TECHNISCHE UNIVERSITÄT DARMSTADT

Metabolic Engineering of Ketocarotenoid Biosynthetic Pathway into the Model Organism *Chlamydomonas reinhardtii*

Vom Fachbereich Biologie der Technischen Universität Darmstadt

zur Erlangung des akademischen Grades

eines *Doctor rerum naturalium*

Dissertation von

NAM TRUNG TRAN

aus Hai Phong, Vietnam

1. Referent: Prof. Dr. Ralf Kaldenhoff

2. Referent: Prof. Dr. Christina Cardoso

Tag der Einreichung: 28.05.2019

Tag der mündlichen Prüfung: 18.07.2019

Darmstadt 2019

Nam Trung Tran, Metabolic Engineering of Ketocarotenoid Biosynthetic Pathway into the Model Organism *Chlamydomonas reinhardtii*

Darmstadt, Technische Universität Darmstadt

Jahr der Veröffentlichung der Dissertation auf TUprints: 2019
Tag der mündlichen Prüfung: 18.07.2019

Θάλατται! Θάλατται!

(The Sea! The Sea!)

Xenophon

Anabasis, Book 4

ABSTRACT

Ketocarotenoids represent a special group of carotenoids characterized by presence of one or several carbonyl (C=O) groups in their ionone rings. Due to their excellent anti-oxidative characteristics, several ketocarotenoids such as canthaxanthin and astaxanthin are valuable pigments highly sought by feed, cosmetical and nutraceutical industries. In this work I aimed to introduce ketocarotenoid biosynthetic pathway into the model organism *Chlamydomonas reinhardtii* via overexpression of its native key enzyme ß-carotene ketolase (CrBKT). High transgene expression and transgene stability were attained with help of the bicistronic Ble2A system in which, the selection marker - zeocin-resistance conferring *ble* gene - is directly linked to gene-of-interest via the so-called self-cleavage foot-and-mounth-disease-virus (FMDV) 2A sequence. Functionality of Ble2A system was proven by successful production of the fluorescence protein mCherry in *Chlamydomonas*. CrBKT's enzymatic activity was also successfully confirmed by heterologous production in carotenoid-producing *E. coli*, indicated by the almost complete conversion of ß-carotene to canthaxanthin and of zeaxanthin to astaxanthin.

Two strains of *Chlamydomonas* were chosen for metabolic engineering: strain UVM-4 which boasted improved transgene expression and strain CC-4102 in which only ß-carotene and zeaxanthin are accumulated due to mutations in α-carotene biosynthetic pathway and xanthophyll cycle. Transformation of both strains with CrBKT overepxression vectors yielded hundreds of zeocin-resistant colonies but only in ~10% of them could the integration of CrBKT be confirmed via PCR. Ketocarotenoid production was not detected in any PCR-positive lines either. Success was only achieved when transformation conditions were changed, namely algal cells were transformed and recovered in dark on growth medium supplemented with yeast extract and tryptone. Under these conditions, I was able to isolate four CrBKT-overproducing transformants. All four lines were characterized by their pale green color as well as their drastically reduced chlorophyll contents. Canthaxanthin production was also detected in two lines, whose concentration stood at about 10% of total cellular carotenoids (~0.1 pg/cell).

An intriguing phenomenon was also observed with these pale green canthaxanthin-producing transformants. When cultivated in light, they promptly reverted back to the normal dark green color. Canthaxanthin could no longer be detected and zeocin resistance was seeminly impaired as well. Though the cause of this phenomenon could not be pinpointed with certainty, it did help explain the failure of my earlier experiments.

Taken together, these results formed the foundation for future projects of ketocarotenoid metabolic engineering in microalgae. Several potential pitfalls that might be encountered were identified and strategies to overcome them were also suggested.

ZUSAMMENFASSUNG

Ketocarotinoide gehören zu einer speziellen Gruppe der Carotinoide, die durch eine oder mehrere Ketogruppen (C=O) in ihren Iononringen charakterisiert werden. Aufgrund ihrer hervorragenden antioxidative Wirkung sind Ketocarotinoide wie Canthaxanthin oder Astaxanthin wertvolle Pigmente, die in der Futter-, Kosmetik- und nutrazeutische Industrie immer begehrt sind. In dieser Arbeit möchte ich anhand Überexprimierung des nativen Schlüsselenzyms ß-Carotinketolase (CrBKT), den ketocarotinoid-biosynthetische Pathway in das Modelorganismus *Chlamydomonas reinhardtii* einbauen. Transgen-Exprimierung bzw. Transgen-Stabilität sollen durch Einsatz des Ble2A-System verbessert werden, in dem der Selektionsmarker - das für Zeocin-Resistenz verantwortliche *ble* Gen – direkt mit dem Gene-of-interest durch die sogenannte selbst-gespaltete 2A-Sequenz aus Maul-und-Klauenseuche-Virus (FMDV) verknüpft wird. Die Funktionalität des Ble2A system wurde durch erfolgreiche Exprimierung des fluoreszierenden Proteins mCherry in *Chlamydomonas* bestätigt. Ebenfalls nachgewiesen war die enzymatische Aktivität von CrBKT, dessen heterologe Exprimierung in carotinoid-produzierenden *E. coli*-Zellen zu fast vollständige Konvertierung von ß-Carotin zu Canthaxanthin bzw. von Zeaxanthin zu Astaxanthin führte.

Zwei *Chlamydomonas*-Stämme wurden für die Metabolic-Engineering-Experimente ausgewählt: Stamm UVM-4, in dem Transgen-Exprimierung erhöht werden sollte, und Stamm CC-4102, in dem wegen Mutationen sowohl in α-carotin-biosynthetischem Pathway als auch im Xanthophyll-Zyklus nur ß-Carotin und Zeaxanthin akkumuliert werden. Nach Transformation der beiden Stämme ergaben sich hunderte zeocin-resistente Kolonien, lediglich ca. 10% wiesen die erfolgreiche Integration des CrBKT-Gens ins Genom auf. In keinen Transformanten war Ketocarotinoid-Produktion nachzuweisen. Erfolgreiche Ergebnisse konnte nur durch Veränerdung der Transformationsbedingungen erreicht werden: die Algenzellen wurden im Dunkeln auf mit Hefeextrakt und Trypton ergänztem Wachstumsmedium transformiert und selektiert. Unter diesen Bedingungen ist es mir gelungen, vier CrBKT-überexprimierende Linien zu isolieren. Alle vier Linien verfügen über eine blassgrüne Farbe und drastisch reduzierten Chlorophyll-Gehalt. In zwei Linien war Canthaxanthin-Produktion nachgewiesen, Canthaxanthin-Konzentration beträgt ca. 10% gesamte Carotinoide-Menge der Zelle (0.1 pg/Zelle).

Ein nicht erwartetes Phänomenon war mit den blassgrünen, canthaxanthin-produzierenden Transformanten zu beobachten. Waren sie im Licht kultiviert, kehrten sie schnell zu der normal grünen Farbe zurück. Canthaxanthin-Produktion war nicht mehr detektierbar und Zeocin-Resistenz war ebenfalls beeinträchtigt.

Zusammen bilden diese Ergebnisse die Grundlage für Ketocarotinoide-Metabolic Engineering-Versuche in Zukunft. Mögliche Schwierigkeiten, denen man begegnen kann, sind identifiziert und Strategien, mit denen man diese Schwierigkeiten beseitigen kann, werden vorgeschlagen.

ACKNOWLEDGEMENTS

September 13th, 2014 was a lovely sunny autumn day when my journey began. There I was, 4 years 7 months 11 days ago, finishing one of the last experiments of my Master Thesis when Professor Kaldenhoff entered the room and offered me a PhD position in his working group. 1684 days later and here I am, older but not necessary much wiser and feeling like Bilbo Baggins when he wrote in the first line of his leather-covered book: “In a hole in the ground there lived a hobbit…” Looking back, it still manages to surprise me of what indeed an adventure it was! Certainly I would never reach where I am today without the help of others, to whom I am all greatly indebted.

First and foremost I would like to express my sincerest gratitude to my doctoral father, Professor Dr. Ralf Kaldenhoff, who not only offered me this wonderful opportunity to continue my pursuit of knowledge but also guided me through each step of my research and provided me with ample supports – academically, materially as well as emotionally – each and every time I am in need. His firm belief in the role science would play in the incoming fight against climate change and his tireless commitments to this noble cause never fail to amaze me. His lead-by-example way of managementship, his exceptional organizational skills, his jovial kindness and his unmovable sangfroid shape our group into an enjoyable and productive work environment. My achievements would be all but impossible without him.

I would like to offer my special thanks to my second supervisor, Professor Dr. M. Cristina Cardoso for her valuable guidance, her richly informative discussions and also her heartfelt encouragements during my research.

My great appreciation is reserved for all current and former members of working group Kaldenhoff: Beate Otto and Dr. Norbert Uehlein-Rössner, Christa Jacob and Ursula Wohner, Dr. Sulabha Sharma, Paul Elsholz, Petra Wurmser and Franziska Joseph, Dr. Christoph Schwarz, Dr. Anastassia Boudichevskaia, Dr. Simon Heppel, Dr. Lei Kai and Dr. Gabriel Glitsos. “We Few, We Happy Few, We

Band of Brothers." Thank you for sharing with me the most friendly and supportive lab I have ever experienced, for our insightful Friday morning's discussion and countless other idea-exchanging and troubleshooting talks, for helping me during preparation and supervision of student's courses and above all, for being my companions during one of the most unforgettable chapter of my life.

I am particularly grateful for the assistance given by Dr. Jürgen Breitenbach from University Frankfurt who kindly donated the plasmids used in my research, Professor Dr. Ralph Bock from Max Planck Institute of Molecular Plant Physiology in Potsdam for so generously sending me UVM strains of *Chlamydomonas*, Marcus Geißler and Elisabeth Bayer from AG Warzecha TU Darmstadt for helping me with HPLC-DAD, Dr. Alexander Rapp from AG Cardoso TU Darmstadt for instructions with the confocal microscope. I also wish to express my gratitude to other people who have also lent me a great hand in various experiments which ultimately, for one reason or another, did not successful and thus were not described in this dissertation: Dr. Michael Ensminger and Dr. Andreas Christmann, who helped me with FACS experiments, Christiane Rudolph and Dr. Olga Avrutina who helped me with HPLC-MS measurements and Benjamin Juretzka and Professor Dr. Christian Hess who helped me with Raman spectroscopy experiments. Even though the results still left much to be desired, your helpfulness, kindness and resourcefulness have forever earned my deepest appreciation.

I am particularly grateful for the assistance given by my undergraduate students Marius Munch, Tanja Habeck, Michael Basic and Amine Achaq.

Last but not least, I wish to say the dearest thanks to my parents Do Thi Tinh and Tran Manh Hai, and my beloved wife Do Hong Hao, who have been standing beside me all these long years. Words fail to describe how deeply I cherish your tenderness, your patience and above all, your endless love.

Darmstadt, April 23rd, 2019

Tran Nam Trung

TABLE OF CONTENTS

I. INTRODUCTION

1. Green algae and *Chlamydomonas reinhardtii*

1.1. Green algae – a brief introduction

The word „alga“ (plural: algae) comes directly from the Latin noun „*alga*” meaning seaweed. The name encloses a huge group of organisms of extreme diversity: from the enormous giant kelp (*Macrocystis pyrifera*) off the coast of Alaska to the tiny, ubiquitous *Euglena gracilis* found in a roadside puddle; from the filamentous *Spirulina* feeding the population around Lake Chad in Africa to the toxic *Karenia brevis* causing the catastrophic Red Tide in the Gulf of Mexico ; from the red *Chlamydomonas nivalis* staining arctic snow patches to *Noctiluca scintillans,* the alga lighting up the ocean at night by their bioluminescence. Even to this day, no single definition of algae has been universally agreed upon. The Merriam Webster's definition is just one among many others: an alga is

> *"A plant or plant-like organism of any of several phyla, divisions, or classes of chiefly aquatic usually chlorophyll-containing nonvascular organisms of polyphyletic origin that usually include the green, yellow-green, brown, and red algae in the eukaryotes and especially formerly the cyanobacteria in the prokaryotes".*

The green algae (Chlorophyta) are taxonomically closely related to land plants; together they form the green lineage (Viridiplantae) **[1]**. Common features of this division are: aquatic habitats, isokont flagella, double-membrane chloroplast, starch storage in plastids and presence of both chlorophylls a and b **[2]**. Several members of phylum Chlorophyta rank among the most important and well-known algae species: *Chlorella, Dunaliella*, *Haematococcus, Scenedesmus, Botryococcus, Volvox* and *Chlamydomona,* each with its own rich and colourful history.

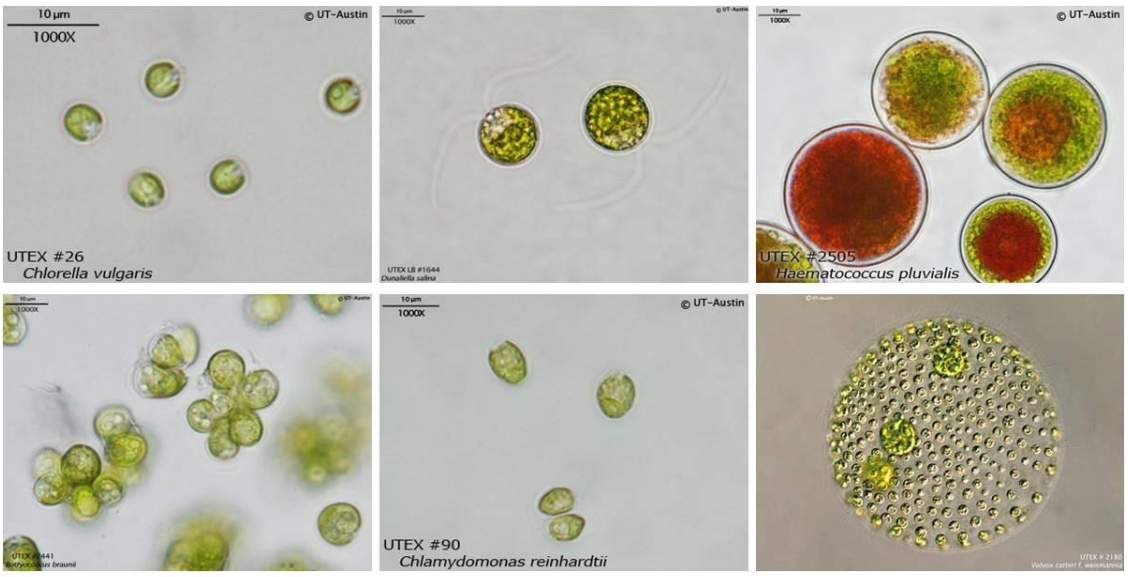

Figure 1: Green algae of the phylum Chlorophyta: *Chlorella vulgaris* (upper left), *Dunaliella salina* (upper middle), *Haematococcus pluvialis* (upper right), *Botryococcus braunii* (lower left), *Chlamydomonas reinhardtii* (lower middle), *Volvox carteri* (lower right). Photo courtesy of Culture Collection of Algae at the University of Texas at Austin (utex.org)

The worlds's first „superstar alga", *Chlorella* got into the limelight in the late 1940s early 1950s, emerging as a highly promising staple food source of the future. With the traumas of World War II still vivid and the world-changing Green Evolution still years in future, 1950s were the time of the so-called „Malthusian Scare": many scientists believed that the world's agricultural capacity was steadily overtaken and would soon be outstripped by its exploding population. A worldwide famine was therefore inevitable if not imminent. In such gloomy atmosphere, the potentials of *Chlorella* - rich in proteins, vitamins and other nutrients; rapid growth consuming nothing but light, water and carbon dioxide - captured the imaginations of not only scientists but also much wider audience. Extensive large-scale experiments however showed that the high expectations on *Chlorella* were rather misplaced: production proved far more costly and difficult than expected and the high photosynthesis efficiency recorded previously under controlled lab conditions was unattainable when uncontrolled outdoor light was used **[3]**. That notwithstanding, *Chlorella* remains one of the most commercially cultivated microalgae today with the annual production exceeds 2,000 metric tonnes, mostly for dietary and nutraceutical purposes **[4]**.

Dunaliella salina and *Haematococcus pluvialis* are often depicted in encyclopaedias and textbooks with their orange-red colouration but they are in fact green algae. The reddening does not even start until cells are exposed to stress conditions (high irradiance, high salinity, nutrient limitation), upon which pigments (termed „haematochrome" in older literature) are produced in large amount and stored inside their intracellular lipid bodies. „Haematochromes" of *Dunaliella* and *Haematococcus* have already been identified as ß-carotene and astaxanthin respectively; both are carotenoids with excellent anti-oxidant activities. While their actual physiological functions in algal cells still remain matters of debate, the beneficial health effects of both dietary ß-carotene and the much more potent astaxanthin are well established by a rich litany of researches, making them highly sought commodities on the market, especially as nutraceutical products. Large-scale commercial production has been achieved in Australia, Israel, China, India (*Dunaliella*) **[5];** Hawaii, Israel, China (*Haematococcus*) **[6]**.

It is often said that the economy of 19th century was built on coal, of 20th century on oil. The world's stock of fossil fuels is however a limited resource which is being rapidly depleted by the booming population. The 1973 oil crisis only served too well as a stern warning to what might happen once fossil fuels run out or become too expensive to collect. Consumption of fossil fuels is also linked to increased atmospheric CO_2 concentration, the Greenhouse Effect and their far reaching environmental consequences. Thus it is small wonder that more and more efforts have been poured into the search of the new sources of sustainable energy. Species of the genus *Botryococcus*, especially *Botryococcus braunii*, are known for their unusual trait of accumulating long-chain hydrocarbon (up to 61% dry weight) in their colony matrix and occluded globes **[7]**, thus making them promising candidates as biofuel producers. A large-scale business evaluation in Japan, 2012 estimated that *Botryococcus*-derived oil would become competitive once oil price exceeded 1.25 $/litre **[8]**.

Volvox is a common entry in many encyclopaedias and biology textbooks not only due to its seniority - it was among the very first microorganisms ever discovered, described by none other than Antonie van Leeuwenhoek, the Father of Microbiology in 1700, himself – but also because of its intriguing cellular organisation. *Volvox* cells form spherical or oval hollow colonies of up to 60,000 cells, large

enough to be visible to the naked eyes. Volvox colonies are thus often seen as “the missing link” between uni- and muticellular organisms. Closely related to *Volvox* is one alga species that is termed „the green yeast”, *the* model organism for researchers of photosynthesis, cell motility, cell’s responses to stimuli and other algal biological processes since the last 70 years. Enter *Chlamydomonas reinhardtii*

1.2. *Chlamydomonas reinhardtii* – the model organism

Consisting of 459 species, the genus *Chlamydomonas* (Greek: *chlamys* – cloak or mantel, perhaps a reference to their proteinous cell wall) belongs to the family Chlamydomonadaceae, order Volvocales, class Chlorophyceae, phylum Chlorophyta. Members of this genus are widely distributed around the world in many different habitats: soil, fresh water, ocean and even snow. By far the most commonly used species for laboratory researches is *Chlamydomonas reinhardtii*.

First described by Dangeard in 1888, *Chlamydomonas reinhardtii* was named in honour of the Ukrainian botanist Ludwig Reinhard(t). Similar to other species in the genus, morphologically cells have two anterior flagella of equal length, a proteinous cell wall, contractile vacuoles, a single cup-shaped chloroplast with one or several prominent pyrenoids and an eyespot. Eyespot, also called stigma, is a bright orange carotenoid-containing organelle located peripherally near cell’s equator and plays important roles in light perception **[9]**. *Chlamydmonas reinhardtii* vegetative cells are haploid with 17 chromosomes and can growth both photoautotrophically in light and heterotrophically in dark when acetate is present. Cells proliferate by means of either asexual cell division or sexual mating of two isogamous gametes. Gametogenesis is induced by nitrogen depletion in presence of blue light. There are two mating types („plus” and „minus”) which are simple Mendelian traits. *Chlamydomonas reinhardtii* is also among the first organisms to have their genome completely sequenced. Sequences of its ~112 Mbp nuclear genome **[10]**, as well as ~15.8 kpb mitochondrial **[11]** and ~205 kbp chloroplast genomes **[12]** have been published.

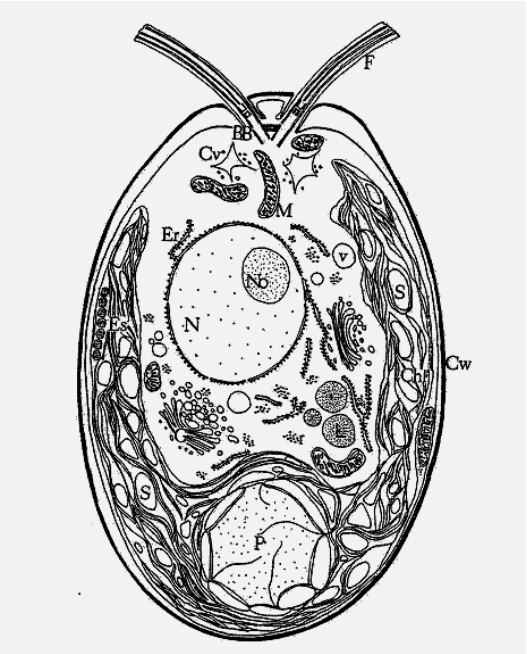

Figure 2: semidiagrammatic representation of an interphase *Chlamydomonas* cell. Abbreviations: F – flagella, BB – basal body, Cv – contractile vacuoles, M – mitochondria, Er – endoplasmic reticulum, v – vacuole, No – nucleolus, N – nucleus, S – starch grain, Es – eye spot, Chl – chloroplast, L – lipid droplet, G – Golgi apparatus, P – pyrenoid. Cw – cell wall. Modified from Harris 2001**[13]**.

In many different ways, *Chlamydomonas reinhardtii* is an attractive model organism. It grows fast and requires neither expensive supplements nor elaborate equipments for cultivation. Capable of sexual reproduction, it is amenable to various crossing techniques of classical genetics. Photosynthesis researches benefit greatly from studying non-photosynthetic mutants of *Chlamydomonas reinhardtii*, which, unlike other obligate phototrophic species, can still survive in presence of acetate. *Chlamydomonas* flagella, built from microtubules, can be easily amputated and regrown, giving insight into how such structures are assembled, controlled and disassembled. The presence of a prominent light perceiving organelle (the eyespot) and cell's ability to move in response to light stimuli (phototaxis) are also of great help to studies of photoreception. Nothing could attest the popularity of *Chlamydmonas reinhardtii* better than the sheer number of mutants accumulated from more than 70 years of works. One of the biggest mutant collections, the Chlamydomonas Resources Centre (CRC), University of Minnesota, United States, regularly maintains and distributes a library of more than 5,000 mutants. Given such impressive lineage, it is rather surprising that all the *Chlamydomonas* laboratory strains and their subsequent mutants could be traced back to a single humble zygospore isolated from a potato field in Massachusetts by G.M. Smith in 1945 **[14]**.

1.3. Genetic manipulation of *Chlamydomonas*

It was discovered relatively early that exogenous bacterial DNA can be taken up into *Chlamydomonas* cells **[15]**. Since then, transformation of cells, integration of exogenous gene into algal genome and transgene expression have been established into a routine techniques for *Chlamydomonas*. Genetic manipulation not only of nuclear **[16]** but also of chloroplast **[17]** and mitochondrial **[18]** genomes has all been achieved.

1.3.1. Methods of DNA delivery

Arguably the simplest method to introduce foreign DNA into *Chlamydomonas* cells is the so-called glass beads transformation **[19]**. In this method, cell-wall-less *Chlamydomonas* cells, DNA and glass beads are agitated together at high speed on an ordinary benchtop vortex mixer. The exact mechanism behind remains unknown but it is generally believed that the mild shear force during agitation facilitates DNA uptake. Cell wall removal requires treatment with autolysin, a lytic enzyme secreted by cells during gametogenesis and hydrolyses components of the protein-rich cell wall. Alternatively, cell-wall-deficient mutants (such as those with the phenotype *cw15*) could be used for transformation.

Particle bombardment (also called biolistics) is another method of DNA delivery into *Chlamydomonas* **[16][18][20]**. DNA-coated sub-micron gold or tungsten particles are accelerated into algal cells by a stream of pressurised helium. The downsides of this technique are the high costs of equipments and consumables as well as the relatively high number of transgene copies integrated into algal genome which could potentially induce gene silencing. On the other hand, particle bombardment is often the method of choice for transformation of chloroplasts and mitochondria where high copies number is desired. No prior removal of the cell wall is required in order to prepare *Chlamydomonas* cells for transformation.

Another popular method of DNA delivery is electroporation **[21][22][23]**. When an electric field is applied on algal cells, their lipid membranes become temporarily permeable allowing DNA to enter. Similar to particle bombardment, cell wall removal is not a requirement. Though limited by the high equipment costs and the large number of parameters that need to be optimised, transformation efficiency is much higher than glass beads method with less deletion at insertion sites **[21]**. Transformation efficiency could be boosted further with special transformation buffer **[24]**.

Agrobacterium tumefaciens is the pathogen of the crown gall disease in plants. In one of the very few examples of inter-kingdom horizontal gene transfer, bacterial DNA (termed T-DNA) is inserted into cells and integrated into host's genome. Co-cultivation with *Agrobacterium tumefaciens* is one of the most popular methods for transformation of higher plants, especially dicotyledons **[25]**. In comparisons however, reports of successful transformation of *Chlamydomonas* with *Agrobacterium* are much fewer and farther between **[26][27]**. Several other methods of DNA delivery are also occasionally reported but not adopted widely: agitation with silicon carbide whiskers **[28]**, sonication **[29]**, cell penetrating peptide-mediated translocation **[30]**, etc.

After entering cells, exogenous DNA would eventually be lost again unless it can integrate itself stably into algal genome. Insertion into chloroplast or mitochondrial genome is facilitated by homologous recombination and the sites of insertions are pre-determined by two guiding homologous arms flanking the sequence of interest **[31][32]**. Transgene incorporation into *Chlamydomonas* nuclear genome is a much more complex process however. In a high-throughput genotyping study of more than 11,000 insertion mutants **[33]**, Zhang et al. found that insertion sites were distributed randomly across the genome, implying a mechanism involved gene insertion into double-stranded breaks (illegitimate recombination). In addition, often found together with the sequence of interest in the insertion site were fragments from transformation plasmid or pieces of *Chlamydomonas* DNA from entirely different genomic loci. Zhang et al. explained this finding by suggesting a model, in which not only plasmid DNA but also genomic DNA from lysed cells were partially digested by endolytic nucleases before or during entry into recipient cells, where they were ligated into double-stranded breaks of the recipient genome. This model also helps to explain an intriguing observation that transformation efficiency of *Chlamydomonas* was enhanced when linearised plasmids (with cleavage site outside expression cassette) are used instead of the intact circular DNA **[34]**.

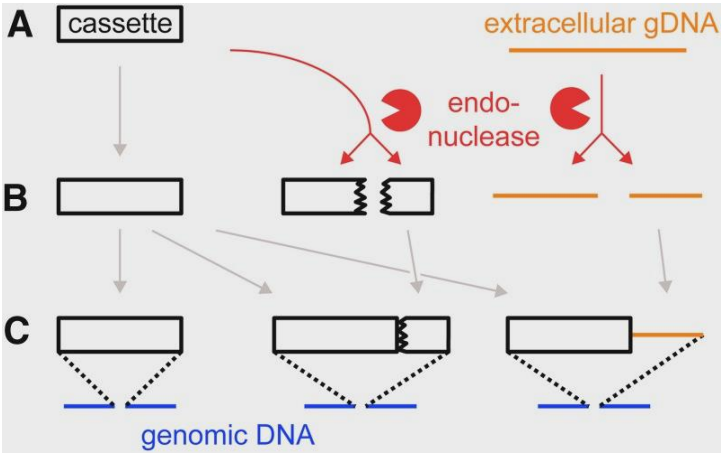

Figure 3: Model of transgene integration into *Chlamydomonas* nuclear genome proposed by Zhang et al. Extracellular DNA (transformation vector, gDNA of lysed cells) are digested by endonuclease(s) upon entering cells. DNA fragments are then inserted into genome via double-stranded breaks. Modified from Zhang et al 2014 **[32]**

Development of a versatile molecular toolkit is *sine qua non* for genetic modification of any organism. Since the first reports of successful transformation of *Chlamydomonas* almost 30 years ago, significant advances have been made in this field. The following sections will discuss most important elements of *Chlamydmonas* molecular toolkit: selection markers, reporter genes, promoters, as well as the difficulties encountered in the *Chlamydomonas* system and outlook to the future.

1.3.2. Molecular toolkit for nuclear transformation of Chlamydomonas

***Selection markers**:* First reports of successful transformations of Chlamydomonas were performed using endogenous genes to rescue auxotrophic mutants. Commonly used auxotrophy selection markers include: *arg*7 for arginine biosynthesis **[35]**, *nit*1 for nitrate metabolism **[19]**, *oee*1 and *atp*C for photosynthesis **[16][36]**. Over the years, antibiotic-resistant genes are also added to the arsenal of selection markers: *ble* from *Streptoalloteichus hindustanus* against phleomycin/ zeocin **[37]**, *aadA* from *E. coli* against spectinomycin **[38]**, *aph*VII from *Streptomyces hygroscopicus* against hygromycin B **[39]**, aphVIII from *Streptomyces rimosus* against paromomycin **[40]**, synthetic *tet*X against tetracycline **[41]**, etc. While other markers confer resistance by enzymatic degradation, Ble inactivates phleomycin/ zeocin through drug sequestration: two molecules of antibiotics are removed through binding with a Ble dimer. As the results, high levels of production are generally required **[42]**.

***Reporter genes**:* Due to their simple, non-invasive and non-destructive modes of detection, fluorescence proteins are popular among researchers as reporter genes of choice. In *Chlamydomonas* however, the use of fluorescence proteins are limited by their low production, conditioned by poor codon optimization, and by high levels of autofluorescence. These limitations are vividly demonstrated by the case of green fluorescence protein (GFP). First report of successful production of GFP in *Chlamydomonas* came in 1999 but only after the authors had exchanged the native *Aequorea victoria* sequence with a *Chlamydomonas* codon-optimized one **[43]**. Since then, expression of codon-optimized GFP alone has been routinely achieved **[44][45][46]**. Detection of GFP-fusion proteins are still hampered by high autofluorescence caused by photosynthetic pigments, and visualisation of such proteins are most successful when they are concentrated in pigment-lacking organelles such as flagella **[47][48]** or nucleus **[46][48]**, or when the pigment-deficient white mutant was used for study **[50]**.

Other fluorescence proteins are also tested for *Chlamydomonas* with positive results. Among these, best signal-to-background ratios were achieved with proteins whose excitation and emission spectra fell within the so-called “green gap” of photosynthesis such as mVenus, mTomato and mCherry **[51][52]**. Alongside fluorescence proteins, other enzyme-based reporter gene systems are being developed as well: luciferase **[53]**, ß-glucuronidase **[54]**, arylsulfatase **[55]** etc. Detection via enzymatic reactions is however often complicated by substrate’s inability to enter cells and their toxicity. The former can be alleviated by secretion of protein into medium **[53][55]**.

Promoters: A library of both constitutive and inducible promoters to drive gene expression is pre-exquisite for any transgene expression. Unfortunately, the choices of strong promoters for *Chlamydomonas reinhardtii* are somewhat limited. The most commonly used promoters are native ones: the constitutive PsaD **[56]**, RBCS2 **[57]**, the fusion promoter HSP70A-RBCS2 **[58]** as well as the

light- and heatshock-inducible HSP70A **[58]**, ammonium-starvation-inducible NIT1 **[59]**, low-CO2-inducible CA1 **[60]**, copper-depletion-inducible CYC6 **[61]**. Though widely applied for higher plants, attempts to utilize constitutive promoters of viral origins such as CaMV35S or SV40 to *Chlamydomonas* were met only with limited success **[62][63]**. To my best knowledge, there is no virus known to infect *Chlamydomonas reinhardtii*, making isolation of new viral promoters difficult.

1.3.3. Difficulties for transgene expression:

Stringent codon bias**:** *Chlamydomonas* genome has a very high GC content. At 66.3%, it is much higher than human (52.3%), *E. coli* (51.4%), *Saccharomyces cerevisiae* (39.8%), *Arabidopsis thaliana* (36.0%), *Caenorhabditis elegans* (35.4%). It was also recognized very early that its codon usage is strongly biased. A statistical analysis of 846 coding sequences (420455 codons) showed that, for example, the frequency ratios of CAG to CAA (both encoding glutamine) was 8.6:1; of CAC to CUA (both encoding histidine) was 6.7:1, of UGC to UGU (both encoding cysteine) was 9.1:1 **[64].** Frequencies of some codons were so low that they were practically unused; for example the frequency ratios of AAG to AAA (both encoding lysine) was 17.7:1. Expressions of many transgenes are thus difficult unless their sequences are specifically codon-optimised for *Chlamydomonas* **[43][65]**.

Gene silencing: Unstable transgene expression represents a serious problem both for researches and for practical applications of transgenic technology. The first study that took a detailed look into the phenomenon of gene silencing was performed by Cerutti et al. in 1997, which came to the conclusions that gene silencing took place on both transcriptional and post-transcriptional levels, though neither chromatin methylation nor genetic alterations of transgene (e.g. deletion, rearrangements, mutations, etc.) were the culprit **[66]**. The important roles of RNA interference in gene silencing was later demonstrated by Fuhrmann et al **[67]** and since then, RNAi has been turned into an important tool for targeted down regulation of gene expression in *Chlamydomonas* **[58][69]**.

1.3.4. Future's outlook: making Chlamydomonas a better model organism

Genetic manipulation of *Chlamydomonas* is plagued by its unusually strict codon usage, low transgene expression and gene silencing, variable of gene expression due to positional effects, lack of adequate molecular tools, etc. As Einstein once said: "In the middle of difficulty lies opportunity", these issues also create rooms for improvement in the future.

The biased codon usage of *Chlamydomonas* necessitates the use of synthetic DNA. Fortunately, recent advances in gene synthesis has significantly both driven down the cost and increased the sequence fidelity of synthetic DNA **[70]**. Together with the rapidly increasing amounts of data from next-generation sequencing, it is not inconceivable to assume that the dearth of suitable genetic elements for *Chlamydomonas* system would soon be thing of the past. Efforts have also been made to standardise the molecular toolkit and turn it into a modular system (i.e. parts such as promoter, coding sequence, regulatory elements etc. can be inserted, swapped or removed with minimal efforts). In a recent cooperation of many laboratories in France, UK, Denmark, Germany and Spain, a molecular cloning toolkit for *Chlamydomonas reinhardtii* based on Golden Gate **[71]** cloning has been created with 119 openly distributed genetic parts (among them 7 promoters, 6 terminators, 12 reporter genes, 6 selection markers and 9 signal and targeting peptide sequences) **[72]**. Such library

would significantly reduce the workload for creating and testing new transformation vectors as well as simplify material sharing between groups.

Mutations of chromatin modification mechanisms could lead to improved transgene expressions. Neupert et al. reported the creation of two new strains of *Chlamydomonas* via UV-mediated mutagenesis where expression of GFP was significantly enhanced compared to their parrent strain **[73]**. While the exact nature and locations of mutation were not yet elucidated, subsequent studies showed that in mutant strains, increased YFP concentration was correlated with higher levels of histone 4 acetylyation and lower levels of histone 3 methylation **[74]**. In another publication, the *met1* mutant in which a DNA cytosine methyltransferase was disrupted by insertional mutagenesis, also displayed improved expressions of squalene synthase (CrSQS) and a SQS-like protein 3 (CrSSL3) **[75]**.

Transgene expression and transgene stability could also be enhanced by the use of polycistronic constructs. The merits and also caveats of this particular approach will be discussed in the next section.

1.3.5. One-promoter approach: polycistronic constructs for Chlamydomonas

„You only find what you are searching for“. Transformation invariably requires co-expression of a selection marker, with the help thereof successfully transformed cells could be screened. It is however not unusual that cells that survived selection does not express the gene of interest, either because expression cassette is fragmented and only part with selection marker is incorporated into genome, or because expression is repressed by transcriptional/ post-transcriptional gene silencing mechanisms. It is further aggravated by the generally low expression levels in *Chlamydomonas* and screening for high-producing transformant lines could be depressingly tedious. Published studies reported success rates (i.e. percentage of lines with high transgene expression among total number of colonies screened) as low as 1% **[76][77]**. Clearly if expression levels of selection marker and gene of interest could be somehow coupled, screening workload would be significantly reduced. Enter the concept of polycistronic constructs. Seymor Benzer, in his classic work „*The elementary units of heredity*“ **[78]**, defined „cistron“ as „a unit of [gene] function”. A polycistronic construct is a construct in which a molecule of messenger RNA encodes two or more proteins. While polycistronic mRNAs is generally the norm among prokaryotes, eukaryotic mRNAs are with few exceptions monocistronic. Polycistronic constructs for use in eukaryotic organisms such as *Chlamydomonas* thus require additions of viral DNA elements such as 2A peptides or internal ribosome binding sites.

Internal ribosome binding sites (IRESs) were first discovered in piconavirus **[79]**. As their name suggests, they direct internal entry of ribosomes amid sequence and initiate downstream translation in a cap-independent manner. Successful applications of IRES-based polycistronic constructs have been reported in animals, fungi and plants **[80][81]**. Even in organisms that are evolutionary far distant from their natural hosts, IRES elements are still functional **[82]**. Interestingly, some putative IRES elements are also identified in non-viral genomes, whose functions remain still unsolved **[83]**. There is only one report of successful application of IRES in *Chlamydomonas* by Onishi in 2016 **[77]**, in which coding sequences of yellow fluorescence protein mVenus and the paromomycin resistance marker APHVIII are linked by seven different viral IRES. Subsequent tests showed that among tested sequences, only IRES elements from potato leafroll virus (PLRV) were functional, with chances of

detecting mVenus-positive colonies increased ten-fold compared to monocistronic construct where *aphVIII* and *mVenus* each had its own promoter. There was still their discrepancy in expression levels, with the upstream *mVenus* more efficiently translated than the downstream *aphVIII*.

First discovered in foot-and-mouth disease virus (FMDV), 2A peptides are short oligopeptides (19-22 amino acids in length) found in many positive-strand RNA viruses **[84]**. Often termed „self-cleaving peptide", translation of a 2A sequence-containing mRNA would yield two instead of one protein, with the ostensible „cleavage site" between glycine and proline residues at the 2A peptide's C-terminus. The term "self-cleaving" is however misleading, since no proteolytic reaction actually takes place. Instead, biosynthesis of the peptide bond between glycine and proline is simply „skipped" by ribosome **[85]**. Compared to IRES and other multi-gene co-expression approaches, 2A peptide enjoys the relatively high expression of downstream proteins (theoretical stochiometric ratio between two daughter proteins should be 1:1) and their smaller sizes mean smaller risk of interference with protein activity. Downsides are the artifacts added to C-terminus of the upstream and N-terminus of the downstream proteins, and the presence of ribosome read-through products, i.e. large fusion protein in which the amide bond between glycine and proline is still successfully formed **[86]**.

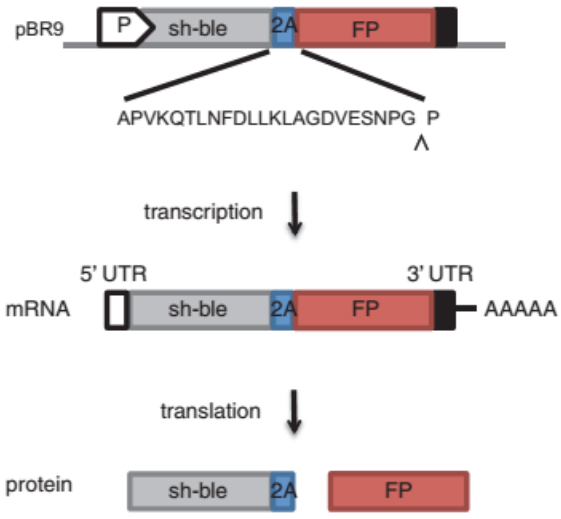

Figure 4: Schematic of 2A peptide-based transgene expression strategy developed for *Chlamydomonas*. Arrowhead symbol (∧) indicates the "cleavage site" within 2A peptide's sequence. Modified from **[51]**

Applications of 2A peptide for transgene expression in *Chlamydomonas* were pioneered by Rasala et al. (2012), in which the coding sequence of xylanase 1 was fused downstream to the zeocin-resistance marker *ble* via FMDV's 2A **[46]**. 2A sequence is found to be properly processed by *Chlamydomonas* and, compared to the conventional two-promoter construct, the novel one-promoter 2A construct's transgene expression is dramatically increased (~100 fold). Subsequent studies showed that the addition of a prolin residue to the N-terminus of the downstream protein does not seem to interfere with organelle targeting, as downstream mCherry fused with transit peptides for nucleus, mitochondria, endoplasmic reticulum and chloroplasts is still properly delivered to the corresponding organelles **[87]**. Transgene stability is enhanced as well because gene silencing would lead to loss of zeocin resistance and cell death. The Ble2A concept has since been widely adopted for production of a plethora of proteins in *Chlamydomonas* such as: squalene synthase **[75]**, calredoxin **[88]**, NAD-dependent phosphite oxidoreductase **[89]**, Orange protein **[90]**, peroxisomal acyl-CoA oxidase **[91]**, etc.

2. Carotenoids

2.1. Carotenoids - overview

Carotenoids (from Latin "*carota"*, carrot) are organic pigments found in a plethora of plants, algae, fungi, bacteria as well as in some animals. They fulfil a wide variety of biological functions. Among the best understood are their roles in photosynthesis: here they act as accessory pigments which expand the wavelength range of light-harvesting antennas, dissipate of excessive absorbed energy and contribute to structural stabilisation of photosynthetic complexes **[92]**. Many carotenoids are also well-known strong UV-absorbers and anti-oxidants. For example, astaxanthin is produced by *Haematococcus pluvialis* under high light to cope with oxidative stress, while staphyloxanthin acts as virulence factor of *Staphylococcus aureus* by protecting the pathogen from reactive oxygen species (ROS) released by host's phagocytic cells **[93]**. The carotenoids in many fruits (tomato, bell pepper, apricot etc.) attract animals, which feed themselves on the fruits and disperse the seeds. Lesser known but equally important are the carotenoid's roles in modulations of lipid membrane physical properties such as fluidity or gas permeability **[94]**. Carotenoids are also precursors of many biological active compounds such as vitamin A, rhodopsin, abscisic acid, fungal pheromones and anti-fungal compounds **[95]**.

Carotenoids belong to the class of terpenes. Like all terpenes, biosynthesis of carotenoids starts with the production of the basic building unit: isopentenyl pyrophosphate (IPP, C_5). While in animals including human, archaea and some bacteria, IPP is synthesized by the mevalonate pathway, in vascular plants and green algae, IPP biosynthesis takes place exclusively inside plastid via the methylerythritol phosphate (MEP) pathway **[96]**. Subsequent reactions between two or more IPP units lead to carbon chain elongation. The vast majority of carotenoids are tetraterpenoids (C_{40}) built from two units of geranyl geranyl pyrophosphate (GGPP, C_{20}). Exceptions are triterpene (C_{30}) carotenoids from some heliobacteria species, built from two molecules of farnesyl pyrophosphate (FPP, C_{15}), and the even rarer C_{50} carotenoids, which could be detected only in small groups of actinobacteria and haloarchaea **[97]**. The C_{40} backbone harbours eleven C=C double bonds, which are responsible for the typical yellow-red tints of carotenoids. It is worth mentioning that carotenoid colors could change quite dramatically once they form complexes with proteins. A classical example is the red carotenoid astaxanthin attached to crustacyanin, a protein found in the exoskeleton of lobsters, that has the blue color but would change back red once the carotenoprotein complex is destroyed upon being cooked.

Carotenoid biosynthetic pathways from GGPP are shown in **Figure 5**. Condensation of two GGPP (C_{20}) molecules gives rise to one molecule of phytoene, the first C_{40} carotenoid in the pathway. Phytoene is further processed into ξ-carotene then lycopene. The open ends of lycopene undergo cyclisation to form two so-called ionone rings. Depending on their ring's configurations, the resulting products are either α- or β-carotene. Two different branches thus emerge: one to biosynthesis of ß-carotene, zeaxanthin, violaxanthin, antheraxanthin and neoxanthin; the other to biosynthesis of α-carotene, lutein and loroxanthin. The former is termed "ß-carotene pathway", the latter "α-carotene pathway".

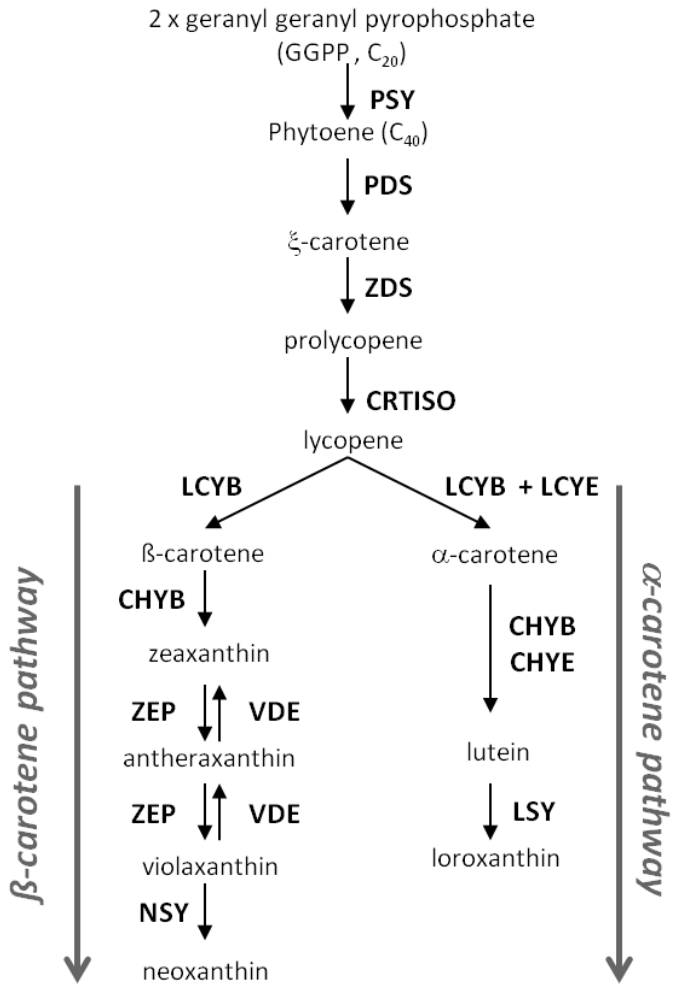

Figure 5: biosynthetic pathways of carotenoids. Biosynthesis starts from condensation of two GGPP molecules to phytoene and branches at lycopene. Involved enzymes are written in bold uppercase. Their full names are as follows: PSY – phytoene synthase, PDS – phytoene desaturase, ZDS - ξ-carotene desaturase, CRTISO – carotenoid isomerase, LCYB – lycopene ß-cyclase, LCYE – lycopene ε-cylase, CHYB – carotene ß-hydroxylase, CHYE – carotene ε-hydroxylase, ZEP – zeaxanthin epoxidase, VDE – violaxanthin deepoxidase, NSY – neoxanthin synthase, LSY – loroxanthin synthase

Commercial demands for carotenoids are constantly on the rise. Global carotenoids market stood at $1.23 billion in 2015 and is expected to grow to $1.81 billion by the year of 2022 **[98]**. Carotenoids are still mainly used as colouring agents for human foods and additives to animal feeds but market trends are changing rapidly. One of the fastest growing segments of carotenoids market is the dietary supplements. Benefiting from numerous studies showing their positive health effects, carotenoids such as astaxanthin or fucoxanthin have seen their demands skyrocketing in the recent years **[99]**. There is also a major shift in carotenoid supply chains. While the market is still dominated by synthetic carotenoids produced by the chemical industry, bio-carotenoids extracted from natural sources attract more and more interest due to both their proven superior bioavailability as well as ever increasing consumer consciousness **[100]**.

2.2. Ketocarotenoids and astaxanthin

Ketocarotenoids belong to a sub-group of carotenoids member of which all contain at least one ketone (C=O) group in their ionone ring. The electron-pulling conjugative effect of the carbonyl group(s) changes the absorption maximum slightly, causing the shift from the yellow color often associated with xanthophylls (the Greek word "*xanthus*" means yellow) to a red tint. Unlike ß-carotene or lutein that are ubiquitous in photosynthetic organisms, ketocarotenoids are distributed among a much smaller number of species. Their names often give clues to the natural sources in which they could be found: echinenone in sea urchins (phylum Echinodermata) **[101]**, adonixanthin and adonirubin in the petals of Adonis flowers **[102]**, canthaxanthin in the chanterelle mushroom (*Cantharellus cinnabarinus)* **[103]** etc.

Astaxanthin (the Greek word "*astakos*" means lobster – the pigment is responsible for the color change of crustacean exoskeleton to red when they are cooked) is a highly valuable ketocarotenoid sought by many industrial sectors. Some of the biggest buyers of commercial astaxanthin come from aquaculture and poultry industry, where astaxanthin is added to animal feeds both for reddening of meat (a factor of great importance for fishes like salmon or trout) and to improve animal's health **[104]**. Demands are also high in cosmetics and nutraceutical sectors, inspired by a considerable body of clinical studies backing beneficial health effects of astaxanthin on human's health **[105]**. Such positive health effects of astaxanthin are explained by its excellent radical scavenging and anti-oxidative activities. A study by Kushirage et al. in 1990 showed that anti-oxidative activity of astaxanthin was 500-fold more potent than of vitamin E and 38-fold more than of ß-carotene **[106]**.

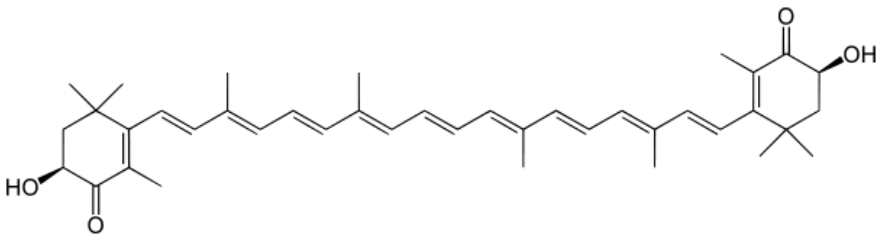

Figure 6: chemical structure of natural astaxanthin (3S, 3'S stereoisomer)

The majority of astaxanthin in the feed market is synthetic astaxanthin supplied by big chemical concerns such as BASF or Roche **[104]**. While synthetic astaxanthin is indeed much cheaper than natural astaxanthin to prodce, the former is also significantly inferior in terms of anti-oxidative activity and bioavailability and may not even be suitable as human nutraceutical supplement **[107]**. Such difference is readily explained by conformation difference: the majority of synthetic astaxanthin is in 3R,3'S conformation, while in natural astaxanthin 3S,3'S stereoisomer is the main form **[104]**. Natural sources of astaxanthin range from bacteria (e.g. *Paracoccus carotinifaciens, Agrobacterium aurantiacum*), yeasts (*Xanthophyllomyces dendrorhous*) to algae (*Haematococcus pluvialis*), higher plants (*Adonis aestivalis* – Adonis flower) and animals (*Euphausia superba* – Antarctic krill). Among these, only *Haematococcus pluvialis* and *Euphausia superba* have been established as production platforms for human consumption. In the recent years, a third species, the green alga *Chromochloris zofingiensis* (earlier *Chlorella zofingiensis*), has also emerged as a promising alternative source of natural astaxanthin **[108]**.

2.3. Astaxanthin biosynthetic pathways

Functional analysis of astaxanthin-biosynthetic enzymes of *Haematococcus pluvialis* **[109]** and *Chromochloris zofingiensis* **[110]**, of *Agrobacterium aurantiacum* **[111]** and of *Xanthophyllomyces dendrorhous* **[112]**, as well as of *Adonis aestivalis* **[113]** all pointed to ß-carotene as the starting point of the biosynthesis. Comparing their chemical structures, ß-carotene differs from astaxanthin by having two extra hydroxyl (-OH) groups at both 3-positions and two extra carbonyl (C=O) groups at both 4-positions of its two ionone rings. The conversion of ß-carotene to astaxanthin is thus catalysed by two classes of enzymes: ß-carotene ketolases (BKT/ CrtW/ CrtO) which add the carbonyl groups; and ß-carotene hydroxylases (CHYb/ CrtY/ CrtR) which add the hydroxyl groups to the ionone ring. Intriguingly, in *Xanthophyllomyces dendrorhous*, both hydroxylation and ketolation reactions are catalysed by a single dual-function enzyme, the astaxanthin synthase CrtS. Like many other secondary metabolism processes, enzymes of astaxanthin biosynthesis are promiscuous, meaning they can accept a wide variety of substrate. For example, BKT is capable of processing ß-carotene to echinenone, echinenone to canthaxanthin, zeaxanthin to adonixanthin and adonixanthin to astaxanthin.

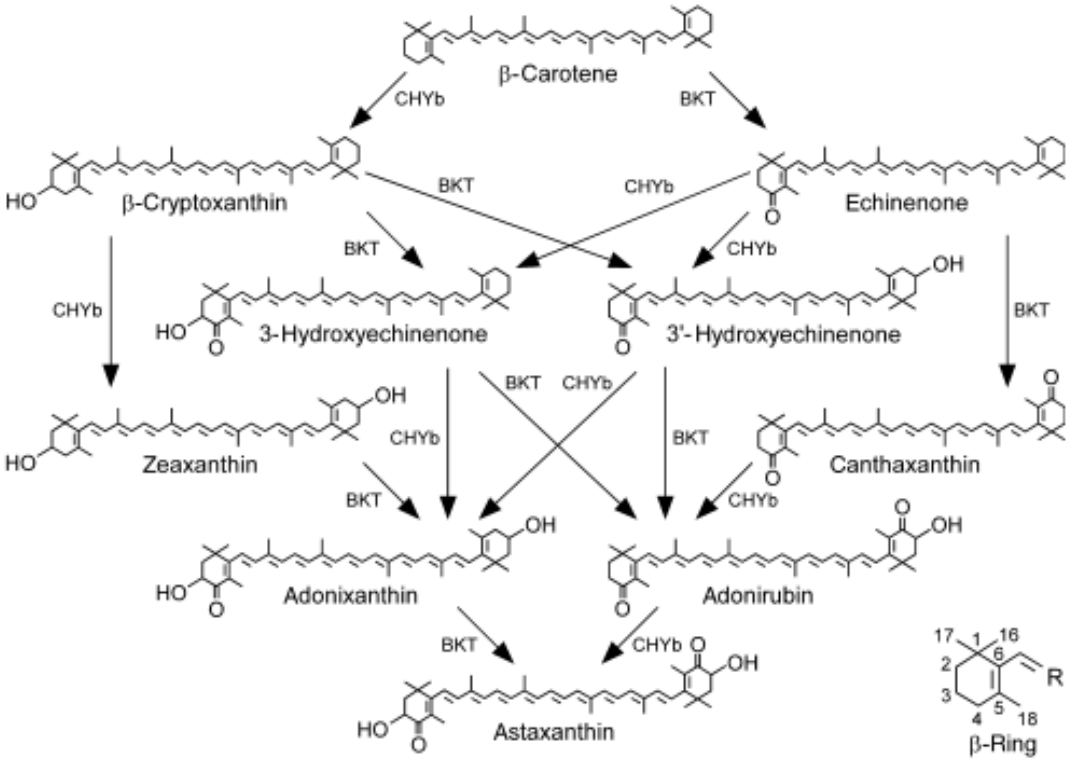

Figure 7: possible routes from ß-carotene to astaxanthin. On the lower right hand side is the numbering of the ß-ionone ring. Modified from **[96]**

Since one enzyme can only add one carbonyl or hydroxyl group to one position at one time, the conversion of ß-carotene to astaxanthin could theoretically go through different routes via many intermediates as showed in **Figure 7**. Which pathways/ intermediates are predominant depends on substrate specificity and enzymatic activity of individual enzymes as well as the balance between hydroxylation and ketolation, which varies greatly from species to species. For example, in *Haematococcoccus pluvialis*, ß-carotene is first converted to canthaxanthin and then hydroxylised to astaxanthin **[109]**, while in *Chromochloris zofingiensis,* first step is the hydroxylation of ß-carotene to zeaxanthin followed by its ketolation to astaxanthin **[110]**. *Haematococcus pluvialis* also accumulates almost exclusively astaxanthin, while significant amounts of zeaxanthin, canthaxanthin and adonixanthin were detected in *Chromochloris zofingiensis* **[108]**.

Much less well-understood is how the astaxanthin biosynthesis is regulated and coordinated with other cellular processes. In both *Haematococcus pluvialis* and *Chromochloris zofingiensis,* expression of genes in the astaxanthin pathway is activated by elevated concentrations of reactive oxygen species (ROS) **[114][115]**. Studies of these astaxanthin-producing algae also found a strong link between astaxanthin biosynthesis and accumulation of neutral lipids **[115][S25]**. In both species, genes involved in neutral lipid production were up-regulated under astaxanthin-inducing conditions; astaxanthin was often esterified and deposited into lipid bodies and lipid synthesis inhibitor also suppressed accumulation of astaxanthin. The conversion of chloroplast-bound ß-carotene to astaxanthin, which is synthesized on ER surface **[118]** and stored in cytosolic lipid droplets, implies an involved plastid-cytosol translocation step of ß-carotene, though the exact mechanism has still not yet fully elucidated.

2.4. Astaxanthin production of *Chlamydomonas reinhardtii*

ß-carotene ketolase is the key enzyme in the biosynthesis of ketocarotenoids. In 2005, Lohr et al. discovered for the first time the sequence of a ß-carotene ketolase homolog in *Chlamydomonas* genome. This finding came as a surprise, since for a long time it was generally assumed that *Chlamydomonas reinhardtii* did not produce astaxanthin or any other ketocarotenoids and thus had no need for a ß-carotene ketolase. Termed CrBKT, this protein shared 70% identity and 85% similarity with the ß-caroten ketolases from *Haematococcus pluvialis* **[96]**. Subsequent functional analysis of heterologously produced CrBKT in *E. coli* confirmed its activity: in *E. coli* cells, CrBKT was able to convert ß-carotene to canthaxanthin and zeaxanthin to astaxanthin almost quantitatively **[117]**. In both cases, only small amounts of mono-ketolated intermediates (echinenone and adonixanthin) were detected, implying that CrBKT was able to ketolate both ionone rings (i.e. a diketolase). Results of functional assays in *E. coli* were corroborated by studies in plants, in which CrBKT was produced in chloroplasts of *Arabidopsis thaliana* **[117]**, tobacco (*Nicotiana tabacum)* **[119]**, tomato (*Solanum lycopersicum)* **[120]** and rice (*Oryza sativa)* **[121].** The results were significant accumulation of astaxanthin and other ketocarotenoids, products from ketolation of photosynthetic carotenoids, and the reddening of plant tissues. These bodies of evidences support the conclusion that CrBKT is a diketolase capable of processing different carotenoids with high efficiency.

Repeated attempts however failed to detect astaxanthin and other carotenoids in *Chlamydomonas* cells, under both nutrient-replete and nutrient-limited conditions (that normally would trigger

ketocarotenoid accumulation in both *Haematococcus pluvialis* and *Chromochloris zofingiensis*) **[96]**. So where is astaxanthin? Turns out that scientist had been looking at the wrong cells. It has been known for a long time that after sexual fusion of two haploid gametes, the *Chlamydomonas* diploid zygotes undergo maturation in dark to the next developmental stage called zygospore – thick-walled diploid resting cells capable of germinating under favourable conditions releasing four haploid daughter cells **[122]**. Dark maturation of zygote to zygospore is accompanied by the change of color from green to orange-red. HPLC analysis by Sonja Werner in her meticulous research revealed drastic changes in the pigment profile, in which chlorophylls were significantly reduced and cells accumulate various ketocarotenoids, among them 4-ketolutein, astaxanthin and canthaxanthin **[123]**. The majority of detected ketocarotenoids was esterified with fatty acids and presumably stored in cytosolic lipid droplets. None of these ketocarotenoids was detected in vegetative cells, gametes or immature zygotes, implying that zygospore is the only developmental stage in which ketocarotenoid accumulation takes place.

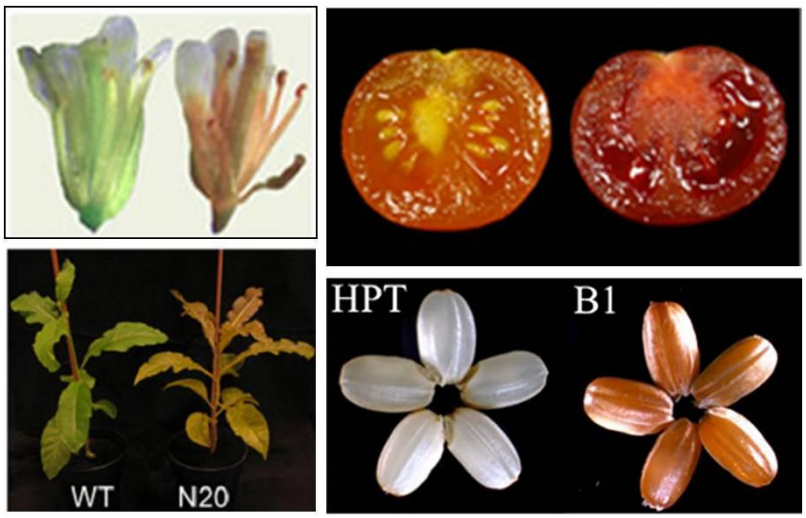

Figure 8: Heterologous production of CrBKT in *Arabidopsis* (upper left), tobacco (lower left), tomato (upper right) and rice (lower right) lead to accumulation of astaxanthin and other carotenoids, resulting in the "reddening" of the plant tissues. Non-transformed plants or plants transformed with the empty vector are shown on the left for comparison. Pictures are collected and combined from cited research papers **[117][119][120][121]**.

Accumulation of ketocarotenoids was also accompanied by increased level of CrBKT transcripts in zygospores **[123]**. It is worth mentioning that production of CrBKT was not completely silent in vegetative *Chlamydomonas* cells. It however does not contradict the fact that no ketocarotenoid was found in vegetative cells. In a similar study *in Haematococcus*, Huang et al. showed that astaxanthin production did not take place until BKT transcripts exceeded the threshold level of 1.6×10^{-6} fmol/ ng total RNA **[124]**.

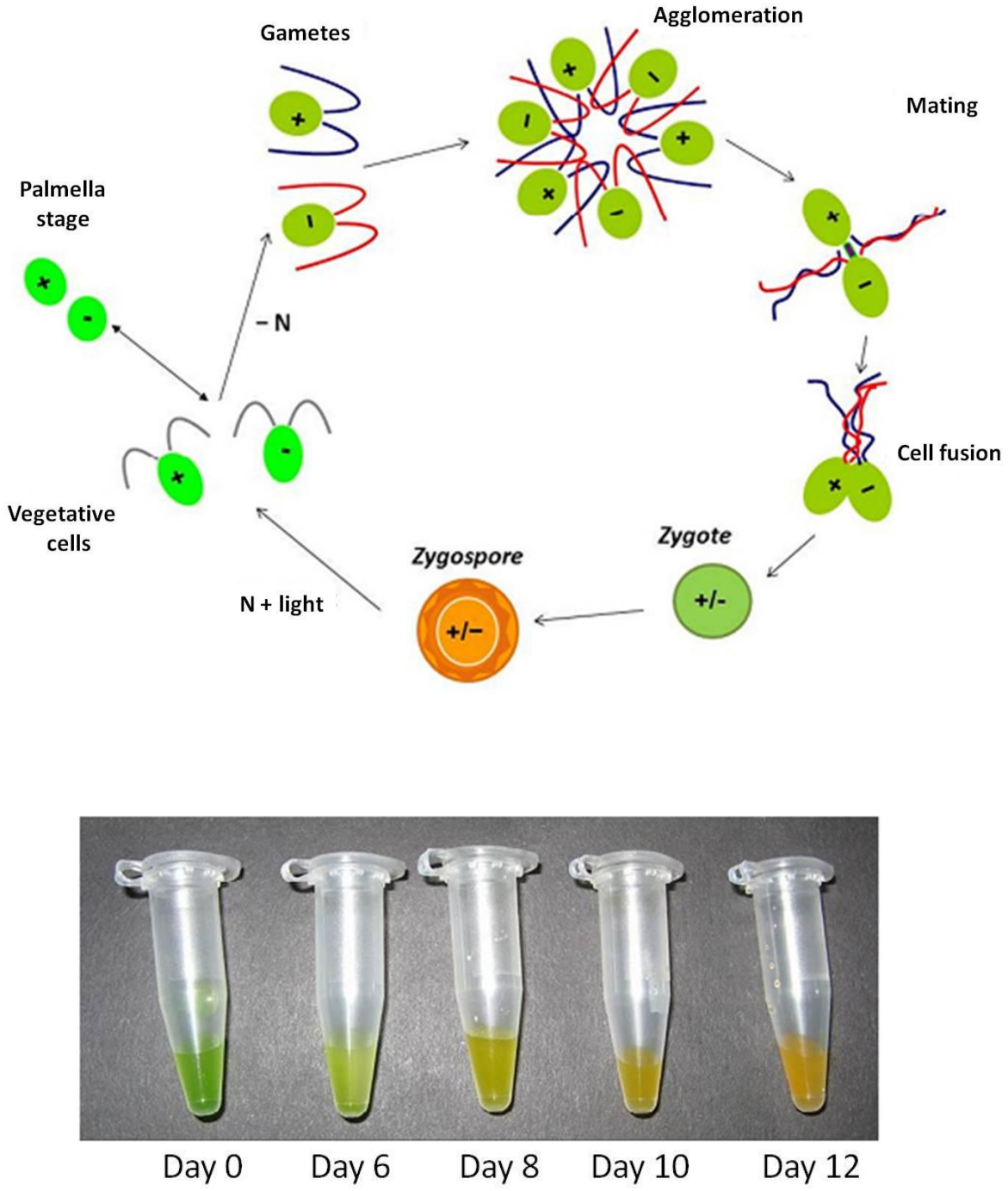

Figure 9: (*Upper*) Schematic of sexual reproduction of *Chlamydomonas reinhardtii*. Gametogenesis took place under nitrogen-limited conditions (-N). Two haploid gametes of opposite mating types (+) and (-) fuse to form a diploid zygote, which matures into zygospore. Under favourable conditions (N + light), meiosis took place releasing four haploid daughter vegetative cells. (*Lower*) Progression of zygote maturation into zygospore from Day 0 to Day 12. The change of colors was caused by degradation of chlorophylls and accumulation of ketocarotenoids. Modified from **[123]**.

2.5. Metabolic engineering of *Chlamydomonas* for astaxanthin production

Astaxanthin is a highly valuable ketocarotenoid which is currently produced on mass scale in the green algae *Haematococcus pluvialis*. As a production species, *Haematococcus* suffers from its slow growth, susceptibility against parasites and high energy demand both for induction of carotenogenesis and for breaking the resistant aplanospore cell walls. Thus it is of great interest to use metabolic engineering to introduce astaxanthin biosynthetic pathway into a more amenable algal species. *Chlamydomonas reinhardtii* appears as a great candidate for this purpose because (1) it is a very well understood model organism with available molecular toolkits and established methods of genetic manipulation and (2) astaxanthin biosynthesis already exists in *Chlamydomonas*, though only limited to zygospore stage. Zygospores, however, are considered unsuitable for astaxanthin production. Though vegetative cells of *Chlamydomonas* do proliferate rapidly under undemanding conditions, these advantages are practically nullified by low efficiency of cell mating (26.4% according to **[123]**, even when using strains considered "high-efficiency mating") and by the sheer length of zygospore maturation (5-6 weeks). The presences of the undesired 4-ketolutein, inevitable side-product from ketolation of lutein, and of the thick zygospore cell wall resistant to mechanical breakage, further lower its value. To address these issues, it is necessary to answer two following questions: (1) how to engineer green vegetative *Chlamydomonas* cells to produce astaxanthin, and (2) how to eliminate undesired side-product 4-ketolutein and increase astaxanthin yield?

The answer to the first question: how to engineer astaxanthin production into green vegetative cells, seems straightforward. Overproduction of a ß-caroten ketolase in the algal chloroplast should theoretically result in ketolation of already existing carotenoids such as ß-carotene, zeaxanthin and lutein, producing canthaxanthin, astaxanthin and 4-ketolutein respectively. Canthaxanthin could also be further hydroxylated by endogenous ß-carotene hydroxylase to astaxanthin. This approach has already been proven in higher plants **[117][119][120][121]**, cyanobacteria **[125]** and microalgae **[126]**. In *Chlamydomonas* however, attempts to overexpress ß-carotene ketolase were met only with limited success. In 2007, Leon et al. over-produced BKT1 from *Haematococcus pluvialis* into Chlamydomonas chloroplast but could detect neither astaxanthin nor canthaxanthin and only a trace amount of 4-ketolutein **[127]**. In a similar study, overproduction of BKT3 from *Haematococcus* and endogenous CrBKT from *Chlamydomonas* in *Chlamydomonas* chloroplast both lead to accumulation of no ketocarotenoid but an unknown chlorophyll-related pigment **[128]**. Among various ketolase, CrBKT is arguably the better choice for production in *Chlamydomonas* due to compatible codon usage and its high activity **[117]**.

The second question could be answered by analysing the carotenoid biosynthetic pathway (**Figure 5**). 4-ketolutein is product from ketolation of lutein, so the logical solution would be the removal of lutein. In *Chlamydomonas*, suppression of lutein production is achieved by the mutation *lor1* in the lycopene ε-cylase gene **[129]**. Zygospore formed from two *lor1* gametes did not produce any 4-ketolutein **[123]**. Another competitive pathway which could potentially lower the astaxanthin yield is the biosynthesis of antheraxanthin, violaxanthin and neoxanthin from zeaxanthin (the xanthophylls cycle). Blocking the xanthophylls cycle lead both to accumulation of zeaxanthin and defective non-photochemical quenching, thus these mutants were called *npq* mutants **[130]**. The triple mutant *npq2-2 nqp1 lor1* was isolated by Baroli et al. in 2003, in which the amounts of accumulated lutein, violaxanthin and antheraxanthin were all drastically reduced **[131]**. This mutant, deposited in the

Chlamydomonas Resources Centre under the name CC-4102, accumulates almost exclusively ß-carotene and zeaxanthin; both could be processed by CrBKT with high efficiency to produce canthaxanthin and astaxanthin, respectively. For this reason, strain CC-4102 represents itself as an excellent candidate for metabolic engineering of astaxanthin biosynthetic pathway.

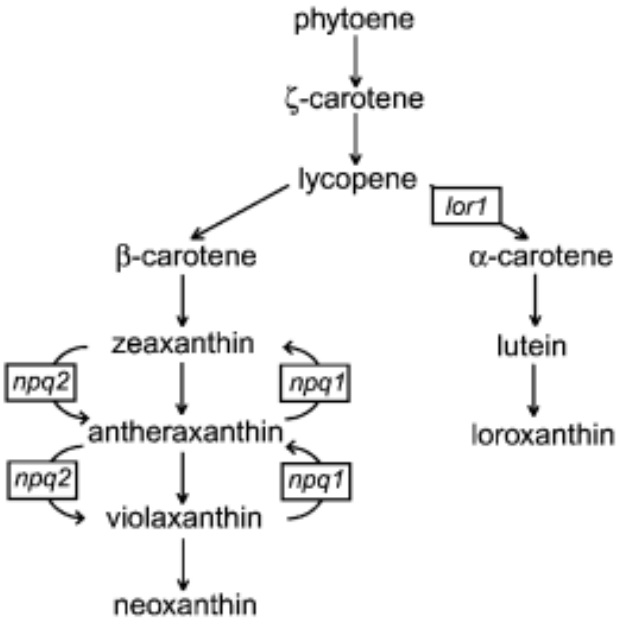

Figure 10. Mutations in both the α-carotene branch (*lor1*) as well as in the xanthophylls cycle (*npq2, npq 1*) result in accumulation of ß-carotene and zeaxanthin in strain CC-4102. Modified from **[131]**

3. Aims of the study

In this project, I aimed to engineer ketocarotenoid production into *Chlamydomonas* green vegetative cells by over production of its endogenous ß-carotene ketolase CrBKT. Two strains of *Chlamydomonas* were chosen for the experiment: strain UVM-4 which produced transgene with high efficiency **[73]** and strain CC-4102 which accumulated ß-carotene and zeaxanthin, both excellent substrates for CrBKT. The expression of CrBKT is to be driven by the strong constitutive promoter HSP70A-RBCS2 **[58]** and coupled with the selection marker through a 2A sequence **[46]**, which should improve both transgene expression and transgene stability. These elements represented some of the best tools for genetic modification of *Chlamydomonas reinhardtii* up-to-date.

Successfully transformed cells should be carefully screened both for production of the protein of interest as well as for production of new ketocarotenoids. Influences of CrBKT production on cell physiology should also be investigated in details.

Results of these experiments would provide useful clues for further researches on astaxanthin metabolic engineering in *Chlamydomonas reinhardtii*.

II. MATERIALS AND METHODS

1. Materials

1.1. Strains

Two *Chlamydomonas* strains were used in this project. Strain UVM-4, described in **[73]** was kindly provided by Professor Dr. Ralph Bock, Max-Planck-Institut für Molekulare Pflanzenphysiologie in Potsdam, Germany. It was a daughter strain of CC-4350 (*cw15 nit1 nit2 arg7-8 mt+*) but no longer required arginine for growth due to earlier plasmid complementation. Strain CC-4102 (genotype *npq2-2 npq1 lor1 arg7 mt+*), described in **[131]**, was purchased from mutant library of Chlamydomonas Resources Centre (CRC), University of Minnesota, United States.

Escherichia coli strain DH5α (*fhuA2 lac(del)U169 phoA glnV44 Φ80' lacZ(del)M15 gyrA96 recA1 relA1 endA1 thi-1 hsdR17*) was used throughout the project.

1.2. Growth media

E. coli cells were grown in LB medium with vigorous shaking (140 rpm) at 37^0C.

LB medium	
Yeast extract	10 g/L
NaCl	5g/L
Tryptone	10 g/L

Chlamydomonas cells were grown in TAP medium with moderate shaking (90 rpm) at room temperature. Light was provided by cold fluorescent tubes. Light intensity measured at the bottom of the flask was 60-80 µE/m^2.s.

TAP medium	
Tris base	0.02 M
TAP salts	25 mL/ 1L
Phosphate solution	380 µL/ 1L
TAP trace elements	1 mL/ 1L
Concentrated acetic acid	1.1 mL/ 1L
pH	6.8

Stock solutions of TAP salts and phosphate solution were mixed as follows and stored without being autoclaved at 4^0C until use. For preparation of trace element solution, first EDTA was dissolved in hot water (60-80^0C) then pH was adjusted to 5.0 with KOH. Trace metals were subsequently added. The finish solution was left at 4^0C for several weeks until its color changed to dark red, at which point it was filtered and stored in plastic container at 4^0C until use.

TAP salts (stored at 4^0C)	
NH_4Cl	15 g/L
$MgSO_4.7H_2O$	4 g/L
$CaCl_2.{}_2H2O$	2 g/L

Phosphate solution (stored at 4^0C)	
KH_2PO_4	288 g/L
K_2HPO_4	144 g/L

TAP trace elements (stored at 4^0C)	
$Na_2EDTA.2H_2O$	50 g/L
$ZnSO_4.7H_2O$	22 g/L
H_3BO_3	11.4 g/L
$MnCl_2.4H_2O$	5 g/L
$FeSO_4.7H_2O$	5 g/L
$CoCl_2.6H_2O$	1.6 g/L
$CuSO_4.5H_2O$	1.6 g/L
$(NH4)_6MoO_3$	1.1 g/L

For cultivation of heterotrophically grown cells (i.e. in dark), yeast extract and tryptone were added to TAP medium at concentration of 0.3% and 0.2% respectively. For preparation of agar plate, agar-agar (Carl-Roth) was added prior autoclaving at concentration of 1.5%. Antibiotics or L-arginine were added after autoclaving to desired concentration.

1.3. Plasmids

Several plasmids were used in this project were either purchased, kindly provided by my collaborator – Dr. Jürgen Breitenbach, University Frankfurt; or cloned by myself. The complete list of plasmids could be seen follows. References to purchased/ donated plasmids are shown on the right.

List of plasmids		
CrBKT CDS plasmid	provided by Dr. Jürgen Breitenbach (Uni Frankfurt)	**[120]**
pACCAR 16 Δ*crt*X	provided by Dr. Jürgen Breitenbach (Uni Frankfurt)	**[111]**
pACCAR 25 Δ*crt*X	provided by Dr. Jürgen Breitenbach (Uni Frankfurt)	**[111]**
pBluescript SK(+)	routine cloning plasmid	
pBluescript KS(+)	routine cloning plasmid	
CrBKT pBluescript KS(+) (CrBKT pBSK)	generated by myself	
CrBKT-mCherry pBluescript KS(+) (CrBKT-mCherry pBSK)	generated by myself	
mCherry-CrBKT pBluescript KS(+) (mCherry-CrBKT pBSK)	generated by myself	
pBR9 mCherry	purchased from Chlamydomonas Resources Centre	**[87]**
pBR32 psaD mCherry	purchased from Chlamydomonas Resources Centre	**[87]**
pChlamy4	purchased from Thermo Fisher	**[132]**
pBR32 psaD CrBKT-mCherry	generated by myself	
pBR32 psaD CrBKT	generated by myself	
pChlamy4 CrBKT 6xHis	generated by myself	

1.4. Primers

All primers used for this project were ordered from Sigma-Aldrich, dissolved in PCR-grade water to concentration of 100 µM and stored at -20^{0}C. The complete list of primers could be found below:

Number	Name	Sequence
389	Shorty	ACC AGC CC
390	Longo	GTA ATA CGA CTC ACT ATA GGG CAC GCG TGG TCG ACG GCC CGG GCT GGT
1147	AP1	GTA ATA CGA CTC ACT ATA GGG C
1148	AP2	TGG TCG ACG GCC CGG GCT GG
1476	EcoRI-mCherry-fw	AAAA GAATTC ATG GTG TCC AAG GGC GAG
1477	HindIII-mCherry-re	AGAG AAGCTT CTT GTA CAG CTC GTC CAT GC
1478	HindIII-psaD-for	ATCG AAGCTT ATG GCC GTC ATG ATG CGC ACC
1479	Ble2A for	GAC CAG GTG GTG CCG GAC AAC ACC
1480	Ble2A rev	TTG CTC TCC ACG TCG CCC GCC AGC TTC
1481	XbaI-6xHis-rev	AGAG TCTAGA TTA GTG GTG GTG GTG GTG GTG ACC
1486	KpnI – mCherry - fw	AAAA GGTACC A ATG GTG TCC AAG GGC GAG
1487	SalI – mCherry – rev	AAAA GTCGAC CTT GTA CAG CTC GTC CAT GC
1488	SalI – CrBKT – fw	AAAA GTCGAC ATG GGC CCT GGG ATA CAA CCC ACT TCC G
1489	HindIII – CrBKT TAA – rev	AAAA AAGCTT TTA CGC CAG GGC TGC GCC GCG
1490	KpnI – CrBKT - fw	AGTC GGTACC A ATG GGC CCT GGG ATA CAA CCC ACT TCC G
1491	SalI – CrBKT – rev	AAAA GTCGAC CGC CAG GGC TGC GCC GCG
1492	SalI – mCherry – fw	AAAA GTCGAC ATG GTG TCC AAG GGC GAG
1493	HindIII – mCherry TAA – rev	ACTG AAGCTT TTA CTT GTA CAG CTC GTC CAT GC
1500	XhoI- mCherry-fw	AAAA CTCGAG ATG GTG TCC AAG GGC GAG GAG G
1501	BclI-CrBKT-TAA-rev	AAAA TGATCA TTA CGC CAG GGC TGC GCC
1502	XhoI-CrBKT-fw	AATA CTCGAG ATG GGC CCT GGG ATA CAA CC
1503	BclI-mCherry-TAA-rev	AAAA TGATCA TTA CTT GTA CAG CTC GTC CAT GCC
1534	XbaI-CrBKT TC rev	AAAA TCTAGA GA CGC CAG GGC TGC GCC
1535	EcoRI psaD for	ATCG GAATTC ATG GCC GTC ATG ATG CGC ACC
1536	XbaI – mCherry TC rev	CGAT TCTAGA GA CTTGTACAGCTCGTCCATGCC
1563	Ble-GSP1	GCC ATA TGC ATG GCC ATC
1564	AR1-GSP2	CGC ACC AAT CAT GTC AAG CCT CAG CG
1565	V5-GSP3	CTGGGCCTGGACAGCACC
1566	3UTR-GSP4	GGCGGGCTGGGCGTATTTGAAGCG

1.5. Carotenoid standards

Carotenoid standards of ß-carotene, zeaxanthin, astaxanthin, canthaxanthin, antheraxanthin, violaxanthin, lutein, neoxanthin were purchased from CaroteNature GmbH (Switzerland), dissolved in *tert*-butyl methyl ether (MTBE) to concentration of 100 mg/L and stored at -20^{0}C until used.

1.6. Antibiotics

Following antibiotics were used for the experiments

List of antibiotics		
Name	**Stock concentration**	**Working concentration**
Ampicillin	100 mg/mL	100 µg/mL
Chloramphenicol	34 mg/mL	34 µg/mL
Zeocin	25 mg/mL	10 and 20 µg/mL

2. Methods

2.1. Determination of cell growth

E. coli cell growth was monitored by measuring the optical density at 600 nm. Growth of *Chlamydomonas* was monitored either by measuring the optical density at 680 nm or through cell counts. Determination of cell counts was performed with the Countess II Automated Cell Counter (Thermo Fisher) according to the manufacturer's instructions. Reliable data were obtained between the OD values of 0.1 to 1 and between cell counts from 10^4 to 10^7 cells /mL. If OD/ cell count were outside these thresholds, sample had to be diluted/ concentrated.

For measuring growth rate, frequent and accurate register of OD under stringently controlled growth conditions is required. Therefore, for determination of algal growth rate I used Multi Cultivator MC1000 (Photo Systems Instruments). It was a photobioreactor system designed for lab-scale cultivation of algae and phototrophic bacteria. The core of the system consisted of eight identical test tubes made of glass serving as growth chambers. Illumination was provided by arrays of cool white LEDs capable of changing both light intensity and colors. Test tubes were immersed in thermostated water bath to maintain constant temperature. Mixing was achieved by air bubbling. Culture's optical densities at two wavelengths, 680 and 720nm, were automatically and periodically measured and documented. Calculation of the growth rate is demonstrated in Section 2.7.

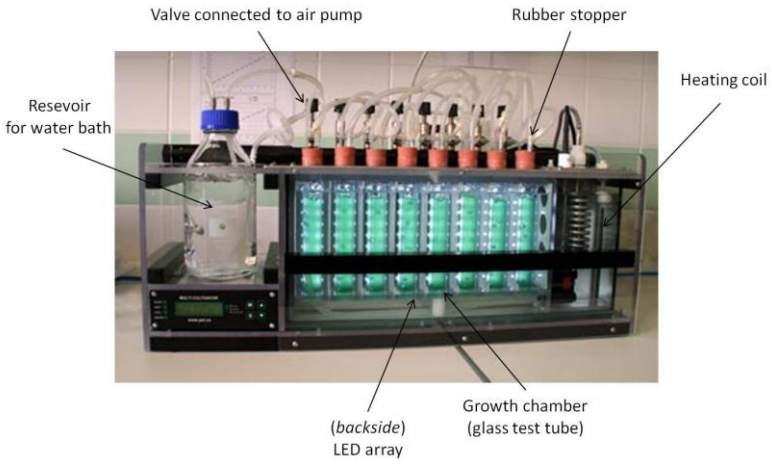

Figure 11: MC1000 Multi Cultivator system. Picture courtesy of Photo Systems Instruments

2.2. Works with DNA

2.2.1. Plasmid minipreparation

- Grow cells overnight with appropriate antibiotic
- Harvest cells from 1.5 mL overnight culture by centrifugation at 13,000 rpm, RT for 30 sec
- Remove the supernatant and add another 1.5 mL overnight culture. Repeat the harvesting step
- Centrifuge shortly to collect all liquid medium at the bottom of the tube and remove it completely
- Add 300 µL of cold P1 buffer containing RNase A (100 mg/L). Resuspend cell thoroughly
- Add 300 µL P2 buffer, mix by gently inverting tube (8 times)
- Add 300 µL of cold P3 buffer, mix by inverting. White precipitate should appear.
- Incubate tubes on ice for 10 min
- Spin down tubes for 10 min at 13,000 rpm, RT
- Transfer 750 µL clear supernatant to fresh tube
- Add 750 µL isopropanol 100%. Mix well
- Centrifuge at 13,000 rpm, RT for 10 min
- Remove the supernatant and wash pellets with 1 mL ethanol 70%
- Centrifuge again at 13,000 rpm, RT for 5 min
- Remove ethanol. Spin down the tubes shortly to collect all liquid at the bottom and remove it completely
- Air-dry the pellet for no more than 5 min
- Resuspend the pellet in 30-50 µL ddH_2O
- (optional: reconstitute DNA by incubation at 37^{0}C for 1h)

P1 buffer
50mM Tris/HCl (pH 8) 10mM EDTA 100µg/mL RNase I, freshly added

P2 buffer
200 mM NaOH 1% SDS

P3 buffer
3M potassium acetate pH 5.5

2.2.2 Extraction of genomic DNA from Chlamydomonas (according to Gernot Gloeckner, University of Freiburg)

- Harvest cells from 2-5 ml of a dense grown culture and spin it down in 2 ml Eppendorff tubes at 3000 rpm, RT, 5 min. Wash cell pellet once with dH_2O
- Resuspend the pellet in 500 µl of CTAB-Buffer.

CTAB buffer
2% (w/v) Cetyl trimethylammonium bromide
100 mM Tris-HCl, pH 8
1,4 M NaCl
20 mM EDTA (pH 8)
2 % (v/v) beta-Mercaptoethanol (freshly added)

- Incubate the solution at 65 degree C for 1 h.
- Add 500 µl of phenol/chloroform/isoamylalcohol (25:24:1), mix well
- Transfer the upper phase to new fresh tube and wash twice with 500 µL chloroform. Collect the upper (aqueous) phase.
- Precipitate DNA with 0.7 volumes of isopropanol for 15 min at 4^0 C. Spin down at 13000 rpm for 20 min, 4^0C. Wash the DNA pellet with 70% ethanol
- Dissolve DNA pellet in dH_2O
- Treat gDNA sample with RNase A overnight, RT to eliminate RNA
- Store gDNA sample at 4^0C / dispense into small aliquots and freeze at -20^0C

2.2.3. DNA electrophoresis

DNA was separated in 0.8% TAE-agarose gel. For loading DNA samples into gel, a 5x concentrated loading buffer was used. Electrophoresis was performed at constant voltage of 80-110V. DNA bands were visualized by ethidium bromide.

TAE electrophoresis buffer (50x concentrated)	
Tris base	242 g/L
Concentrated acetic acid	57.1 mL/ 1L
EDTA	0.5
pH	8.0

5x DNA loading buffer
2% Ficoll
0.5% SDS
50mM EDTA
0.2% Orange G
10% Glycerol

2.2.4. DNA quantification

DNA was quantified either by photometric measurement or by band densitometry (i.e. measurement of band density) after electrophoresis. Photometric measurements involved measuring sample's absorbance at 260nm on WPA Biowave S2100 UV/Vis Diode Array Spectrophotometer; DNA concentration was calculated by photometer's built-in software. In band densitometry, the to-be-quantified band was compared with band of comparable size from DNA markers, which were loaded and ran on the same gel. Measurement of band density was carried out with ImageJ software. Circular DNA was to be linearised prior to electrophoresis by restriction digestion.

2.2.5. Restriction digest

Restriction digest of DNA was performed as recommended by restriction enzyme's manufacturer. For complete digestion of large amount of DNA, reaction time was extended to overnight (16-18h). After digestion, restriction enzymes were removed by Nucleospin Gel and PCR clean up kit (Macherey Nagel) or heat-inactivated as recommended by manufacturers. The following table lists all restriction enzymes used in the project, their manufacturers and reaction temperatures.

Restriction enzyme		
Name	**Manufacturer**	**Reaction temperature**
*Bam*HI	Thermo Fisher	37^0C
*Bcl*I	Thermo Fisher	50^0C
*Eco*RI	Thermo Fisher	37^0C
*Eco*RV	Thermo Fisher	37^0C
*Hind*III	Thermo Fisher	37^0C
*Kpn*I	Thermo Fisher	37^0C
*Nru*I	Thermo Fisher	37^0C
*Pvu*II	Thermo Fisher	37^0C
*Sal*I	Thermo Fisher	37^0C
*Sca*I-HF	New England Biolabs	37^0C
*Xba*I	New England Biolabs	37^0C
*Xho*I	New England Biolabs	37^0C

2.2.6. Cloning

All plasmids generated during the project were created by classic cut-and-ligation cloning. Briefly, backbone and insert fragments were digested with appropriate restriction enzymes to generate sticky ends. After restriction enzymes were removed or heat-inactivated, ligation took place in presence of T4 ligase (Thermo Fisher). Ligation mixtures were used to transform chemically competent *E. coli*. Surviving colonies were first screened by colony PCR, from those which were positive plasmids were isolated and further confirmed with both restriction assays and PCRs.

2.2.7. Polymerase chain reaction (PCR)

PCR reaction mixture (total volume: 25 µL)	
PCR-grade water	19 µL
10x DreamTaq buffer containing 25 mM $MgCl_2$	2.5 µL
dNTPs (25mM each)	0.5 µL
DreamTaq polymerase (0.5 U/µL)	1 µL
Forward primer (10 mM)	0.5 µL
Reverse primer (10 mM)	0.5 µL
DNA template (10-50 ng DNA)	1 µL

Thermocycler's temperature settings		
1. 95^0C	5 min	
2. 95^0C	30 sec	30 cycles
3. T_m - 5^0C	30 sec	
4. 72^0C	varied	
5. 72^0C	7 min	
6. 4^0C	∞	

Notes:

- Preparation of template: as a rule of thumb, plasmid DNA from minipreparation was diluted 1:10 or 1:50 before it was used as template for PCR. For colony PCR, template was prepared by resuspending a medium size colony in 11 µL ddH_2O. 10 µL would be used for PCR, while the remaining 1 µL was put on a LB-selection plate and grown for several hours/ overnight.
- Melting point (T_m) of a primer was estimated by many online tools such as North-western University's Oligocalc (http://biotools.nubic.northwestern.edu/OligoCalc), the free software Serial Cloner or NEB's T_m calculator (http://tmcalculator.neb.com). For DreamTaq polymerase, elongation time (step 4) was estimated using the thump rule of 1 min/ 1kb DNA length
- For difficult PCR (GC-rich templates or primers with high secondary structures, such as *Chlamydmonas* genomic DNA), DMSO was added to the reaction mixture to concentration of 5%.
- When fidelity was important (e.g. for cloning purpose), high-fidelity Q5 DNA polymerase (New England Biolabs) was used in lieu of DreamTaq polymerase. Protocols followed NEB's recommendation.

2.3. Works with proteins

2.3.1. Protein extraction

- Harvest cells by centrifugation (1 mL of overnight grown E. coli or 1 x 10^7 *Chlamydomonas* cells). Wash cell pellet once with 1 mL of ddH_2O
- Resuspend cells in 60 µL extraction buffer

Protein extraction buffer
50 mM Na_2HPO4
1 mM EDTA
5% glycerin
pH 7.5
1x cOmplete protease inhibitor cocktail
(Sigma Alrich) – freshly added

- Add a small amount of acid-washed glass beads (∅ 0.5mm)
- Break cells with BioZym's BeadBlaster24: 4 x 15 sec (100% power – 7 m/s), with 60 sec pause in between
- Add 20 µL of 4x protein loading buffer, mix well but avoid creating air bubbles

4x protein loading buffer
0.25M Tris/HCl pH 6.8
8% SDS
40% Glycerin
0.2 M DTT
0.01% bromophenol blue

- Incubate samples at room temperature for 2-3h. This step was necessary to solubilise very hydrophobic proteins such as CrBKT **[109]**
- Remove insoluble materials by centrifugation. Collect the protein samples into new tubes and store at -20^0C until use.

2.3.2. SDS – polyacrylamide gel electrophoresis (SDS-PAGE)

Proteins were separated on standard Laemmli polyacrylamide gel **[133]** at constant current of 20 mA/ gel. After electrophoresis, protein bands were visualized by Coomassie Brilliant Blue R-250 staining. Gel was immersed in staining solution (1.5 mg/mL CBB, 50% v/v methanol, 10% v/v acetic acid) and shaken for one hour at RT. Staining solution was decanted and gel was subsequently destained in destaining solution (30% v/v methanol, 10% v/v acetic acid) for several hours or overnight. Destaining process could be accelerated by briefly boiling the stained gel in ddH2O in microwave before adding destaining solution. Once protein bands were clearly visible, gels were photographed.

Laemmli polyacrylamide gel		
	Stacking gel	**Separation gel**
AA/BAA (37.5 : 1)	4%	13.3 %
Tris/ HCl	125 mM	375 mM
SDS	0.1 %	0.1%
TEMED	0.08 %	0.033 %
APS	0.05 %	0.05 %
Bromophenol blue	0.00025 %	_
pH	6.8	8.8

1x Laemmli running buffer
3 g/L Tris base
144 g/L glycine
0.1% SDS

2.3.3. Western blot

V5-tagged proteins were detected by immunoblotting. Main steps of this procedure were: protein transfer, blocking, apply of primary antibody, apply of secondary antibody and development.

a) Protein transfer: Protein transfer was performed with the tank-blot system (Bio-Rad). After electrophoresis, the gel was taken out and washed in transfer buffer (10 mM CAPS/NaOH, pH 11) for 10 minutes at RT. Meanwhile, an 8 x 6 cm piece of PVDF membrane was activated by immersing in methanol for 15 seconds, washing briefly with deionized water and finally incubated in transfer

buffer for 5 minutes. Transferring clamp was assembled by sandwiching gel and membrane between several sheets of Whatman paper (3 on each side) soaked in transfer buffer. It was then inserted to blotting tank with gel facing cathode and membrane facing anode. The tank was filled with transfer buffer and protein transfer took place overnight under constant voltage of 30 V at 5^0C (cold storage room). A small stirring rod was also added to the tank to keep the solution well-mixed and thus the electric current relatively constant.

On the following day, the membrane was removed from blotting sandwich, washed briefly with methanol for 10 seconds and then kept under PBS-T (PBS/ 0.5% Tween 20).

b) Blocking: Blocking solution was prepared by resuspending 250 mg skimmed milk powder in 5 mL PBS-T. By applying blocking solution on the protein-side of the membrane, any potential unspecific binding site was blocked. Blocking took place for 2.5-3 hours at RT or alternatively over night.

c) Apply of primary antibody: After blocking, the membrane was taken out and placed between two normal plastic sheets to form an *ad hoc* incubation bag. The bag was heat-sealed on three sides and solution of primary antibody (mouse anti-V5 IgG, 1:500 diluted in blocking solution) was applied on the protein-side. The bag's remaining opening was subsequently heat-sealed as well, forming a water-tight incubation chamber. After one hour, the bag was cut open, primary antibody removed and the membrane washed with PBS-T (once with 10 mL PBS-T for 30 minutes, then twice with 5 mL PBST-T for 10 minutes). Primary antibody was frozen at -20^0C and could be reused several times.

d) Apply of secondary antibody: Secondary antibody solution (alkaline phosphatase conjugated anti-mouse IgG (whole molecule) antibody) was prepared by diluting stock solution 30,000-fold with PBS-T. It was then added onto the membrane's protein side and incubated for 40 minutes under shaking. After this period of incubation, the membrane was washed once with 10 mL PBST-T for 20 minutes, then once again with 10 mL PBS-T for another 10 minutes.

e) Development: Membrane was washed twice with 10 mL assay B buffer (20 mM Tris/HCl pH 9.8, 10 mM $MgCl_2$) for 10 minutes. The membrane was again sealed in another plastic incubation bag containing 5 mL of staining solution (165 µg/mL 5-bromo-4-chloro-3-indolyl phosphate and 330 µg/mL nitroblue tetrazolium in assay B buffer) and incubated over night at 4^0C. Reaction was stopped by washing the membrane in ddH_2O. Positive bands were stained dark purple on the membrane.

2.3.4. In-gel fluorescence detection

Since proteins were not completely denatured by heating to 95^0C, it was still possible to detect fluorescence from mCherry and mCherry-tagged proteins in polyacrylamide gel. In-gel fluorescence detection of mCherry was carried out with AI600 Imager System (GE Healthcare). Measurements settings are listed in Section 2.5.

2.4. Transformation protocols

2.4.1. Transformation of chemically competent E. coli

Preparation of chemically competent E. coli cells with $CaCl_2$ method

- Inoculate 3 ml LB medium (+ corresponding antibiotic) with a colony or a piece of glycerin culture and incubate overnight at 37°C, 180 rpm.
- Inoculate 50 ml LB medium (+ corresponding antibiotic) with 1 ml of the overnight tube culture. Incubate at 37°C and 180 rpm until OD_{600} is 0.4 (around 2 hours).
- Leave the cells in ice for 10 minutes.
- Centrifuge 5 minutes at 3000 rpm and 4°C
- Resuspend carefully the pellet in cold 20 ml 50 mM $CaCl_2$.
- Incubate in ice for 30 minutes.
- Centrifuge 5 minutes at 3000 rpm and 4°C
- Resuspend the pellet (should be white) in 3 ml of 50 mM $CaCl_2$ plus 15% glycerin.
- Prepare 250 µl aliquots and store at -80°C.

Heat-shock transformation of chemically competent E. coli

- Thaw chemically competent cells on ice. Start experiment right after the last ice crystal disappears.
- Disperse 100 µL competent cells into pre-chilled 1.5 mL Eppendorf tubes
- Add DNA (0.5 - 1 µL for plasmid DNA, 5 - 10 µL for ligation mixture), mix by swirling gently
- Incubate on ice for another 30 min
- Heat shock at 42^0C in water bath for exactly 45 sec
- Immediately put the tubes back on ice and let them recover for 2 min
- Add 400 µL SOC medium to each tube. Mix by inverting
- Incubate on rotary shaker for 1h at 37^0C
- Plate cells (50 & 200 µL) on selection plates. Incubate plates at 37^0C over night.

SOC medium
2% bactotryptone
0.5% yeast extract
10 mM NaCl
2.5 mM KCl
10 mM $MgCl_2$
10 mM $MgSO_4$
20 mM glucose (autoclaved separately)

2.4.2. Transformation of cell-wall-less Chlamydomonas UVM-4 cells with glass beads

- Inoculation of *Chlamydomonas* seed culture (500 mL TAP in 1L Erlenmeyer flask) with a pea-sized cell pellet (∅ 4mm) from agar plate (~ 3 week old). Flask was shaken at 90 rpm, RT under cold fluorescent light (~ 60 µE/m^2.s, 24/24h)
- After 3 days, cell density reached ~ 1.0 x 10^6 cells/ mL (see **Fig. 12a & b**). Cells were then sub-cultured into two 100 mL cultures (20 mL seed culture + 80 mL fresh TAP medium in 1L Erlenmeyer flask, initial cell density 2 x 10^5 cells/mL) and shaken under the same conditions (**Fig.12c & d**) for another 2 days.

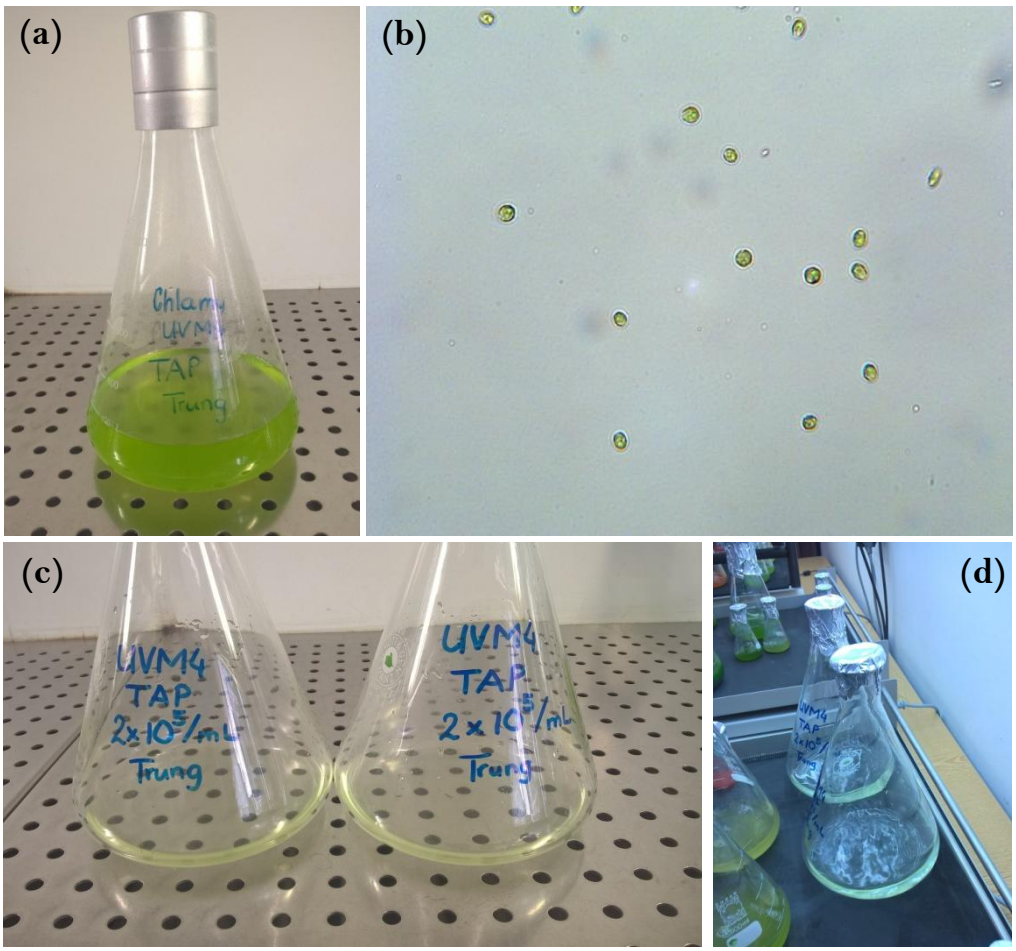

Figure 12: (a) First seed culture after 3 days of cultivation. Cell density was estimated at 1.0 x 10^6 cells/mL. (b) Microscopic picture of cells from seed culture (400x magnification). (c) Seed culture was diluted 1:5 with fresh TAP medium and shaken further for another 2 days on a rotary shaker (d).

- Cell density reached ~ 1.0 x 10^6 cells/ mL over night. 100mL fresh TAP medium were added to bring cell density down to 5.0 x 10^5 cells/mL
- Plasmid was prepared by minipreparation (alkaline lysis protocol) from 16 mL overnight E. coli liquid culture. DNA was precipitated by isopropanol and dissolved in total of 80 µL ddH_2O. The whole batch was linearized with ScaI-HF (NEB) in total reaction volume of 100 µL at 37^{0}C, overnight.

- On the day of transformation, cell density reached 2.4 x 10^6 cells/ mL (**Fig. 13a&b**).

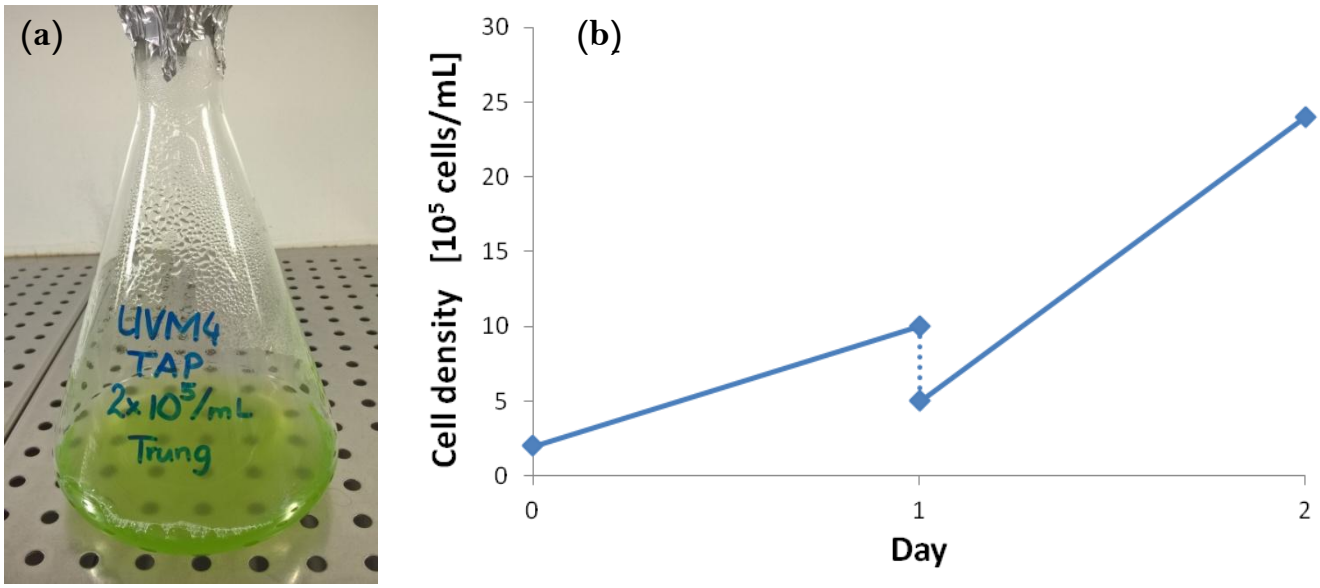

Figure 13: (a) After 2 days of cultivation, Chlamydomonas liquid culture reached cell density of 2.4 x 10^6 cells/mL and was used for transformation. (b) Growth curve during cultivation

- Plasmid linearization was verified by gel electrophoresis and linearized plasmid was purified by gel excision with Macherey Nagel's Nucleospin Gel and PCR clean up kit. DNA was eluted from column with 50 µL ddH2O. DNA concentration was estimated via photometric measurement at 500 ng/ µL. 10 µL DNA (5 µg) were used for each transformation.
- 300 mg of acid-washed glass beads (∅ 0.5mm) were weighted and autoclaved in 2mL Eppendorf reaction tube.
- Cells from 100 mL culture were harvested by centrifugation (2500 rpm, 5 min, RT) and resuspended in 1mL TAP medium (cell concentration 2.4 x 10^8 cells/mL)
- 20% PEG-6000 solution was freshly prepared and sterile by passing through Roth's 0.22µm-pore membrane.
- To each tube following was added sequentially:
    - 300 µL cell suspension (7.2 x 10^7 cells)
    - 10 µL DNA (5 µg)
    - 100 µL freshly prepared PEG-6000 20% (final concentration 5%)

  Mixtures were gently mixed by swirling with the pipette tip.

- The tubes were vortexed on Vortex Mixer (Neolab) at ca. 3000rpm for exactly 15 sec.
- Cells were washed off glass beads with TAP medium and collected in total 10 mL TAP medium in 25mL Erlenmeyer flasks. All recovery cultures were gently shaken (90 rpm) at ~ 60 µE/m^2.s light intensity over night.
- After overnight recovery, 1 mL (1/10 reactions) of recovery suspension was plated out on each ∅ 9cm agar plate (TAP + zeocin) and incubated at 25^{0}C, 20µE/m2.s for 2 weeks.
- For selection under heterotrophic conditions, cells were plated out on TAP + zeocin + yeast extract + tryptone agar plates and incubated dark at 25^{0}C for 3-4 weeks.

2.4.3. Transformation of cell-wall-intact Chlamydomonas CC-4102 cells by electroporation

- Prior to transformation, cells were cultivated similar to UVM-4. A seed culture ((500 mL TAP supplemented with 200 µg/mL L-arginine in 1L Erlenmeyer flask) was prepared by inoculating pea-sized cell pellet (∅ 4mm) from agar plate (~ 3 week old). Flask was shaken at 90 rpm, RT under cold fluorescent light (~ 60 µE/m^2.s, 24/24h). After 3 days, the seed culture was again diluted 1:5 by fresh TAP-arginine medium and grown over night. The following day, culture was once again diluted 1:2 by fresh TAP-arginine medium and grown over night. On the day of transformation, cell density should reach 2-3 x 10^6 cells/mL.
- Cultivation of CC-4102 required supplementation of L-arginine at concentration of 200 mg/L.
- Plasmids were prepared, linearised and concentrated as described earlier.
- Harvest cells from 200 mL culture by centrifugation (2500 rpm, 5 min, RT)
- Resuspend cells in 10 mL MAX Efficiency electroporation buffer (Thermo Fisher) and incubate for 5 min at RT. Harvest cells afterwards by centrifugation (2500 rpm, 5 min, RT)
- Repeat the wash step once more
- Resuspend cells in 2 mL MAX Efficiency electroporation buffer (cell density: 2-3 x 10^8 cells/mL). Disperse cells into several 250 µL aliquots
- Add 10 µL DNA (5 µg) to each aliquot. Mix by swirling and incubate at 4^0C for 5 min
- Chill electroporation cuvettes (4mm, Bio-Rad) on ice
- Transfer cells-DNA mixture to ice-cold cuvettes just before electroporation
- Proceed with electroporation with GenePulser Xcell (Bio-Rad) with the following settings
    - 500 V
    - 50 µF
    - 800 Ω

  With these settings, the time constants (T_m) should be around 50 milliseconds.

- Let the cells to recover at RT for 15 min
- Transfer the cells to 10 mL of TAP - arginine – 40 mM sucrose in 25mL Erlenmeyer flasks. All recovery cultures were gently shaken (90 rpm) at ~ 60 µE/m^2.s light intensity over night.
- After overnight recovery, cells were harvested and resuspended in 10 mL TAP-arginine.
- 1 mL (1/10 reactions) of the cell suspension was plated out on each ∅ 9cm agar plate (TAP + arginine + zeocin) and incubated at 25^0C, 20µE/m2.s for 2 weeks.
- For selection under heterotrophic conditions, cells were plated out on TAP + zeocin + yeast extract + tryptone agar plates and incubated dark at 25^0C for 3-4 weeks.

2.5. Microscopy and fluorescence detection

Bright-field microscopy was performed with Novex Holland BBS 86 microscope. Pictures were recorded by Micam software.

Fluorescence microscopy was performed Leica TCS SP5 II Confocal Microscope. Chlorophyll autofluorescence was recorded at laser excitation of 488 nm, emission 650-700 nm, gain 50. mCherry fluorescence was recorded at laser excitation 561 nm, emission 580-640 nm, gain 200.

Fluorescence detection of colonies on agar plates and of fluorescence protein bands on polyacrylamide gels was performed with AI600 Imager System (GE Healthcare). Settings for detection of chlorophyll autofluorescence were: laser excitation 630 nm, emission filter 705 band pass 40nm; of mCherry were: laser excitation 520 nm, emission filter 605 band pass 40nm.

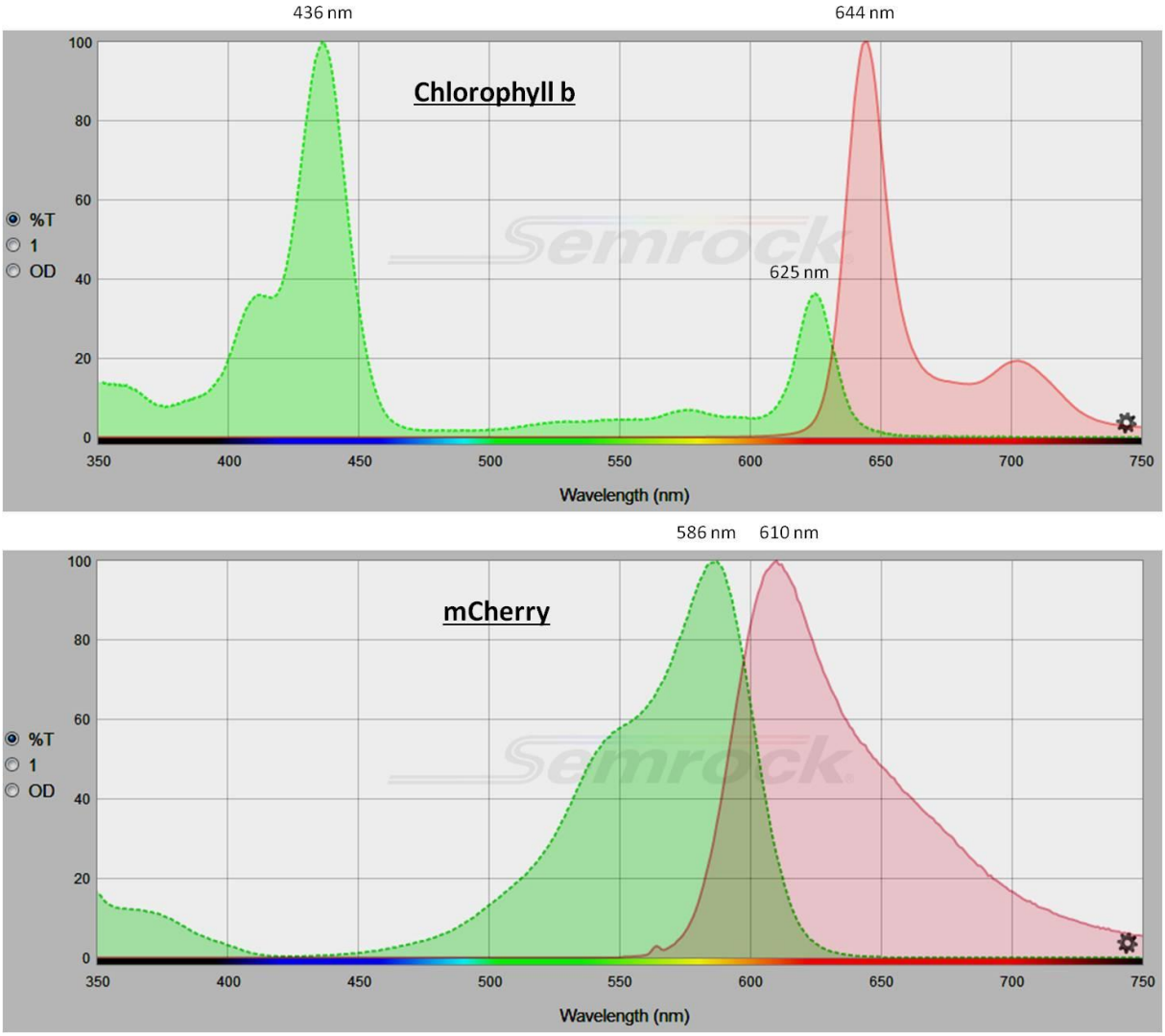

Figure 14: Excitation (green) and emission (red) spectra of Chlorophyll b and mCherry. Fluorescence data from Semrock SearchLight (https://searchlight.semrock.com)

2.6. Pigment analysis

2.6.1. Measurements of chlorophylls and total carotenoids

The protocol based on Lichtenthaler **[134]** provided a quick and reliable method for determination of chlorophyll a, b and total carotenoids concentrations. Cells from 1 mL of dense grown algal culture were harvested by centrifugation (2500 rpm, 5 min, RT). Supernatant was discarded and cell pellet was washed once with 1 mL ddH_2O. 1 mL methanol and 300 mg acid-washed glass beads (∅ 0.5mm) were then added. Cell disruption was achieved with BioZym's BeadBlaster24: 4 x 15 sec (100% power – 7 m/s), with 60 sec pause between cycles. Methanol extract was cleared from cell debris and glass beads by short centrifugation (13,000 rpm, 1 min, RT) and transferred to new fresh tube.

Absorbance at 470, 652 and 665 nm was measured by photometer and concentrations of chlorophyll a, b and total carotenoids were calculated as follows:

c[*Chlorophyll a*] (µg/mL) = $16.72 \times A_{665} - 9.16 \times A_{652}$

c[*Chlorophyll b*] (µg/mL) = $34.09 \times A_{652} - 15.28 \times A_{665}$

$$c[\textit{Total carotenoids}]\ (\mu g/mL) = \frac{1000 \times A470 - c[\textit{Chlorophyll a}] \times 1.63 - c[\textit{Chlorophyll b}] \times 104.96}{221}$$

2.6.2. Pigment extraction

The following protocol was used for extraction of pigments from bacterial and algal samples for analysis with high performance liquid chromatography. All solvents used were of HPLC-grade.

- Harvest cells via centrifugation. Wash cell pellets with ddH_2O.
- Add 300 mg acid-washed glass beads (∅ 0.5mm)
- Add subsequently 200 µL methanol, 200 µL acetone and 200 µL chloroform. After each time a solvent was added, samples were treated with BioZym's BeadBlaster24 (4 x 15 sec -100% power, 60 sec pause in between)
- After three rounds of beads beating, the tubes were centrifuged at 13,000 rpm, 5 min, RT. Clear organic solvent extracts were collected and transferred to new tubes
- Add 1000 µL ddH_2O to the clear extract and centrifuge at 13,000 rpm, 1 min, RT. This step would force methanol, acetone and more polar contaminants into the aqueous (upper) phase, while carotenoids and chlorophylls remained in the chloroform (lower) phase.
- Collect the chloroform phase.
- Dry the solvent at 40^0C under a stream of dry nitrogen gas
- Dissolve the pigments in a small volume of methanol

If saponification was desired, methanol – 0.02M KOH was added instead of methanol. Acetone and chloroform were subsequently added with beads beating in between as described above. The extract was cleared by centrifugation and incubated in dark at 4^0C for 4h. Afterwards, water was added and samples were treated in the same manner as described above.

2.6.3. High performance liquid chromatography (HPLC)

Pigment analysis was performed with reversed phase HPLC. Important components of the HPLC system (Agilent 1100 Series) were:

- *Injector:* was carried out automatically by G1329A Autosampler module (Agilent). Pigment samples were contained in 2mL screw cap glass vials with septa.
- *Pumps:* The HPLC system was equipped with G1312A binary pumps (Agilent). Solvents before entering pumps were degassed by the G1322A degasser unit (Agilent). At the flow rate of 1 mL/min, pressure typically ranged from 9 – 13 MPa.
- *Column:* The heart of the system, the column, was the revesed phase C30 YMC-carotenoid column (YMC, Japan). The column was 250 mm in length, 4.6 mm in diameter with particle size of 5 µm. With much longer chain length than the classical C18 columns, this column was much more hydrophobic and thus better suited for analysis of carotenoids.
- *Detector:* Pigments were detected by their absorbance at 450 nm, measured by the G1314A detector (Agilent). G1314A was a variable wavelength detector capable of monitoring a single (but variable between 190-450nm) wavelength at one time.

For pigment analysis, following program was used based on published protocol of Richins et al. **[135]**. Injection volumes were typically between 5-20 µL. Flow rate was set at 1 mL/min. Mobile phase consisted of a linear gradient from two solvents: Solvent A and Solvent B.

Solvent A	Solvent B
81% (v/v) methanol 15% (v/v) MTBE 4% (v/v) H_2O	8% (v/v) methanol 88% (v/v) MTBE 4% (v/v) H_2O

HPLC program consisted of a linear gradient for 30 minutes followed by wash/ reconditioning steps was as follows:

Time [min]	Solvent A	Solvent B
0	100%	0%
30	33%	67%
31	0%	100%
34	0%	100%
35	100%	0%
39	100%	0%

For detection of carotenoids and chlorophylls, detector was set at wavelength of 450 nm. Measurements of absorption spectra of peaks of interest were performed in the working group of Professor Warzecha, TU Darmstadt with the same setup except for the diode array detector G4212B (Agilent)**.** Absorbance was monitored from 280 to 640nm. Chromatograms were recorded with detection wavelength set at 450 nm and reference wavelength at 570 nm.

2.7. Insertion mapping

Insertion sites of *Chlamydomonas* transformants were mapped with genome walking method as described by Siebert et al. (1999) **[136]** and Pollock et al. (2017) **[137]**. Briefly, genomic DNA was extracted from *Chlamydomonas* transformants and blunt-ended DNA libraries were generated via overnight digestion at 37^0C by a mixture *Eco*RV, *Nru*I and *Pvu*II. A blunt-ended adaptor was prepared by mixing primers 389 and 390 (500 pmol each) in 1x Green buffer (Thermo Fisher), which were then heated to 950C for 10 minutes then allowed to slowly cool down to 4^0C over a time period of two hours (cool down rate 1.5^0C/min). Prior to annealing, primer 389 was phosphorylated for 2h at 37^0C by T4 polynucleotide kinase (NEB) in 1x T4 ligase buffer supplemented with 1mM ATP. Subsequently, adaptor was ligated to the blunt end of DNA fragments by T4 ligase at 16^0C overnight. Ligation mixture consisted of 40 ng digested genomic DNA, 4 µL adaptor, 1 mM ATP, 8 units of T4 ligase (Thermo Fisher) and 1x T4 ligase buffer. The reaction was stopped by heating at 65^0C for 20min and ligation mixtures were diluted 1:10 with dH_2O before they were used as template for PCR.

For amplification of the 5'-upstream- and 3'-downstream flanking sequences of the transgene, two rounds of PCR were required. First round of PCR was performed with an adaptor primer (primer 1147) and a gene-specific primer (primer 1563 or 1565, recognizing *ble* and *V5* sequences respectively). In the second "nested" PCR, PCR products from the first round were diluted 1:50 with ddH_2O and amplified using adaptor primer 1148 and gene-specific primers 1564 (recognizing promoter sequence) and 1566 (recognizing 3'-UTR sequence). For both PCRs, touch-down programs (see below) and high-processivity Taq polymerase (Genaxxon) in reaction buffer S were used. Obtained PCR products were cloned in the EcoRV site of pBluescript II SK(+)via TA cloning (Li et al. 1999) and sent for sequencing at Mycrosynth Seqlab (Göttingen, Germany) using M13 Forward (-20) (TGT AAA ACG ACG GCC AG) or M13 reverse primers (CAG GAA ACA GCT ATG AC). Insertion sites were identified by comparing sequencing data to *Chlamydomonas* genome database of Phytozome (https://phytozome.jgi.doe.gov).

Touch-down PCR protocols for insertion mapping

1st PCR

	Temperature	Time
	94^0C	3 minutes
20 cycles	94^0C	30 seconds
	65^0C -> 51^0C (- 0.7^0C/ cycle)	45 seconds
	72^0C	6 minutes
20 cycles	94^0C	30 seconds
	50^0C	45 seconds
	72^0C	6 minutes
	72^0C	7 minutes

2nd „nested" PCR

	Temperature	Time
	94^0C	3 minutes
20 cycles	94^0C	30 seconds
	72^0C -> 58^0C (- 0.7^0C/ cycle)	45 seconds
	72^0C	6 minutes
20 cycles	94^0C	30 seconds
	58^0C	45 seconds
	72^0C	6 minutes
	72^0C	7 minutes

2.8. Nile Red staining

Nile Red (Sigma Alrich) was dissolved in DMSO to concentration of 1 mg/mL. To stain lipid droplets, Nile Red stock solution was added to algal suspension to final concentration of 0.1 mg/mL and incubated for 10 min. Afterwards the samples were ready for imaging with fluorescence microscope (Leica TCS SP5 II System, Excitation 514 nm, Emission 580-590nm, gain 200). No wash step was necessary because fluorescence of Nile Red was quenched by water.

2.9. Bioinformatic tools

Following bioinformatic tools were used during the project:

- For protein sequence alignment: PRALINE (http://www.ibi.vu.nl/programs/pralinewww/) from University of Amsterdam **[138]**
- For prediction of structure and trans-membrane domains:
  - TMHMM Server v. 2.0 (http://www.cbs.dtu.dk/services/TMHMM-2.0/) from Department of Health and Bio-Informatics, Technical University of Denmark **[139]**
  - PHYRE2 Protein Fold Recognition Server (www.sbg.bio.ic.ac.uk/phyre2) from Imperial College London, UK **[140]**
- For prediction of transit peptides: PredAlgo (https://giavap-genomes.ibpc.fr/predalgo/) from Institut de Biologie Physico−Chimique (IBPC), Paris, France **[141]**

2.10. Data analysis

For determination of growth performance, model of exponential growth was applied. This model was characterised by following equation:

$$N = N_0 e^{\mu t}$$

in which, N is cell quantity, N_0 cell quantity at time point zero, t the duration of cultivation and μ the specific growth rate. In the case of algal growth, N was represented by optical density. The model was only applicable when cells were still in their early *log* phase.

Various statistical analyses (t-test, ANOVA, histogram, normal probability plot) were executed with Microsoft Excel 2007 software.

HPLC peaks were quantified by calculated their area under the curve (AUC). For comparison, chromatograms were normalized between the highest peak (set at 1) and baseline (set at 0).

3. RESULTS

3.1. Comparisons of strains UVM-4 and CC-4102

Two *Chlamydomonas* strains, UVM-4 and CC-4102 were used for my project. Prior to the experiments, two strains were compared with regards to appearance and morphology, growth performance, pigment profile as well as their amenability to different transformation methods.

3.1.1. Appearance and morphology

Strain UVM-4, harboring the mutation *cw-15*, is a cell wall deficient mutant. Under microscope, UVM-4 cells appeared as small green round cells lacking both the proteinous cell wall layer and distinctive flagella. On agar plates, UVM-4 colonies displayed smooth, glossy and shiny surface (**Figure 15**). In liquid cultures, cells did not seem to be actively swimming but moved instead passively around by Brownian motions.

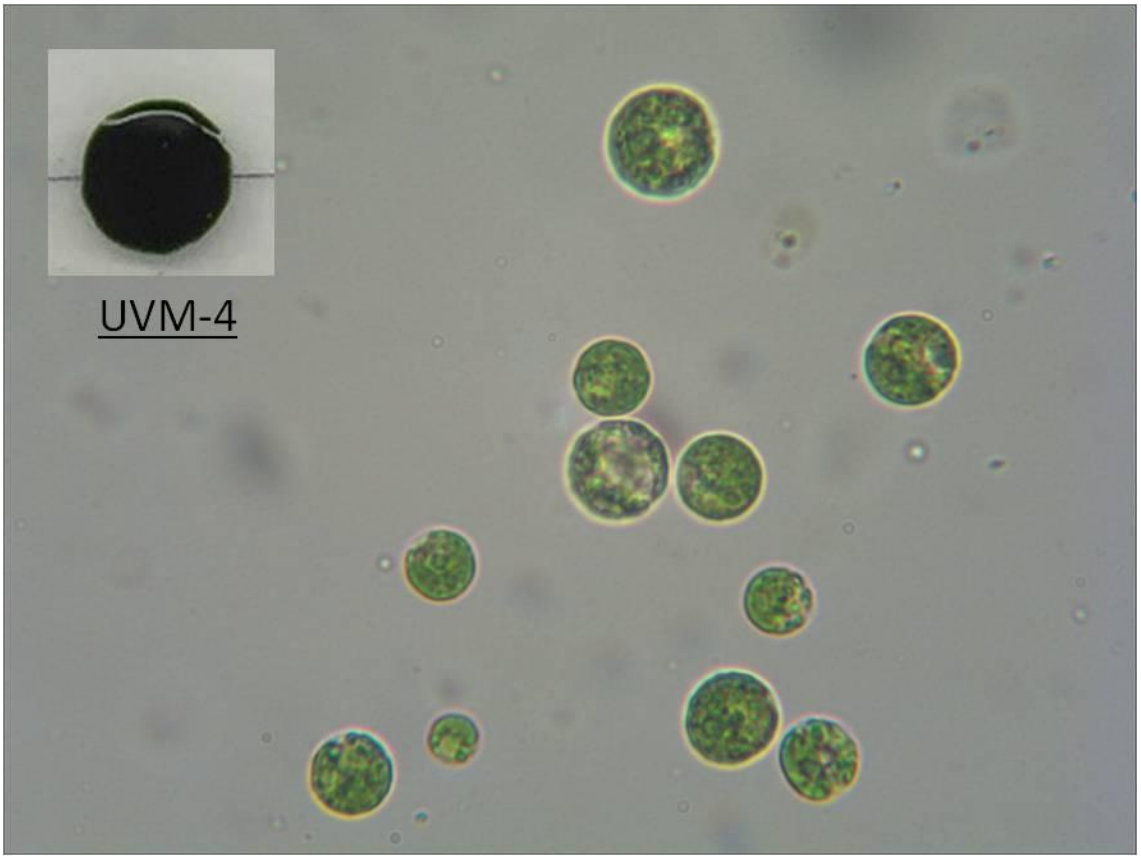

Figure 15: UVM-4 cells under light microscope (1000x magnification).
In the small window is a UVM-4 colony on agar plate.

The strain CC-4102 in contrast, where the cell wall was still intact, displayed quite different morphology. On agar plates, CC-4102 colonies had a rough, dull surface. Under microscope, CC-4102 cells did not appeared individually but as what E. H. Harris **[142]** termed "palmelloid colonies": clusters of four to eight adherent, non-motile, non-flagellated oval cells trapped within a gelatinous mucilage layer. Upon transferred from growth medium to distilled water, small cells rapidly swam out using their two swirling flagella (**Figure 16**).

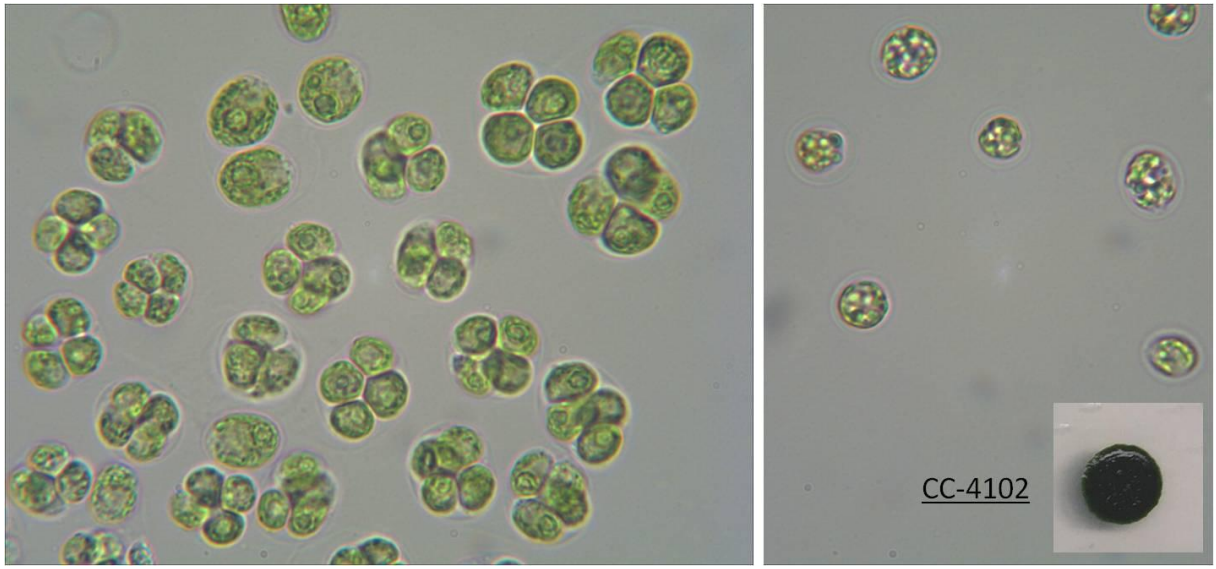

Figure 16: CC-4102 cells under light microscope (1000x magnification): "palmelloid colonies" (left) and actively swimming cells upon transferred to distilled water (right). In the small window is a CC-4102 colony on agar plate.

In both strains, autofluorescence of chlorophylls revealed the characteristic cup-shaped chloroplasts which occupied almost the whole cell volume and enveloped other organelles (**Figure 17**).

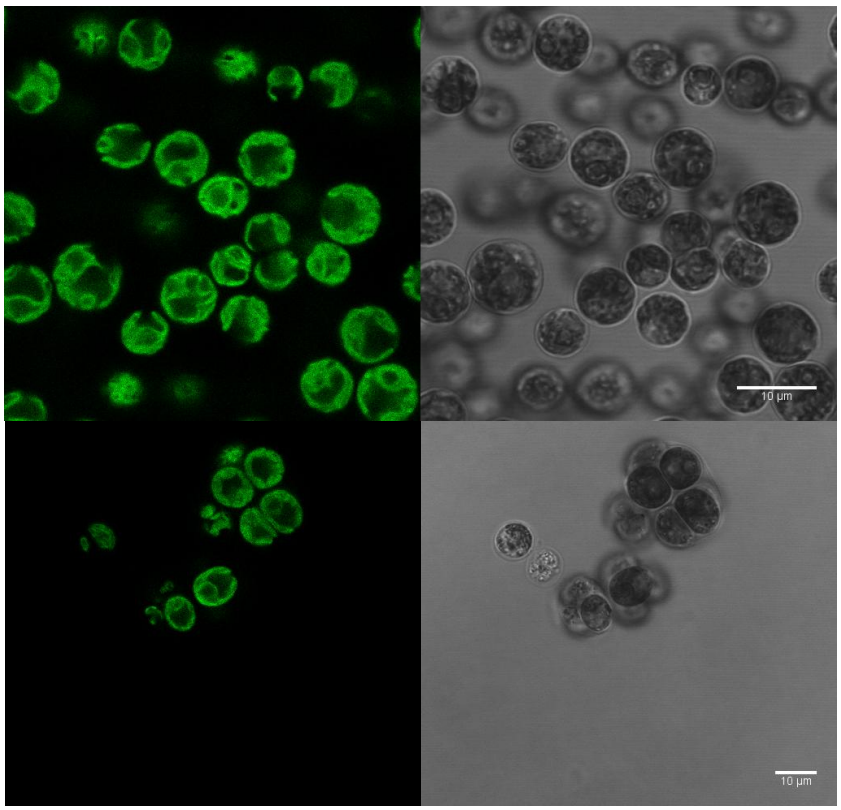

Figure 17: Chlorophyll autofluorescence of strains UVM-4 (upper panel) and CC-4102 (lower panel) revealed the characteristic cup-shaped chloroplasts. On the left are false-colored fluorescence image (excitation: 488 nm, emission: 650-700 nm). On the right are differential interference contrast (DIC) images. Scale bars are 10 µm.

3.1.2. Growth performance

Both strains grew equally well in TAP medium (**Figure 18**), though CC-4102, harbouring the genotype *arg7-8* required supplementation of L-arginine. Specific growth rates (μ) of UVM-4 and CC-4102 under test conditions (TAP-arginine medium, 20^0C, 80μE/m^2.s light 24/24h) were estimated at 1.88 and 1.69 day^{-1}, respectively.

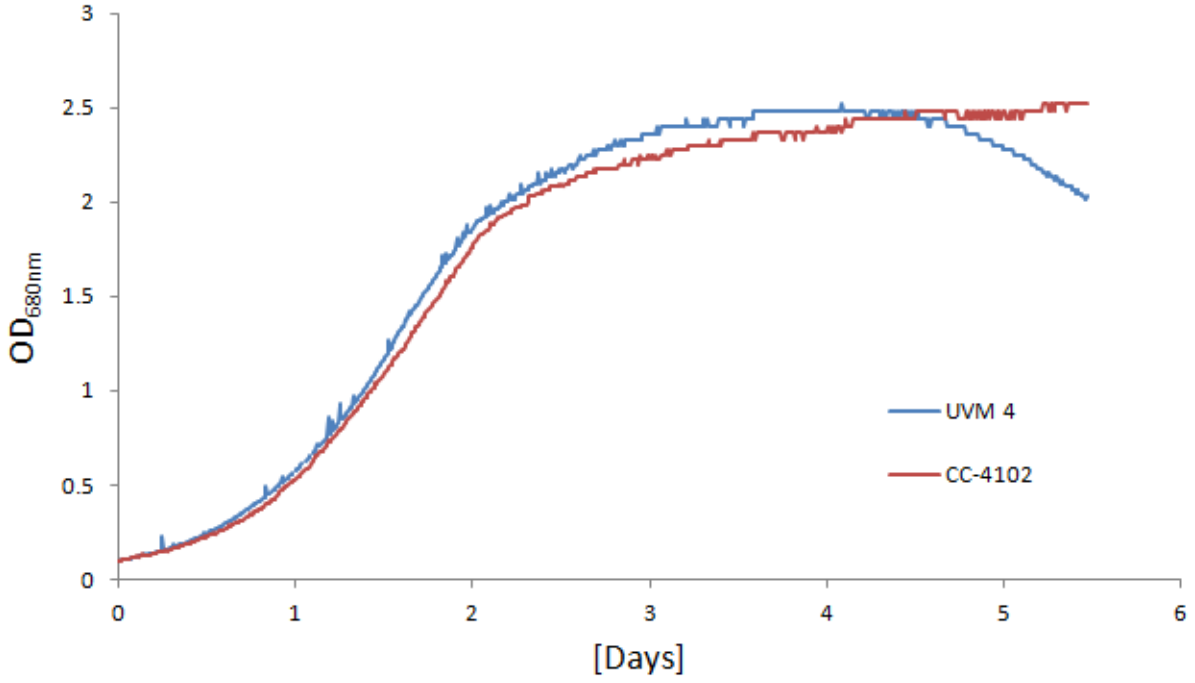

Figure 18: Growth curve of UVM-4 (blue) and CC-4102 cells (red) in TAP medium supplemented with L-arginine (200 mg/L) at temperature of 20^0C and light intensity of 80 μE/m^2.s . On the vertical axis are measurements of culture's optical density at 680nm. Data points were collected automatically by MC1000 system every 10 minutes.

3.1.3. Pigment compositions

Estimation of chlorophylls and carotenoid contents according to Lichtenthaler **[134]** failed to reveal any significant difference between these two strains (**Table 1**). On the other hand, their carotenoid compositions were quite different. The major carotenoids of UVM-4 were loroxanthin, violaxanthin, antheraxanthin, lutein and ß-carotene. On the other hand, in CC-4102 cells, only trace amounts of loroxanthin, violaxanthin and antheraxanthin could be detected, while the concentration of lutein was greatly diminished. In contrast, zeaxanthin was accumulated in great amount and ß-carotene concentration was also increased by 72% (**Figure 19**).

These findings are in good agreement with published results of Baroli et al. 2003 **[131]**

Table 1: Estimated contents of chlorophylls and carotenoid in UVM-4 and CC-4102 cells according to Lichtenthaler method.

	UVM-4	CC-4102
Chlorophyll a	60.61 ± 0.35%	62.73 ± 0.11%
Chlorophyll b	15.01 ± 0.85%	12.35 ± 0.42%
Total carotenoids	24.38 ± 0.52%	24.92 ± 0.31%

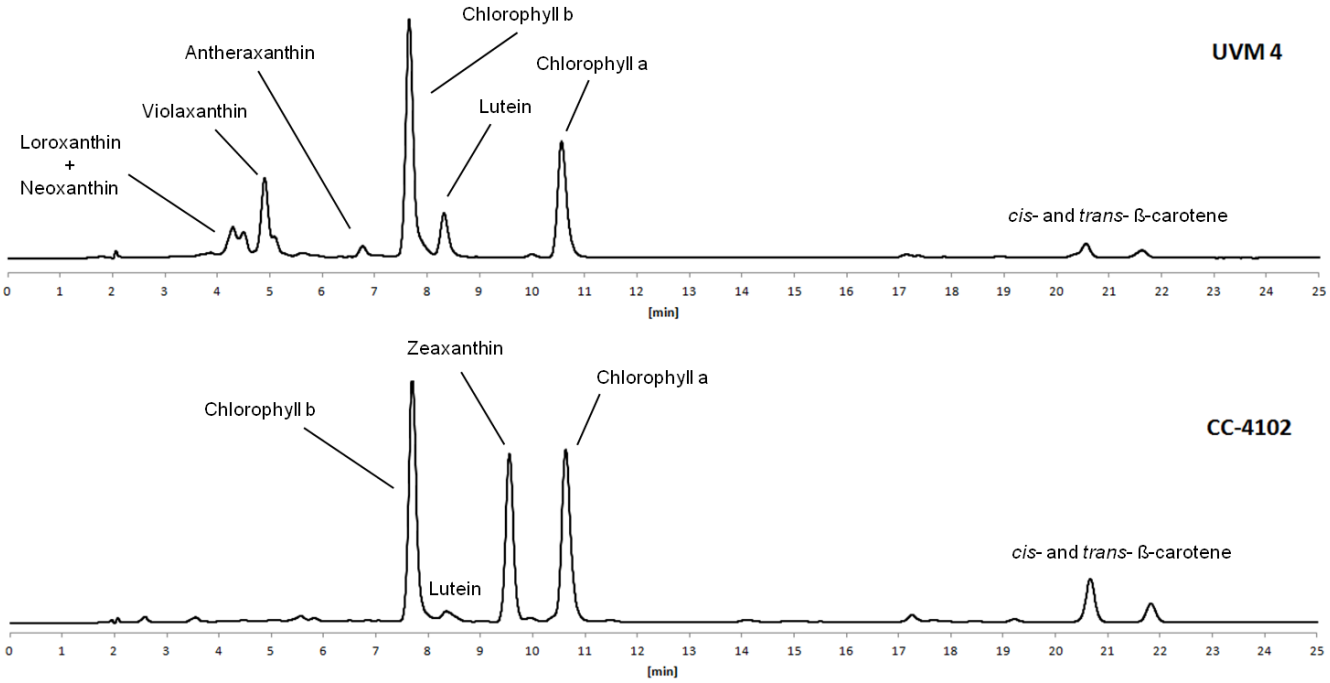

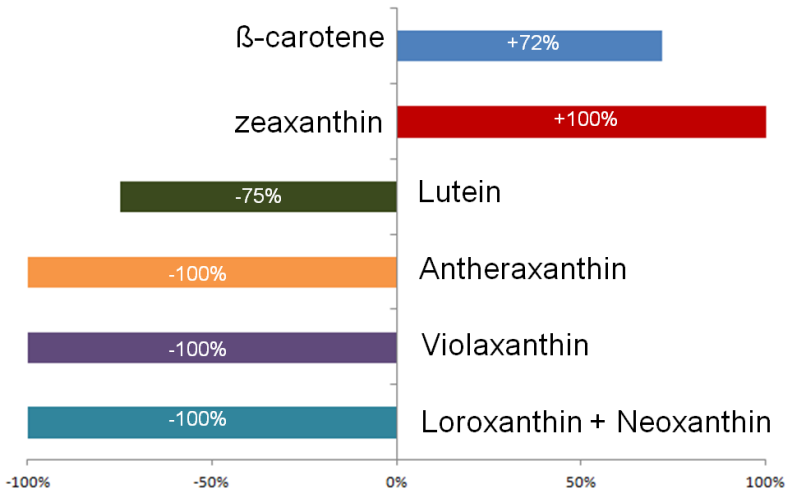

Figure 19: (*Upper*) HPLC analysis of pigments extracted from UVM-4 and CC-4102 cells. (*Lower*) Relative contents (pigment/ chlorophyll a) of carotenoids of strain CC-4102 compared to those of strain UVM-4. A change of ±100% means the complete gain/ loss of the corresponding pigment

3.1.4. Amenability to transformation methods

Several transformation methods such as electroporation, bioballistics, glass beads transformation, etc. are available for *Chlamydomonas reinhardtii*. CC-4102 is not amenable to glass beads transformation due to the presence of the intact cell wall. In a preliminary experiment, it was also discovered that electroporation with cell wall deficient UVM-4 lead to disruption of large number of cells, resulting in low transformation efficiency (data not shown). Thus it was decided that henceforth, UVM-4 would be transformed with glass beads, while CC-4102 were transformed via electroporation.

To test the transformation efficiency as well as the functionality of the Ble2A concept, I transformed both strains with 5 µg of the plasmid pBR9 mCherry **[51]** linearized with *Sca*I. This plasmid harboured an expression cassette containing the bicistronic construct of *ble* selection marker fused to codon-optimized mCherry gene via 2A sequence. Successful transformation was expected to cause accumulation of fluorescent mCherry in the cytosol.

Surviving colonies were selected on TAP-arginine agar plate supplemented with zeocin at concentrations of 10 and 20 mg/L. Results are shown in **Table 2**.

Table 2: Transformation of UVM-4 and CC-4102 with 5 µg pBR9 mCherry

Strains	10 mg/L zeocin	20 mg/L zeocin
UVM-4	102 colonies / 2 plates (102 colonies/ µg DNA)	8 colonies / 2 plates (8 colonies/ µg DNA)
CC-4102	Selection was insufficient	93 colonies / 1 plate (186 colonies/ µg DNA)

Unexpectedly, two strains showed different susceptibility to zeocin. While zeocin killed UVM-4 cells at both concentrations, 20 mg/L was required for effective selection of CC-4102 cells. This discrepancy could be attributed to different morphology and the presence of the cell wall. For following transformations of UVM-4 and CC-4102 cells, it was thus decided that zeocin concentrations of 10 mg/L and 20 mg/L would be used respectively.

Production of mCherry and its variability among transformants were assessed by spotting about 50 independent transformant lines from each strain on a TAP-zeocin plate followed by fluorescence measurements with AI600 fluorescence imager. Under the tested conditions, non-transformed *Chlamydomonas* emitted very weak mCherry fluorescence. Results (**Figure 20**) indicate that mCherry production among transformants varied significantly and seemed to follow the pattern of a normal distribution. 20% of UVM-4 transformants and 76% of CC-4102 transformants displayed higher mCherry fluorescence than non-transformed cells.

Successful mCherry production was also corroborated by the results of in-gel fluorescence detection of mCherry **(Figure 21)** as well as fluorescence microscopy **(Figure 22)**. mCherry was predominantly detected in cytosol, implying efficient cleavage at 2A peptide by *Chlamydomonas* cells.

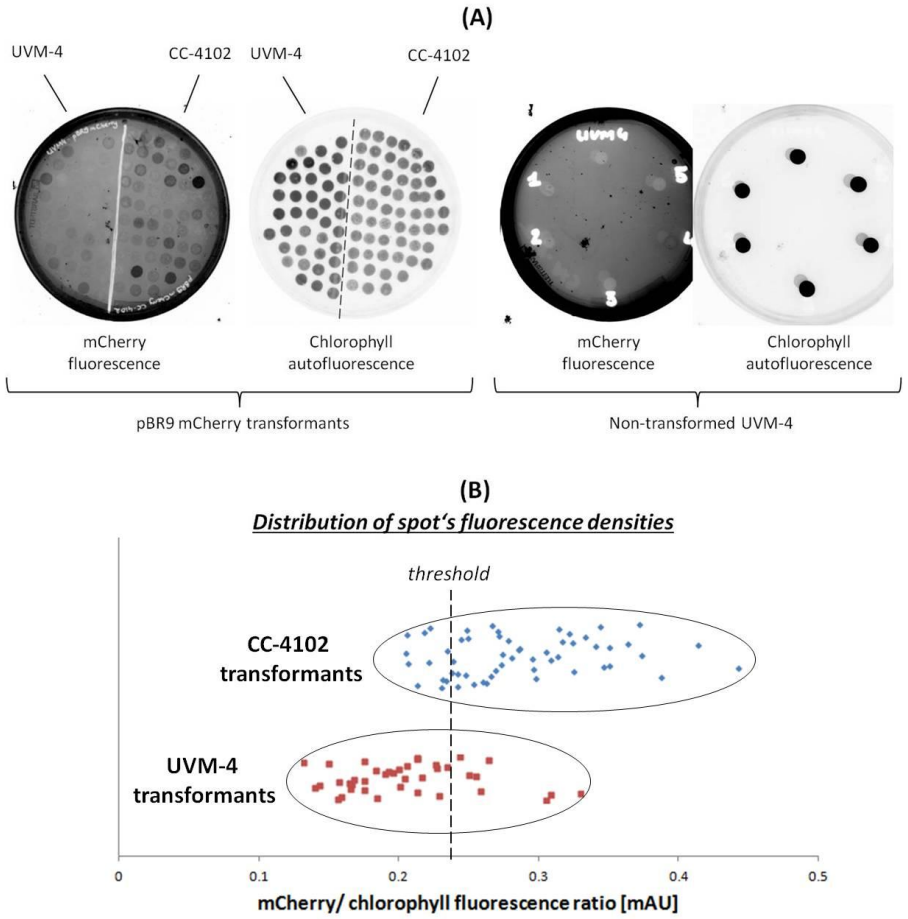

Figure 20: (A) Fluorescence measurements of pBR9 mCherry transformants compared to untranformed cells. UVM-4 transformants were spotted on the left half of the agar plate, CC-4102 transformants on the right half. Darker spots means stronger fluorescence signal. **(B)** Distribution of fluorescence densities (mCherry to chlorophyll signal ratio) among spots as seen in (A). Threshold value (dotted line) was averaged fluorescence density of non-transformed cells plus three times standard deviation.

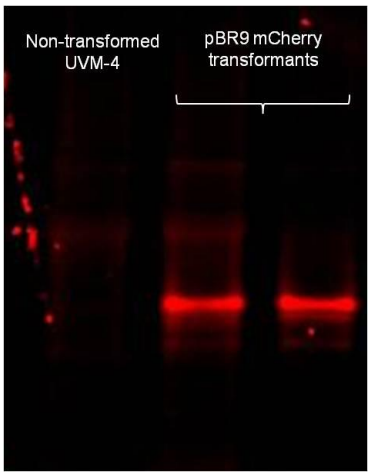

Figure 21: In-gel fluorescence detection of mCherry extracted from non-transformed UVM-4 cells (*left*) as well as from two independent pBR9 mCherry UVM-4 transformants (middle and right). Excitation wavelength 520 nm, emission filter 605BP40

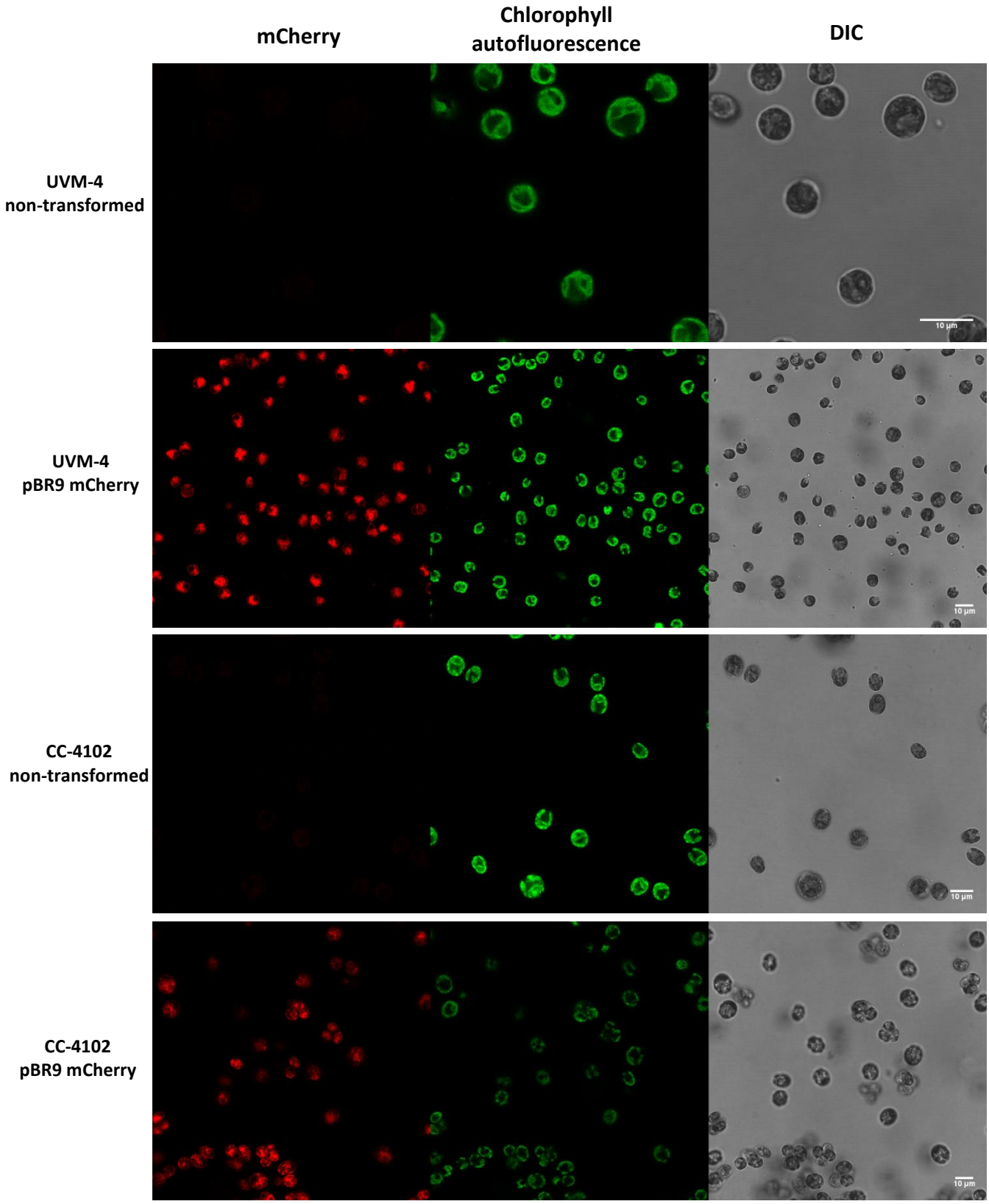

Figure 22: Detection of mCherry (excitation 561nm, emission 580-640 nm) and chlorophyll (excitation 488nm, emission 650-700 nm) fluorescence of pBR9 mCherry transformants. Scale bars are 10 µm.

3.2. Verification of CrBKT's ketolase activity

3.2.1. Protein sequence analysis of CrBKT

Peptide sequence alignment of CrBKT (328 amino acids) with CzBKT from *Chromochloris zofingiensis* (Genbank AY772713.1, 312 amino acids) and three isoforms from *Haematococcus pluvialis* (HpBKT1, 329 amino acids, GenBank: GU143688.1; HpBKT2, 320 amino acids, GenBank: GU143689.1 and HpBKT3, 320 amino acids, GenBank: AY603347.1) revealed a remarkably similarity between these enzymes. Exception was the N-terminus of CrBKT, which contained a completely unconserved sequence - 24 amino acids in length that could not be found in any of the other BKTs.

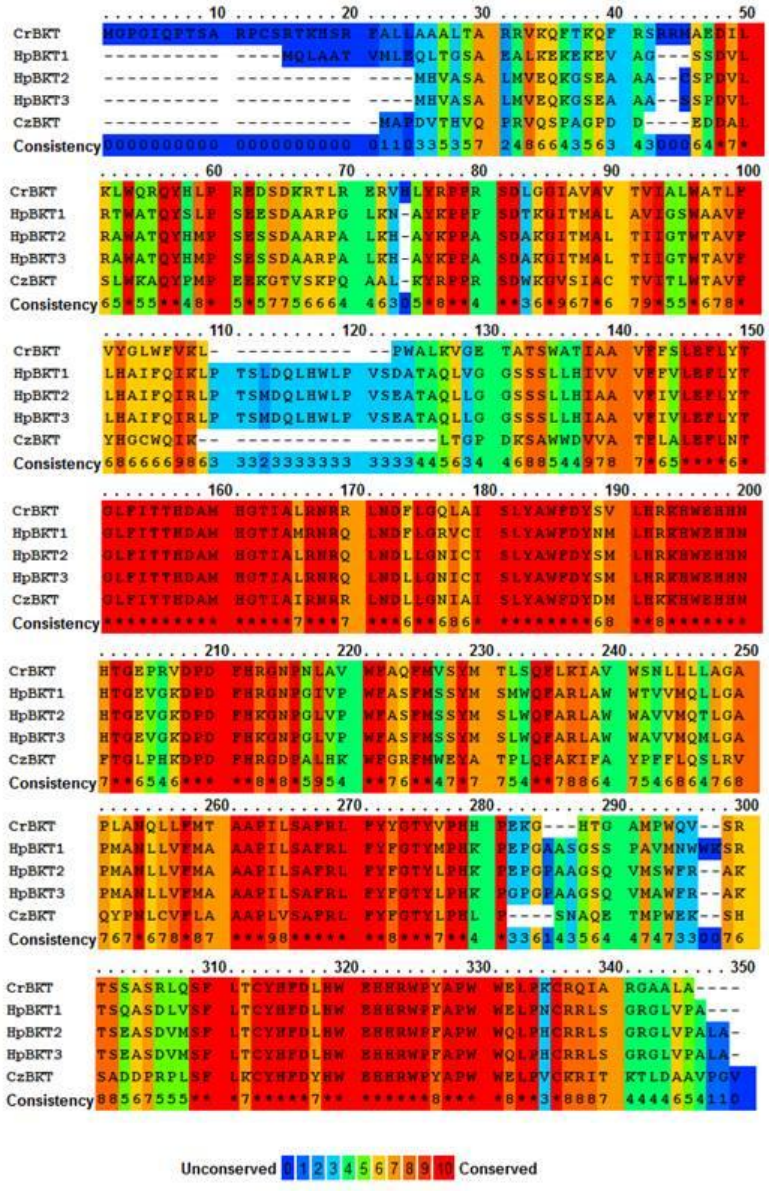

Figure 23: Sequence alignment of CrBKT, HpBKT 1,2,3 and CzBKT. Level of sequence conservation is displayed by color scale in which blue means 0% and red means 100% conversed sequences.

Structural prediction of CrBKT with PHYRE2 and TMHMM showed that it was a very hydrophobic protein with five membrane-spanning helices **(Figure 24)**.

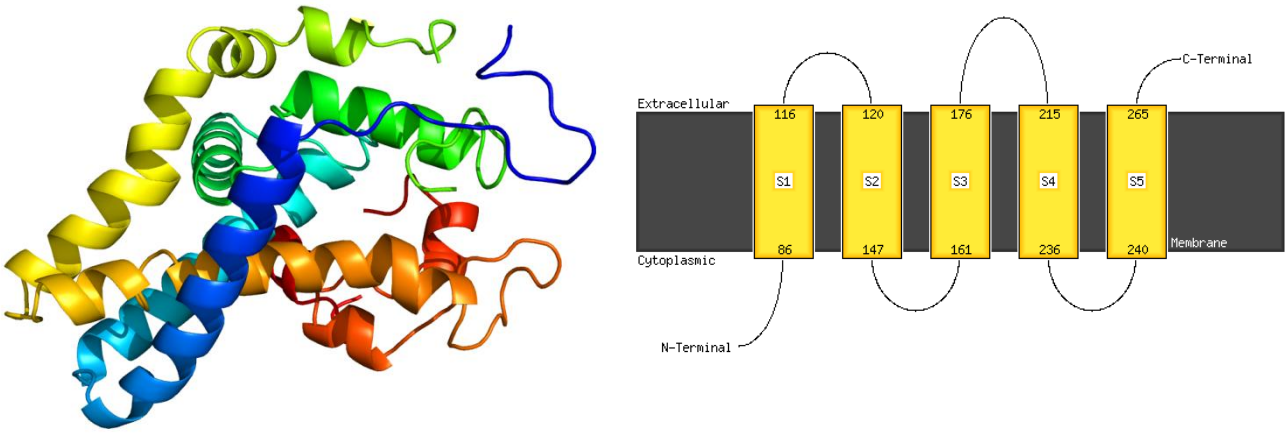

Figure 24: Predicted structure of CrBKT (left) with its five trans-membrane helices (right). N-terminus is colored dark blue, C-terminus dark-red. Predictions were made using PHYRE2 algorithms.

Unexpectedly, the transit peptide-predicting PredAlgo algorithms predicted the presence of a hitherto undiscovered 40 amino-acid-long chloroplastic transit peptide in the sequence of CrBKT. Applying the same algorithms to either CzBKT or HpBKT 1,2 and 3 failed to reveal any transit peptide (**Table 3**), which is in good agreement with published reports of these BKTs being located in cytosol **[109][116]**.

Table 3: PredAlgo predictions for different BKT proteins. C-score represents the likelihood of one protein to be located in chloroplast. Cutoff value for C-score was 0.41

PredAlgo predictions	
Protein	**C-score**
CrBKT	1.0302315
CzBKT	0.0003020
HpBKT1	0.0026631
HpBKT2	0.0033693
HpBKT3	0.0073585

3.2.2. Ketolase activity of CrBKT heterologously produced in E. coli

The plasmid harbouring coding sequence of CrBKT was kindly donated by Dr. Breitenbach, University Frankfurt. The ketolase activity of this acquired CrBKT was verified using *in vivo* assay in *E. coli* described by Zhong et al. **[117]**. In this assay, CrBKT was heterologously produced in carotenoid-accumulating *E. coli* cells. Ketolation lead to changes in carotenoid profile which could be detected by HPLC.

Carotenoid-accumulating *E. coli* were generated by introducing plasmids pACCAR16 Δ*crt*X or pACCAR25 Δ*crt*X **[111]** into cells. These plasmids harboured carotenoid biosynthetic genes from the bacterium *Erwinia uredovora* – *crt*E, *crt*B, *crt*I, *crt*Y and in case of pACCAR25 Δ*crt*X also *crt*Z. Host's farnesyl pyrophosphate (FPP) served as starting substrate. HPLC analysis confirmed the accumulation of ß-carotene and zeaxanthin in pACCAR16 Δ*crt*X and pACCAR25 Δ*crt*X transformants respectively **(Figure 25)**.

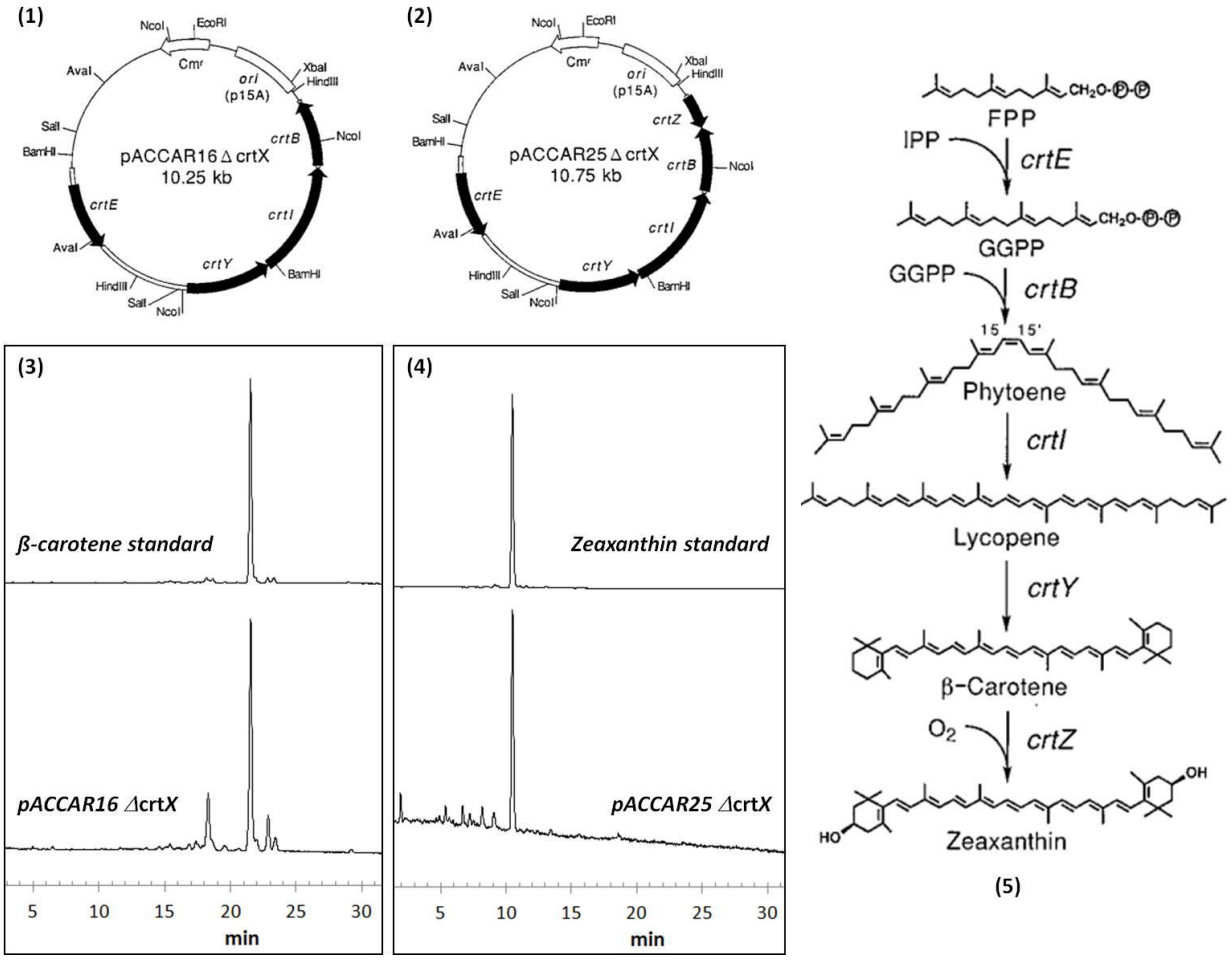

Figure 25: Carotenoid-accumulating *E. coli* strains. (1) & (2): plasmid maps of pACCAR16 ΔcrtX and pACCAR25 ΔcrtX. (3) & (4): HPLC analysis of carotenoids extracted from p pACCAR16 ΔcrtX and pACCAR25 ΔcrtX transformants, in comparison with ß-carotene and zeaxanthin standards. (5): Biosynthetic steps from FPP to ß-carotene and zeaxanthin. (1), (2) and (5) contain modified pictures from **[111]**, (3), (4) are my own analyses. Y-axis (absorbance) of all chromatograms was normalized between 0 and 1. Detection at 450nm.

In the next step, coding sequence of CrBKT was cloned between *Xba*I and *Hind*III sites of pBluescript KS(+) plasmid. The new plasmid, CrBKT pBluescript KS(+) – short CrBKT pBSK, was co-transformed with either pACCAR16 Δ*crt*X or pACCAR25 Δ*crt*X into *E. coli* cells. Expression of CrBKT was driven by *lac* promoter. Co-transformation lead to cell color change from yellow to orange-red. HPLC analyses revealed accumulation of canthaxanthin and astaxanthin – ketolation products of ß-carotene and zeaxanthin (**Figures 26 & 27**). Intriguingly, a small amount of canthaxanthin was also detected in pACCAR25 Δ*crt*X – CrBKT pBSK transformant, indicating that CrBKT and CrtZ competed with each other for usage of ß-carotene as substrate..

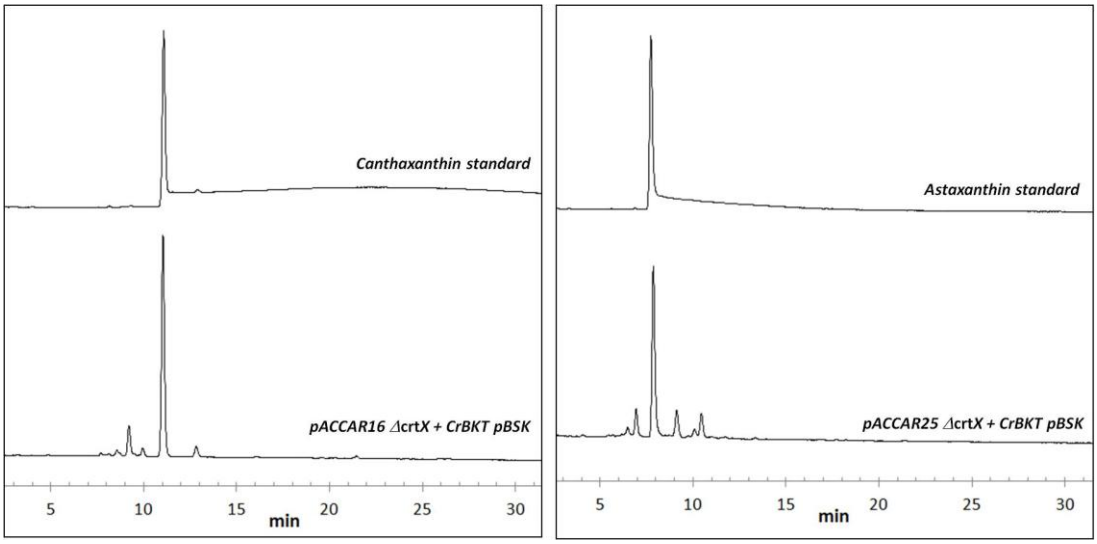

Figure 26: Accumulation of canthaxanthin and astaxanthin in pACCAR16 Δ*crt*X – CrBKT pBSK and pACCAR25 Δ*crt*X- CrBKT pBSK double transformants respecitive. Y-axis (absorbance) of all chromatograms was normalized between 0 and 1. Detection at 450nm.

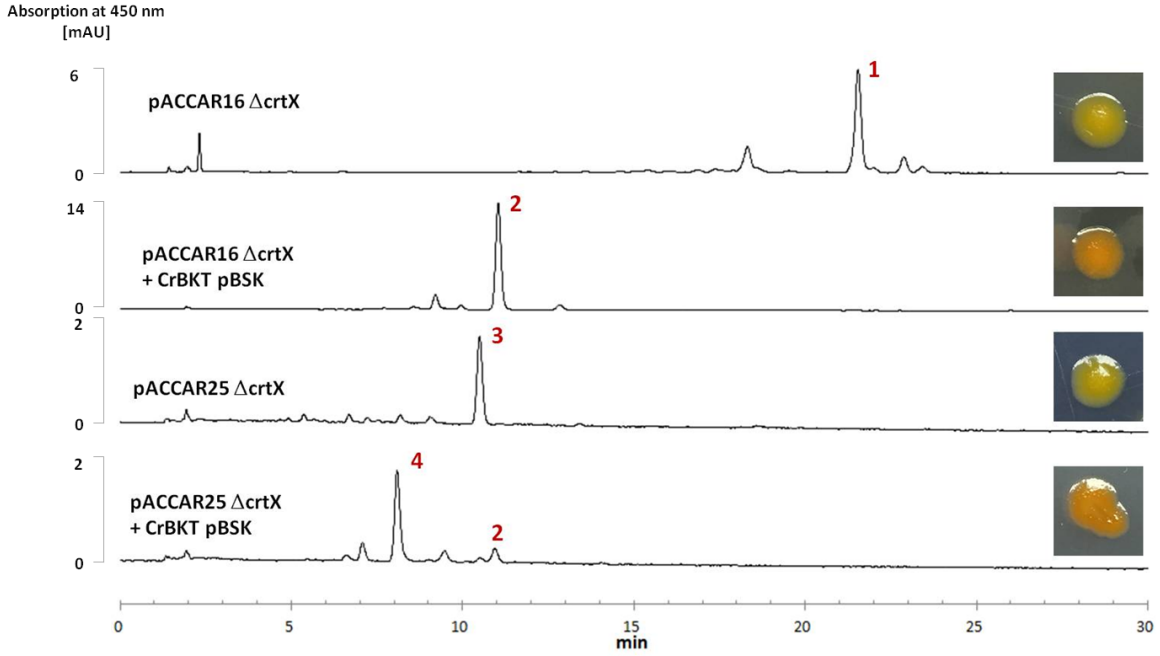

Figure 27: Conversion of ß-carotene to canthaxanthin and of zeaxanthin to astaxanthin when CrBKT pBSK was introduced into carotenoid-accumulating *E. coli* strains. *E. coli* colonies on agar plates are showed in small windows on the left. Pigments: 1 – ß-carotene, 2 – canthaxanthin, 3 – zeaxanthin, 4 - astaxanthin. Y-axis (absorbance) of all chromatograms was normalized between 0 and 1. Detection at 450nm.

3.2.3. Ketolase activities of mCherry-fused CrBKT constructs

It was of great interest to tag CrBKT with a fluorescence protein both for quick quantification of protein production and easier assessment of protein localization. However, tagging a very hydrophobic protein (i.e. CrBKT) with a hydrophilic fluorescence protein could potential lead to misfolding and loss of function. To rule out this contingency, first I assessed the ketolase activities of both N-terminal and C-terminal CrBKT-mCherry fusion constructs using assay method described in previous Section.

N-terminal mCherry-fused CrBKT construct was created by cloning between the *Sal*I and *Hind*III sites of pBluescript KS(+) the coding sequence of CrBKT and between the *Kpn*I and *Sal*I sites the codon-optimized coding sequence of mCherry omitted stop codon. C-terminal mCherry-fused CrBKT construct was created by cloning between the *Sal*I and *Hind*III sites the codon-optimized coding sequence of mCherry and between the *Kpn*I and *Sal*I sites the coding sequence of CrBKT omitted stop codon. The two constructs were termed mCherry-CrBKT and CrBKT-mCherry respectively. In both cases, mCherry and CrBKT were connected by the Val-Asp (VD) linker **(Figure 29)**. Sequence analysis of both fusion constructs using TMHMM algorithms predicted no changes in the trans-membranes helices compared to native CrBKT (data not shown).

Both fusion proteins remained fluorescent, as seen in the results of in-gel fluorescence detection (**Figure 28**).

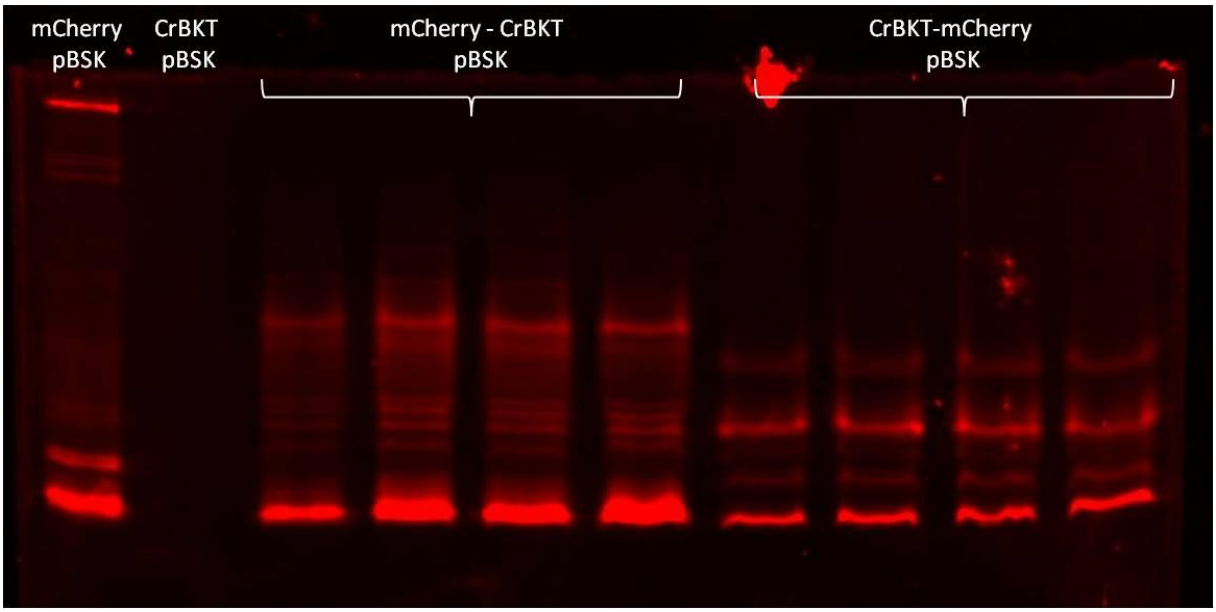

Figure 28: In-gel fluorescence detection of mCherry and mCherry-tagged proteins extracted from transformed *E. coli* cells. From left to right: positive control – *E. coli* cells producing mCherry (encoded in mCherry pBluescript plasmid); negative control – CrBKT pBSK transformant, four independent lines of mCherry-CrBKT transformants and four independent lines of CrBKT-mCherry transformants.

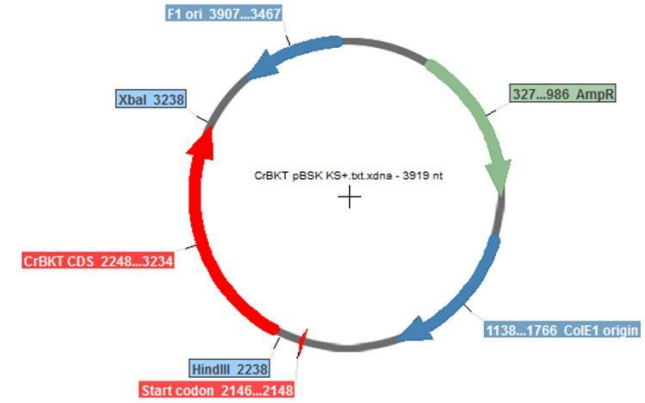

CrBKT

MTMITPSAQLTLTKGNKSWVPGPPSRSTVSISLTMGPGIQPTSARPCSRTKH
SRFALLAAALTARRVKQFTKQFRSRRMAEDILKLWQRQYHLPREDSDKRTL
RERVHLYRPPRSDLGGIAVAVTVIALWATLFVYGLWFVKLPWALKVGETAT
SWATIAAVFFSLEFLYTGLFITTHDAMHGTIALRNRRLNDFLGNLAISLYAW
FDYSVLHRKHWEHHNHTGEPRVDPDFHRGNPNLAVWFAQFMVSYMTLS
QFLKIAVWSNLLLLAGAPLANQLLFMTAAPILSAFRLFYYGTYVPHHPEKGH
TGAMPWQVSRTSSASRLQSFLTCYHFDLHWEHHRWPYAPWWELPKCRQ
IARGAALA

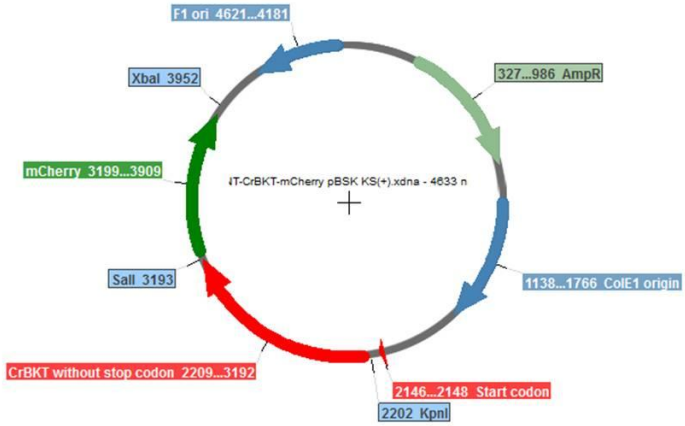

CrBKT-mCherry

MTMITPSAQLTLTKGNKSWVPMGPGIQPTSARPCSRTKHSRFALLAAALTA
RRVKQFTKQFRSRRMAEDILKLWQRQYHLPREDSDKRTLRERVHLYRPPRS
DLGGIAVAVTVIALWATLFVYGLWFVKLPWALKVGETATSWATIAAVFFSL
EFLYTGLFITTHDAMHGTIALRNRRLNDFLGNLAISLYAWFDYSVLHRKHW
EHHNHTGEPRVDPDFHRGNPNLAVWFAQFMVSYMTLSQFLKIAVWSNLL
LLAGAPLANQLLFMTAAPILSAFRLFYYGTYVPHHPEKGHTGAMPWQVSR
TSSASRLQSFLTCYHFDLHWEHHRWPYAPWWELPKCRQIARGAALAVDM
VSKGEEDNMAIIKEFMRFKVHMEGSVNGHEFEIEGEGEGRPYEGTQTAKL
KVTKGGPLPFAWDILSPQFMYGSKAYVKHPADIPDYLKLSFPEGFKWERV
MNFEDGGVVTVTQDSSLQDGEFIYKVKLRGTNFPSDGPVMQKKTMGWE
ASSERMYPEDGALKGEIKQRLKLKDGGHYDAEVKTTYKAKKPVQLPGAYN
VNIKLDITSHNEDYTIVEQYERAEGRHSTGGMDELYK

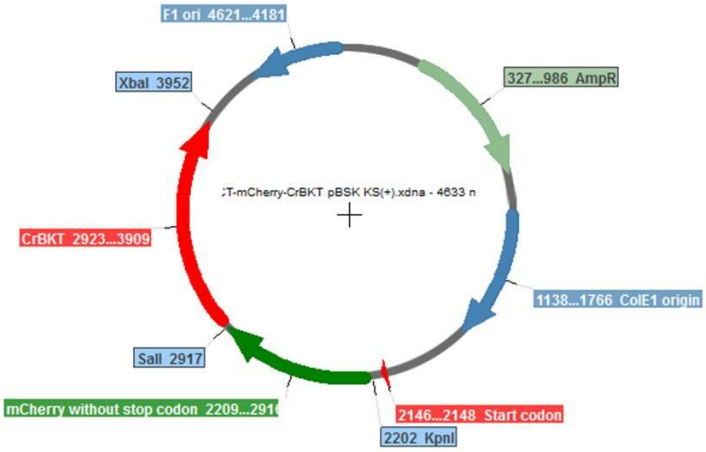

mCherry-CrBKT

MTMITPSAQLTLTKGNKSWVPMVSKGEEDNMAIIKEFMRFKVHMEGSVNG
HEFEIEGEGEGRPYEGTQTAKLKVTKGGPLPFAWDILSPQFMYGSKAYVKHP
ADIPDYLKLSFPEGFKWERVMNFEDGGVVTVTQDSSLQDGEFIYKVKLRGTN
FPSDGPVMQKKTMGWEASSERMYPEDGALKGEIKQRLKLKDGGHYDAEVK
TTYKAKKPVQLPGAYNVNIKLDITSHNEDYTIVEQYERAEGRHSTGGMDELYK
VDMGPGIQPTSARPCSRTKHSRFALLAAALTARRVKQFTKQFRSRRMAEDI
LKLWQRQYHLPREDSDKRTLRERVHLYRPPRSDLGGIAVAVTVIALWATLF
VYGLWFVKLPWALKVGETATSWATIAAVFFSLEFLYTGLFITTHDAMHGTI
ALRNRRLNDFLGNLAISLYAWFDYSVLHRKHWEHHNHTGEPRVDPDFHR
GNPNLAVWFAQFMVSYMTLSQFLKIAVWSNLLLLAGAPLANQLLFMTAA
PILSAFRLFYYGTYVPHHPEKGHTGAMPWQVSRTSSASRLQSFLTCYHFDL
HWEHHRWPYAPWWELPKCRQIARGAALA

Figure 29: CrBKT and CrBKT-mCherry fusion constructs. On the left are plasmid maps of CrBKT pBSK, CrBKT-mCherry pBSK and mCherry-CrBKT pBSK. On the right are the corresponding peptide sequences of produced proteins. In red is the sequence of CrBKT, in green of mCherry. At the N-termini of all three proteins are short amino sequences originated from backbone plasmid pBluescript.

When produced in ß-carotene- and zeaxanthin-accumulating *E. coli* strains, both constructs still displayed ketolase activities, indicated by conversion of ß-carotene to canthaxanthin and zeaxanthin to astaxanthin. In general, the results with fusion constructs were remarkably similar to those with native CrBKT. Exception was the case of N-terminally fused mCherry-CrBKT, in which the conversion of ß-carotene to canthaxanthin was incomplete, indicated by significant amount of ß-carotene that could still be detected **(Figure 30)**. Consequently, C-terminal fused CrBKT-mCherry was chosen for overproduction in *Chlamydomonas*.

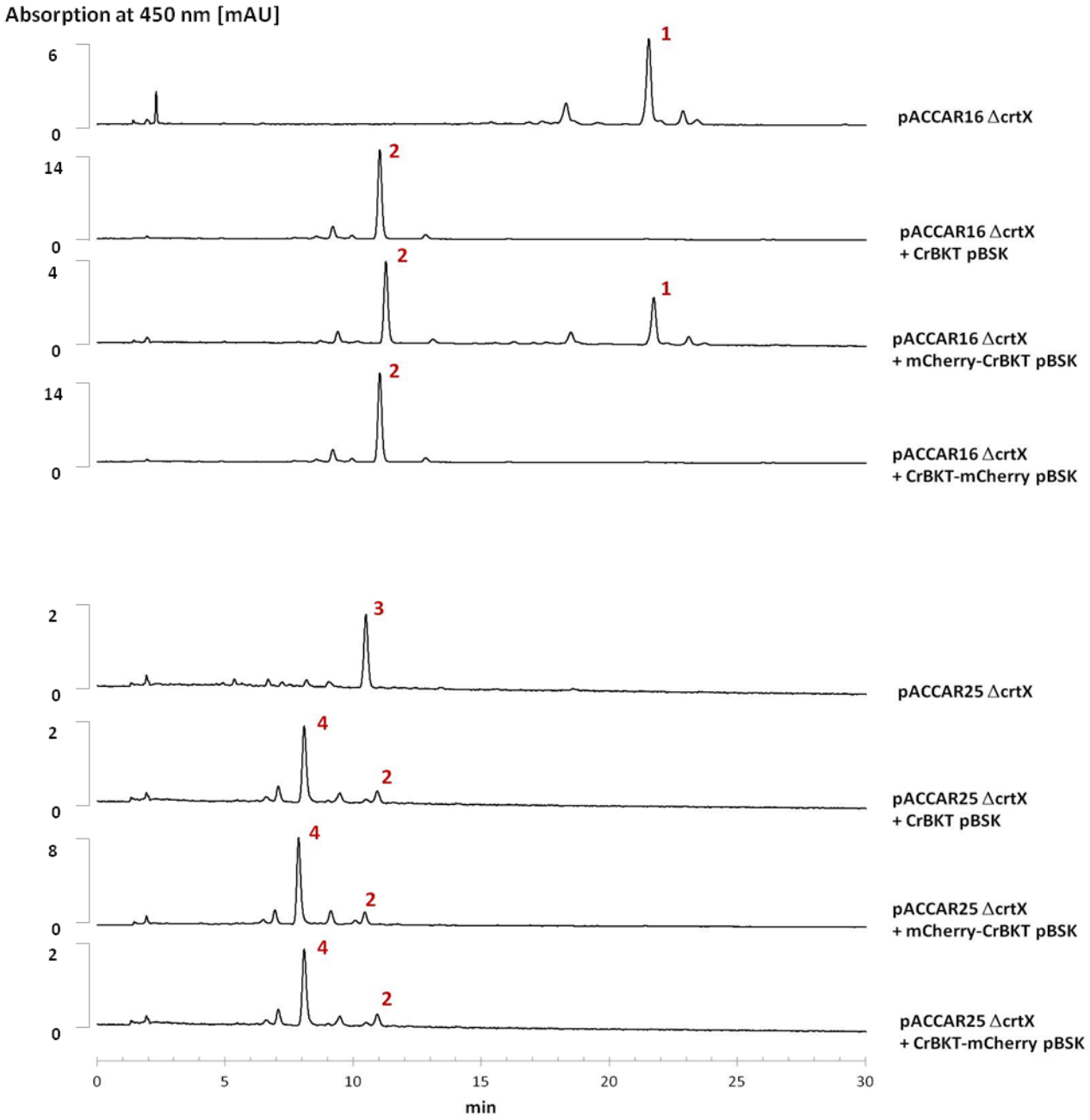

Figure 30: Ketolase activity assay of CrBKT and its mCherry fusion constructs produced in ß-carotene- and zeaxanthin-accumulating *E. coli*. Ketolation lead to conversion of ß-carotene to canthaxanthin and of zeaxanthin to astaxanthin. Pigments: 1 – ß-carotene, 2 – canthaxanthin, 3 – zeaxanthin, 4 - astaxanthin. Y-axis (absorbance) of all chromatograms was normalized between 0 and 1. Detection at 450nm.

3.3. Overproduction of CrBKT targeted to chloroplasts in *Chlamydomonas*

For metabolic engineering of ketocarotenoid production in *Chlamydomonas*, I repeated the commonly used strategy of over-producing ketolase (in my case CrBKT) in the chloroplasts **[117][119][120][121][125][126]**. To attain this goal, CrBKT needed to be fused on its N-terminus with a chloroplast-targeting transit peptide (cTP). The 39-amino acid long transit peptide of photosystem I's subunit psaD from *Chlamydomonas* itself **[56]** was chosen for this purposed.

3.3.1. Functionality of psaD transit peptide

The functionality of psaD transit peptide was tested by transforming *Chlamydomonas* UVM-4 cells with plasmid pBR32 psaD-mCherry **[87]** and followed the subsequent localization of mCherry. In the construct pBR32 psaD-mCherry, the codon-optimized coding sequence of mCherry was fused on its N-terminus with the psaD transit peptide. Also harboured in the plasmid was a Ble2A expression cassette, to which the psaD-mCherry sequence was fused to. Protein production was driven by constitutive HSP70/RBCS2 promoter. Surviving colonies were selected on TAP-agar plate with 10 mg/L zeocin.

Fluorescence microscopy with transformed *Chlamydomonas* cells showed that, in contrast to pBR9 mCherry transformants where signal of mCherry fluorescence and chlorophyll autofluorescence were separated (mCherry was produced in cytosol), in pBR32 psaD-mCherry cells these two clearly co-localized, indicating that the produced mCherry was directed to chloroplasts (**Figure 31**).

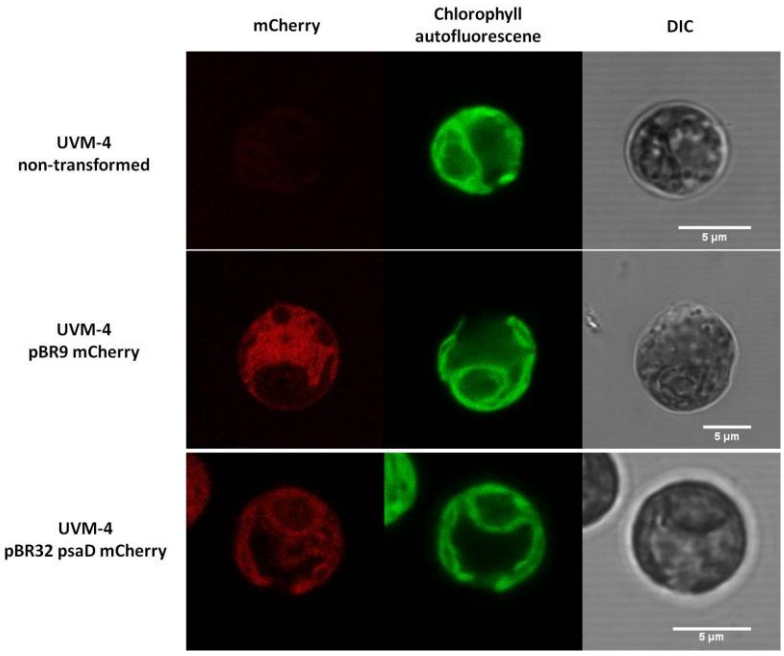

Figure 31: mCherry fluorescence (*left*), chlorophyll autofluorescence (*middle*) and DIC pictures (*right*) from non-transformed UVM-4 cells as well as its pBR9 mCherry and pBR32 psaD mCherry transformants. Scale bars are 5µm

3.3.2. Cloning of plastid-targeted CrBKT over-production constructs and transformation

Two constructs were created for over-production of CrBKT targeted to *Chlamydomonas* chloroplasts: pBR32 psaD CrBKT and pBR32 psaD CrBKT-mCherry. These plasmids were generated by cloning the coding sequence of CrBKT and CrBKT-mCherry fusion protein between the *Xho*I and *Bam*HI sites of plasmid pBR32 psaD mCherry. Due to the presence of a *Bam*HI recognition site in the sequence of CrBKT, inserted sequences were amplified with extension containing *Bcl*I site, which upon restriction digest generated sticky ends compatible to those of *Bam*HI.

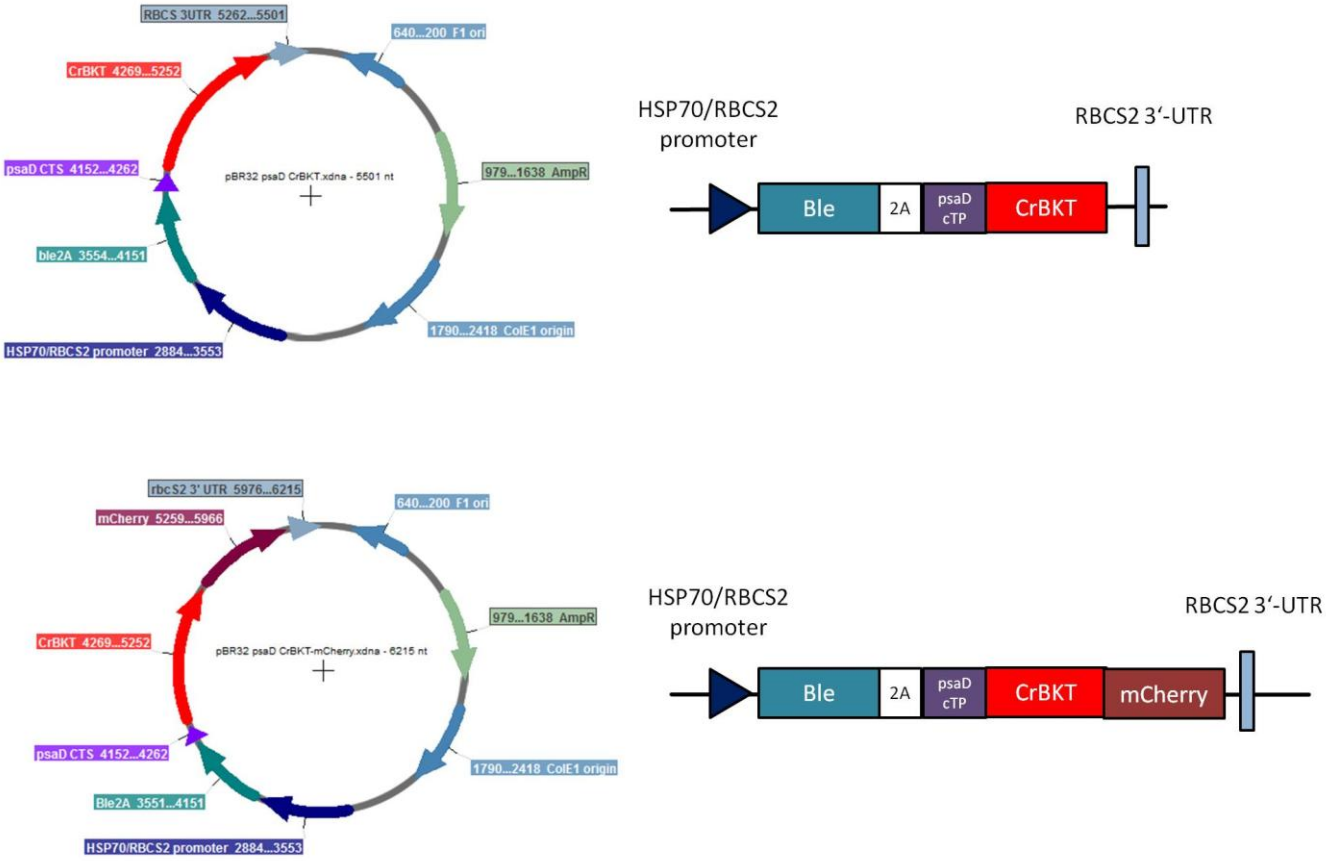

Figure 32: Constructs for over-production of CrBKT in *Chlamydomonas* chloroplasts.

Both strains UVM-4 and CC-4102 were transformed with these two constructs using standard transformation protocol. Colonies appeared 10-14 days after transformation. In general, transformation efficiencies were much lower compared to control batches transformed with pBR32 psaD mCherry. Results are shown in **Table 4**.

Table 4: Transformation of UVM-4 and CC-4102 with pBR32 psaD CrBKT and pBR32 psaD CrBKT-mCherry. In parallel, another transformation with pBR32 psaD mCherry was carried out as control.

Strains	pBR32 psaD CrBKT	pBR32 psaD CrBKT-mCherry	pBR32 psaD mCherry
UVM-4	*1st transformation with 2.5 µg DNA* 1 colonies / 3 plates (1.4 colonies/ µg DNA) *2nd transformation with 5 µg DNA* 9 colonies / 6 plates (3 colonies/ µg DNA)	*1st transformation with 2.5µg DNA* 2 colonies / 3 plates (2.7 colonies/ µg DNA) *2nd transformation with 5 µg DNA* 11 colonies / 6 plates (3.7 colonies/ µg DNA)	*Transformation with 3 µg DNA* 49 colonies/ 2 plates (81.7 colonies/ µg DNA)
CC-4102	*1st transformation with 2.5µg DNA* 4 colonies / 3 plates (5.3 colonies/ µg DNA) *2nd transformation with 5 µg DNA* 17 colonies / 6 plates (5.7 colonies/ µg DNA)	*1st transformation with 2.5µg DNA* 6 colonies / 3 plates (8 colonies/ µg DNA) *2nd transformation with 5 µg DNA* 23 colonies / 6 plates (7.7 colonies/ µg DNA)	*Transformation with 3 µg DNA* > 100 colonies/ 3 plates (> 111 colonies/ µg DNA)

3.3.3. PCR-screening of zeocin-resistant transformants

In total, 73 zeocin-resistant colonies were isolated from transformation of two *Chlamydomonas* strains with two psaD-CrBKT constructs. In the first round of screening, successful integration of transgene into genome was checked by PCR. Primers 1501 and 1502 were used, which amplified the whole length (984 bp) of CrBKT coding sequence. Test with a CrBKT-containing plasmid (pBR32 psaD CrBKT) confirmed the functionality of the primers as well as PCR conditions. Amplification using genomic DNA of non-transformed *Chlamydomonas* as template resulted in bands of size around 400 base pairs. It was postulated that these were products from aborted amplification of the native CrBKT gene in *Chlamydomonas* genome, which was 5kb in length and thus could not be amplified effectively by Taq polymerase.

Genomic DNA were extracted from all 73 zeocin-resistant transformant lines and used as templates for PCR screening. Transformants which displayed a band at ~ 1kb were considered PCR-positive. In total, only 8 of such lines were identified (**Table 5** and **Figure 33**).

Table 5: PCR screening of 73 transformants from transformation of UVM-4 and CC-4102 with pBR32 psaD CrBKT and pBR32 psaD CrBKT-mCherry

Strains	Plasmids	Zeocin-resistant	PCR-positive	Percentage
UVM-4	pBR32 psaD CrBKT	10	1	10%
	pBR32 psaD CrBKT-mCherry	13	1	7.7%
CC-4102	pBR32 psaD CrBKT	21	2	9.5%
	pBR32 psaD CrBKT-mCherry	29	4	13.7%
Total		**73**	**8**	**11%**

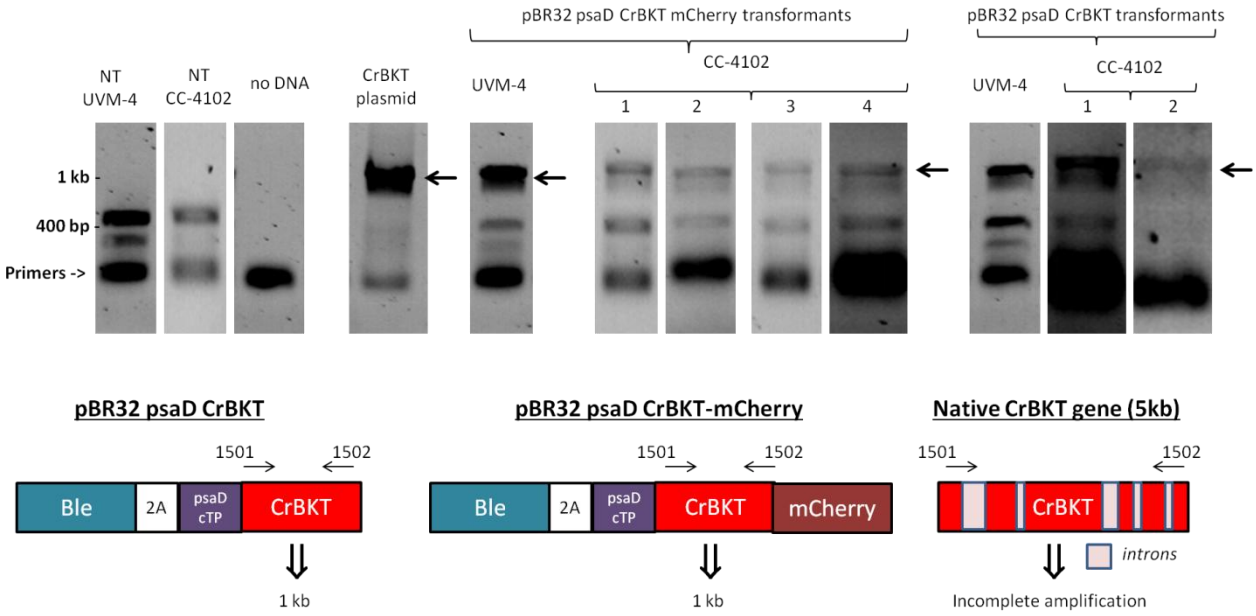

Figure 33: PCR screening of transformants from transformation of UVM-4 and CC-4102 with pBR32 psaD CrBKT and pBR32 psaD CrBKT-mCherry. First four lanes from the left are controls: PCR amplification from genomic DNA extracted from non-transformed (NT) UVM-4 and CC-4102 cells, from sample without DNA template and from pBR32 psaD CrBKT-mCherry plasmid. Next are PCR amplifications from 8 positive lines. For PCR, primers 1501 and 1502 were used, which bound to the beginning and the end of CrBKT sequence, resulting in ~ 1kb products (black arrows). These primers also recognized the native CrBKT gene in *Chlamydomonas* genome, which was 5 kb because of introns and thus could not be completely amplified with *Taq* polymerase.

The low percentage of PCR-positive lines among zeocin-resistant transformants prompted me to the question: could zeocin resistance be conferred by another element rather than the *Ble* gene? To answer this question, I proceed to check the presence of *Ble* gene in 2 PCR-positive and 6 PCR-

negative lines among CC-4102 pBR32 psaD CrBKT-mCherry transformants. Primers 1479 and 1480 were used, which would result in the amplification of a ~ 300bp fragment from Ble2A sequence. No amplification was observed when either water or genomic DNA from non-transformed *Chlamydomonas* CC-4102 was used as template. Positive control with transformation vector yielded as expected the ~ 300bp fragment. Among 8 tested lines, all eight were positive (**Figure 34**). Results indicated that among PCR-negative transformants, the expression cassette was probably fragmented and only the Ble2A part was incorporated into genome.

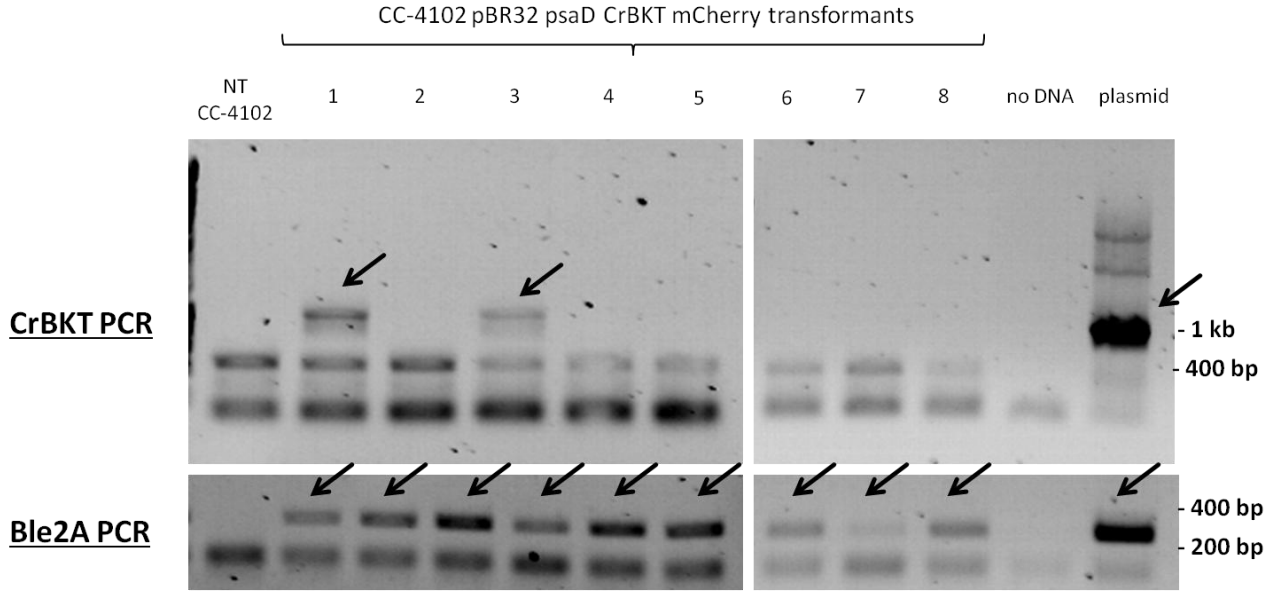

Figure 34: PCR screening of 8 transformants from transformation of CC-4102 with pBR32 psaD CrBKT-mCherry for presence of CrBKT (*upper*) and Ble2A gene (*lower*). Also tested were samples with genomic DNA from non-transformed (NT) CC-4102 cells, with water and with pBR32 psaD CrBKT-mCherry plasmid as templates. Expected amplicon sizes were ~ 1kb for CrBKT PCR and ~ 300bp for Ble2A PCR (black arrows). Only lines 1 and 3 were positive with CrBKT PCR, while all eight lines were positive with Ble2A PCR.

Eight transformants positive to CrBKT PCR were subsequently named UVM-BM1, UVM-B6, CC-BM2, CC-BM4, CC-BM 18, CC-BM28, CC-B8 and CC-B13. The abbreviations UVM and CC denote if the mother strain used for transformation was UVM-4 or CC-4102, respectively. The abbreviations BM and B denote if the plasmid used for transformation harboured the fusion construct CrBKT-mCherry or only CrBKT.

3.3.4. Analysis of PCR-positive transformants

In the next step, I tried to detect mCherry fluorescence from the PCR positive transformants. Three pBR32 psaD CrBKT transformants: UVM-B6, CC-B8 and CC-B13, as well as non-transformed cells did not show any mCherry fluorescence as expected. Among five pBR32 psaD CrBKT-mCherry transformants, only the UVM-BM1 line showed very weak signal, while again no mCherry fluorescence was observed in the other four lines (**Figure 35**). In UVM-BM1 cells, mCherry and chlorophyll fluorescence signal seemed to co-localize. Attempts of detect mCherry in-gel fluorescence with proteins extracted from UVM-BM1 were however not successful (data not shown).

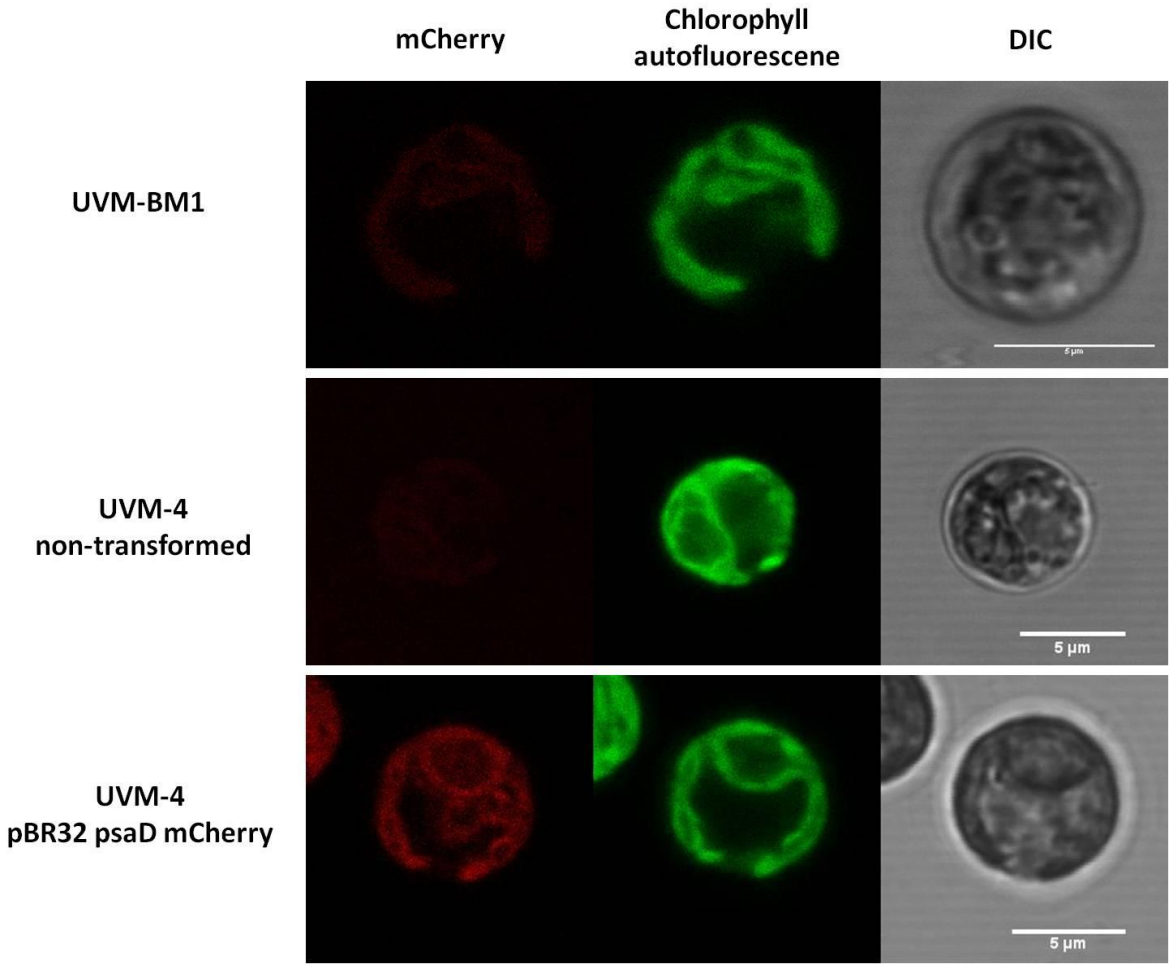

Figure 35: mCherry fluorescence (*left*), chlorophyll autofluorescence (*middle*) and DIC pictures (*right*) from UVM-BM1 cells, non-transformed UVM-4 cells as well as its pBR32 psaD mCherry and pBR32 psaD CrBKT-mCherry transformants. Scale bars are 5µm

Pigments were extracted from all eight transformant lines and saponified with KOH. Saponification removed chlorophylls, which were deesterified and went into aqueous phase during extraction. The subsequent carotenoid fractions were analysed via HPLC. Neither canthaxanthin, astaxanthin nor any new pigments were observed. No difference in the carotenoid profiles between transformants and their non-transformed cells could be detected either (**Figure 36**).

3.3.5. Summary

For over-production of CrBKT and its C-terminal mCherry fusion protein in *Chlamydomonas* chloroplasts, cells from two strains: UVM-4 and CC-4102, were transformed with vectors pBR32 psaD CrBKT or pBR32 psaD CrBKT-mCherry. In total, 73 zeocin-resistant colonies were isolated. Test with 8 transformants showed the presence of the selection marker, the *Ble2A* gene, in 100% tested. In contrast, presence of CrBKT sequence could be detected only in eight among 73 lines, a success ratio of 11%. Among five positive pBR32 psaD CrBKT-mCherry transformants, only one (UVM-BM1) showed very weak mCherry fluorescence, though the presence of fusion protein could not be confirmed via in-gel fluorescence detection. Among eight PCR-positive transformants, none produced astaxanthin, canthaxanthin or any new pigments.

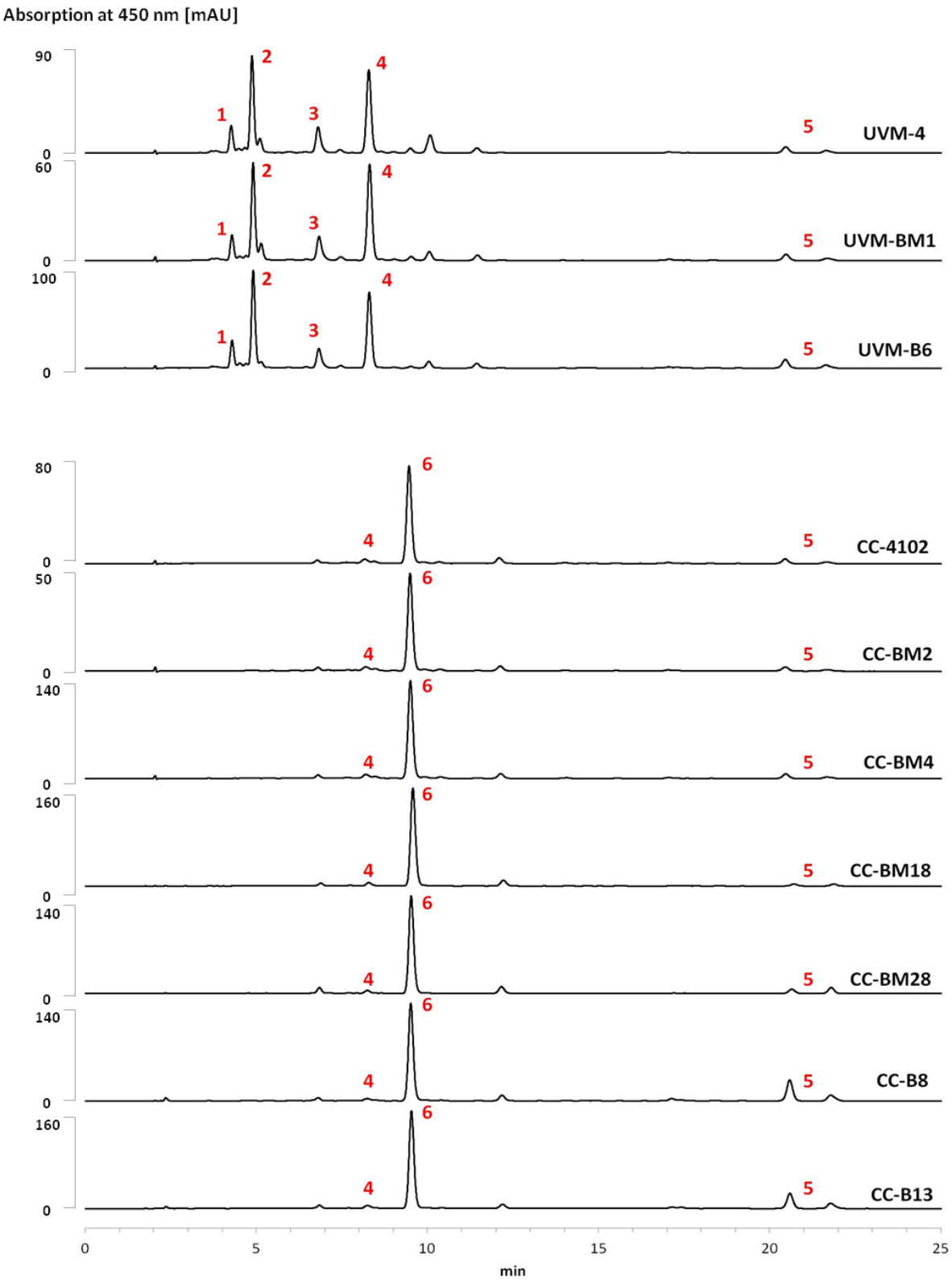

Figure 36: HPLC analysis of carotenoids extracted from 8 PCR-positive, zeocin-positive lines from transformation of Chlamydomonas strains UVM-4 and CC-4102 with pBR32 psaD CrBKT-mCherry and pBR32 psaD CrBKT. Pigments: 1 = loroxanthin + neoxanthin, 2 = violaxanthin, 3 = antheraxanthin, 4 = lutein, 5 =α- and ß-carotene, 6 = zeaxanthin. Y-axis (absorbance) of all chromatograms was normalized between 0 and 1. Detection at 450nm.

3.4. Over-production of V5-tagged CrBKT in *Chlamydomonas*

After transformation of *Chlamydomonas* with pBR32 psaD CrBKT and pBR32 psaD CrBKT-mCherry failed to induce ketocarotenoid production, I modified my strategy. Previous experiments showed that protein production was very low, thus I intended to tag CrBKT with an epitope tag, allowing detection with the much more sensitive Western blot. Also the putative chloroplastic transit peptide at the N-terminus of CrBKT was another point of concern, since double stacking of two different transit peptides after each other could lead to mistargeting as well as faulty post-import processing. Therefore I intended to omit the chloroplastic transit peptide altogether. The third change in strategy was in the selection conditions. Last but not least, since there were reports in higher plants of detrimental effects of ketocarotenoid production on photosynthesis **[143][144]**, in addition to normal practice of antibiotic selection in light, I also included dark (heterotrophic) selection conditions.

3.4.1. Cloning of V5-tagged CrBKT over-production constructs and transformation

Another construct was generated for over-production of V5-tagged CrBKT in *Chlamydomonas*. The coding sequence of CrBKT without stop codon was cloned between *Xho*I and *Xba*I sites of plasmid pChlamy4. pChlamy4 (Thermo Fisher) was a commercialized plasmid designed for protein production in *Chlamydomonas*. It shared the same Ble2A concept as in others of our plasmids. As the result of cloning, a 26-amino acid-long extension containing both V5 (GKPIPNPLLGLDST) 6xHis (HHHHHH) epitopes was added to CrBKT's C-terminus. The new plasmid, pChlamy4 CrBKT V5H (Figure 37) was used for transformation.

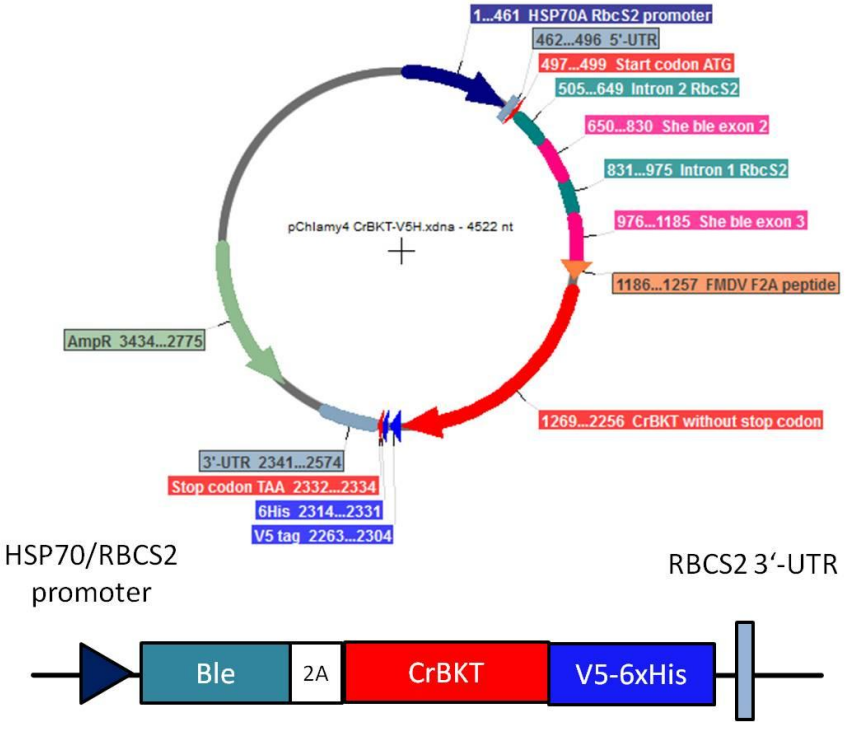

Figure 37: pChlamy4 CrBKT V5H for over-production of V5-tagged CrBKT in *Chlamydomonas*

Both strains UVM-4 and CC-4102 were transformed with these two constructs using standard transformation protocol. After transformation, cells were incubated either in light on TAP-zeocin agar plates as normal, or in dark on TAP-zeocin agar plates supplemented with yeast extract and tryptone (short: TAP-YP-zeocin). Colonies appeared 10-14 days after transformation on light-incubated plates, 3-4 weeks after transformation on dark-incubated plates. Results of transformation are shown in **Table 6**.

Table 6: Transformation of UVM-4 and CC-4102 with 5µg pChlamy4 CrBKT V5H. In parallel, another transformation with 5µg pBR9 mCherry with subsequent selection in light was carried out as control.

Strains	pChlamy4 CrBKT V5H Light incubation	pChlamy4 CrBKT V5H Dark incubation	Control transformation: pBR9 mCherry
UVM-4	10 colonies / 4 plates (5 colonies/ µg DNA)	8 colonies / 4 plates (4 colonies/ µg DNA)	102 colonies/ 2 plates (102 colonies/ µg DNA)
CC-4102	184 colonies / 2 plates (184 colonies/ µg DNA)	56 colonies / 2 plates (56 colonies/ µg DNA)	93 colonies/ 1 plates (186 colonies/ µg DNA)

Compared with previous experiment, transformation efficiencies with test plasmid were similar: 102 colonies/ µg DNA with strain UVM-4 (earlier: 81.7 colonies/ µg DNA); 186 colonies/ µg DNA with strain CC-4102 (earlier: > 111 colonies/ µg DNA). Regardless of light conditions, transformation of UVM-4 with CrBKT-containing plasmid also yielded very low number of colonies: 5 & 4 colonies / µg DNA (earlier: 3 & 3.7 colonies/ µg DNA). However, transformation efficiencies of CC-4102 with pChlamy4 CrBKT V5H were much improved than earlier transformation with pBR32 psaD CrBKT and pBR32 psaD CrBKT-mCherry (184 colonies/ µg DNA vs.5.7 and 7.7 colonies/ / µg DNA). Dark incubation yielded only a third as many colonies as light incubation.

Interestingly, among 56 colonies isolated on dark-incubated plates from transformation of CC-4102 cells, 4 appeared to have the pale green color, making them standing out among other dark green colonies. These lines were subsequently termed DP (**d**ark-incubated, **p**ale green).

3.4.2. PCR-screening of zeocin-resistant transformants

In total, 258 zeocin-resistant colonies were isolated from transformation of two *Chlamydomonas* strains with pChlamy4 CrBKT V5H. Among them, 110 were tested further with PCR. Primers 1479 and 1491 were chosen which would amplify a ~ 1300 bp-long sequence bridging *Ble2A* and *CrBKT* sequences. Test with transformation vector confirmed the functionality of the primers as well as PCR conditions. Amplification using genomic DNA of non-transformed *Chlamydomonas* as template resulted in faint bands with size around 1000 and 200 base pairs, possibly from one-side amplification of the native CrBKT gene with primer 1491.

Genomic DNA were extracted from 110 zeocin-resistant transformant lines and used as templates for PCR screening. Transformants which displayed a band at ~ 1.3 kb were considered PCR-positive. In total, 15 PCR-positive lines were identified (**Table 7** and **Figure 38**).

Table 7: PCR screening of 112 transformants from transformation of UVM-4 and CC-4102 with pChlamy4 CrBKT V5H

Strains	Light/ Dark	Zeocin-resistant	Tested	PCR-positive	Percentage
UVM-4	Light	10	8	3	37.5%
	Dark	8	6	1	16.7%
CC-4102	Light	184	40	4	10%
	Dark (dark green colonies)	52	52	3	5.8%
	Dark (pale green colonies)	4	4	4	100%
Total		**258**	**110**	**15**	**13.6%**

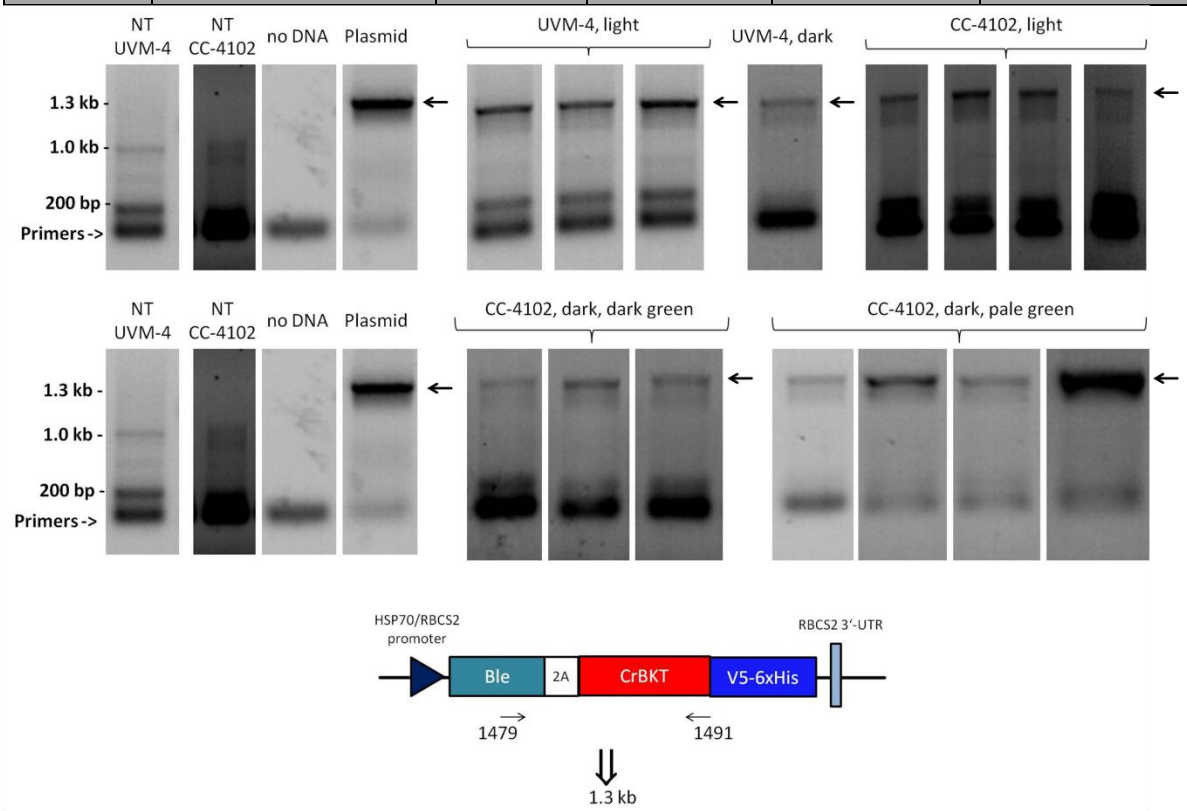

Figure 38: PCR screening of transformants from transformation of UVM-4 and CC-4102 with pChlamy4 CrBKT V5H. First four lanes from the left are controls: PCR amplification from genomic DNA extracted from non-transformed (NT) UVM-4 and CC-4102 cells, from sample without DNA template and from pChlamy4 CrBKT V5H plasmid. Following are PCR amplifications from 15 positive lines. For PCR, primers 1479 and 1491 were used, which resulted in the amplification of a ~ 1.3kb products (black arrows).

Based on their mother strains (UVM-4 or CC-4102), selection light condition (light on TAP-zeocin or dark on TAP-YP-zeocin agar) and their colors (green or pale green), the 15 PCR-positive transformants were named accordingly:

- UVM-4 transformants, selected in light: UVM-L6, UVM-L8 and UVM-L9
- UVM-4 transformant, selected in dark: UVM-D6
- CC-4102 transformants, selected in light: CC-L31, CC-L33, CC-L36 and CC-L39
- CC-4102 transformants, selected in dark, green: CC-D3, CC-D4, CC-D29
- CC-4102 transformants, selected in dark, pale green: CC-DP1, CC-DP2, CC-DP3, CC-DP4

3.4.3. Pigment compositions of PCR-positive transformants

Relative contents of chlorophlyll a, chlorophyll b and total carotenoids were determined photometrically according to Lichtenthaler **[134]**. Results were shown in **Table 8** and **Figure 39**. In general, there was no difference between non-transformed cells and green transformants. In contrast, in all four DP lines (pale-green) the content of both chlorophyll a and b were significantly reduced. The much lower chlorophylls/ total carotenoid ratios explained their pale green tints.

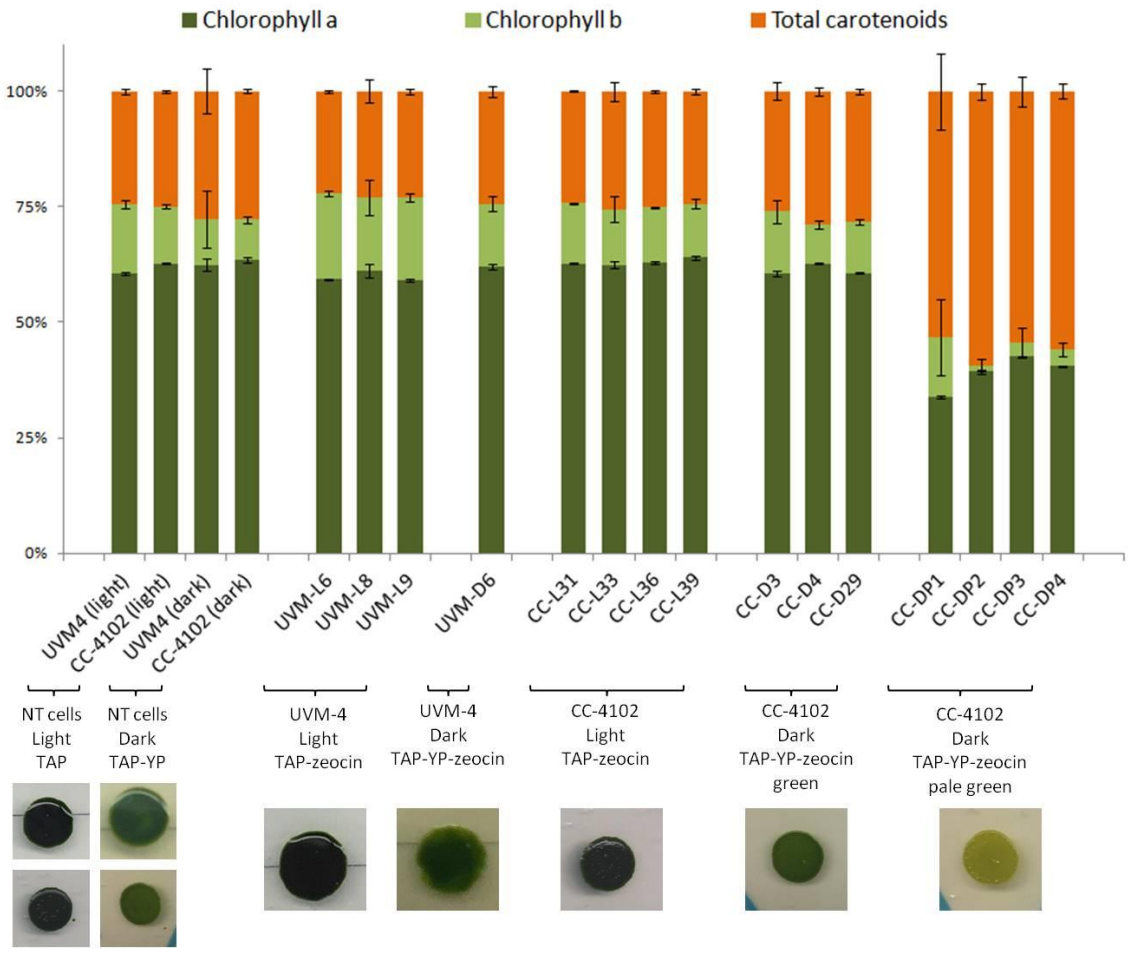

Figure 39: Percentage of chlorophyll a, chlorophyll b and total carotenoids of 15 PCR-positive pChlamy4 CrBKT V5H transformants, compared to those of non-transformed (NT) UVM-4 and CC-4102. Light conditions and growth media are specified. In the small windows are pictures of algal colonies on agar plates. Measurements were performed in triplicates. Error bars are standard deviations.

Table 8: Cellular contents of chlorophyll a, chlorophyll b and total carotenoids of 15 PCR-positive pChlamy4 CrBKT V5H transformants, compared to those of non-transformed (NT) UVM-4 and CC-4102.

Strains	Light/ Dark	Chlorophyll a [pg/cell]	Chlorophyll b [pg/cell]	Total carotenoids [pg/cell]	Chlorophylls/ Total carotenoids
UVM-4	Light	1.10 ± 0.09	0.27 ± 0.01	0.44 ± 0.04	3.10 ± 0.09
UVM-4	Dark	0.96 ± 0.07	0.16 ± 0.11	0.42 ± 0.03	2.68 ± 0.06
CC-4102	Light	2.03 ± 0.23	0.40 ± 0.06	0.80 ± 0.08	3.01 ± 0.05
CC-4102	Dark	1.88 ± 0.03	0.26 ± 0.03	0.51 ± 0.02	2.60 ± 0.06
UMV-L6	Light	1.23 ± 0.05	0.39 ± 0.01	0.46 ± 0.02	3.54 ± 0.06
UVM-L8	Light	1.31 ± 0.07	0.34 ± 0.08	0.49 ± 0.07	3.34 ± 0.51
UVM-L9	Light	1.31 ± 0.08	0.40 ± 0.01	0.51 ± 0.04	3.34 ± 0.09
UVM-D6	Dark	1.29 ± 0.01	0.28 ± 0.04	0.51 ± 0.02	3.09 ± 0.18
CC-L31	Light	1.78 ± 0.08	0.37 ± 0.02	0.69 ± 0.03	3.12 ± 0.02
CC-L33	Light	1.26 ± 0.28	0.25 ± 0.12	0.51 ± 0.08	2.92 ± 0.31
CC-L36	Light	1.97 ± 0.34	0.37 ± 0.06	0.79 ± 0.13	2.98 ± 0.04
CC-L39	Light	2.04 ± 0.25	0.37 ± 0.03	0.78 ± 0.10	3.10 ± 0.10
CC-D3	Dark	1.54 ± 0.03	0.34 ± 0.06	0.66 ± 0.06	2.84 ± 0.28
CC-D4	Dark	1.75 ± 0.04	0.23 ± 0.03	0.81 ± 0.02	2.45 ± 0.11
CC-D29	Dark	1.65 ± 0.06	0.30 ± 0.01	0.77 ± 0.04	2.54 ± 0.07
CC-DP1	Dark	0.64 ± 0.06	0.25 ± 0.18	0.99 ± 0.09	0.90 ± 0.30
CC-DP2	Dark	0.62 ± 0.03	0.03 ± 0.02	0.93 ± 0.06	0.68 ± 0.05
CC-DP3	Dark	0.87 ± 0.05	0.07 ± 0.07	1.11 ± 0.02	0.84 ± 0.11
CC-DP4	Dark	0.66 ± 0.02	0.06 ± 0.02	0.91 ± 0.06	0.79 ± 0.05

3.4.4. HPLC analysis of PCR-positive transformants

Pigment profiles of the transformants were analysed more closely with HPLC. According to several publications **[145]**, saponification could cause degradation of ketocarotenoids. Thus in contrast to earlier experiment, pigment extracts were not saponified prior to HPLC. As the results, both carotenoids and chlorophylls were detected in the chromatograms.

Among eleven green transformant lines (light-selected UVM-L6, UVM-L8, UVM-L9, CC-L31, CC-L33, CC-L36, CC-L39 as well as dark-selected UVM-D6, CC-D3, CC-D4 and CC-D29), no astaxanthin, canthaxanthin nor any other ketocarotenoids could be detected. Neither was any conspicuous change in composition of major pigments. I was however able to detect the increased accumulation of several chlorophyll-related products which hitherto only existed at trace levels in non-transformed cells, especially in CC-DP1 and CC-DP4 lines. Absorption spectra of the new peaks all reveal "humps" at 580-640 nm, which is typical for chlorophylls but non-existent in carotenoids (**Figure 40**). Absorption spectrum's shapes of these peaks were very similar to those of chlorophyll a and b, and their absorption maxima between 400 and 500 nm were also very close as well. It was thus postulated that these peaks were intermediates from chlorophyll biosynthesis or degradation pathways.

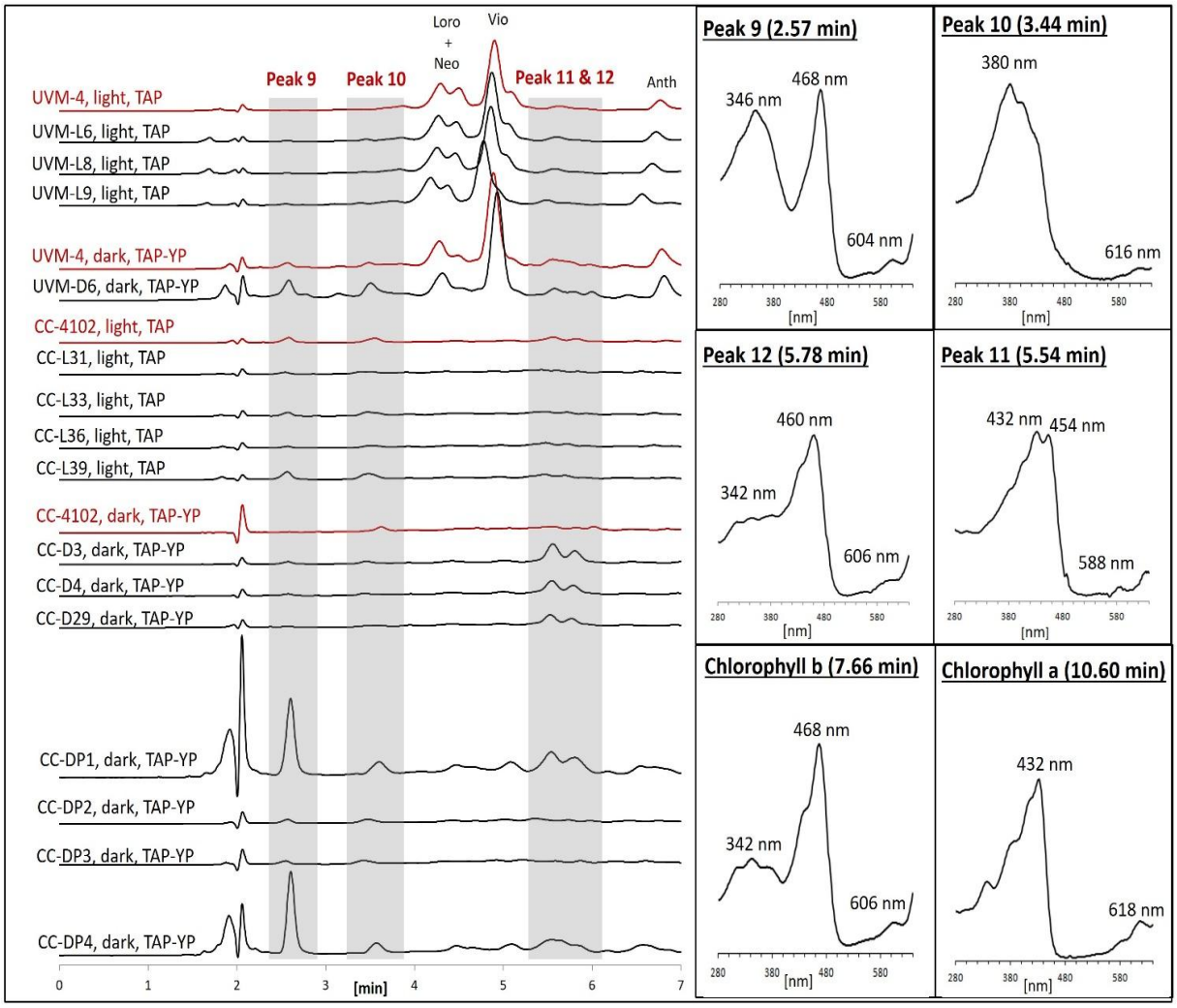

Figure 40 *(previous page)***:** Detection of chlorophyll-like products (peaks 9, 10, 11 and 12) in several pChlamy4 CrBKT-V5H transformants. Cell lines, light conditions and growth media are specified on the right hand side. Chromatograms from non-transformed cells are marked red. Loro, neo, vio and anth are abbreviations of loroxanthin, neoxanthin, violaxanthin and antheraxanthin. On the left hand side are absorption spectra between 280 and 640nm, as well as retention time of peaks 9 -12 and of chlorophyll a and b.

In contrast, HPLC analysis of dark-screened, pale green DP lines revealed significant differences compared to non-transformed cells. Corroborating the earlier determination of pigment compositions (***Section 3.4.3***), in DP lines both chlorophyll a and b peaks were visibly reduced. Chlorophyll b was no longer the highest peak in the chromatogram but now zeaxanthin **(Figure 41)**. Unidentified chlorophyll-related products that were previously observed (peaks 9, 10, 11 and 12) were also detected in DP lines as well **(Figure 40)**. Intriguingly, in two DP lines (CC-DP1 and CC-DP4), I detected a new small peak eluted between zeaxanthin (9.5 min) and chlorophyll a (10.6 min). This new peak, peak 13, was eluted at the same time as canthaxanthin standard (9.78 min) **(Figure 42)**. Furthermore, the absorption spectra of peak 13 (maximum: 468nm) and canthaxanthin (maximum: 476 nm) were also remarkably similar. **Figure 43** shows the comparisons of absorption spectra of peak 14 with canthaxanthin as well as with zeaxanthin and chlorophyll a - two major adjacent peaks.

I thus postulated that peak 13 was canthaxanthin contaminated by a small amount of zeaxanthin and chlorophyll a - two major adjacent peaks. To test this hypothesis, I simulated a combined absorption spectrum from individual spectra of canthaxanthin, zeaxanthin and chlorophyll a with weighting factors **Wc**, **Wz** and **Wa** respectively. At any wavelength, the absorbance of the simulated mixture was:

$$A\,[simulated] = \boldsymbol{Wc}\ x\ A[canthaxanthin] + \boldsymbol{Wz}\ x\ A[zeaxanthin] + \boldsymbol{Wa}\ x\ A[chlorophyll\ a]$$

A very good fit was achieved with: **Wc** = 0.894, **Wz** = 0,109 and **Wa** = 0.221, indicating that the dominant substance in peak 13 was indeed canthaxathin with some chlorophyll a and zeaxanthin contamination. The simulated spectrum was also shown in **Figure 43**.

By comparing the areas under curve (AOC) of canthaxanthin, zeaxanthin and ß-carotene peaks with those of standards, it was possible to estimate the contents of canthaxanthin, which stood at less than 10% of the total carotenoids content **(Table 9)**.

Table 9: Canthaxanthin content of the DP lines

Strains	**Pigment content (*m/m % total carotenoids)***		
	Canthaxanthin	**Zeaxanthin**	**ß-carotene**
CC-DP1	8.35%	75.98%	15.66%
CC-DP2	0%	56.83%	43.17%
CC-DP3	0%	56.39%	43.61%
CC-DP4	9.02%	78.72%	12.26%
Non-transformed CC-4012	0%	81.44%	18.56%

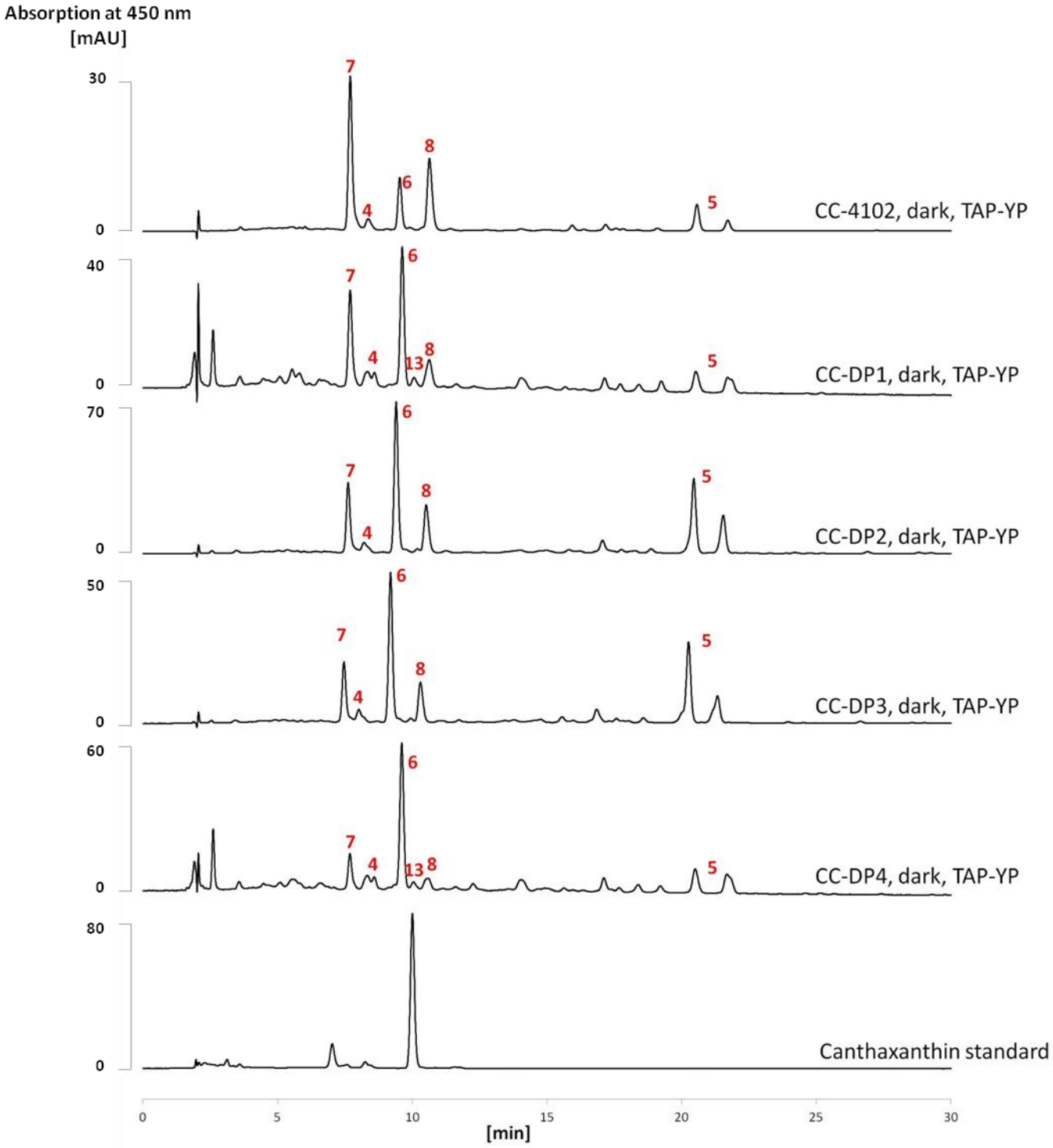

Figure 41: The pale green color of DP lines was elucidated by HPLC analysis, which saw dramatic shift in pigment profiles compared to non-transformed cells: chlorophyll-to-carotenoid ratios were significantly reduced, and zeaxanthin became the highest peak in the chromatogram. Pigments: 4 = lutein, 5 =α- and ß-carotene, 6= zeaxanthin, 7 = chlorophyll b, 8 = chlorophyll a, 13 = canthaxanthin. Y-axis (absorbance) of all chromatograms was normalized between 0 and 1. Detection at 450nm.

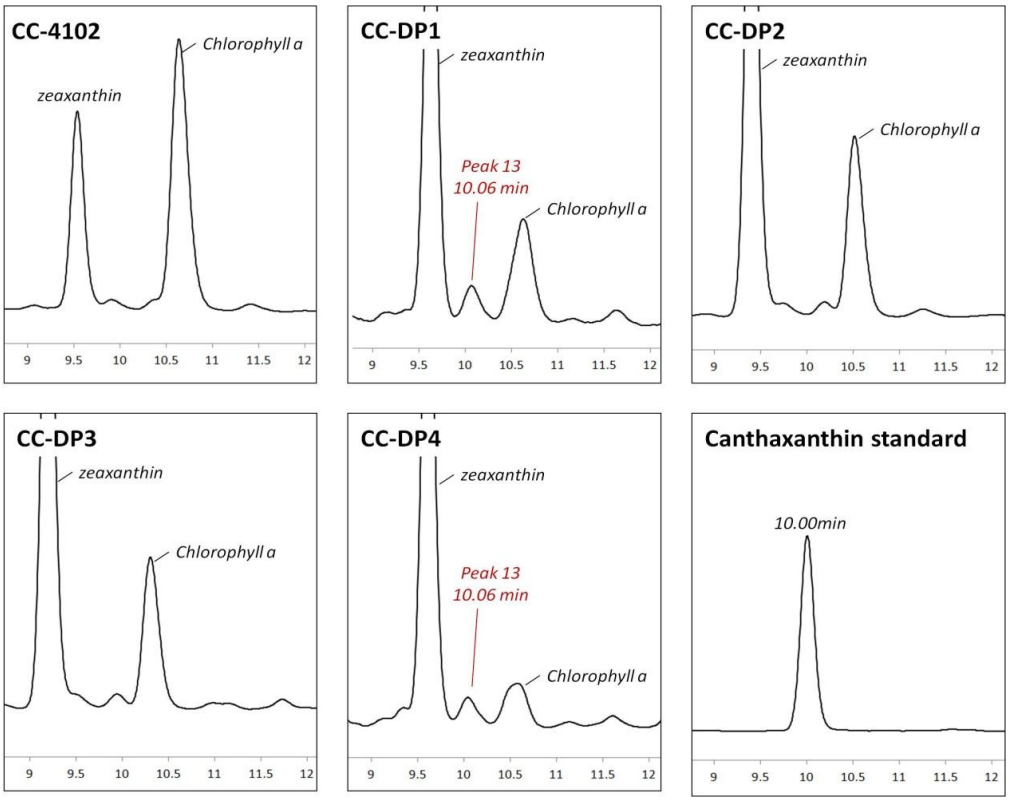

Figure 42: Peak 13 was eluted at the same time as canthaxanthin standard.

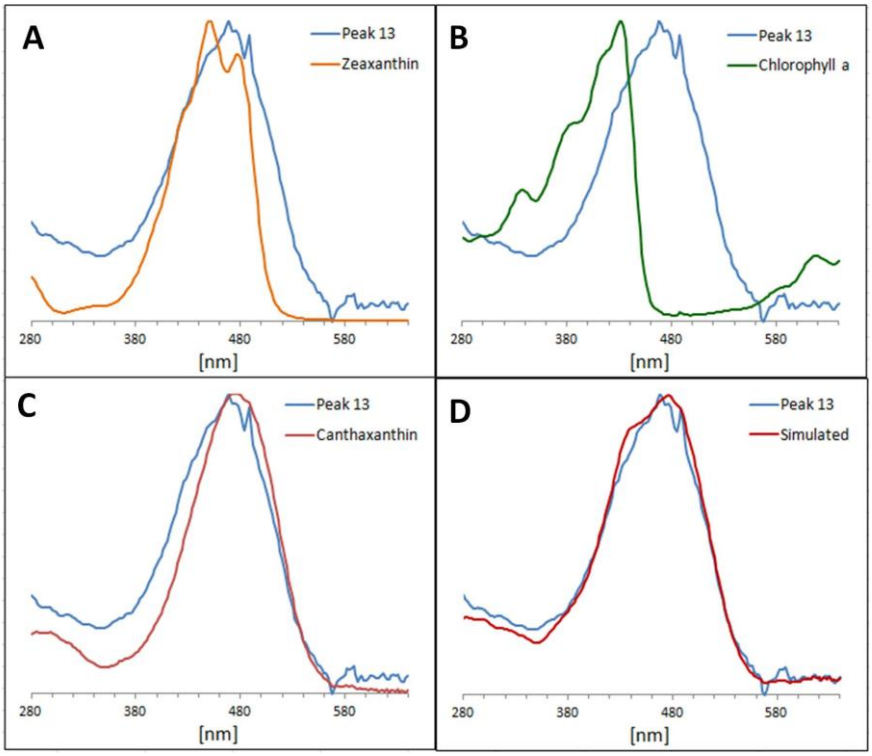

Figure 43*:* Comparisons of absorption spectrum from 280 to 640nm of the unidentified peak 13 with (A) zeaxanthin, (B) chlorophyll a, (C) canthaxanthin and (D) the simulated weighted sum of these three substances with weighting factors of 0.894, 0.109 and 0.221 respectively.

3.4.5. Summary

For over-production of V5-tagged CrBKT in *Chlamydomonas* chloroplasts, cells from two strains: UVM-4 and CC-4102, were transformed with the vector pChlamy4 CrBKT-V5H. After transformation, cells were selected either in light under mixotrophic conditions or in dark under heteroptrophic conditions. In total, 258 zeocin-resistant colonies (194 light-selected and 64 dark-selected) were isolated. Among 110 tested lines (48 light-selected and 62 dark-selected), presence of CrBKT sequence could be detected only in 15 (7 light-selected and 8 dark-selected), an average success ratio of 13.6% (14.6% among light-selected, 12.9% among dark-selected lines).

Neither any ketocarotenoids nor any changes in pigment profiles were detected among all seven light-selected lines. Among eight dark-selected transformants, four were still dark green in color, the other four were pale green. Photometrical measurements as well as HPLC analysis indicated that the "de-greening" was caused by significantly reduced contents of both chlorophyll a and b. Accumulation of chlorophyll-liked products were also detected in several transformants. Canthaxanthin, product from ketolation of ß-carotene, was detected in two pale green lines at concentration of less than 10% total carotenoids. Neither astaxanthin nor any other ketocarotenoids were confirmed in any transformant.

Taken together, the results seem to suggest a relationship between light regime, chlorophyll biosynthesis and carotenoid ketolaion.

3.5. Further analysis of DP lines

3.5.1. Immunodetection of V5 epitope

The presence of V5-tagged CrBKT in DP cells was confirmed by immunodetection with anti-V5 antibody **(Figure 44)**. Theoretical molecular weight of CrBKT-V5H is 41.4 kb, however I was only able to detected bands with sizes at >70, 100 and 130-180 kDa, which might be caused by oligomerisation (protein samples were not boiled before SDS-PAGE). Small bands (around 25kDa) were also observed on the blot in all samples included the non-transformed cells.

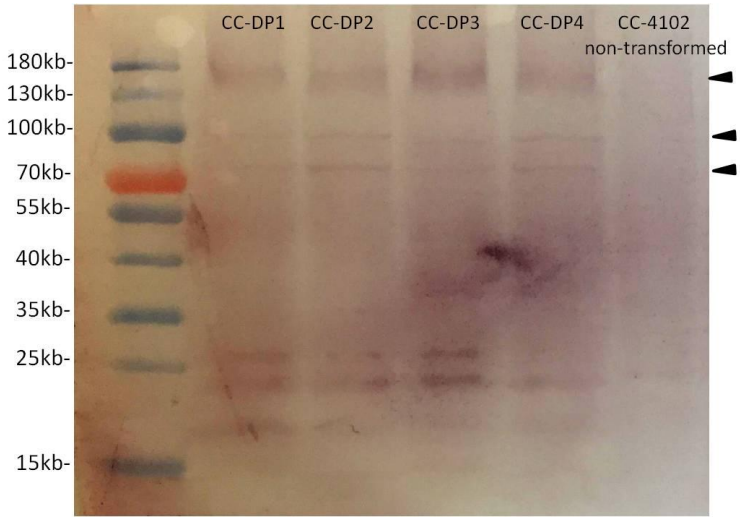

Figure 44: Immunodetection of V5-tagged CrBKT in four DP lines. Total proteins were extracted and separated with SDS-PAGE. V5-tagged proteins were recognized by anti-V5 antibody from rabbit, which was in turn detected by anti-rabbit IgG secondary antibodies conjugated with alkaline phosphatase. Protein bands were visualized by BCIP-NBT reaction overnight. Protein markers are Prestained PageRuler (Thermo Fisher). Black arrows indicate positive bands.

3.5.2. Nile Red staining

In other ketocarotenoid-accumulating algae (*Haematococcus pluvialis* and *Chromochloris zofingiensis,* also in *Chlamydomonas* zygospores), production of ketocarotenoids is accompanied by massively increased production of neutral lipids in form of lipid droplets. To compare neutral lipid production of DP cells with non-transformed ones, I stained neutral lipid bodies with Nile Red and detected their presence with fluorescence microscope. Strain CC-DP4, the transformant line with the highest content of canthaxanthin, was chosen for the analysis. Results were shown in **Figure 45**.

In general, no increased in lipid production was confirmed for CC-DP4. No large lipid bodies were detected either. Only small lipid droplets were seen in both CC-DP4 and non-transformed CC-4102 cells. Chlorophyll autofluorescence indicated that the chloroplast of CC-DP4 was intact and retained its cup-shaped form.

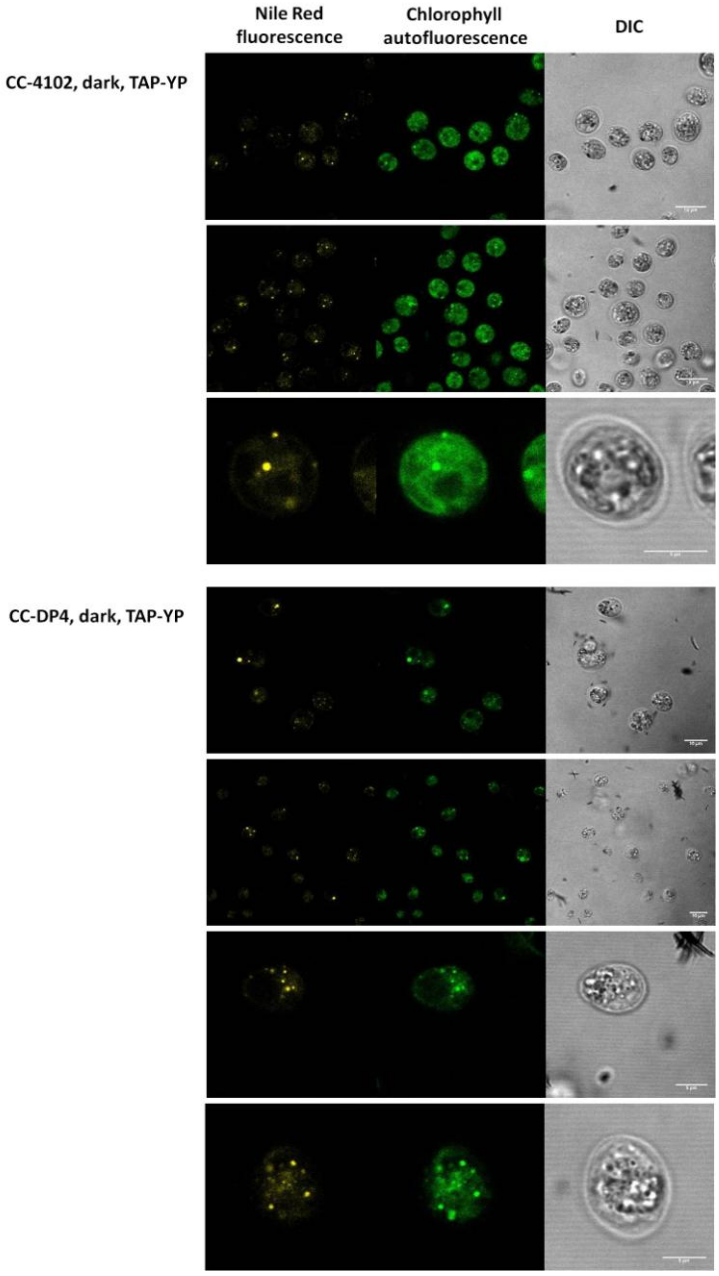

Figure 45: Nile Red staining. Nile Red fluorescence (*left*), chlorophyll autofluorescence (*middle*) and DIC pictures (*right*) from non-transformed CC-4102 and canthaxanthin-accumulating CC-DP4 cells. Note that the bright spots in chlorophyll fluorescence channel were in fact fluorescence of Nile Red in lipid droplets. Scale bars are 10µm

3.5.3. Insertion mapping

Flanking 5'-upstream and 3'-downstream sequences of CrBKT overproduction cassette in all four DP lines were amplified via Genome walking. Results after the second (nested) PCR are shown in **Figure 46**. The highest band from each sample were excised from gel, cloned into pBluescript SK(+) vector via TA cloning and sequenced with Sanger sequencing. Sequencing results are summarized in **Table 10**.

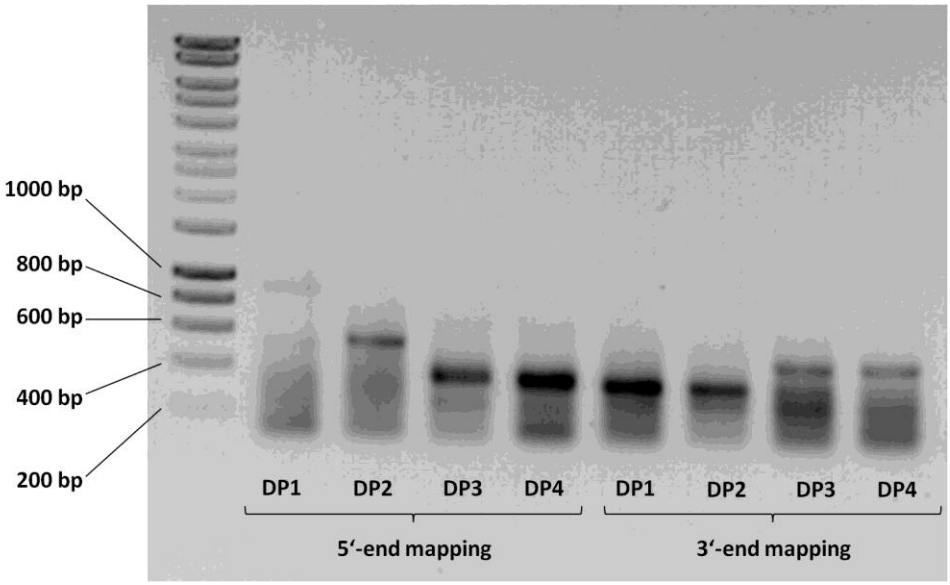

Figure 46: Amplification of 5'- and 3'-end flanking sequences for insertion mapping of four DP lines. Shown are results after the second (nested) PCR.

Table 10: Insertion mapping of DP transformants

		Obtained sequence	Positions/ annotations
CC-DP1	5'-end	0.8 kb	Chromosome 12:2721079..2721880 (intron sequence)
	3'-end	0.3 kb	Chromosome 14:2789910..2790198 (Unconventional Myosin-XIX)
CC-DP2	5'-end	0.55 kb	Unsuccessful, only 4 nucleotides from *Chlamydomonas* genome is identified, the rest are from plasmid
	3'-end	0.3 kb	Chromosome 12:4680191..4680470 Oligosaccharyltransferase, alpha subunit (ribophorin I)
CC-DP3	5'-end	0.3 kb	Unsuccessful, only plasmid sequence is obtained
	3'-end	0.3 kb	Contaminating sequence
CC-DP4	5'-end	0.45 kb	Unsuccessful, only plasmid sequence is obtained
	3'-end	0.45 kb	Contaminating sequence

It was only possible to identify the 5'-upstream region of CC-DP1 as well as 3'-downstream regions of insertion sites in CC-DP1 and CC-DP2. 5'-end insertion mapping of CC-DP2, CC-DP3 and CC-DP4 was unsuccessful, probably because the insertion sites were either very close or identical to positions recognized and cut by restriction enzymes during genome walking. 3'-end mapping of CC-DP3 and CC-DP4 yielded contaminating sequences 87% identical to *Microbacterium* sp. genomic DNA, implying that these samples were contaminated with bacteria. 5'-end and 3'-end mapping results of CC-DP1 revealed insertion sites in two different chromosomes (chromosome 14 and 12, respectively).

3.5.4 Influence of light on pigment profile of DP transformants

An interesting phenomenon was observed regarding the changes of DP lines when dark-grown cells were transferred back to light. Initially DP lines were maintained in dark on TAP-YP agar plates supplemented with zeocin (20 mg/L). Attempts to grow DP cells on zeocin-containing agar plates in light, failed repeatedly. A dilution series of different zeocin concentrations indicated that light-grown DP cells were only resistant to zeocin concentrations up to 10 mg/L. while dark-grown cells survived 20 mg/L zeocin (**Figure 47**). Intriguingly, light-grown DP cells no longer had their distinctive pale green color, instead they were dark green similar to non-transformed CC-4102 cells. HPLC analysis revealed the return of non-transformed chlorophyll/ carotenoid ratio, as well as the absence of canthaxanthin in light-grown DP cells (**Figure 48 & 49**).

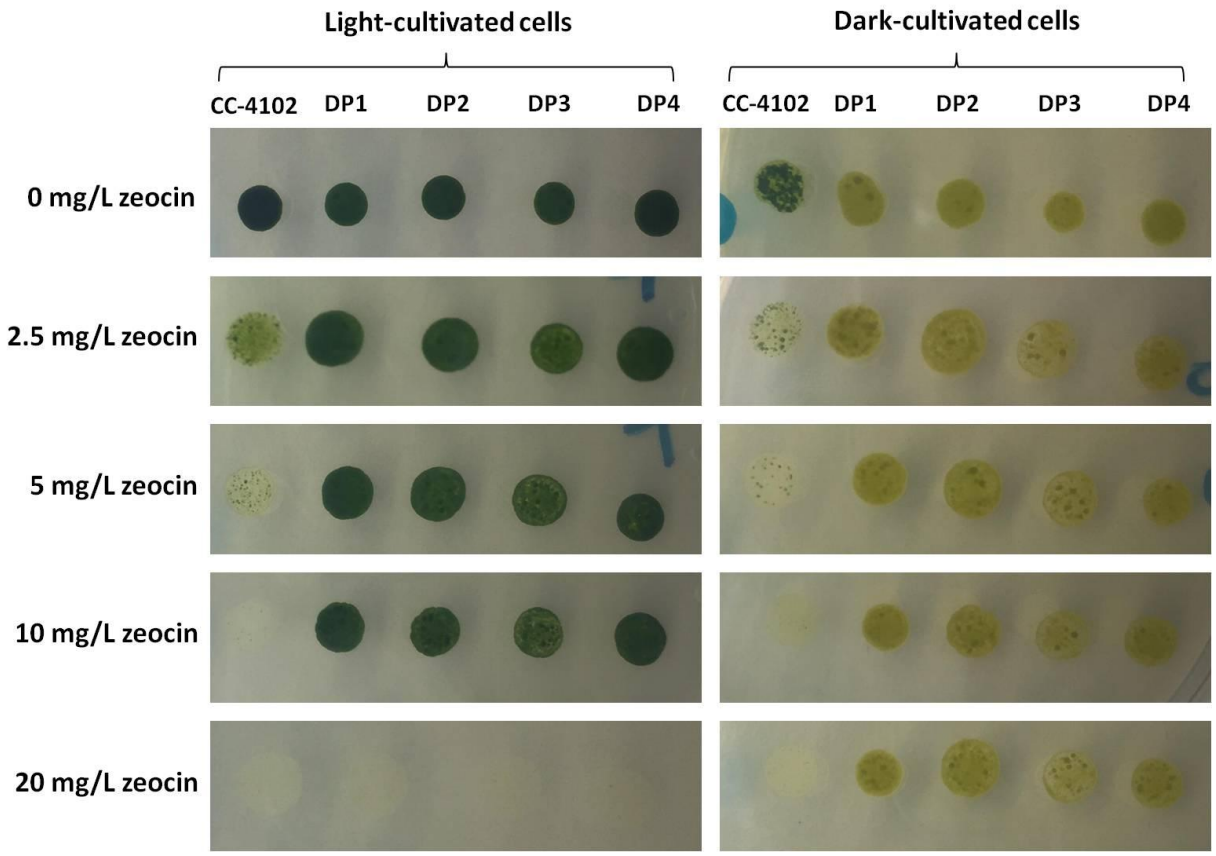

Figure 47: DP cells grown in dark and in light: light-grown DP cells did not survive 20 mg/L zeocin and returned to the dark-green color of non-transformed cells. Non-transformed CC-4102 cells were also spotted for comparision. All experiments were carried out on TAP-YP agar plate.

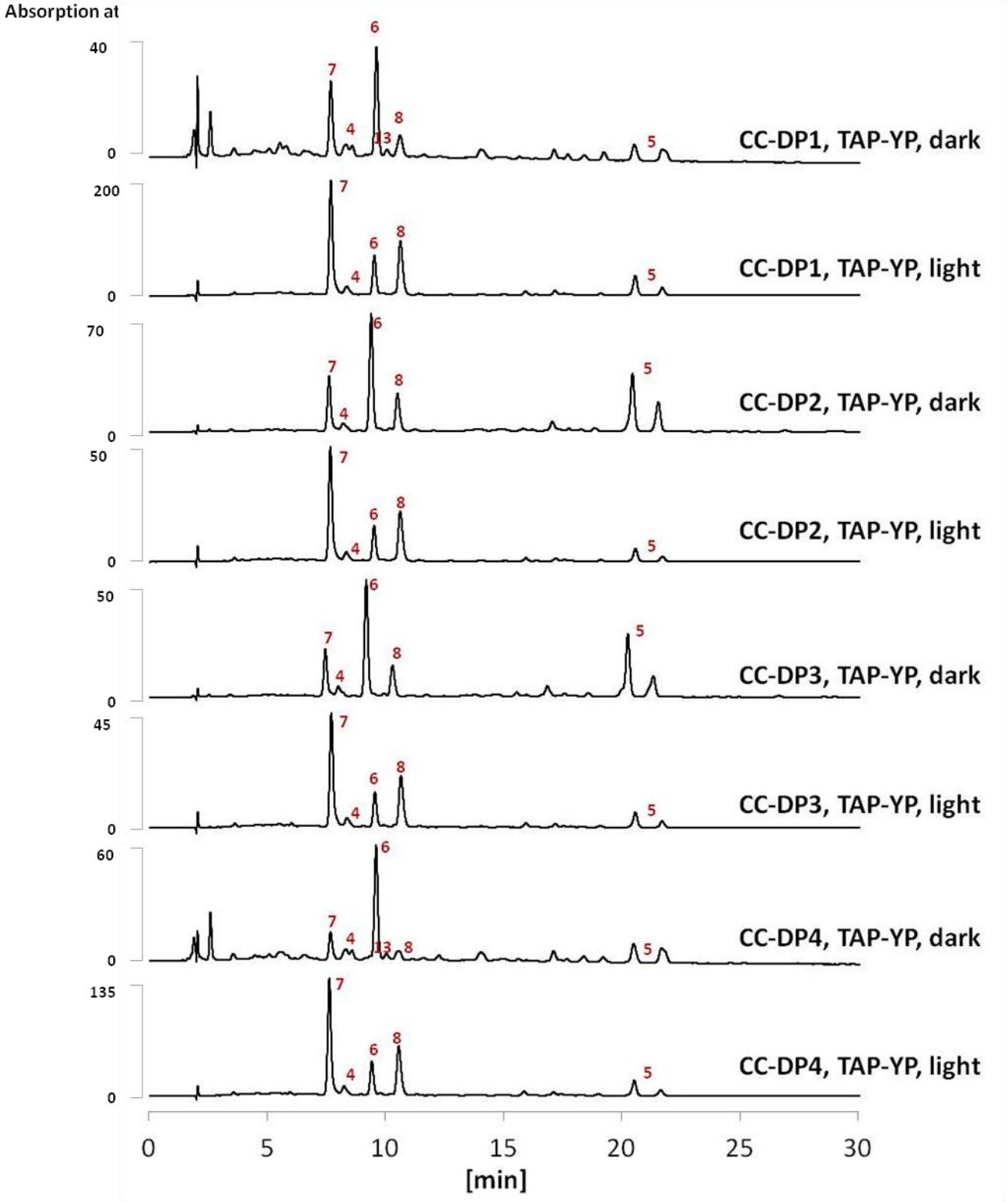

Figure 48: When DP cells were cultivated in light, their pigment profile changes dramatically. HPLC analysis revealed the return of chlorophylls, which reverted cell's color from pale green to dark green. Also canthaxanthin was no longer detectable. Pigments: 4 = lutein, 5 =α- and ß-carotene, 6= zeaxanthin, 7 = chlorophyll b, 8 = chlorophyll a, 13 = canthaxanthin. Y-axis (absorbance) of all chromatograms was normalized between 0 and 1. Detection at 450nm.

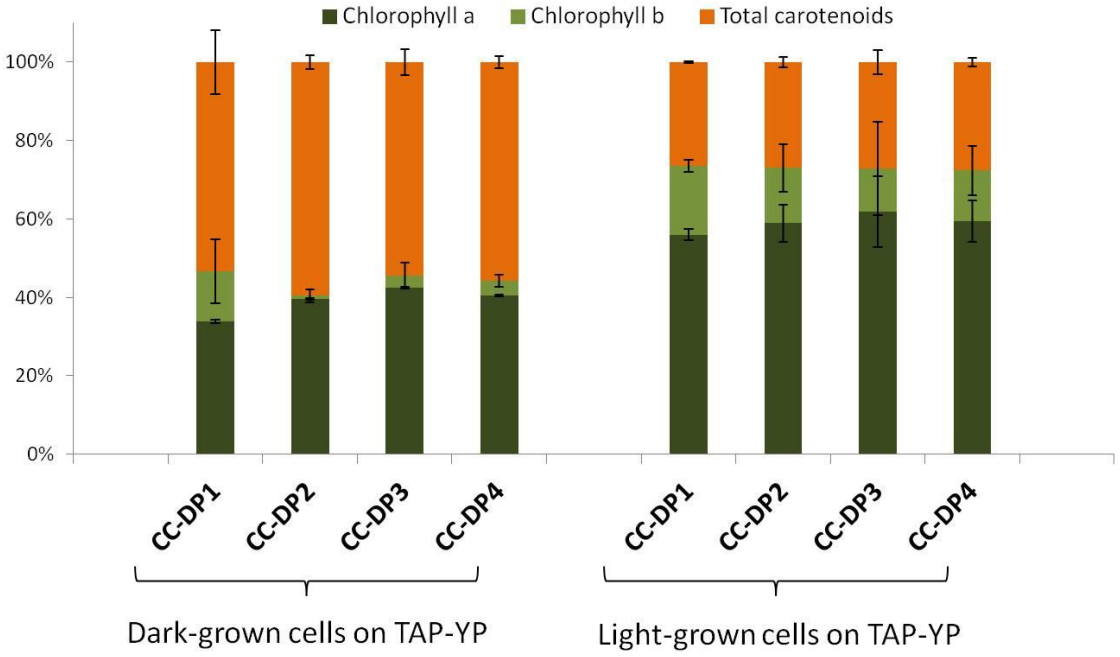

Figure 49: Differences in pigment compositions when DP cells were grown either in light or in dark. Light-grown cells saw their chlorophylls/carotenoids ratio reverted back to normal values of non-transformed cells.

PCR analysis with three different primer pairs showed that both *ble* and *CrBKT* genes were still present in the genome and correctly connected via 2A sequence after DP cells were cultivated in light (**Figure 50**).

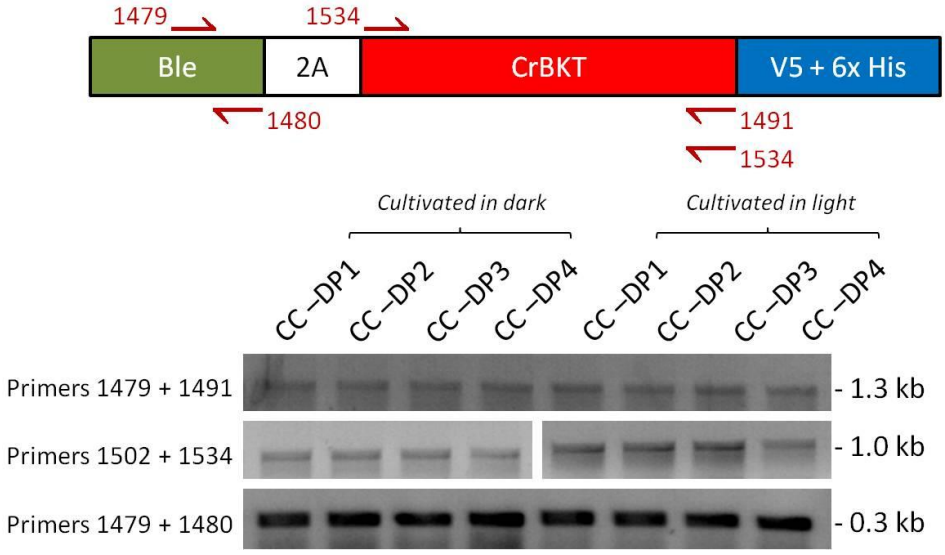

Figure 50: The Ble2A-CrBKT was still in DP cell's genome regardless if they were cultivated in dark or in light. Three primers pairs were used to confirm the transgene: 1479 + 1491 (Ble2A-CrBKT gene), 1502 + 1534 (CrBKT gene) and 1479 + 1480 (Ble gene). Expected amplicon sizes were 1.3 kb, 1.0 kb and 0.3 kb respectively. Primer binding positions were also shown.

4. DISCUSSION

4.1. Ketolase activity of CrBKT was confirmed by *in vivo* assay in *E. coli*

Ketolase activity of CrBKT was to be confirmed by *in vivo* assay in *E. coli* **[117]**. In this assay, CrBKT was heterologously produced in carotenoid-accumulating *E. coli* cells. Ketolation lead to changes in carotenoid profile which could be detected by HPLC. ß-carotene- and zeaxanthin-accumulating strains of *E. coli* were successfully generated by introducing into cells the plasmids pACCAR16 Δ*crt*X or pACCAR25 Δ*crt*X **[111].** pACCAR25 Δ*crt*X differed from pACCAR16 Δ*crt*X by harbouring the gene for crtZ, which catalyzed the oxidation of ß-carotene to zeaxanthin. HPLC data confirmed that ß-carotene and zeaxanthin were the main carotenoids in these strains. In cells, these carotenoids were probably incorporated into plasma membrane **[146]**.

In the next step, CrBKT, encoded in plasmid CrBKT pBSK, was produced in cells under the control of the *lac* promoter. Due to its high hydrophobicity, CrBKT was likely to be also incorporated into *E coli* plasma membrane as well, where it met the substrates – ß-carotene and zeaxanthin - and ketolation took place. As the results, canthaxanthin and astaxanthin were formed. Only traces of residual ß-carotene and zeaxanthin, and very small amount of monoketolation intermediates (echinenone and adonixanthin) could still be detected. These data confirmed the earlier published results that CrBKT was a diketolase capable of adding carbonyl group to both ionone rings with high efficiency **[117]**. In our double-transformant of CrBKT pBSK and pACCAR25 Δ*crt*X, a small amount of canthaxanthin, ketolation product of ß-carotene, was discovered belongside astaxanthin, ketolation product of zeaxanthin. This result could be explained by the competition between CrBKT and CrtZ, and a small amount of ß-carotene, instead of being hydrolyzed by CrtZ to zeaxanthin, was instead converted into canthaxanthin by CrBKT.

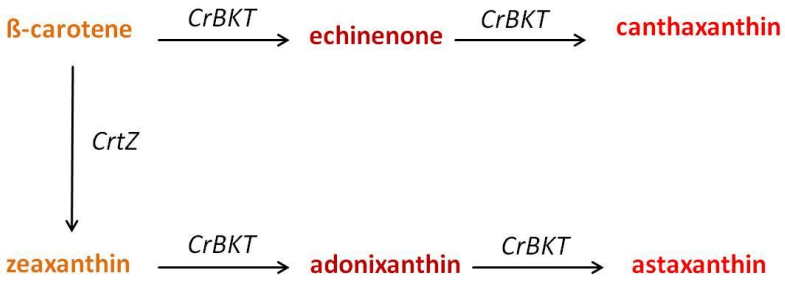

Figure 51: Reactions involved in *E. coli*-based ketolase activity assay.

After the ketolase activity of CrBKT had been successfully confirmed, in the next experiments I tried to answer the question if fusion of mCherry onto the N- or C-terminus of CrBKT would affect its activity. The addition of a hydrophilic domain (i.e. mCherry) to a generally hydrophobic protein could potentially interfere with protein folding and thus affect its activity. Using the same *E. coli* approach, I introduced mCherry-CrBKT and CrBKT-mCherry into carotenoid-accumulating cells and analyzed the changes in carotenoid profiles. Protein production was successfully confirmed by in gel fluorescence detection of mCherry. Production of the C-terminal fusion construct, CrBKT-mCherry, also resulted in complete ketolation of ß-carotene to canthaxanthin and of zeaxanthin to astaxanthin, implying that C-terminal fusion did not affect the ketolase activity. In light of the *in silico* sequence analysis,

CrBKT's C-terminus is predicted to not be anchored in the lipid membrane, thus any change here is unlikely to interfere with the reaction center.

In the case of mCherry-CrBKT, conversion of zeaxanthin to astaxanthin was also complete. In contrast, conversion of ß-carotene to canthaxanthin was incomplete, as indicated by a significant amount of residual ß-carotene. These results implied that N-terminal mCherry fusion seemed to affect not only its activity but also, intriguingly, substrate specificity, though the N-terminus of CrBKT is also predicted to not be membrane-anchored. However, before any conclusion could be drawn, caution is advised since many factors that could also affect ß-carotene conversion rate such as protein production level, protein folding, carotenoid production level, availability of cofactors etc. remain largely unknown.

In retrospect, the *in vivo* assay in *E. coli* was a quick and reliable method to confirm the ketolase activity of CrBKT. On the other hand, this approach suffers from several drawbacks. Absolute quantification of protein activity was difficult due to discrepancies in protein production levels, substrates as well as cell's own metabolism. Produced proteins could form inclusion bodies and do not display its full activity. Coordination between protein production and carotenoid production also prove problematic: CrBKT was predominantly produced during the *log* phase while carotenoid accumulation only started in the earnest after cells had reached stationary phase (personal communication with Dr. Breitenbach, University Frankfurt). A better alternative for assessment of ketolase activity would be an *in vitro* enzymatic assay. To my best knowledge, no *in vitro* assay has been established for CrBKT. *In vitro* assays of other carotenoid-processing enzymes were only limitedly successful due to lack of co-factors as well as insolubility of both enzyme and substrate **[147]**. The latter requires addition of organic solvents or lipids. Ideally, both enzyme and substrate should be together incorporated into artificial lipid membrane (e.g. liposome, nanodiscs). In the working group Kaldenhoff, we have successfully established the protocol to express and incorporate proteins into lipid membrane using cell-free production system **[148]**. Such approaches would be promising for future research of carotenoid-processing proteins.

4.2. Transformation of *Chlamydomonas reinhardtii*

Transformation was the crucial step for generation of any transgenic *Chlamydomonas* lines. As tool to assess and optimize transformation protocol of *Chlamydomonas reinhardtii* as well as protein production with ble2A system, test plasmid pBR9 mCherry **[51]** was used. As seen in **Section 3.1.4**, both *Chlamydomonas* strains, UVM-4 and CC-4102, were well amendable for transformation. Due to their difference in cell wall structure, different transformation methods were used: glass bead transformation for UVM-4 and electroporation for CC-4102. From each batch of transformation, 100-200 colonies appeared on agar plates, providing enough transformants for subsequent analysis. Fluorescence measurements of independent transformant lines on agar plates revealed a random distributed pattern among mCherry signal, supporting the model of Zhang et al **[33]** in which transgene is randomly incorporated into host's genome via illegitimate recombination. Interestingly, electroporation-transformed CC-4102 yielded not only better transformation efficiency but also better protein production than glass-beads-transformed UVM-4. It was also observed that among ~ 50 randomly picked zeocin-resistant transformants, both the ratio of mCherry-fluorescent cells (defined as cells with fluorescence higher than fluorescence of non-transformed cells plus three

standard deviation) and the mean fluorescence were higher in CC-4102 than UVM-4. This finding came as surprise since UVM-4 is a *Chlamydomonas* strain specifically engineered for better transgene expression (it is the exact reason why it was chosen for this project). To my best knowledge there has not yet been any report of transgene expression in CC-4102 but since its mutations are in carotenoid biosynthetic pathways, the change that it could somehow display significantly higher than wild-type *Chlamydomonas* is minute. In literature, while UVM-4 has been successfully used for protein production by many working groups **[52]**, **[73]**, **[149]**, there are also several reports of failure to attain higher production levels with this strain **[75]**, **[150]**. Our failure to achieve high mCherry production and later to detect any ketocarotenoid-producing UVM-4 indicates that UVM-4 is not suitable for our experiment.

Once transformation protocols had been established, I proceeded with transformation of CrBKT-containing plasmids into *Chlamydomonas*. Despite a large number of colonies were obtained from agar plates, screening process was significantly hampered by very low ratio with which CrBKT integration into genome could be confirmed. In both cases of pBR32 psaD CrBKT-mCherry and pChlamy4 CrBKT V5H, only around 10% of the zeocin-positive lines did indeed harbor the CrBKT gene. On the other hand, PCR also revealed that 8/8 (100%) of randomly picked zeocin-resistant lines did indeed contain the *ble*2A gene, implying that the presence of this gene is essential for antibiotic survival. Taken together, these data pointed to a very low co-integration rate of selection marker *ble*2A and the gene of interest *CrBKT*. This finding is in stark contrast of generally very high co-integration rates reported for ble2A system in literature: 70% **[46]**, 90% **[151]**, 51.3% **[75]**. Unfortunately, no PCR was performed with ble2A-mCherry transformants to assess co-integration rate here. Analysis of mCherry fluorescence however did show that 76% of CC-4102 transformants displayed higher mCherry-to-chlorophyll signal than non-transformed cells, implying that also here co-transformation rate must be high as well.

What could possibly cause such low co-integration rates? The model in which transgene is incorporated into *Chlamydomonas* genome **[33]** could shed light into this puzzling question. According to this model, plasmid DNA is subjected to digestion by sequence-specific endonucleases before and during entry into recipient cells during transformation. If the sequence of CrBKT somehow contains one or several recognition sites of these endonucleases, endonucleolytic cleavage would destroy the expression cassette, resulting in two separate DNA fragments: one with promoter and the intact ble2A gene, the other with fragmented CrBKT gene and terminator. Though lacking the terminator sequence, the former could still be incorporated into *Chlamydomonas* genome, yielding zeocin-resistant colonies without CrBKT gene. Though highly speculative, this hypothesis could explain very well why low co-transformation rates only occurred with our two CrBKT plasmids.

The next question is obviously how to prove that such endonuclease recognition sites exist within CrBKT sequence. To answer this question, I devise the following experiment (**Figure 52**): genome of *Chlamydomonas reinhardtii* is cleaved specifically by CRISPR/ Cas9. The choice of CRISPR/ Cas9 allows rapid sequencing of insertion sites without the time-consuming genome walking. Cleavage locus is carefully chosen to facilitate quick visual screening of insertion transformants based on disrupted phenotype. Several candidates could be named: CpSPR43 (whose disruption results in abnormally high chlorophyll a/ b ratio), ChlM (severe reduction of chlorophylls concentration) **[152]**, PSY1 (white colonies due to knock-out of both carotenoids and chlorophylls biosynthesis) **[153]**. sgRNA-Cas9

ribonucleoprotein together with PCR-amplified CrBKT are introduced into cells via electroporation **[152]**. Upon obtaining insertion transformants, the whole insertion sites are sequenced using known flanking primers. If CrBKT is susceptible to endonucleases during transformation, it is likely that only a fraction of this gene would be insertion into Cas9-induced double strand break. Careful alignment of several insertion site sequences would probably reveal if any endonuclease recognition sites exist within CrBKT gene.

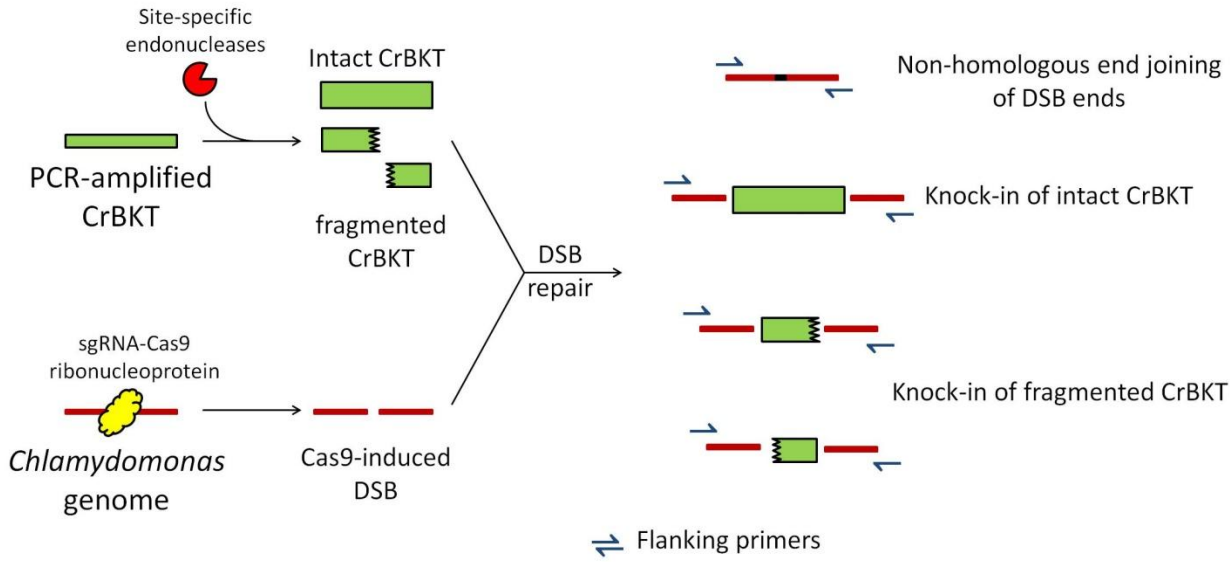

Figure 52: Proposed experiment for elucidation of putative endonuclease site(s) within CrBKT sequence. DSB: double-strand break

4.3. Overproduction of CrBKT leads to accumulation of canthaxanthin

At least two transformant lines from transformation of CC-4102 were found accumulating canthaxanthin, the ketolation product of ß-carotene, implying that CrBKT was produced and active in *Chlamydomonas* cells. The localization of CrBKT is an interesting point of discussion. Inside the cells, ß-carotene is located in chloroplast and either associated to photosynthetic complexes or stored in the eyespot **[154]**. In order for the ketolation reaction to take place, it is logically presumed that CrBKT would have to be located in chloroplast as well. This presumption is further reinforced by the finding of a putative chloroplastic transit peptide in the sequence of CrBKT. In this aspect, CrBKT differs greatly from *Haematococcus pluvialis* HpBKT and *Chromochloris zofingiensis* CzBKT. Both HpBKT and CzBKT are localized in cytosol **[109]**, **[116]**; their sequence analysis failed to detect any chloroplast transit peptide. Such difference may reflect the different pathways with which ketocarotenoids are formed in these microalgae. In *Haematococcus pluvialis*, astaxanthin is produced from *de novo* synthesized ß-carotene which is presumably exported from chloroplast into cytosol **[155]**. The ketolation and hydroxylation of ß-carotene to astaxanthin takes place on the surface of ER-associated lipid droplets **[156]**. On the other hand, in *Chlamydomonas* zygospores ketocarotenoids are produced directly from existing primary (photosynthetic) carotenoids **[123]**. In this case, the localization of CrBKT to chloroplast makes perfect sense.

The complete absense of astaxanthin also gives some food for thought. No astaxanthin was confirmed in any transformants, despite the fact that zeaxanthin was the predominant carotenoid in

CC-4102 cells. As seen with *E. coli* assay, CrBKT is capable of converting zeaxanthin to astaxanthin with high efficiency. The lack of astaxanthin could be attributed to one of the following causes:

(1) Zeaxanthin and CrBKT were spatially separated. In CC-4102 cells, zeaxanthin were located in thylakoid membrane as part of the light harvesting antenna **[157]**. *Chlamydomonas* chloroplast is however a complex structure with many distinct compartments (**Figure 53**). If CrBKT is not located in thylakoid membrane but incorporated into other parts of the chloroplast such as pyrenoid or eyespot, then no reaction could take place because of enzyme-substrate separation.

(2) Zeaxanthin was co-localized with CrBKT but its association with proteins from light harvesting complexes prevents ketolation. Ketolation reaction requires free carotenoids, which are actually rare in microalgae. In *Chlamydomonas*, all carotenoids are one way or the other associated into some caroteno-protein complexes. This is one aspect where the *in vivo* test in *E. coli* poorly represents the reality in algal cells. In carotenoid-accumulating *E. coli*, carotenoids are freely available in the plasma membrane and no such constrain is put on CrBKT. Many authors working on higher plants also commented on the low substrate availability as potential reason for failure/ low level of ketocarotenoid accumulation **[158]**, **[159]**.

(3) Zeaxanthin and CrBKT were co-localized but reaction could not take place due to lack of substrate or unfavorable redox-conditions. It is easy to forget that the ketolation reaction is a redox reaction and another reaction partner is oxygen. Several co-factors are also required without which no reaction could take place. Study of *Haematococcus pluvialis* HpBKT showed that the presence Fe^{2+}, ascorbic acid, 2-oxoglutarate and catalase were essential for ketolase activity **[160]**. The lack of suitable lipid environment could also be a contributing factor. Both CrBKT and its carotenoid substrates are highly hydrophobic and thus require hydrophobic milieu for maximal efficiency. In all ketocarotenoid-producing microalgae, ketocarotenoid biosynthesis is always preceded by significant neutral lipid biosynthesis, which forms lipid bodies and serves as metabolite sinks **[110]**, **[123]**. Inhibition of lipid synthesis also suppresses ketocarotenoid formation **[123], [161]**. As seen with the Nile Red staining, no significant formation of lipid bodies was observed in DP lines. The fact that canthaxanthin could still be detected could be explained by the fact that ß-carotene containing eyespots are structurally similar to lipid bodies **[154]**, thus providing the suitable surrounding for ketolation reaction.

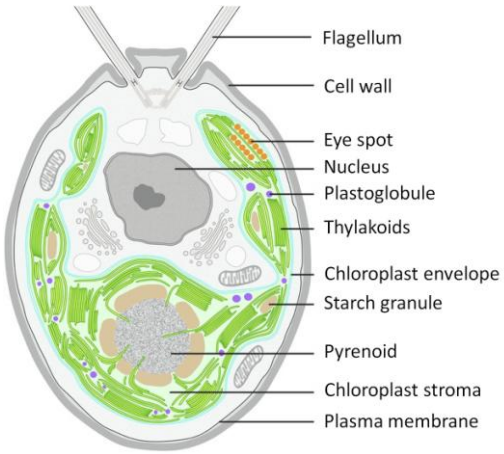

Figure 53: Structure of *Chlamydomonas* chloroplast. Modified from **[162]**

4.4. Reduction of chlorophylls in DP transformants

Four transformant lines, CC-DP1, 2, 3 and 4, stood out due to their pale green color. The pale color is explained by their much reduced chlorophylls/ total carotenoids ratio. Among these, canthaxanthin could be discovered in at least two lines (CC-DP1 and CC-DP4). Also in these two lines, elevated accumulation of several chlorophyll-like products, presumably either degradation products of chlorophyll or intermediates from chlorophyll biosynthesis pathways, were detected. On the other hand, in all dark green transformants, no trace of ketocarotenoids could be confirmed. Insertion mapping data, though still incomplete, implied it is unlikely that the expression cassette was inserted amid any chlorophyll-biosynthetic gene, thus the reduction of chlorophylls could not be attributed to mere gene disruption. Interestingly enough, the same phenomenon has also been repeatedly reported in ketocarotenoid-producing higher plants **[143], [144], [163], [164], [165], [166]**. The plant species, used variants of BKT and (if specified) decrease of chlorophyll content in these studies are listed in **Table 11**. Evidences thus point to a general correlation between ketocarotenoid production and chlorophyll reduction/ degradation regardless of species, ketocarotenoids or BKT variants.

Table 11: Correlation between ketocarotenoid production and chlorophyll reduction in many metabolic engineering studies

Studies	Plant (tissue)	ß-carotene ketolase	Detected ketocarotenoids	Reduction of chlorophylls
Gerjets et al. 2007	*Nicotiana tabacum* (leaves)	*Synechocystis* CrtO	Echinenone 4-ketolutein	26%
Zhu et al. 2007	*Nicotiana glauca* (leaves)	*Synechocystis* CrtO	Echinenone 3-Hydroxy echinenone 4-ketolutein 4-ketozeaxanthin	34%
Hasunuma et al. 2008	*Nicotiana tabacum* (leaves)	*Brevundimonas* CrtW	Fritschiellaxanthin Canthaxanthin 3-Hydroxy echinenone Adonirubin 4-Ketoantheraxanthin Astaxanthin	58%
Röding et al. 2015	*Nicotiana tabacum* (leaves)	*Chlamydomonas* CrBKT	Astaxanthin Canthaxanthin 4-Ketoantheraxanthin Echinenone 3-Hydroxy echinenone Adonirubin Adonixanthin	not specified
Fujii et al. 2016	*Lactuca sativa* (leaves)	*Brevundimonas* CrtW	Astaxanthin Canthaxanthin Echinenone	not specified
Mortimer et al. 2017	*Nicotiana glauca* (leaves)	*Brevundimonas* CrtW	Echinenone 4-ketolutein	not specified
Own study	*Chlamydomonas* CC-4102	*Chlamydomonas* CrBKT	Canthaxanthin	~ 60%

It is worth noticing that chlorophyll reduction also occurs naturally during the course of ketocarotenoid biosynthesis in microalgae. The green vegetative *Haematococcus pluvialis* cells, for example, are photosynthesis-active and accumulate little to no astaxanthin. Upon exposed to stress conditions (e.g. nitrogen limitation, strong light, etc.), cell growth is arrested and cellular chlorophyll contents are rapidly reduced by factor of 2 over a period of just 2 days, afterwards they stay more or less stable. Astaxanthin production starts later and takes also much longer to reach the final concentration **[167]**. Similarly, the green haploid *Chlamydomonas reinhardtii* cells do not produce ketocarotenoid either. After mating, the diploid zygotes undergo maturation in dark to zygospores. It is discovered that from the onset of zygote maturation, chlorophyll contents decrease constantly and in just two weeks, sink to 5% of their original amounts. At the same time, concentrations of ketocarotenoids rise continuously and reach their final concentration after 2-3 weeks **[123]**. (There is almost no lag between chlorophyll reduction and ketocarotenoid biosynthesis in case of *Chlamydomonas* zygospore because, as already stated, CrBKT utilizes existing primary carotenoids as substrate instead of having to wait for *de novo* synthesized ß-carotene as in case of *Haematococcus*).

To my best knowledge, there is yet to be a study which directly addresses the relationship between ketocarotenoid biosynthesis and chlorophyll reduction. Until then, the mechanism behind such correlation still remains a mystery. Chlorophyll reduction is seen as a potential problem if any engineered plants or microalgae are to be used as industrial production platform of ketocarotenoids because it hampers photosynthetic performance. In higher plants, it is possible to limit ketocarotenoid biosynthesis to non-photosynthetic tissues such as fruits, seedlings or flowers **[120], [121], [164]**. Such solution is hardly applicable to unicellular organism such as microalgae. Thus understanding the mechanism behind the correlation between ketocarotenoid biosynthesis and chlorophyll reduction is vital for the prospect of any microalgal ketocarotenoid-producing platform in future.

4.5. Drastic changes in pigment profiles of DP lines when they are grown in light

Pigment profiles of DP lines changed drastically depending if they were grown in dark or in light. In dark, DP cells were pale green in color and produced canthaxanthin. In light, cells returned to normal dark green hue and canthaxanthin production could no longer be detected. The light-grown cells were also more susceptible to zeocin. While dark-grown cells could survive zeocin concentration of 20 mg/L, such concentration was lethal to light-grown cells. Since both dark- and light-grown cells were cultivated in TAP-YP medium, the influence of medium could be excluded as explanation. Genomic instability (i.e. loss of transgene) could also be excluded, since presence of the intact ble2A-CrBKT was confirmed in both dark-and light-grown cells via PCR.

The reduced zeocin resistance on the other hand points to decrease in transgene expression level. Zeocin resistance is conferred by Ble protein not as result of enzymatic degradation but through drug sequestration: two molecules of antibiotics are removed through binding with a Ble dimer **[42]**. Consequently, Ble production levels are positively correlated to zeocin resistance **[168]**. Furthermore, as the result of bicistronic ble2A-CrBKT construct, the ratio of Ble to CrBKT is theoretically 1:1. Thus decrease in Ble concentratration also means production of CrBKT in light-grown cells was lower. This hypothesis is also in good agreement with the observation of DP cells returning to dark green color

and losing canthaxanthin, since ketocarotenoid production interferes with chlorophyll biosynthesis, as discussed in **Section 4.4**.

What caused the decrease of transgene expression? The decrease of both Ble (lower zeocin resistance) and CrBKT levels (loss of phenotypes associated with ketocarotenoid biosynthesis) hints to gene silencing on RNA level. In our bicistronic construct, ble2A-CrBKT was transcribed as one mRNA molecule before individual proteins were formed separately during translation. Transcription is driven by strong constitutive promoter HSP70/ RBCS2, which shows similar activities both in dark and in light **[58]**, thus transcriptional gene silencing is unlikely the cause. Unfortunately, post-transcriptional gene silencing (PTGS) in *Chlamydomonas reinhardtii* is still largely a poorly understood topic. The pioneering work of Cerutti et al. **[66],** who transformed *Chlamydomonas* with the *aadA* gene conferring spectinomycin resistance and observed that its transcripts were degraded post-transcriptionally, remains the first and sadly, only study so far which addresses directly the questions of mechanisms behind PTGS in *Chlamydomonas*. On the other hand, available genomics and transcriptomics data of *Chlamydomonas* prove valuable for identifying the participating components. Small interfering RNA (siRNA), microRNA (miRNA) as well as orthologs of Argonaute proteins, essential component of RNA-induced silencing complex (RISC) have been successfully identified in *Chlamydomonas reinhardii* **[169]**, **[170]**. Targeted gene silencing by RNAi is also achieved in *Chlamydomonas* as well **[171]**, **[172]**. However, to my best knowledge, there still has not been any report of a light-dependent PTGS mechanism. Such mechanis, if exists, could explain the changes in DP cell's pigment profile under different light conditions.

The aforementioned phenomenon could also explain my failure to detect any ketocarotenoid-producing transformants among light-selected ones with either pBR32 psaD-CrBKT-mCherry or pChlamy4 CrBKT V5H. It is entirely possible that one or several of such lines did harbor the CrBKT genes, however CrBKT production was suppressed by light and thus phenotypes (reduction of chlorophylls, production of canthaxanthin) could not be discovered.

4.6. Future outlooks: towards astaxanthin production in *Chlamydomonas reinhardtii*

I started the project with the aim of engineering the ketocarotenoid biosynthetic pathway into *Chlamydomonas reinhardtii* green haploid vegetative cells by overproducing its own CrBKT, which would hopefully lead to production of the valuable pigments canthaxanthin and astaxanthin. Though quite straightforward, several unforeseeable obstacles have to be overcome along the way: very low CrBKT incorporation rate, low protein production, light-independent phenotypes, etc. At the end, only biosynthesis of canthaxanthin is confirmed and at quite low level (10% total carotenoids). This section is devoted to the discussion of future approaches to finally turn *Chlamydomonas reinhardtii* as a feasible industrial astaxanthin-producing organism.

The encounter with so many unexpected problems during my project is a good indication that our knowledge of *Chlamydomonas* genetic engineering is still very limited. Until more researches are carried out in this direction, such problems are sadly unavoidable. The future outlook of *Chlamydomonas* genetic engineering has already been discussed in **Section 1.3.4**. With better promoters, better reporter genes, better strains, better transformation methods, more precise

genome editing approaches, better understanding of gene silencing mechanisms, it is expected that transgene expression in *Chlamydomonas* would not be as troublesome as it is today and researchers could confidently try their hand at more novel and more radical concepts with still a reasonable chance of success.

The conversion from ß-carotene to astaxanthin involves two different reactions: ketolation and hydroxylation, thus requires both ketolase and hydroxylase. Since ß-carotene hydroxylase is ubiquitous among plants and microalgae (it catalyzes the step from ß-carotene to zeaxanthin), some studies opted to rely on host's indigenous hydroxylase for the hydroxylation of canthaxanthin to astaxanthin. While this approach simplifies experiments (dealing only with ketolase instead of both enzymes), the low activity of native hydroxylase could result in metabolic bottlenecks, low level of astaxanthin and accumulation of non- and partly hydroxylated intermediates **[121]**. Thus to ensure the formation of astaxanthin, cooperation of both enzymes is required. Several hydroxylases from astaxanthin-producing microalgae *Haematococcus pluvialis* **[173]**, *Chromochloris zofingiensis* **[116]** as well as *Chlamydomonas reinhardtii* **[174]** have been identified and characterized. Better ketolase-hydroxylase cooperation could be achieved via novel concepts such as artificial enzyme channel **[175]**, in which they are organized with help of scaffolding protein together into a multienzyme complex **(Figure 54)**. Alternatively, the unique dual functionality of *Xanthophyllomyces dendrorhous*, astaxanthin synthase CrtS (i.e. it could catalyze both ketolation and hydroxylation reaction **[112]**) could also be exploited.

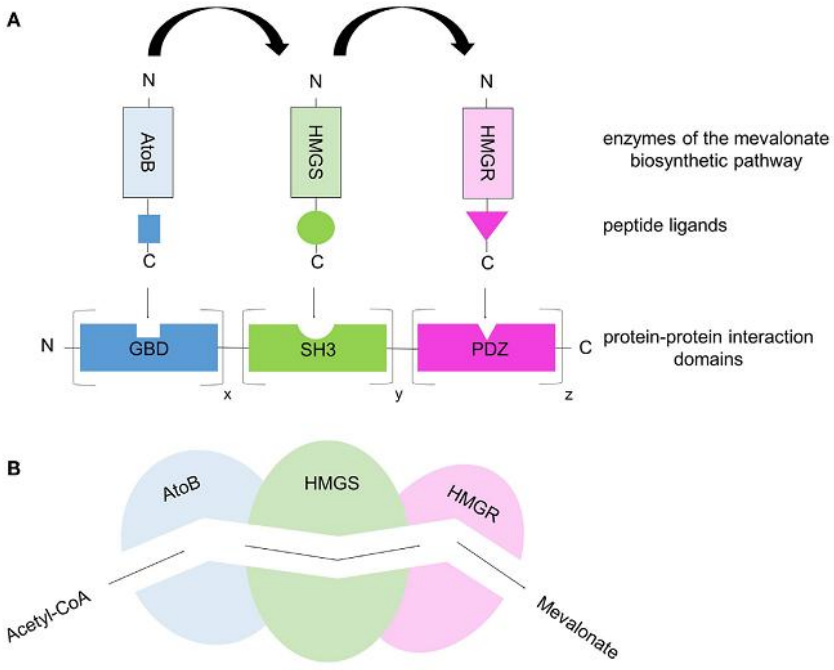

Figure 54: the artificial enzyme channel concept. Three individual enzymes (in this case, from mevalonate pathway) are connected together via scaffolding proteins into multienzyme complex that enable direct conversion from acetyl-coA to mevalonate with little interference from competing pathways. Modified from **[175]**

Introduction of foreign proteins is however only the beginning of metabolic engineering. The interference between ketocarotenoid- and chlorophyll biosynthesis makes it imperative that these

two processes should be separated. The *Chlamydomonas* eyespot is probably a good candidate as location for ketocarotenoid production. In *Chlamydomonas reinhardtii*, eyespot is formed from layers of carotenoid-rich (predominantly ß-carotene) lipid globule inside chloroplast, thus provides both substrate and the required hydrophobic environment for the ketolation reaction. Eyespot is also the location of many proteins involved in photoreception, phototaxis and Circadian cycle. Though no transit peptide is known to specifically target proteins into eyespot, it is not inconceivable that such sequence exists and could be discovered from sequence alignment of known eyespot proteins. By moving the ketocarotenoid biosynthesis into eyespot, not only is the problem with interference into chlorophyll biosynthesis eliminated but higher yield is also expected due to more favourable reaction conditions there.

Substrates for ketocarotenoid biosynthesis are supplied by the general carotenoid biosynthetic network. Thus to attain high yield of ketocarotenoids, it is essential that overall output of carotenoid biosynthesis should be increased as well. Carotenoid biosynthesis begins with the production of isopentenyl pyrophosphate (IPP), the common building unit of all terpenoids. In *Chlamydomonas reinhardtii*, IPP is synthesized via the non-mevalonate pathway (also called the MEP pathway). The attempt to increase IPP production by over-producing key enzymes of the non-mevalonate pathway, 1-deoxy-D-xylulose 5-phosphate synthase (DXS) and reductase (DXR), was met with only moderate success **[90]**. On the other hand, overproduction of *Chromochloris zofingiensis* phytoene synthase (PSY) in *Chlamydomonas* leads to significant increase of violaxanthin and lutein, indicating that the reaction from GGPP to phytoene might represent the rate-limiting step of the whole process **[176]**. Another successful strategy to enhance carotenoid contents is the overproduction of the Orange protein (OR). Orange gene is first identified in a cauliflower mutant with abnormal orange color (hence its name) and encodes a plastid-localized DnaJ-like molecular chaperone **[177]**. An OR-like gene has been identified in *Chlamydomonas* genome and its overproduction leads to almost doubled amounts of lutein and ß-carotene **[90]**. It is postulated that OR supports the action of PSY as its chief posttranscriptional regulator. It remains to be seen if the overexpression of PSY and OR genes, in combination with our CrBKT cassette, could lead to significant accumulation of ketocarotenoids.

Once high yield production of ketocarotenoids has been achieved, the valuable pigments still have to be extracted from cells. Compared to the thick cell walls of *Haematococcus pluvialis* and *Chromochloris zofingiensis*, the soft proteinous cell wall of *Chlamydomonas reinhardtii* is immensely advantageous regarding cell breakage and pigment extraction. Still, cells have to be collected and concentrated, which contribute to a significant part of production cost. Ideally, ketocarotenoids should be automatically secreted into media. In *Chlamydomonas*, secretion of recombinant proteins has been routinely achieved **[46]**, **[52]**, **[178]**. Researches on secretion of other substances are however much rarer. In this aspect, perhaps strategies from other species could be applied for *Chlamydomonas* as well. Carotenoid secretion facilitated by transporters from ATP-binding cassette protein family (ABC transporters) has been reported in *E. coli* **[179]** and *Saccharomyces cerevisiae* **[180]**, though in both case the cultures have to be layered with a hydrophobic solvent (decane or vegetable oil), which serves as metabolite sink for carotenoids. Alternatively, ketocarotenoids could also be exported together in a complex with carotenoid-binding protein. Several of such proteins have already been identified and characterized: orange carotenoid proteins (OCP) from cyanobacteria **[181]**, crustacyanin from crustaceans **[182]**.

LIST OF ABBREVIATIONS

ABC	ATP-binding cassette protein family
BKT	ß-carotene ketolase
Ble	Selection marker against zeocin
Ble2A	Bicistronic construct in which ble gene is fused to FMDV's 2A sequence
CHYB	Carotene ß-hydroxylase
CHYE	Carotene ε-hydroxylase
Cr	*Chlamydomonas reinhardtii*
CRC	Chlamydomonas Resource Center
CRTISO	Carotenoid isomerise
CTAB	Cetyl trimethylammonium bromide
cTP	Chloroplast transit peptide
Cz	*Chromochloris zofingiensis*
DMSO	Dimethyl sulfoxide
DNA	Deoxyribonucleic acid
DP	Dark-cultivated pale green transformants
DXR	Deoxy-D-xylulose 5-phosphate reductase
DXS	Deoxy-D-xylulose 5-phosphate synthase
ER	Endoplasmic reticulum
FMDV	Foot-and-month disease virus
FPP	Farnesyl pyrophosphate
GFP	Green fluorescence protein
GGPP	Geranyl geranyl pyrophosphate
Hp	*Haematococcus pluvialis*
HPLC	High performance liquid chromatography
IPP	Isopentenyl pyrophosphate

IRES	Internal ribosome binding site
LCYB	Lycopene ß-cyclase
LCYE	Lycopene ε-cylase
LSY	Loroxanthin synthase
MEP	Methylerythritol phosphate
miRNA	MicroRNA
MTBE	Methyl *tert*-butyl ether
NPQ	Non-photochemical quenching
NSY	Neoxanthin synthase
OCP	Orange carotenoid protein
OR	Orange protein
PBS	Phosphate-buffered saline
pBSK	pBluescript plasmid
PCR	Polymerase chain reaction
PDS	Phytoene desaturase
PLRV	Potato leafroll virus
PSY	Phytoene synthase
RNA	Ribonucleic acid
RNAi	RNA interference
RISC	RNA-induced silencing complex
ROS	Reactive oxygen species
SDS-PAGE	SDS-polyacrylamide gel electrophoresis
siRNA	Small interfering RNA
TAP	Tris-acetate-phosphate
VDE	Violaxanthin deepoxidase
ZDS	ξ-carotene desaturase
ZEP	Zeaxanthin epoxidase

LIST OF FIGURES

Figure 12*(Page 32)***:** (a) First seed culture after 3 days of cultivation. Cell density was estimated at 1.0 x 10^6 cells/mL. (b) Microscopic picture of cells from seed culture (400x magnification). (c) Seed culture was diluted 1:5 with fresh TAP medium and shaken further for another 2 days on a rotary shaker (d).

Figure 13*(Page 33)***:** (a) After 2 days of cultivation, Chlamydomonas liquid culture reached cell density of 2.4 x 10^6 cells/mL and was used for transformation. (b) Growth curve during cultivation

Figure 14*(Page 35)***:** Excitation (green) and emission (red) spectra of Chlorophyll b and mCherry. Fluorescence data from Semrock SearchLight (https://searchlight.semrock.com)

Figure 15*(Page 40)**:* UVM-4 cells under light microscope (1000x magnification). In the small window is a UVM-4 colony on agar plate.

Figure 16*(Page 41)**:* CC-4102 cells under light microscope (1000x magnification): "palmelloid colonies" (left) and actively swimming cells upon transferred to distilled water (right). In the small window is a CC-4102 colony on agar plate.

Figure 17*(Page 41)**:* Chlorophyll autofluorescence of strains UVM-4 (upper panel) and CC-4102 (lower panel) revealed the characteristic cup-shaped chloroplasts. On the left are false-colored fluorescence image (excitation: 488 nm, emission: 650-700 nm). On the right are differential interference contrast (DIC) images. Scale bars are 10 µm.

Figure 18*(Page 42)***:** Growth curve of UVM-4 (blue) and CC-4102 cells (red) in TAP medium supplemented with L-arginine (200 mg/L) at temperature of 20^0C and light intensity of 80 µE/m^2.s . On the vertical axis are measurements of culture's optical density at 680nm. Data points were collected automatically by MC1000 system every 10 minutes.

Figure 19*(Page 43)***:** (*Upper*) HPLC analysis of pigments extracted from UVM-4 and CC-4102 cells. (*Lower*) Relative contents (pigment/ chlorophyll a) of carotenoids of strain CC-4102 compared to those of strain UVM-4. A change of $\pm$100% means the complete gain/ loss of the corresponding pigment

Figure 20*(Page 45)***:** **(A)** Fluorescence measurements of pBR9 mCherry transformants compared to untranformed cells. UVM-4 transformants were spotted on the left half of the agar plate, CC-4102 transformants on the right half. Darker spots means stronger fluorescence signal. **(B)** Distribution of fluorescence densities (mCherry to chlorophyll signal ratio) among spots as seen in (A). Threshold value (dotted line) was averaged fluorescence density of non-transformed cells plus three times standard deviation.

Figure 21*(Page 45)***:** In-gel fluorescence detection of mCherry extracted from non-transformed UVM-4 cells (*left*) as well as from two independent pBR9 mCherry UVM-4 transformants (middle and right). Excitation wavelength 520 nm, emission filter 605BP40

Figure 22*(Page 46)***:** Detection of mCherry (excitation 561nm, emission 580-640 nm) and chlorophyll (excitation 488nm, emission 650-700 nm) fluorescence of pBR9 mCherry transformants. Scale bars are 10 µm.

Figure 23*(Page 47)***:** Sequence alignment of CrBKT, HpBKT 1,2,3 and CzBKT. Level of sequence conservation is displayed by color scale in which blue means 0% and red means 100% conversed sequences.

Figure 24*(Page 48)***:** Predicted structure of CrBKT (left) with its five trans-membrane helices (right). N-terminus is colored dark blue, C-terminus dark-red. Predictions were made using PHYRE2 algorithms.

Figure 25*(Page 49)***:** Carotenoid-accumulating *E. coli* strains. (1) & (2): plasmid maps of pACCAR16 ΔcrtX and pACCAR25 ΔcrtX. (3) & (4): HPLC analysis of carotenoids extracted from p pACCAR16 ΔcrtX and pACCAR25

Figure 36*(Page 60)***:** HPLC analysis of carotenoids extracted from 8 PCR-positive, zeocin-positive lines from transformation of Chlamydomonas strains UVM-4 and CC-4102 with pBR32 psaD CrBKT-mCherry and pBR32 psaD CrBKT. Pigments: 1 = loroxanthin + neoxanthin, 2 = violaxanthin, 3 = antheraxanthin, 4 = lutein, 5 =α- and ß-carotene, 6 = zeaxanthin. Y-axis (absorbance) of all chromatograms was normalized between 0 and 1. Detection at 450nm.

Figure 37*(Page 61)***:** pChlamy4 CrBKT V5H for over-production of V5-tagged CrBKT in *Chlamydomonas*

Figure 38*(Page 63)***:** PCR screening of transformants from transformation of UVM-4 and CC-4102 with pChlamy4 CrBKT V5H. First four lanes from the left are controls: PCR amplification from genomic DNA extracted from non-transformed (NT) UVM-4 and CC-4102 cells, from sample without DNA template and from pChlamy4 CrBKT V5H plasmid. Following are PCR amplifications from 15 positive lines. For PCR, primers 1479 and 1491 were used, which resulted in the amplification of a ~ 1.3kb products.

Figure 39*(Page 64)***:** Percentage of chlorophyll a, chlorophyll b and total carotenoids of 15 PCR-positive pChlamy4 CrBKT V5H transformants, compared to those of non-transformed (NT) UVM-4 and CC-4102. Light conditions and growth media are specified. In the small windows are pictures of algal colonies on agar plates. Measurements were performed in triplicates. Error bars are standard deviations.

Figure 40*(Page 66)***:** Detection of chlorophyll-like products (peaks 9, 10, 11 and 12) in several pChlamy4 CrBKT-V5H transformants. Cell lines, light conditions and growth media are specified on the right hand side. Chromatograms from non-transformed cells are marked red. Loro, neo, vio and anth are abbreviations of loroxanthin, neoxanthin, violaxanthin and antheraxanthin. On the left hand side are absorption spectra between 280 and 640nm, as well as retention time of peaks 9 -12 and of chlorophyll a and b.

Figure 41*(Page 68)***:** The pale green color of DP lines was elucidated by HPLC analysis, which saw dramatic shift in pigment profiles compared to non-transformed cells: chlorophyll-to-carotenoid ratios were significantly reduced, and zeaxanthin became the highest peak in the chromatogram. Pigments: 4 = lutein, 5 =α- and ß-carotene, 6= zeaxanthin, 7 = chlorophyll b, 8 = chlorophyll a, 13 = canthaxanthin. Y-axis (absorbance) of all chromatograms was normalized between 0 and 1. Detection at 450nm.

Figure 42*(Page 59)***:** Peak 13 was eluted at the same time as canthaxanthin standard.

Figure 43*(Page 69):* Comparisons of absorption spectrum from 280 to 640nm of the unidentified peak 13 with (A) zeaxanthin, (B) chlorophyll a, (C) canthaxanthin and (D) the simulated weighted sum of these three substances with weighting factors of 0.894, 0.109 and 0.221 respectively.

Figure 44*(Page 70)*: Immunodetection of V5-tagged CrBKT in four DP lines. Total proteins were extracted and separated with SDS-PAGE. V5-tagged proteins were recognized by anti-V5 antibody from rabbit, which was in turn detected by anti-rabbit IgG secondary antibodies conjugated with alkaline phosphatase. Protein bands were visualized by BCIP-NBT reaction overnight. Protein markers are Prestained PageRuler (Thermo Fisher). Black arrows indicate positive bands.

Figure 45*(Page 71)***:** Nile Red staining. Nile Red fluorescence (*left*), chlorophyll autofluorescence (*middle*) and DIC pictures (*right*) from non-transformed CC-4102 and canthaxanthin-accumulating CC-DP4 cells. Note that the bright spots in chlorophyll fluorescence channel were in fact fluorescence of Nile Red in lipid droplets. Scale bars are 10µm

Figure 46*(Page 72)**:* Amplification of 5'- and 3'-end flanking sequences for insertion mapping of four DP lines. Shown are results after the second (nested) PCR.

Figure 47*(Page 73)***:** DP cells grown in dark and in light: light-grown DP cells did not survive 20 mg/L zeocin and returned to the dark-green color of non-transformed cells. Non-transformed CC-4102 cells were also spotted for comparision. All experiments were carried out on TAP-YP agar plate.

Figure 48*(Page 74)***:** When DP cells were cultivated in light, their pigment profile changes dramatically. HPLC analysis revealed the return of chlorophylls, which reverted cell's color from pale green to dark green. Also canthaxanthin was no longer detectable. Pigments: 4 = lutein, 5 =α- and ß-carotene, 6= zeaxanthin, 7 = chlorophyll b, 8 = chlorophyll a, 13 = canthaxanthin. Y-axis (absorbance) of all chromatograms was normalized between 0 and 1. Detection at 450nm.

Figure 49*(Page 75)***:** Differences in pigment compositions when DP cells were grown either in light or in dark. Light-grown cells saw their chlorophylls/carotenoids ratio reverted back to normal values of non-transformed cells.

Figure 50*(Page 75)***:** The Ble2A-CrBKT was still in DP cell's genome regardless if they were cultivated in dark or in light. Three primers pairs were used to confirm the transgene: 1479 + 1491 (Ble2A-CrBKT gene), 1502 + 1534 (CrBKT gene) and 1479 + 1480 (Ble gene). Expected amplicon sizes were 1.3 kb, 1.0 kb and 0.3 kb respectively. Primer binding positions were also shown.

Figure 51*(Page 76)***:** Reaction involved in *E. coli*-based ketolase activity assay.

Figure 52*(Page 79)***:** Proposed experiment for elucidation of putative endonuclease site(s) within CrBKT sequence. DSB: double-strand break

Figure 53*(Page 80)***:** Structure of *Chlamydomonas* chloroplast. Modified from **[162]**

Figure 54*(Page 84)*: the artificial enzyme channel concept. Three individual enzymes (in this case, from mevalonate pathway) are connected together via scaffolding proteins into multienzyme complex that enable direct conversion from acetyl-coA to mevalonate with little interference from competing pathways. Modified from **[175]**

LIST OF TABLES

APPENDIX

Plasmid pBR9 mCherry

GCACTTTTCGGGGAAATGTGCGCGGAACCCCTATTTGTTTATTTTTCTAAATACATTCAAATATGTATCCGCTCATGAGACAATAACCCTGATAAATGCTTCA
ATAATATTGAAAAAGGAAGAGTATGAGTATTCAACATTTCCGTGTCGCCCTTATTCCCTTTTTTGCGGCATTTTGCCTTCCTGTTTTTGCTCACCCAGAAACGC
TGGTGAAAGTAAAAGATGCTGAAGATCAGTTGGGTGCACGAGTGGGTTACATCGAACTGGATCTCAACAGCGGTAAGATCCTTGAGAGTTTTCGCCCCGA
AGAACGTTTTCCAATGATGAGCACTTTTAAAGTTCTGCTATGTGGCGCGGTATTATCCCGTATTGACGCCGGGCAAGAGCAACTCGGTCGCCGCATACACT
ATTCTCAGAATGACTTGGTTGAGTACTCACCAGTCACAGAAAAGCATCTTACGGATGGCATGACAGTAAGAGAATTATGCAGTGCTGCCATAACCATGAGT
GATAACACTGCGGCCAACTTACTTCTGACAACGATCGGAGGACCGAAGGAGCTAACCGCTTTTTTGCACAACATGGGGGATCATGTAACTCGCCTTGATCG
TTGGGAACCGGAGCTGAATGAAGCCATACCAAACGACGAGCGTGACACCACGATGCCTGTAGCAATGGCAACAACGTTGCGCAAACTATTAACTGGCGAA
CTACTTACTCTAGCTTCCCGGCAACAATTAATAGACTGGATGGAGGCGGATAAAGTTGCAGGACCACTTCTGCGCTCGGCCCTTCCGGCTGGCTGGTTTATT
GCTGATAAATCTGGAGCCGGTGAGCGTGGGTCTCGCGGTATCATTGCAGCACTGGGGCCAGATGGTAAGCCCTCCCGTATCGTAGTTATCTACACGACGG
GGAGTCAGGCAACTATGGATGAACGAAATAGACAGATCGCTGAGATAGGTGCCTCACTGATTAAGCATTGGTAACTGTCAGACCAAGTTTACTCATATATA
CTTTAGATTGATTTAAAACTTCATTTTTAATTTAAAAGGATCTAGGTGAAGATCCTTTTTGATAATCTCATGACCAAAATCCCTTAACGTGAGTTTTCGTTCCA
CTGAGCGTCAGACCCCGTAGAAAAGATCAAAGGATCTTCTTGAGATCCTTTTTTTCTGCGCGTAATCTGCTGCTTGCAAACAAAAAAACCACCGCTACCAGC
GGTGGTTTGTTTGCCGGATCAAGAGCTACCAACTCTTTTTCCGAAGGTAACTGGCTTCAGCAGAGCGCAGATACCAAATACTGTTCTTCTAGTGTAGCCGTA
GTTAGGCCACCACTTCAAGAACTCTGTAGCACCGCCTACATACCTCGCTCTGCTAATCCTGTTACCAGTGGCTGCTGCCAGTGGCGATAAGTCGTGTCTTAC
CGGGTTGGACTCAAGACGATAGTTACCGGATAAGGCGCAGCGGTCGGGCTGAACGGGGGGTTCGTGCACACAGCCCAGCTTGGAGCGAACGACCTACAC
CGAACTGAGATACCTACAGCGTGAGCTATGAGAAAGCGCCACGCTTCCCGAAGGGAGAAAGGCGGACAGGTATCCGGTAAGCGGCAGGGTCGGAACAG
GAGAGCGCACGAGGGAGCTTCCAGGGGGAAACGCCTGGTATCTTTATAGTCCTGTCGGGTTTCGCCACCTCTGACTTGAGCGTCGATTTTTGTGATGCTCG
TCAGGGGGGCGGAGCCTATGGAAAAACGCCAGCAACGCGGCCTTTTTACGGTTCCTGGCCTTTTGCTGGCCTTTTGCTCACATGTTCTTTCCTGCGTTATCC
CCTGATTCTGTGGATAACCGTATTACCGCCTTTGAGTGAGCTGATACCGCTCGCCGCAGCCGAACGACCGAGCGCAGCGAGTCAGTGAGCGAGGAAGCGG
AAGAGCGCCCAATACGCAAACCGCCTCTCCCCGCGCGTTGGCCGATTCATTAATGCAGCTGGCACGACAGGTTTCCCGACTGGAAAGCGGGCAGTGAGCG
CAACGCAATTAATGTGAGTTAGCTCACTCATTAGGCACCCCAGGCTTTACACTTTATGCTTCCGGCTCGTATGTTGTGTGGAATTGTGAGCGGATAACAATT
TCACACAGGAAACAGCTATGACCATGATTACGCCAAGCGCGCAATTAACCCTCACTAAAGGGAACAAAAGCTGGAGCTCCACCGCGGTGGCGGCCGCTCT
AGAcggcggggagctcgctgaggcttgacatgattggtgcgtatgtttgtatgaagctacaggactgatttggcgggctatgagggcgggggaagctctggaagggccgcgatggggcgcgcggcgtcc
agaaggcgccatacggcccgctggcggcacccatccggtataaaagcccgcgaccccgaacggtgacctccactttcagcgacaaacgagcacttatacatacgcgactattctgccgctatacataacc
actcagctagcttaagatcccatcaagcttgcatgccgggcgcgccagaaggagcgcagccaaaccaggatgatgtttgatggggtatttgagcacttgcaaccctatccggaagcccccctggcccacaa
aggctaggcgccaatgcaagcagttcgcatgcagcccctggagcggtgccctcctgataaaccggccaggggcctatgttctttacttttttacaagagaagtcactcaacatcttaaaatggccaggtga
gtcgacgagcaagcccggcggatcaggcagcgtgcttgcagatttgacttgcaacgcccgcattgtgtcgacgaaggcttttggctcctctgtcgctgtctcaagcagcatctaaccctgcgtcgccgtttcc
atttgcaggatggccatgcatatggccaagctgaccagcgccgttccggtgctcaccgcgcgcgacgtcgccggagcggtcgagttctggaccgaccggctcgggttctcccgggacttcgtggaggacga
cttcgccggtgtggtccgggacgacgtgaccctgttcatcagcgcggtccaggaccaggtgagtcgacgagcaagcccggcggatcaggcagcgtgcttgcagatttgacttgcaacgcccgcattgtgtc
gacgaaggcttttggctcctctgtcgctgtctcaagcagcatctaaccctgcgtcgccgtttccattttccaggaccaggtggtgccggacaacaccctggcctgggtgtgggtgcgcggcctggacgagctgt
acgccgagtggtcggaggtcgtgtccacgaacttccgggacgcctccgggccggccatgaccgagatcggcgagcagccgtgggggcgggagttcgccctgcgcgacccggccggcaactgcgtgcact
tcgtggccgaggagcaggacGCCCCGGtGAAGCAGACCCtGAACttCGACctgctgaagctggcgggcGACgtggagagcaacCCGGGCcccCTCGAGATGGTGTCCAAGGG
CGAGGAGGACAACATGGCCATCATCAAGGAGTTCATGCGCTTCAAGGTGCACATGGAGGGCAGCGTGAACGGCCACGAGTTCGAGATCGAGGGCGAGG
GCGAGGGCCGCCCCTACGAGGGCACCCAGACCGCCAAGCTGAAGGTGACCAAGGGCGGCCCCCTGCCCTTCGCCTGGGACATCCTGAGCCCCCAGTTCAT
GTACGGCAGCAAGGCCTACGTGAAGCACCCCGCCGACATCCCCGACTACCTGAAGCTGAGCTTCCCCGAGGGCTTCAAGTGGGAGCGCGTGATGAACTTC
GAGGACGGCGGCGTGGTGACCGTGACCCAGGACAGCAGCCTCCAGGACGGCGAGTTCATCTACAAGGTGAAGCTGCGCGGCACCAACTTCCCCAGCGAC
GGCCCCGTGATGCAGAAGAAGACCATGGGCTGGGAGGCCAGCAGCGAGCGCATGTACCCCGAGGACGGCGCCCTGAAGGGCGAGATCAAGCAGCGCCT
GAAGCTGAAGGACGGCGGCCACTACGACGCCGAGGTGAAGACCACCTACAAGGCCAAGAAGCCCGTGCAGCTGCCCGGCGCCTACAACGTGAACATCAA
GCTGGACATCACCAGCCACAACGAGGACTACACCATCGTGGAGCAGTACGAGCGCGCTGAGGGCCGCCACAGCACCGGCGGCATGGACGAGCTGTACAA
GTAAggatccCCGCTCCGTGTAAATGGAGGCGCTCGTTGATCTGAGCCTTGCCCCCTGACGAACGGCGGTGGATGGAAGATACTGCTCTCAAGTGCTGAAGC
GGTAGCTTAGCTCCCCGTTTCGTGCTGATCAGTCTTTTTCAACACGTAAAAAGCGGAGGAGTTTTGCAATTTTGTTGGTTGTAACGATCCTCCGTTGATTTTG
GCCTCTTTCTCCATGGGCGGGCTGGGCGTATTTGAAGCGGGTACCCAATTCGCCCTATAGTGAGTCGTATTACGCGCGCTCACTGGCCGTCGTTTTACAACG
TCGTGACTGGGAAAACCCTGGCGTTACCCAACTTAATCGCCTTGCAGCACATCCCCCTTTCGCCAGCTGGCGTAATAGCGAAGAGGCCCGCACCGATCGCC
CTTCCCAACAGTTGCGCAGCCTGAATGGCGAATGGGACGCGCCCTGTAGCGGCGCATTAAGCGCGGCGGGTGTGGTGGTTACGCGCAGCGTGACCGCTA
CACTTGCCAGCGCCCTAGCGCCCGCTCCTTTCGCTTTCTTCCCTTCCTTTCTCGCCACGTTCGCCGGCTTTCCCCGTCAAGCTCTAAATCGGGGGCTCCCTTTA
GGGTTCCGATTTAGTGCTTTACGGCACCTCGACCCCAAAAAACTTGATTAGGGTGATGGTTCACGTAGTGGGCCATCGCCCTGATAGACGGTTTTTCGCCCT
TTGACGTTGGAGTCCACGTTCTTTAATAGTGGACTCTTGTTCCAAACTGGAACAACACTCAACCCTATCTCGGTCTATTCTTTTGATTTATAAGGGATTTTGCC
GATTTCGGCCTATTGGTTAAAAAATGAGCTGATTTAACAAAAATTTAACGCGAATTTTAACAAAATATTAACGCTTACAATTTAGGTG

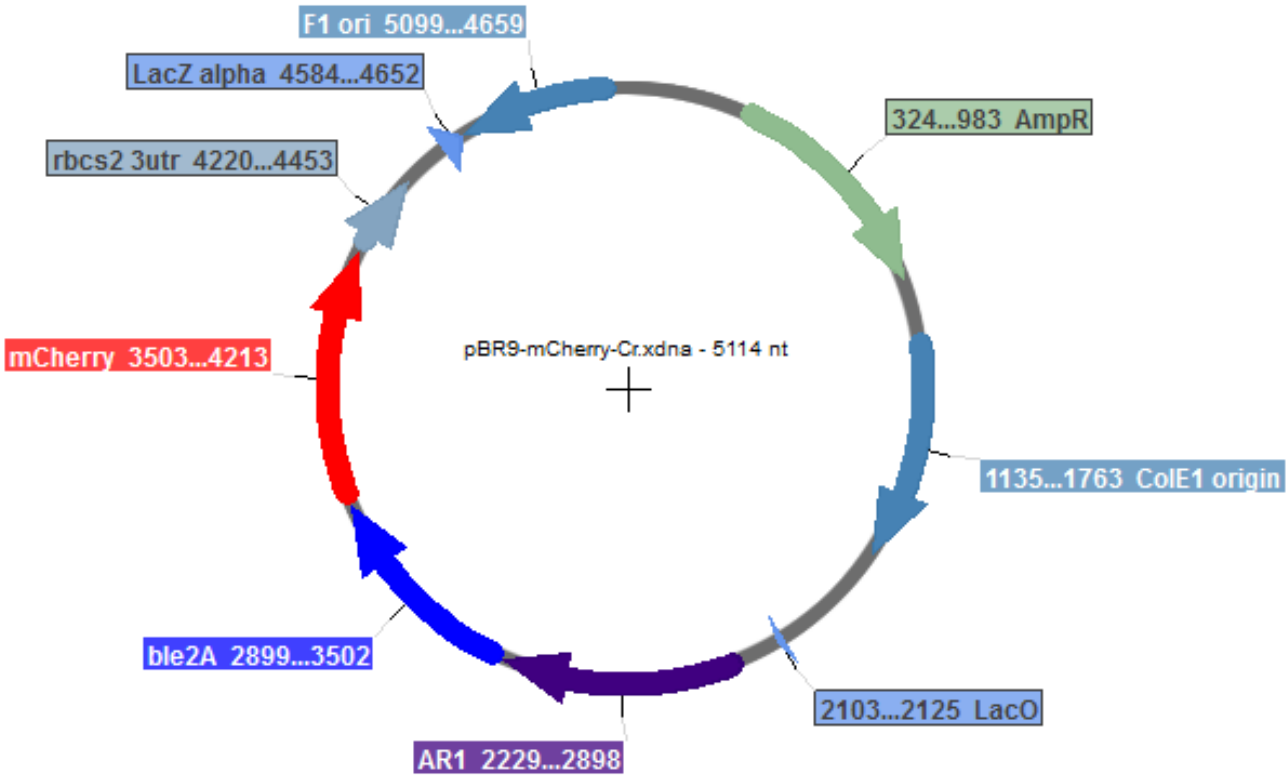

Features:

Ampicillin resistance marker AmpR	324 – 983
HSP70/ RBCS2 promoter (AR1 promoter)	2229 – 2898
ble gene from *Streptoalloteichus hindustanus*	2899 - 3424
FMDV 2A sequence	3425 - 3496
Codon-optimized mCherry coding sequence	3503 – 4213
RBCS2 3'-UTR sequence	4220 – 4453

Plasmid pBR32 psaD mCherry

caattcgccctatagtgagtcgtattacgcgcgctcactggccgtcgttttacaacgtcgtgactgggaaaaccctggcgttacccaacttaatcgccttgcagcacatcccccttttcg
ccagctggcgtaatagcgaagaggcccgcaccgatcgcccttcccaacagttgcgcagcctgaatggcgaatgggacgcgccctgtagcggcgcattaagcgcggcgggtgtggt
ggttacgcgcagcgtgaccgctacacttgccagcgccctagcgcccgctcctttcgctttcttcccttcctttctcgccacgttcgccggctttccccgtcaagctctaaatcgggggctc
cctttagggttccgatttagtgctttacggcacctcgaccccaaaaaacttgattagggtgatggttcacgtagtgggccatcgccctgatagacggtttttcgccctttgacgttgga
gtccacgttctttaatagtggactcttgttccaaactggaacaacactcaaccctatctcggtctattcttttgatttataagggattttgccgatttcggcctattggttaaaaaatgag
ctgatttaacaaaaatttaacgcgaattttaacaaaatattaacgcttacaatttaggtggcacttttcggggaaatgtgcgcggaaccccctatttgtttatttttctaaatacattcaa
atatgtatccgctcatgagacaataaccctgataaatgcttcaataatattgaaaaaggaagagtatgagtattcaacatttccgtgtcgcccttattcccttttttgcggcattttgcc
ttcctgtttttgctcacccagaaacgctggtgaaagtaaaagatgctgaagatcagttgggtgcacgagtgggttacatcgaactggatctcaacagcggtaagatccttgagagtt
ttcgccccgaagaacgttttccaatgatgagcacttttaaagttctgctatgtggcgcggtattatcccgtattgacgccgggcaagagcaactcggtcgccgcatacactattctcag
aatgacttggttgagtactcaccagtcacagaaaagcatcttacggatggcatgacagtaagagaattatgcagtgctgccataaccatgagtgataacactgcggccaacttactt
ctgacaacgatcggaggaccgaaggagctaaccgcttttttgcacaacatgggggatcatgtaactcgccttgatcgttgggaaccggagctgaatgaagccataccaaacgacg
agcgtgacaccacgatgcctgtagcaatggcaacaacgttgcgcaaactattaactggcgaactacttactctagcttcccggcaacaattaatagactggatggaggcggataaa
gttgcaggaccacttctgcgctcggcccttccggctggctggtttattgctgataaatctggagccggtgagcgtgggtctcgcggtatcattgcagcactggggccagatggtaagc
cctcccgtatcgtagttatctacacgacggggagtcaggcaactatggatgaacgaaatagacagatcgctgagataggtgcctcactgattaagcattggtaactgtcagaccaa
gtttactcatatatactttagattgatttaaaacttcatttttaatttaaaaggatctaggtgaagatccttttgataatctcatgaccaaaatcccttaacgtgagttttcgttccactg
agcgtcagaccccgtagaaaagatcaaaggatcttcttgagatcctttttttctgcgcgtaatctgctgcttgcaaacaaaaaaaccaccgctaccagcggtggtttgtttgccggat
caagagctaccaactctttttccgaaggtaactggcttcagcagagcgcagataccaaatactgttcttctagtgtagccgtagttaggccaccacttcaagaactctgtagcaccgc
ctacatacctcgctctgctaatcctgttaccagtggctgctgccagtggcgataagtcgtgtcttaccgggttggactcaagacgatagttaccggataaggcgcagcggtcgggctg
aacgggggttcgtgcacacagcccagcttggagcgaacgacctacaccgaactgagatacctacagcgtgagctatgagaaagcgccacgcttcccgaagggagaaaggcgg
acaggtatccggtaagcggcagggtcggaacaggagagcgcacgagggagcttccagggggaaacgcctggtatctttatagtcctgtcgggtttcgccacctctgacttgagcgt
cgatttttgtgatgctcgtcaggggggcggagcctatggaaaaacgccagcaacgcggccttttacggttcctggccttttgctggccttttgctcacatgttctttcctgcgttatccc
ctgattctgtggataaccgtattaccgcctttgagtgagctgataccgctcgccgcagccgaacgaccgagcgcagcgagtcagtgagcgaggaagcggaagagcgcccaatacg
caaaccgcctctccccgcgcgttggccgattcattaatgcagctggcacgacaggtttcccgactggaaagcgggcagtgagcgcaacgcaattaatgtgagttagctcactcatta
ggcaccccaggctttacactttatgcttccggctcgtatgttgtgtggaattgtgagcggataacaatttcacacaggaaacagctatgaccatgattacgccaagcgcgcaattaac
cctcactaaagggaacaaaagctggagctccaccgcggtggcggccgctctagacggcggggagctcgctgaggcttgacatgattggtgcgtatgtttgtatgaagctacaggac
tgatttggcgggctatgagggcgggggaagctctggaagggccgcgatggggcgcgcggcgtccagaaggcgccatacggcccgctggcggcacccatccggtataaaagcccg
cgaccccgaacggtgacctccactttcagcgacaaacgagcacttatacatacgcgactattctgccgctatacataaccactcagctagcttaagatcccatcaagcttgcatgcc
gggcgcgccagaaggagcgcagccaaaccaggatgatgtttgatggggtatttgagcacttgcaacccttatccggaagccccctggcccacaaaggctaggcgccaatgcaagc
agttcgcatgcagcccctggagcggtgccctcctgataaaccggccagggggcctatgttctttacttttttacaagagaagtcactcaacatcttaaaatggccaggtgagtcgacg
agcaagcccggcggatcaggcagcgtgcttgcagatttgacttgcaacgcccgcattgtgtcgacgaaggcttttggctcctctgtcgctgtctcaagcagcatctaaccctgcgtcg
ccgtttccatttgcaggatggccatgcatatggccaagctgaccagcgccgttccggtgctcaccgcgcgcgacgtcgccggagcggtcgagttctggaccgaccggctcgggttct
cccgggacttcgtggaggacgacttcgccggtgtggtccgggacgacgtgaccctgttcatcagcgcggtccaggaccaggtgagtcgacgagcaagcccggcggatcaggcagc
gtgcttgcagatttgacttgcaacgcccgcattgtgtcgacgaaggcttttggctcctctgtcgctgtctcaagcagcatctaaccctgcgtcgccgtttccatttgcaggaccaggtgg
tgccggacaacaccctggcctgggtgtgggtgcgcggcctggacgagctgtacgccgagtggtcggaggtcgtgtccacgaacttccgggacgcctccgggccggccatgaccga
gatcggcgagcagccgtgggggcgggagttcgccctgcgcgacccggccggcaactgcgtgcacttcgtggccgaggagcaggacgccccggtgaagcagaccctgaacttcga
cctgctgaagctggcgggcgacgtggagagcaacccgggccccatggccgtcatgatgcgcacccaggcgcccgctgccactcgcgcttcatcgcgcgtcgctgttgccgctcgcc
cggctgctcgccgcgccgtggtggtccgcgccgaggctctcgagatggtgtccaagggcgaggaggacaacatggccatcatcaaggagttcatgcgcttcaaggtgcacatgga
gggcagcgtgaacggccacgagttcgagatcgagggcgagggcgagggccgcccctacgagggcacccagaccgccaagctgaaggtgaccaagggcggccccctgcccttcg
cctgggacatcctgagcccccagttcatgtacggcagcaaggcctacgtgaagcaccccgccgacatccccgactacctgaagctgagcttccccgagggcttcaagtgggagcgc
gtgatgaacttcgaggacggcggcgtggtgaccgtgacccaggacagcagcctccaggacggcgagttcatctacaaggtgaagctgcgcggcaccaacttccccagcgacggc
cccgtgatgcagaagaagaccatgggctgggaggccagcagcgagcgcatgtaccccgaggacggcgccctgaagggcgagatcaagcagcgcctgaagctgaaggacggcg
gccactacgacgccgaggtgaagaccacctacaaggccaagaagcccgtgcagctgcccggcgcctacaacgtgaacatcaagctggacatcaccagccacaacgaggactac
accatcgtggagcagtacgagcgcgctgagggccgccacagcaccggcggcatggacgagctgtacaagtaaggatccccgctccgtgtaaatggaggcgctcgttgatctgagc
cttgccccctgacgaacggcggtggatggaagatactgctctcaagtgctgaagcggtagcttagctccccgtttcgtgctgatcagtctttttcaacacgtaaaaagcggaggagtt
ttgcaattttgttggttgtaacgatcctccgttgattttggcctctttctccatgggcgggctgggcgtatttgaagcgggtacc

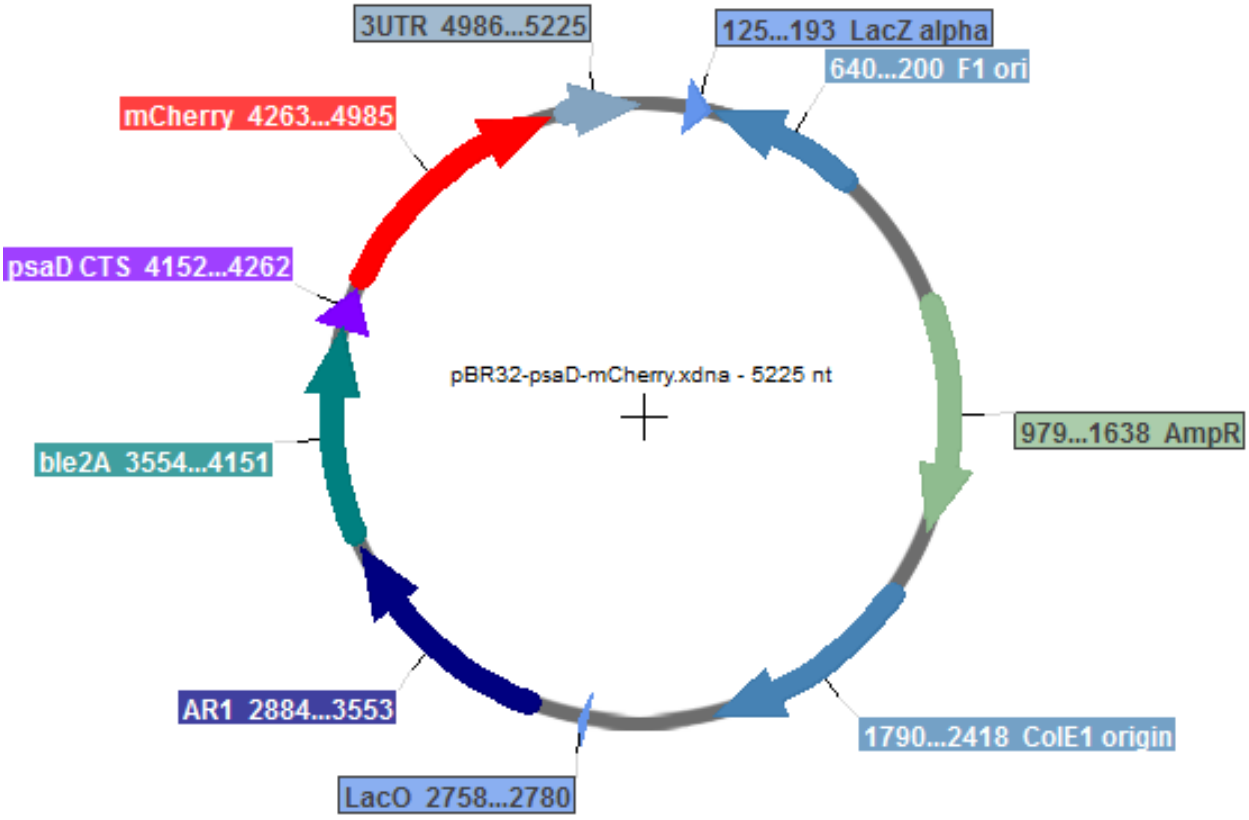

Features:

Ampicillin resistance marker AmpR	979 – 1638
HSP70/ RBCS2 promoter (AR1 promoter)	2884 – 3553
ble gene from *Streptoalloteichus hindustanus*	3554 - 4079
FMDV 2A sequence	4080 – 4151
Chlamydomonas psaD cTP	4152 - 4262
Codon-optimized mCherry coding sequence	4263 – 4985
RBCS2 3'-UTR sequence	4986 – 5225

Plasmid pChlamy4

TCGCTGAGGCTTGACATGATTGGTGCGTATGTTTGTATGAAGCTACAGGACTGATTTGGCGGGCTATGAGGGCGGGGGAAGCTCTGGA
AGGGCCGCGATGGGGCGCGCGGCGTCCAGAAGGCGCCATACGGCCCGCTGGCGGCACCCATCCGGTATAAAAGCCCGCGACCCCGAA
CGGTGACCTCCACTTTCAGCGACAAACGAGCACTTATACATACGCGACTATTCTGCCGCTATACATAACCACTCAGCTAGCTTAAGATCCC
ATCAAGCTTGCATGCCGGGCGCGCCAGAAGGAGCGCAGCCAAACCAGGATGATGTTTGATGGGGTATTTGAGCACTTGCAACCCTTATC
CGGAAGCCCCCTGGCCCACAAAGGCTAGGCGCCAATGCAAGCAGTTCGCATGCAGCCCCTGGAGCGGTGCCCTCCTGATAAACCGGCCA
GGGGGCCTATGTTCTTTACTTTTTTACAAGAGAAGTCACTCAACATCTTAAAATGGCCAGGTGAGTCGACGAGCAAGCCCGGCGGATCA
GGCAGCGTGCTTGCAGATTTGACTTGCAACGCCCGCATTGTGTCGACGAAGGCTTTTGGCTCCTCTGTCGCTGTCTCAAGCAGCATCTAA
CCCTGCGTCGCCGTTTCCATTTGCAGGATGGCCATGCATATGGCCAAGCTGACCAGCGCCGTTCCGGTGCTCACCGCGCGCGACGTCGCC
GGAGCGGTCGAGTTCTGGACCGACCGGCTCGGGTTCTCCCGGGACTTCGTGGAGGACGACTTCGCCGGTGTGGTCCGGGACGACGTGA
CCCTGTTCATCAGCGCGGTCCAGGACCAGGTGAGTCGACGAGCAAGCCCGGCGGATCAGGCAGCGTGCTTGCAGATTTGACTTGCAACG
CCCGCATTGTGTCGACGAAGGCTTTTGGCTCCTCTGTCGCTGTCTCAAGCAGCATCTAACCCTGCGTCGCCGTTTCCATTTGCAGGACCAG
GTGGTGCCGGACAACACCCTGGCCTGGGTGTGGGTGCGCGGCCTGGACGAGCTGTACGCCGAGTGGTCGGAGGTCGTGTCCACGAACT
TCCGGGACGCCTCCGGGCCGGCCATGACCGAGATCGGCGAGCAGCCGTGGGGGCGGGAGTTCGCCCTGCGCGACCCGGCCGGCAACT
GCGTGCACTTCGTGGCCGAGGAGCAGGACGCCCCGGTGAAGCAGACCCTGAACTTCGACCTGCTGAAGCTGGCGGGCGACGTGGAGA
GCAACCCGGGCCCCGAATTCCTCGAGCACCACCACCACCACCACGGCAAGCCCATCCCCAACCCCCTGCTGGGCCTGGACAGCACCGAG
AACCTGTACTTCCAGGGGGTACCAGGATCCGGAAGATCTGGTCTAGAGGGCAAGCCCATCCCCAACCCCCTGCTGGGCCTGGACAGCAC
CCGTACCGGTCACCACCACCACCACCACTAACTGCAGCCGCTCCGTGTAAATGGAGGCGCTCGTTGATCTGAGCCTTGCCCCCTGACGAA
CGGCGGTGGATGGAAGATACTGCTCTCAAGTGCTGAAGCGGTAGCTTAGCTCCCCGTTTCGTGCTGATCAGTCTTTTTCAACACGTAAAA
AGCGGAGGAGTTTTGCAATTTTGTTGGTTGTAACGATCCTCCGTTGATTTTGGCCTCTTTCTCCATGGGCGGGCTGGGCGTATTTGAAGC
GGCGGTATTTCACACCGCATCAGGTGGCACTTTTCGGGGAAATGTGCGCGGAACCCCTATTTGTTTATTTTTCTAAATACATTCAAATATG
TATCCGCTCATGAGATTATCAAAAAGGATCTTCACCTAGATCCTTTTAAATTAAAAATGAAGTTTTAAATCAATCTAAAGTATATATGAGTA
AACTTGGTCTGACAGTTACCAATGCTTAATCAGTGAGGCACCTATCTCAGCGATCTGTCTATTTCGTTCATCCATAGTTGCCTGACTCCCCG
TCGTGTAGATAACTACGATACGGGAGGGCTTACCATCTGGCCCCAGTGCTGCAATGATACCGCGAGACCCACGCTCACCGGCTCCAGATT
TATCAGCAATAAACCAGCCAGCCGGAAGGGCCGAGCGCAGAAGTGGTCCTGCAACTTTATCCGCCTCCATCCAGTCTATTAATTGTTGCC
GGGAAGCTAGAGTAAGTAGTTCGCCAGTTAATAGTTTGCGCAACGTTGTTGCCATTGCTACAGGCATCGTGGTGTCACGCTCGTCGTTTG
GTATGGCTTCATTCAGCTCCGGTTCCCAACGATCAAGGCGAGTTACATGATCCCCCATGTTGTGCAAAAAAGCGGTTAGCTCCTTCGGTCC
TCCGATCGTTGTCAGAAGTAAGTTGGCCGCAGTGTTATCACTCATGGTTATGGCAGCACTGCATAATTCTCTTACTGTCATGCCATCCGTA
AGATGCTTTTCTGTGACTGGTGAGTACTCAACCAAGTCATTCTGAGAATAGTGTATGCGGCGACCGAGTTGCTCTTGCCCGGCGTCAATA
CGGGATAATACCGCGCCACATAGCAGAACTTTAAAAGTGCTCATCATTGGAAAACGTTCTTCGGGGCGAAAACTCTCAAGGATCTTACCG
CTGTTGAGATCCAGTTCGATGTAACCCACTCGTGCACCCAACTGATCTTCAGCATCTTTTACTTTCACCAGCGTTTCTGGGTGAGCAAAAA
CAGGAAGGCAAAATGCCGCAAAAAAGGGAATAAGGGCGACACGGAAATGTTGAATACTCATACTCTTCCTTTTTCAATATTATTGAAGC
ATTTATCAGGGTTATTGTCTCATGACCAAAATCCCTTAACGTGAGTTTTCGTTCCACTGAGCGTCAGACCCCGTAGAAAAGATCAAAGGAT
CTTCTTGAGATCCTTTTTTTCTGCGCGTAATCTGCTGCTTGCAAACAAAAAAACCACCGCTACCAGCGGTGGTTTGTTTGCCGGATCAAGA
GCTACCAACTCTTTTTCCGAAGGTAACTGGCTTCAGCAGAGCGCAGATACCAAATACTGTTCTTCTAGTGTAGCCGTAGTTAGGCCACCAC
TTCAAGAACTCTGTAGCACCGCCTACATACCTCGCTCTGCTAATCCTGTTACCAGTGGCTGTTGCCAGTGGCGATAAGTCGTGTCTTACCG
GGTTGGACTCAAGACGATAGTTACCGGATAAGGCGCAGCGGTCGGGCTGAACGGGGGGTTCGTGCACACAGCCCAGCTTGGAGCGAA
CGACCTACACCGAACTGAGATACCTACAGCGTGAGCTATGAGAAAGCGCCACGCTTCCCGAAGGGAGAAAGGCGGACAGGTATCCGGT
AAGCGGCAGGGTCGGAACAGGAGAGCGCACGAGGGAGCTTCCAGGGGGAAACGCCTGGTATCTTTATAGTCCTGTCGGGTTTCGCCAC
CTCTGACTTGAGCGTCGATTTTTGTGATGCTCGTCAGGGGGGCGGAGCCTATGGAAAAACGCCAGCAACGCGGCCTTTTTACGGTTCCTG
GCCTTTTGCTGGCCTTTTGCTCACATGTTCTTTCCTGCGTTATCCCCTGATTCTGTGGATAACCGTATTACCGCCTTTGAGTGAGCTGATAC
CGCTCGCCGCAGCCGAACGACCGAGCGCAGCGAGTCAGTGAGCGAGGAAGCGG

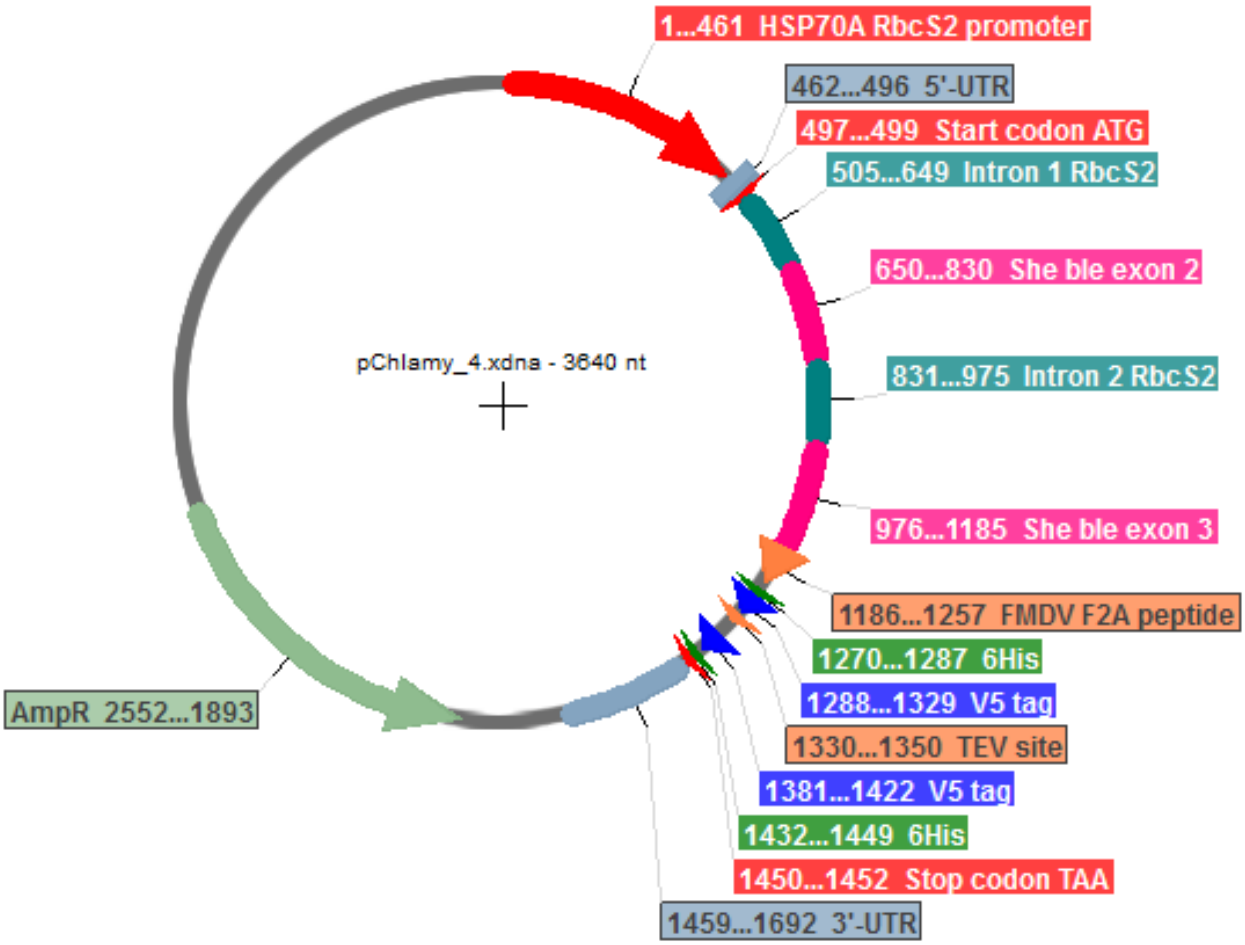

Features:

HSP70/ RBCS2 promoter (AR1 promoter)	1 - 461
ble gene from *Streptoalloteichus hindustanus*	497 - 1185
FMDV 2A sequence	1186 - 1257
N-terminal dual epitope 6xHis – V5	1270 - 1329
C-terminal dual epitope V5 – 6xHis	1381 – 1449
RBCS2 3'-UTR sequence	1459 – 1692
Ampicillin resistance marker AmpR	979 – 1638

Multiple cloning site

CrBKT coding sequence

atgggccctgggatacaacccacttccgcgcgaccgtgttctaggaccaaacacagtcgatttgcgctacttgccgcagcgctgaccgcacgacgcgtcaagcagttcacgaagcagttccgctcgcgtag
gatggcggaggacatactgaagctgtggcagcgccaatatcacctgccgcgcgaggattctgacaagcgcacgctgcgcgagcgcgttcacctgtaccgcccgccgcgttcagacctaggtggcattgcg
gtcgctgtgacagtcatcgcgctgtgggcgacgctgtttgtctacgggctgtggttcgtcaagctgccatgggcgctcaaagtgggcgagacagccacgtcctgggcaaccattgctgctgtattctttagcc
tggaattccttacaccgggctcttcatcaccacgcacgacgcgatgcatggcaccatcgcgctgcgcaaccggcgcctgaacgactttctgggcaacctggcaatcagcctatacgcctggtttgactactc
cgtcctgcaccgcaagcactgggagcaccacaaccacaccggggagccgcgtgtggatccggacttccaccgcggcaaccccaacctggcggtgtggttcgcgcagttcatggtgtcgtacatgaccctc
agccagttcctcaagatcgcggtctggtccaacctgctgctgctggcgggtgcgccgctggccaaccagctgctgttcatgacggcggcgcccatcctgtccgccttccgcctgttctactacggcacctacg
tgccgcaccacccggagaaggggcacaccggcgccatgccctggcaggtatcccgcaccagctccgcctcccggctgcagtcgttcctcacctgctaccacttcgacctgcactgggagcaccaccgctgg
ccctacgcgccctggtgggagctgcccaagtgccgccagattgcccgcggcgcagccctggcgtga

Peptide sequences

CrBKT

MGPGIQPTSARPCSRTKHSRFALLAAALTARRVKQFTKQFRSRRMAEDILKLWQRQYHLPREDSDKRTLRERVHLY
RPPRSDLGGIAVAVTVIALWATLFVYGLWFVKLPWALKVGETATSWATIAAVFFSLEFLYTGLFITTHDAMHGTIAL
RNRRLNDFLGNLAISLYAWFDYSVLHRKHWEHHNHTGEPRVDPDFHRGNPNLAVWFAQFMVSYMTLSQFLKIA
VWSNLLLLAGAPLANQLLFMTAAPILSAFRLFYYGTYVPHHPEKGHTGAMPWQVSRTSSASRLQSFLTCYHFDLH
WEHHRWPYAPWWELPKCRQIARGAALA

HpBKT1

MQLAATVMLEQLTGSAEALKEKEKEVAGSSDVLRTWATQYSLPSEESDAARPGLKNAYKPPPSDTKGITMALAVI
GSWAAVFLHAIFQIKLPTSLDQLHWLPVSDATAQLVGGSSSLLHIVVVFFVLEFLYTGLFITTHDAMHGTIAMRNR
QLNDFLGRVCISLYAWFDYNMLHRKHWEHHNHTGEVGKDPDFHRGNPGIVPWFASFMSSYMSMWQFARLA
WWTVVMQLLGAPMANLLVFMAAAPILSAFRLFYFGTYMPHKPEPGAASGSSPAVMNWWKSRTSQASDLVSF
LTCYHFDLHWEHHRWPFAPWWELPNCRRLSGRGLVPA

HpBKT2

MHVASALMVEQKGSEAAACSPDVLRAWATQYHMPSESSDAARPALKHAYKPPASDAKGITMALTIIGTWTAVFL
HAIFQIRLPTSMDQLHWLPVSEATAQLLGGSSSLLHIAAVFIVLEFLYTGLFITTHDAMHGTIALRNRQLNDLLGNICI
SLYAWFDYSMLHRKHWEHHNHTGEVGKDPDFHKGNPGLVPWFASFMSSYMSLWQFARLAWWAVVMQTLGA
PMANLLVFMAAAPILSAFRLFYFGTYLPHKPEPGPAAGSQVMSWFRAKTSEASDVMSFLTCYHFDLHWEHHRWP
FAPWWQLPHCRRLSGRGLVPALA

HpBKT3

MHVASALMVEQKGSEAAASSPDVLRAWATQYHMPSESSDAARPALKHAYKPPASDAKGITMALTIIGTWTAVFL
HAIFQIRLPTSMDQLHWLPVSEATAQLLGGSSSLLHIAAVFIVLEFLYTGLFITTHDAMHGTIALRNRQLNDLLGNICI
SLYAWFDYSMLHRKHWEHHNHTGEVGKDPDFHKGNPGLVPWFASFMSSYMSLWQFARLAWWAVVMQMLG
APMANLLVFMAAAPILSAFRLFYFGTYLPHKPGPGPAAGSQVMAWFRAKTSEASDVMSFLTCYHFDLHWEHHR
WPFAPWWQLPHCRRLSGRGLVPALA

CzBKT

MAPDVTHVQPRVQSPAGPDDEDDALSLWKAQYPMPEEKGTVSKPQAALKYRPPRSDWKGVSIACTVITLWTAV
FYHGCWQIKLTGPDKSAWWDVVATFLALEFLNTGLFITTHDAMHGTIAIRNRRLNDLLGNIAISLYAWFDYDMLHK
KHWEHHNFTGLPHKDPDFHRGDPALHKWFGRFMWEYATPLQFAKIFAYPFFLQSLRVQYPNLCVFLAAAPLVSAF
RLFYFGTYLPHLPSNAQETMPWEKSHSADDPRPLSFLKCYHFDYHWEHHRWPYAPWWELPVCKRITKTLDAAVP
GVQSDGTKKSQLVN

REFERENCES

[1] F. Not et al. **Advances in Botanical Research, Volume 64, Chapter One - Diversity and Ecology of Eukaryotic Marine Phytoplankton**, *ISSN 0065-2296, http://dx.doi.org/10.1016/B978-0-12-391499-6.00001-3*

[2] Kirsten Heimann, Roger Huerlimann, **Handbook of Marine Microalgae: Biotechnology Advances, Chapter 3 - Microalgal Classification: Major Classes and Genera of Commercial Microalgal Species**, *ISBN 978-0-12-800776-1*

[3] W. Belasco, **Algae Burgers for a Hungry World? The Rise and Fall of Chlorella Cuisine**, *Technology and Culture, Vol. 38, No. 3 (Jul., 1997), pp. 608-634*

[4] A. Guccione, **Chlorella for protein and biofuels: from strain selection to outdoor cultivation in a Green Wall Panel photobioreactor**, *Biotechnol Biofuels. 2014; 7: 84.*

[5] M.A. Borowitzka, **Handbook of Microalgal Culture Applied Phycology and Biotechnology, Second Edition, *Chapter 18: Dunaliella: Biology, Production, and Markets***, *ISBN 978-0-470-67389-8*

[6] M. Olaizola and M. E. Huntley, **Recent advances in commercial production of astaxanthin from microalgae**, *Recent Advances in Marine Biotechnology. Volume 9. Biomaterials and Bioprocessing Science Publishers, New Hampshire, pp: 143-164. 2003*

[7] M. A. Borowitzka, **Single Cell Oils (Second Edition), Microbial and Algal Oils 2010, Chapter 13: Algae Oils for Biofuels: Chemistry, Physiology, and Production**, *Pages 271-289, https://doi.org/10.1016/B978-1-893997-73-8.50017-7*

[8] Shiho, M., Kawachi, M., Horioka, K., Nishita, Y., Ohashi, K., Kaya, K. & Watanabe, M.M. **Business evaluation of an oil production system with green microalgae *Botryococcus braunii***. *Procedia Environ. Sci. 15: 90–109 (2012)*

[9] Melanie Schmidt, Gunther Geßner, Matthias Luff, Ines Heiland, Volker Wagner, Marc Kaminski, Stefan Geimer, Nicole Eitzinger, Tobias Reißenweber, Olga Voytsekh, Monika Fiedler, Maria Mittag, Georg Kreimer, **Proteomic Analysis of the Eyespot of *Chlamydomonas reinhardtii* Provides Novel Insights into Its Components and Tactic Movements**, *The Plant Cell, Vol. 18, 1908–1930, August 2006*

[10] Merchant, S.S., Prochnik, S.E., Vallon, O. et al. **The *Chlamydomonas* genome reveals the evolution of key animal and plant functions**. *Science, 318, 245–250. (2007)*

[11] Vahrenholz, C., Riemen, G., Pratje, E., Dujon, B. and Michaelis, G. **Mitochondrial DNA of *Chlamydomonas reinhardtii*: the structure of the ends of the linear 15.8-kb genome suggests mechanisms for DNA replication**. *Curr. Genet. 24, 241–247. (1993)*

[12] Maul, J.E., Lilly, J.W., Cui, L., dePamphilis, C.W., Miller, W., Harris, E.H. and Stern, D.B. **The *Chlamydomonas reinhardtii* plastid chromosome: islands of genes in a sea of repeats**. *Plant Cell, 14, 2659–2679. (2002)*

[13] E.H. Harris, ***Chlamydomonas* as a Model Organism**, *Annu. Rev. Plant Physiol. Plant Mol. Biol. 2001. 52:363–406*

[14] T. Pröschold, E.H. Harris, A.W. Coleman, **Portrait of a Species *Chlamydomonas reinhardtii***, *Genetics. 2005 Aug; 170(4): 1601–1610.doi: 10.1534/genetics.105.044503*

[15] Lurquin P.F., Behki R.M., **Uptake of bacterial DNA by *Chlamydomonas reinhardi***, *Mutat. Res., 29 (1975), pp. 35-51*

[16] Mayfield S.P., Kindle K.L., **Stable nuclear transformation of *Chlamydomonas reinhardtii* by using a *C. reinhardtii* gene as the selectable marker**, *Proc. Natl. Acad. Sci. U. S. A., 87 (1990), pp. 2087-2091*

[17] K. L. Kindle, K. L. Richards and D. B. Stern, **Engineering the chloroplast genome: techniques and capabilities for chloroplast transformation in *Chlamydomonas reinhardtii***, *PNAS March 1, 1991 88 (5) 1721-1725; https://doi.org/10.1073/pnas.88.5.1721*

[18] Claire Remacle, Pierre Cardol, Nadine Coosemans, Mauricette Gaisne, and Nathalie Bonnefoy, **High-efficiency biolistic transformation of *Chlamydomonas* mitochondria can be used to insert mutations in complex I genes**, PNAS March 21, 2006 103 (12) 4771-4776

[19] Kindle KL, **High-frequency nuclear transformation of *Chlamydomonas reinhardtii***, *Proc Natl Acad Sci U S A. 1990 Feb;87(3):1228-32.*

[20] Ramesh VM, Bingham SE, Webber AN, **A simple method for chloroplast transformation in *Chlamydomonas reinhardtii***, *Methods Mol Biol. 2011;684:313-20. doi: 10.1007/978-1-60761-925-3_23.*

[21] Shimogawara K., Fujiwara S., Grossman A., Usuda H., **High-efficiency transformation of *Chlamydomonas reinhardtii* by electroporation**, *Genetics, 148 (1998), pp. 1821-1828*

[22] Ladygin V.G., **Efficient transformation of mutant cells of *Chlamydomonas reinhardtii* by electroporation**, *Process Biochem., 39 (2004), pp. 1685-1691*

[23] Azencott H.R., Peter G.F., Prausnitz M.R., **Influence of the cell wall on intracellular delivery to algal cells by electroporation and sonication***, Ultrasound Med. Biol., 33 (2007), pp. 1805-1817*

[24] **Manual: GeneArt Max Efficiency Transformation Reagent for Algae**, Life Technologies, November 2013

[25] Hau-Hsuan Hwang, Manda Yu and Erh-Min Lai, ***Agrobacterium*-Mediated Plant Transformation: Biology and Applications**, *The Arabidopsis Book 15: e0186. 2017 https://doi.org/10.1199/tab.0186*

[26] Kumar S.V., Misquitta R.W., Reddy V.S., Rao B.J., Rajam M.V.,**Genetic transformation of the green alga *Chlamydomonas reinhardtii* by *Agrobacterium tumefaciens***, *Plant Sci., 166 (2004), pp. 731-738*

[27] Hema R., Senthil-Kumar M., Shivakumar S., Reddy P.C., Udayakumar M., ***Chlamydomonas reinhardtii,* a model system for functional validation of abiotic stress responsive genes**, *Planta, 226 (2007), pp. 655-670*

[28] Dunahay T.G., **Transformation of *Chlamydomonas reinhardtii* with silicon carbide whiskers**, *BioTechniques, 15 (1993), pp. 452-460*

[29] Wyber JA1, Andrews J, D'Emanuele A., **The use of sonication for the efficient delivery of plasmid DNA into cells***, Pharm Res. 1997 Jun;14(6):750-6.*

[30] Joel M. Hyman, Erika I. Geihe, Brian M. Trantow, Bahram Parvin, and Paul A. Wender, **A molecular method for the delivery of small molecules and proteins across the cell wall of algae using molecular transporters**, *PNAS August 14, 2012 109 (33) 13225-13230; https://doi.org/10.1073/pnas.1202509109*

[31] Véronique Larosa and Claire Remacle**, Transformation of the mitochondrial genome***, Int. J. Dev. Biol. 57: 659 - 665 (2013), doi: 10.1387/ijdb.130230cr*

[32] Muhamed Adem, Dereje Beyene and Tileye Feyissa, **Recent achievements obtained by chloroplast transformation**, *Plant Methods. 2017; 13: 30 doi: 10.1186/s13007-017-0179-1*

[33] Zhang R, Patena W, Armbruster U, Gang SS, Blum SR, Jonikas MC, **High-Throughput Genotyping of Green Algal Mutants Reveals Random Distribution of Mutagenic Insertion Sites and Endonucleolytic Cleavage of Transforming DNA**, *Plant Cell. 2014 Apr;26(4):1398-1409. Epub 2014 Apr 4.*

[34] Meslet-Cladière L1, Vallon O, **Novel shuttle markers for nuclear transformation of the green alga *Chlamydomonas reinhardtii***, *Eukaryot Cell. 2011 Dec;10(12):1670-8. doi: 10.1128/EC.05043-11. Epub 2011 Oct 14.*

[35] Debuchy R., Purton S., Rochaix J.-D.,**The argininosuccinate lyase gene of *Chlamydomonas reinhardtii:* an important tool for nuclear transformation and for correlating the genetic and molecular maps of the ARG7 locus**, *EMBO J., 8 (1989), pp. 2803-2809*

[36] Smart E.J., Selman B.R, **Complementation of *a Chlamydomonas reinhardtii* mutant defective in the nuclear gene encoding the chloroplast coupling factor 1 (CF1) gamma subunit (atpC)**, *J. Bioenerg. Biomembr., 25 (1993), pp. 275-284*

[37] Stevens DR, Rochaix JD, Purton S, **The bacterial phleomycin resistance gene *ble* as a dominant selectable marker in *Chlamydomonas***, *Mol Gen Genet. 1996 Apr 24;251(1):23-30*

[38] Cerutti H , Johnson AM, Gillham N W et al. **A eubacterial gene conferring spectinomycin resistance on *Chlamydomonas reinhardtii*: Integration into the nuclear genome and gene expression.** *Genetics 1997; 145:97-110.*

[39] Berthold P, Schmitt R, Mages W, **An engineered Streptomyces hygroscopicus aph 7" gene mediates dominant resistance against hygromycin B in *Chlamydomonas reinhardtii***. *Protist. 2002 Dec;153(4):401-12.*

[40] Sizova I, Fuhrmann M, Hegemann P., **A Streptomyces rimosus aphVIII gene coding for a new type phosphotransferase provides stable antibiotic resistance to *Chlamydomonas reinhardtii***.*Gene. 2001 Oct 17;277(1-2):221-9.*

[41] Sergio A Garcia-Echauri and Guy A Cardineau, **TETX: a novel nuclear selection marker for *Chlamydomonas reinhardtii* transformation**, *Plant Methods 2015 11:27, doi.org/10.1186/s13007-015-0064-8*

[42] Hayes, J.D., Wolf, C.R., 1990. **Molecular mechanisms of drug resistance**. *Biochem. J. 272, 281–295.*

[43] Markus Fuhrmann, Wolfgang Oertel and Peter Hegemann, **A synthetic gene coding for the green fluorescent protein (GFP) is a versatile reporter in *Chlamydomonas reinhardtii***, *The Plant Journal (1999) 19(3), 353-361*

[44] Franklin S, Ngo B, Efuet E, Mayfield SP**, Development of a GFP reporter gene for *Chlamydomonas reinhardtii* chloroplast**, *Plant J. 2002 Jun;30(6):733-44.*

[45] Jinxia Wu, Zhangli Hu, Chaogang Wang, Shuangfei Li, Anping Lei, **Efficient expression of green fluorescent protein (GFP) mediated by a chimeric promoter in *Chlamydomonas reinhardtii***, *Chinese Journal of Oceanology and Limnology, August 2008, 26:242*

[46] BA Rasala, PA Lee, Z Shen, SP Briggs, M Mendez, SP Mayfield, **Robust Expression and Secretion of Xylanase1 in *Chlamydomonas reinhardtii* by Fusion to a Selection Gene and Processing with the FMDV 2A Peptide**, *PLOS ONE, August 2012, Volume 7, Issue 8, e43349*

[47] Schoppmeier, J., Mages, W. and Lechtreck, K.-F. (2005) **GFP as a tool for the analysis of proteins in the flagellar basal apparatus of *Chlamydomonas***. *Cell Motil. Cytoskelet. 61, 189–200*.

[48] Diener, D. (2009) **Analysis of cargo transport by IFT and GFP imaging of IFT in *Chlamydomonas***. *In Methods in Cell Biology, Vol. 93 (King, S.M. and Pazour, G.J., eds). Burlington, MA: Academic Press, pp. 111–119.*

[49] Yubing Li, Dianyi Liu, Cristina López-Paz, Bradley JSC Olson, James G Umen, **A new class of cyclin dependent kinase in *Chlamydomonas* is required for coupling cell size to cell division**, *eLife 2016;5:e10767. DOI: 10.7554/eLife.10767*

[50] Yoshihara, C., Inoue, K., Schichnes, D., Ruzin, S., Inwood, W. and Kustu, S. (2008) **An Rh1-GFP fusion protein is in the cytoplasmic membrane of a white mutant strain of *Chlamydomonas reinhardtii***. *Mol. Plant, 1, 1007–1020.*

[51] Beth A. Rasala, Daniel J. Barrera, Jenny Ng, Thomas M. Plucinak, Julian N. Rosenberg, Donald P. Weeks, George A. Oyler, Todd C. Peterson, Farzad Haerizadeh and Stephen P. Mayfield, **Expanding the spectral palette of fluorescent proteins for the green microalga *Chlamydomonas reinhardtii***, *The Plant Journal (2013) 74, 545–556*

[52] Kyle J. Lauersen, Olaf Kruse, Jan H. Mussgnug, **Targeted expression of nuclear transgenes in *Chlamydomonas reinhardtii* with a versatile, modular vector toolkit**, *Appl Microbiol Biotechnol (2015) 99:3491–3503 DOI 10.1007/s00253-014-6354-7*

[53] Eichler-Stahlberg, A., Weisheit, W., Ruecker, O. and Heitzer, M. (2009) **Strategies to facilitate transgene expression in *Chlamydomonas reinhardtii***. *Planta, 229, 873–883.*

[54] Pratheesh, P.T., Vineetha, M. and Kurup, G.M. (2014) **An efficient protocol for the *Agrobacterium*-mediated genetic transformation of microalga *Chlamydomonas reinhardtii***. *Mol. Biotechnol. 56, 507–515.*

[55] Specht, E.A., Nour-Eldin, H.H., Hoang, K.T.D. and Mayfield, S.P. (2015) **An improved ARS2-derived nuclear reporter enhances the efficiency and ease of genetic engineering in *Chlamydomonas***. *Biotechnol. J. 10, 473–479.*

[56] Fischer N., Setif P., Rochaix J.-D., **Site-directed mutagenesis of the PsaC subunit of photosystem I-FB is the cluster interacting with soluble ferredoxin**, *J. Biol. Chem., 274 (1999), pp. 23333-23340*

[57] Kozminski K.G., Johnson K.A., Forscher P., Rosenbaum J.L., **A motility in the eukaryotic flagellum unrelated to flagellar beating**, *Proc. Natl. Acad. Sci. U. S. A., 90 (1993), pp. 5519-5523*

[58] Schroda M., Blöcker D., Beck C.F., **The HSP70A promoter as a tool for the improved expression of transgenes in *Chlamydomonas***, *Plant J., 21 (2000), pp. 121-131*

[59] Ohresser M, Matagne RF, Loppes R. **Expression of the arylsulphatase reporter gene under the control of the nit1 promoter in *Chlamydomonas reinhardtii***. *Curr Genet. 1997;31:264–271.*

[60] Villand P, Eriksson M, Samuelsson G. **Carbon dioxide and light regulation of promoters controlling the expression of mitochondrial carbonic anhydrase in *Chlamydomonas reinhardtii.*** *Biochem J. 1997;327(Pt 1):51–57.*

[61] Quinn JM, Kropat J, Merchant S. **Copper response element and Crr1-dependent Ni(2+)-responsive promoter for induced, reversible gene expression in *Chlamydomonas reinhardtii.*** *Eukaryot Cell. 2003;2:995–1002.*

[62] Díaz-Santos E, de la Vega M, Vila M, Vigara J, León R., **Efficiency of different heterologous promoters in the unicellular microalga *Chlamydomonas reinhardtii***., *Biotechnol Prog. 2013 Mar-Apr;29(2):319-28. doi: 10.1002/btpr.1690*

[63] Ladygin, V.G. & Boutanaev A.M., **Transformation of *Chlamydomonas reinhardtii* CW-15 with the Hygromycin Phosphotransferase Gene as a Selectable Marker**, *Russian Journal of Genetics (2002) 38: 1009. https://doi.org/10.1023/A:1020279429009*

[64] Kazusa Codon Usage Database (Nakamura, Y., Gojobori, T. and Ikemura, T. (2000) *Nucl. Acids Res. 28, 292.)* Status: October 2018

[65] Barahimipour R, Strenkert D, Neupert J, Schroda M, Merchant SS, Bock R, **Dissecting the contributions of GC content and codon usage to gene expression in the model alga *Chlamydomonas reinhardtii***, *Plant J. 2015 Nov;84(4):704-17. doi: 10.1111/tpj.13033. Epub 2015 Oct 16.*

[66] H Cerutti, A M Johnson, N W Gillham, J E Boynton, **Epigenetic silencing of a foreign gene in nuclear transformants of *Chlamydomonas***, *The Plant Cell, June 1997. DOI: https://doi.org/10.1105/tpc.9.6.925*

[67] Fuhrmann M., Stahlberg A., Govorunova E., Rank S., Hegemann P., **The abundant retinal protein of the *Chlamydomonas* eye is not the photoreceptor for phototaxis and photophobic responses**, *J. Cell Sci., 114 (2001), pp. 3857-3863*

[68] Pfannenschmid F., Wimmer V.C., Rios R.M., Geimer S., Kröckel U., Leiherer A., Haller K., Nemcová Y., Mages W., ***Chlamydomonas* DIP13 and human NA14: a new class of proteins associated with microtubule structures is involved in cell division**, *J. Cell Sci., 116 (2003), pp. 1449-1462*

[69] Chen H.C., Melis A**., Localization and function of SulP, a nuclear-encoded chloroplast sulfate permease in *Chlamydomonas reinhardtii***, *Planta, 220 (2004), pp. 198-210*

[70] Randall A. Hughes and Andrew D. Ellington, **Synthetic DNA Synthesis and Assembly: Putting the Synthetic in Synthetic Biology**, *Cold Spring Harb Perspect Biol 2017;9:a023812*

[71] Engler C, Marillonnet S, **Golden Gate cloning**, *Methods Mol Biol. 2014;1116:119-31. doi: 10.1007/978-1-62703-764-8_9.*

[72] Pierre Crozet, Francisco J. Navarro, Felix Willmund, Payam Mehrshahi, Kamil Bakowski, Kyle J. Lauersen, Maria-Esther Pérez-Pérez, Pascaline Auroy, Aleix Gorchs Rovira, Susana Sauret-Gueto, Justus Niemeyer, Benjamin Spaniol, Jasmine Theis, Raphael Trösch, Lisa-Desiree Westrich, Konstantinos Vavitsas, Thomas Baier, Wolfgang Hübner, Felix de Carpentier, Mathieu Cassarini, Antoine Danon, Julien Henri, Christophe H. Marchand, Marcello de Mia, Kevin Sarkissian, David C. Baulcombe, Gilles Peltier, José-Luis Crespo, Olaf Kruse, Poul-Erik Jensen, Michael Schroda, Alison G. Smith, and Stéphane D. Lemaire, **Birth of a Photosynthetic Chassis: A MoClo Toolkit Enabling Synthetic Biology in the Microalga *Chlamydomonas reinhardtii***, *ACS Synthetic Biology 2018 7 (9), 2074-2086, DOI: 10.1021/acssynbio.8b00251*

[73] Juliane Neupert, Daniel Karcher and Ralph Bock, **Generation of *Chlamydomonas* strains that efficiently express nuclear transgenes**, *The Plant Journal (2009) 57, 1140–1150*

[74] Rouhollah Barahimipour, Daniela Strenkert, Juliane Neupert, Michael Schroda, Sabeeha S. Merchant and Ralph Bock, **Dissecting the contributions of GC content and codon usage to gene expression in the model alga *Chlamydomonas reinhardtii***, *The Plant Journal (2015) 84, 704–717*

[75] Fantao Kong, Tomohito Yamasaki, Sari Dewi Kurniasih, Liyuan Hou, Xiaobo Li, Nina Ivanova, Shigeru Okada and Takeshi Ohama, **Robust expression of heterologous genes by selection marker fusion system in improved *Chlamydomonas* strains**, *Journal of Bioscience and Bioengineering, VOL. 120 No. 3, 239e245, 2015*

[76] Masayuki Onishi and John R. Pringle, **Robust Transgene Expression from Bicistronic mRNA in the Green Alga *Chlamydomonas reinhardtii***, *G3: Genes, Genomes, Genetics December 1, 2016 vol. 6 no. 12 4115-4125; https://doi.org/10.1534/g3.116.033035*

[77] Fantao Kong, Tomohito Yamasaki, Sari Dewi Kurniasih, Liyuan Hou, Xiaobo Li, Nina Ivanova, Shigeru Okada and Takeshi Ohama, **Robust expression of heterologous genes by selection marker fusion system in improved *Chlamydomonas* strains**, *J. Biosci. Bioeng., (2015), http://dx.doi.org/10.1016/j.jbiosc.2015.01.005*

[78] *Benzer S (1957).* ***"The elementary units of heredity****". In McElroy WD, Glass B. The Chemical Basis of Heredity. Baltimore, Maryland: Johns Hopkins Press. pp. 70–93*

[79] Jang S. K., Krausslich H. G., Nicklin M. J., Duke G. M., Palmenberg A. C., et al., 1988 ***A segment of the 5' nontranslated region of encephalomyocarditis virus RNA directs internal entry of ribosomes during in vitro translation****. J. Virol. 62: 2636–2643.*

[80] Martínez-Salas E., , 1999 ***Internal ribosome entry site biology and its use in expression vectors****. Curr. Opin. Biotechnol. 10: 458–464.*

[81] Hunt A. G., Maiti I. B., , 2001 ***Strategies for expressing multiple foreign genes in plants as polycistronic constructs****. In Vitro Cell. Dev. Biol. Plant 37: 313–320.*

[82] Dorokhov Y. L., Skulachev M. V., Ivanov P. A., Zvereva S. D., Tjulkina L. G., et al., , 2002 ***Polypurine (A)-rich sequences promote cross-kingdom conservation of internal ribosome entry.*** *Proc. Natl. Acad. Sci. USA 99: 5301–5306.*

[83] Jackson, R. J., 2013 **The current status of vertebrate cellular mRNA IRESs**, *Cold Spring Harb. Perspect. Biol. 5: a011569*

[84] Yuancheng Wang, Feng Wang, Riyuan Wang, Ping Zhao & Qingyou Xia, **2A self-cleaving peptide-based multi-gene expression system in the silkworm *Bombyx mori***, *Scientific Reports volume 5, Article number: 16273 (2015)*

[85] Donnelly ML, et al. **Analysis of the aphthovirus 2A/2B polyprotein 'cleavage' mechanism indicates not a proteolytic reaction, but a novel translational effect: a putative ribosomal 'skip'** The *Journal of general virology. 2001;82:1013–1025. doi: 10.1099/0022-1317-82-5-1013.*

[86] Ziqing Liu, Olivia Chen, J. Blake Joseph Wall, Michael Zheng, Yang Zhou, Li Wang, Haley Ruth Vaseghi, Li Qian and Jiandong Liu, **Systematic comparison of 2A peptides for cloning multi-genes in a polycistronic vector**, *Sci Rep. 2017; 7: 2193. Published online 2017 May 19. doi: 10.1038/s41598-017-02460-2*

[87] Beth A. Rasala, Syh-Shiuan Chao, Matthew Pier, Daniel J. Barrera, Stephen P. Mayfield**, Enhanced Genetic Tools for Engineering Multigene Traits into Green Algae**, *PLOS One, Published: April 7, 2014 https://doi.org/10.1371/journal.pone.0094028*

[88] Hochmal AK, Zinzius K, Charoenwattanasatien R, Gäbelein P, Mutoh R, Tanaka H, Schulze S, Liu G, Scholz M, Nordhues A, Offenborn JN, Petroutsos D, Finazzi G, Fufezan C, Huang K, Kurisu G, Hippler M, **Calredoxin represents a novel type of calcium-dependent sensor-responder connected to redox regulation in the chloroplast**, *Nat Commun. 2016 Jun 14;7:11847. doi: 10.1038/ncomms11847.*

[89] Maribel M. Loera-Quezada, Marco Antonio Leyva-González, Gilberto Velázquez-Juárez, Lenin Sanchez-Calderón, Mauro Do Nascimento, Damar López-Arredondo, Luis Herrera-Estrella, **A novel genetic engineering platform for the effective management of biological contaminants for the production of microalgae**, *Plant Biotechnology Journal, Volume14, Issue10, October 2016, Pages 2066-2076*

[90] Morikawa T, Uraguchi Y, Sanda S, Nakagawa S, Sawayama S, **Overexpression of DnaJ-Like Chaperone Enhances Carotenoid Synthesis in *Chlamydomonas reinhardtii,*** *Appl Biochem Biotechnol. 2018 Jan;184(1):80-91. doi: 10.1007/s12010-017-2521-5. Epub 2017 Jun 13.*

[91] Kong F, Liang Y, Légeret B, Beyly-Adriano A, Blangy S, Haslam RP, Napier JA, Beisson F, Peltier G, Li-Beisson Y, ***Chlamydomonas*** **carries out fatty acid β-oxidation in ancestral peroxisomes using a bona fide acyl-CoA oxidase**.*Plant J. 2017 Apr;90(2):358-371. doi: 10.1111/tpj.13498.*

[92] Hashimoto H, Uragami C, Cogdell RJ, **Carotenoids and Photosynthesis**.*Subcell Biochem. 2016;79:111-39. doi: 10.1007/978-3-319-39126-7_4.*

[93] Liu GY, Essex A, Buchanan JT, Datta V, Hoffman HM, et al. (2005) ***Staphylococcus aureus*** **golden pigment impairs neutrophil killing and promotes virulence through its antioxidant activity**. *J Exp Med 202: 209–215.*

[94] Gruszecki WI, Strzalka K (2005) **Carotenoids as modulators of lipid membrane physical properties**. *Biochim Biophys Acta 1740: 108–115*.

[95] Jonathan L. Klassen, **Phylogenetic and Evolutionary Patterns in Microbial Carotenoid Biosynthesis Are Revealed by Comparative Genomics**, *PLOS One, Published: June 22, 2010, https://doi.org/10.1371/journal.pone.0011257*

[96] Martin Lohr, Chung-Soon Im, and Arthur R. Grossman, **Genome-Based Examination of Chlorophyll and Carotenoid Biosynthesis in *Chlamydomonas reinhardtii,*** *Plant Physiology, May 2005, Vol. 138, pp. 490–515*

[97] Ying Yang, Rie Yatsunami, Ai Ando, Nobuhiro Miyoko, Toshiaki Fukui, Shinichi Takaichi, Satoshi Nakamura, **Complete Biosynthetic Pathway of the C50 Carotenoid Bacterioruberin from Lycopene in the Extremely Halophilic Archaeon *Haloarcula japonica,*** *Journal of Bacteriology Apr 2015, 197 (9) 1614-1623; DOI: 10.1128/JB.02523-14*

[98] **Carotenoids Market Size, Share, Report, Analysis, Trends & Forecast to 2022**, *Stratistics Market Research Consulting, 2017*

[99] **Carotenoids market by type, by source, by application and by region – Global trends and forecast to 2019** – *MarketsandMarkets, 2015*

[100] **The global market for carotenoids** - *BCC Research, 2015*

[101] Symonds RC, Kelly MS, Caris-Veyrat C, Young AJ.**Carotenoids in the sea urchin Paracentrotus lividus: occurrence of 9'-cis-echinenone as the dominant carotenoid in gonad color determination**.*Comp Biochem Physiol B Biochem Mol Biol. 2007 Dec;148(4):432-44.*

[102] Takashi Maoka, Tetsuji Etoh, Sanae Kishimoto and Syusaku Sakata, **Carotenoids and Their Fatty Acid Esters in the Petals of *Adonis aestivalis,*** *. Oleo Sci. 60, (2) 47-52 (2011)*

[103] Francis Haxo, **Carotenoids of the Mushroom *Cantharellus cinnabarinus***, *Botanical Gazette 112(2) , December 1950*

[104] Miguel Olaizola and Mark E. Huntley, **Recent advances in commercial production of astaxanthin from microalgae**, *Recent Advances in Marine Biotechnology. Volume 9. Science Publishers, New Hampshire, pp: 143-164. 2003*

[105] Hussein G, Sankawa U, Goto H, Matsumoto K, Watanabe H, **Astaxanthin, a carotenoid with potential in human health and nutrition**, *J Nat Prod. 2006 Mar;69(3):443-9.*

[106] Kurashige, M., E. Okimasu, M. Inoue and K. Utsumi. 1990. **Inhibition of oxidative injury of biological membranes by astaxanthin**. *Physiol. Chem. Phys. Med. NMR 22: 27-38*.

[107] Bob Capelli, Debasis BagchiGerald R. Cysewski, **Synthetic astaxanthin is significantly inferior to algal-based astaxanthin as an antioxidant and may not be suitable as a human nutraceutical supplement**, *Nutrafoods (2013) 12: 145. https://doi.org/10.1007/s13749-013-0051-5*

[108] Jin Liu, Zheng Sun, Henri Gerken, Zheng Liu, Yue Jiang, Feng Chen, **Chlorella zofingiensis as an Alternative Microalgal Producer of Astaxanthin: Biology and Industrial Potential**, *Mar Drugs. 2014 Jun; 12(6): 3487–3515.doi: [10.3390/md12063487]*

[109] Kay Grünewald, Joseph Hirschberg, and Christoph Hagen**, Ketocarotenoid Biosynthesis Outside of Plastids in the Unicellular Green Alga *Haematococcus pluvialis***, *THE JOURNAL OF BIOLOGICAL CHEMISTRY Vol. 276, No. 8, Issue of February 23, pp. 6023–6029, 2001*

[110] Danxiang Han, Yantao Li and Qiang Hu, **Astaxanthin in microalgae: pathways, functions and biotechnological implications,** *ALGAE 2013;28(2): 131-147.*

[111] Norihiko Misawa,Yoshiko Satomi,Keiji Kondo, Akihiro Yokoyama, Susumu Kajiwara, Toshiko Saito, Takeshi Ohtani and Wataru Miki, **Structure and Functional Analysis of a Marine Bacterial Carotenoid Biosynthesis Gene Cluster and Astaxanthin Biosynthetic Pathway Proposed at the Gene Level**, *JOURNAL OF BACTERIOLOGY, Nov. 1995, p. 6575–6584*

[112] Jose L. Barredo, Carlos García-Estrada, Katarina Kosalkova and Carlos Barreiro, **Biosynthesis of Astaxanthin as a Main Carotenoid in the Heterobasidiomycetous Yeast *Xanthophyllomyces dendrorhous***, *J Fungi (Basel). 2017 Sep; 3(3): 44.*

[113] Francis X. Cunningham Jr and Elisabeth Gantt**, A study in scarlet: enzymes of ketocarotenoid biosynthesis in the flowers of *Adonis aestivalis*,** *The Plant Journal (2005) 41, 478–492*

[114] Makio Kobayashi, **Astaxanthin biosynthesis enhanced by reactive oxygen species in the green alga *Haematococcus pluvialis***, *M. Biotechnol. Bioprocess Eng. (2003) 8: 322.*

[115] Mirash Zhekisheva, Aliza Zarka, Inna Khozin-Goldberg, Zvi Cohen, and Sammy Boussiba, **INHIBITION OF ASTAXANTHIN SYNTHESIS UNDER HIGH IRRADIANCE DOES NOT ABOLISH TRIACYLGLYCEROL ACCUMULATION IN THE GREEN ALGA *HAEMATOCOCCUS PLUVIALIS* (CHLOROPHYCEAE)**, *J. Phycol. 41, 819–826 (2005)*

[116] Roth MS, Cokus SJ, Gallaher SD, Walter A, Lopez D, Erickson E Endelman B, Westcott D, Larabell CA, Merchant SS, Pellegrini M, Niyogi KK, **Chromosome-level genome assembly and transcriptome of the green alga *Chromochloris zofingiensis* illuminates astaxanthin production**, *Proc Natl Acad Sci U S A. 2017 May 23;114(21):E4296-E4305.*

[117] Yu- Juan Zhong, Jun-Chao Huang, Jin Liu, Yin Li, Yue Jiang, Zeng-Fu Xu, Gerhard Sandmann and Feng Chen**, Functional characterization of various algal carotenoid ketolases reveals that ketolating zeaxanthin efficiently is essential for high production of astaxanthin in transgenic *Arabidopsis***, *Journal of Experimental Botany, Vol. 62, No. 10, pp. 3659–3669, 2011*

[118] Guanqun Chen, Baobei Wang, Danxiang Han, Milton Sommerfeld, Yinghua Lu, Feng Chen and Qiang Hu, **Molecular mechanisms of the coordination between astaxanthin and fatty acid biosynthesis in *Haematococcus pluvialis* (Chlorophyceae),** *The Plant Journal (2015) 81, 95–107*

[119] Junchao Huang, Yujuan Zhong, Gerhard Sandmann, Jin Liu, Feng Chen, **Cloning and selection of carotenoid ketolase genes for the engineering of high-yield astaxanthin in plants**, *Planta (2012) 236:691–699*

[120] Jun-Chao Huang, Yu-Juan Zhong, Jin Liu, Gerhard Sandmann, Feng Chen, **Metabolic engineering of tomato for high-yield production of astaxanthin***, Metabolic Engineering 17 (2013) 59–67*

[121] Chao Bai, Judit Berman, Gemma Farre, Teresa Capell, Gerhard Sandmann, Paul Christou, Changfu Zhu, **Reconstruction o f the astaxanthin biosynthesis pathway in rice endosperm reveals a metabolic bottleneck at the level of endogenous b-carotene hydroxylase activity***, Transgenic Res (2017) 26:13–23*

[122] Cavalier-Smith T, **Electron microscopy of zygospore formation in *Chlamydomonas reinhardtii***, *Protoplasma 87: 297-315 (1976)*

[123] Sonja Werner, **Nachweis und Charakterisierung der Ketocarotinoidakkumulation in Zygosporen des Modellorganismus *Chlamydomonas reinhardtii***, *Dissertation Zur Erlangung des Grades Doktor der Naturwissenschaften, Fachbereich Biologie Der Johannes Gutenberg-Universität Mainz 2011*

[124] Huang J, Chen F and Sandmann G (2006): **Stress-related differential expression of multiple ß-carotene ketolase genes in the unicellular green alga *Haematococcus pluvialis.*** *Journal of Biotechnology 122: 176–185*

[125] Albrecht M, Steiger S, Sandmann G., **Expression of a ketolase gene mediates the synthesis of canthaxanthin in *Synechococcus* leading to tolerance against photoinhibition, pigment degradation and UV-B sensitivity of photosynthesis**, *Photochem Photobiol. 2001 May;73(5):551-5.*

[126] Anila N, Simon DP, Chandrashekar A, Ravishankar GA, Sarada R, **Metabolic engineering of *Dunaliella salina* for production of ketocarotenoids**, *Photosynth Res. 2016 Mar;127(3):321-33. doi: 10.1007/s11120-015-0188-8. Epub 2015 Sep 3.*

[127] Rosa Leon, Inmaculada Couso, Emilio Fernandez**, Metabolic engineering of ketocarotenoids biosynthesis in the unicelullar microalga *Chlamydomonas reinhardtii***, *Journal of Biotechnology 130 (2007) 143–152*

[128] Wong, K. (2006). **Transgenic *Chlamydomonas reinhardtii* as an experimental system to study the regulation of carotenoid biosynthesis in green microalgae**. (Thesis). University of Hong Kong, Pokfulam, Hong Kong SAR.

[129] Chunaev, A., Mirnaya, O., Maslov, V., and Boschetti, A. (1991). **Chlorophyll b- and loroxanthin-deficient mutants of *Chlamydomonas reinhardtii***. *Photosynthetica 25, 291–301.*

[130] Krishna K. Niyogi, Olle Bjorkman and Arthur R. Grossman, ***Chlamydomonas* Xanthophyll Cycle Mutants Identified by Video Imaging of Chlorophyll Fluorescence Quenching**, *The Plant Cell, Vol. 9, 1369-1 380, August 1997 O 1997 American Society of Plant Physiologists*

[131] Irene Baroli, An D. Do, Tomoko Yamane, and Krishna K. Niyogi, Zeaxanthin **Accumulation in the Absence of a Functional Xanthophyll Cycle Protects *Chlamydomonas reinhardtii* from Photooxidative Stress**, *The Plant Cell, Vol. 15, 992–1008, April 2003*

[132] **Manual: GeneArt™ Chlamydomonas Protein Expression Vector For expression of recombinant proteins in *Chlamydomonas reinhardtii***, Thermo Fisher 2017

[133] Laemmli, U. K. (1970). **Cleavage of structural proteins during the assembly of the head of bacteriophage T4***. Nature 227(5259): 680-685.*

[134] Hartmut K. Lichtenthaler and Claus Buschmann, **Chlorophylls and Carotenoids: Measurement and Characterization by UV-VIS Spectroscopy**, *Current Protocols in Food Analytical Chemistry (2001) F4.3.1-F4.3.8*

[135] Richard D. Richins, James Kilcrease, Laura Rodgriguez-Uribe and Mary A. O'Connell, **Carotenoid Extraction and Quantification from *Capsicum annuum***, *Bio-protocol Vol 4, Iss 19, Oct 05, 2014 (http://www.bio-protocol.org/e1256)*

[136] Siebert PD, Chenchik A, Kellog DE, Lukyanov KA and Lukyanov SA (1995) **An improved PCR method for walking in uncloned genomic DNA**. *Nucleic Acids Res., 23, 1087-1088.*

[137] Steve V. Pollock, Bratati Mukherjee, Joanna Bajsa‐Hirschel, Marylou C. Machingura, Ananya Mukherjee, Arthur R. Grossman, James V. Moroney, **A robust protocol for efficient generation, and genomic characterization of insertional mutants of *Chlamydomonas reinhardtii***, *Plant Methods (2017) 13:22 DOI 10.1186/s13007-017-0170-x*

[138] Simossis VA, Heringa J, **PRALINE: a multiple sequence alignment toolbox that integrates homology-extended and secondary structure information**, *Nucleic Acids Res. 2005 Jul 1;33(Web Server issue):W289-94.*

[139] Krogh A, Larsson B, von Heijne G, Sonnhammer EL, **Predicting transmembrane protein topology with a hidden Markov model: application to complete genomes,** *J Mol Biol. 2001 Jan 19;305(3):567-80.*

[140] Kelley LA, Mezulis S, Yates CM, Wass MN, Sternberg MJ, **The Phyre2 web portal for protein modeling, prediction and analysis***, Nat Protoc. 2015 Jun;10(6):845-58*

[141] Marianne Tardif, Ariane Atteia, Michael Specht, Guillaume Cogne, Norbert Rolland, Sabine Brugière, Michael Hippler, Myriam Ferro, Christophe Bruley, Gilles Peltier, Olivier Vallon, Laurent Cournac, **PredAlgo: A New Subcellular Localization Prediction Tool Dedicated to Green Algae, Molecular Biology and Evolution,** *Volume 29, Issue 12, December 2012, Pages 3625–3639, https://doi.org/10.1093/molbev/mss178*

[142] E.H. Harris, **Chlamydomonas Source Book, Volume 1, 2nd Edition** *2009, Elsevier Inc. ISBN 978-0-12-370873-1*

[143] Ritsuko Fujii, Nami Yamano, Hideki Hashimoto, Norihiko Misawa, Kentaro Ifuku, **Photoprotection vs. Photoinhibition of Photosystem II in Transplastomic Lettuce (*Lactuca sativa*) Dominantly Accumulating Astaxanthin***, Plant Cell Physiol. 57(7): 1518–1529 (2016) doi:10.1093/pcp/pcv187*

[144] Cara L. Mortimer, Norihiko Misawa, Laura Perez-Fons, Francesca P. Robertson, Hisashi Harada, Peter M. Bramley, Paul D. Fraser, **The Formation and Sequestration of Nonendogenous Ketocarotenoids in Transgenic *Nicotiana glauca***, *Plant Physiology Mar 2017, 173 (3) 1617-1635; DOI: 10.1104/pp.16.01297*

[145] Matthew B. Toomey, Kevin J. McGraw; **Modified Saponification and HPLC Methods for Analyzing Carotenoids from the Retina of Quail: Implications for Its Use as a Nonprimate Model Species**. *Invest. Ophthalmol. Vis. Sci. 2007;48(9):3976-3982. doi: 10.1167/iovs.07-0208.*

[146] Céline Bourcier de Carbon, Adrien Thurotte, Adjélé Wilson, François Perreau & Diana Kirilovsky, **Biosynthesis of soluble carotenoid holoproteins in *Escherichia coli,*** *Scientific Reports volume 5, Article number: 9085 (2015)*

[147] Paul D. FRASER, Hiroshi SHIMADA and Norihiko MISAWA, **Enzymic confirmation of reactions involved in routes to astaxanthin formation, elucidated using a direct substrate *in vitro* assay**, *Eur. J. Biochem. 252, 2292236 (1998)*

[148] Kai L, Kaldenhoff R, Lian J, et al. **Preparative scale production of functional mouse aquaporin 4 using different cell-free expression modes**. *PLoS One. 2010;5(9):e12972. Published 2010 Sep 24. doi:10.1371/journal.pone.0012972*

[149] Komsic-Buchmann, Karin & Wöstehoff, Luisa & Becker, Burkhard. (2014). **The Contractile Vacuole as a Key Regulator of Cellular Water Flow in *Chlamydomonas reinhardtii***. *Eukaryotic cell. 13. 10.1128/EC.00163-14.*

[150] Anil Kumar, **Optimization of Transgene Expression in *Chlamydomonas reinhardtii* and its Biotechnological Applications**, *Ph.D. DISSERTATION, The Ohio State University 2010*

[151] Thomas M. Plucinak, **MAKING CHLAMYDOMONAS REINHARDTII A BETTR MODEL ORGANISM: TACKLING THE INEFFICIENCY OF NUCLEAR TRASGENE EXPRESSION AND IMPROVING METHODS FOR THE GENERAION AND CHARATERIZATION OF INSERTIONAL MUTANT LIBRARIES**, *Ph.D. dissertation, University of Nebraska, 2013*

[152] Sung-Eun Shin, Jong-Min Lim, Hyun Gi Koh, Eun Kyung Kim, Nam Kyu Kang, Seungjib Jeon, Sohee Kwon, Won-Sub Shin, Bongsoo Lee, Kwon Hwangbo, Jungeun Kim, Sung Hyeok Ye, Jae-Young Yun, Hogyun Seo, Hee-Mock Oh, Kyung-Jin Kim, Jin-Soo Kim, Won-Joong Jeong, Yong Keun Chang & Byeong-ryool Jeong, **CRISPR/Cas9-induced knockout and knock-in mutations in *Chlamydomonas reinhardtii***, *Scientific Reports volume 6, Article number: 27810 (2016)*

[153] Andre Greiner, Simon Kelterborn, Heide Evers, Georg Kreimer, Irina Sizova, Peter Hegemann, **Targeting of Photoreceptor Genes in *Chlamydomonas reinhardtii* via Zinc-Finger Nucleases and CRISPR/Cas9**, *The Plant Cell Oct 2017, 29 (10) 2498-2518; DOI: 10.1105/tpc.17.00659*

[154] Melanie Schmidt, Gunther Geßner, Matthias Luff, Ines Heiland, Volker Wagner, Marc Kaminski, Stefan Geimer, Nicole Eitzinger, Tobias Reißenweber, Olga Voytsekh, Monika Fiedler, Maria Mittag, Georg Kreimer, **Proteomic Analysis of the Eyespot of *Chlamydomonas reinhardtii* Provides Novel Insights into Its Components and Tactic Movements**, *The Plant Cell Aug 2006, 18 (8) 1908-1930; DOI: 10.1105/tpc.106.041749*

[155] Grünewald, K. & Hagen, **β-carotene is the intermediate exported from the chloroplast during accumulation of secondary carotenoids in *Haematococcus pluvialis***, *C. Journal of Applied Phycology (2001) 13: 89. https://doi.org/10.1023/A:1008183328839*

[156] Chen, G, Wang, B, Han, D, Sommerfeld, M, Lu, Y, Chen F. and Hu Q.(2015), **Molecular mechanisms of the coordination between astaxanthin and fatty acid biosynthesis in *Haematococcus pluvialis* (Chlorophyceae).** *Plant J, 81: 95-107. doi:10.1111/tpj.12713*

[157] Polle JE, Niyogi KK, Melis A, **Absence of lutein, violaxanthin and neoxanthin affects the functional chlorophyll antenna size of photosystem-II but not that of photosystem-I in the green alga *Chlamydomonas reinhardtii*,** *Plant Cell Physiol. 2001 May;42(5):482-91.*

[158] Ducreux LJ, Morris WL, Hedley PE, Shepherd T, Davies HV, Millam S, Taylor MA. **Metabolic engineering of high carotenoid potato tubers containing enhanced levels of beta-carotene and lutein***. J Exp Bot. 2005;56:81–89.*

[159] L Ralley, EMA Enfissi, N Misawa, W Schuch, PM Bramley, PD Fraser, **Metabolic engineering of ketocarotenoid formation in higher plants**, *The Plant Journal, 39 (2004), pp. 477-486*

[160] Paul D. Fraser, Yutaka Miura, and Norihiko Misawa, ***In Vitro* Characterization of Astaxanthin Biosynthetic Enzymes**, *THE JOURNAL OF BIOLOGICAL CHEMISTRY Vol. 272, No. 10, Issue of March 7, pp. 6128–6135, 1997*

[161] Zhekisheva, Mirash & Zarka, Aliza & Khozin-Goldberg, Inna & Cohen, Zvi & Boussiba, Sammy. (2005). **Inhibition of astaxanthin synthesis under high irradiance does not abolish triacylglycerol accumulation in the green alga *Haematococcus pluvialis* (Chlorophyceae).** *Journal of Phycology. 41. 819 - 826. 10.1111/j.0022-3646.2005.05015.x.*

[162] Benjamin D Engel, Miroslava Schaffer, Luis Kuhn Cuellar, Elizabeth Villa, Jürgen M Plitzko, Wolfgang Baumeister, **Native architecture of the Chlamydomonas chloroplast revealed by in situ cryo-electron tomography***, eLife 2015;4:e04889 doi: 10.7554/eLife.04889*

[163] Tanja Gerjets, Manuela Sandmann, Changfu Zhu, Gerhard Sandmann, **Metabolic engineering of ketocarotenoid biosynthesis in leaves and flowers of tobacco species***, Biotechnol. J. 2007, 2, 1263–1269 DOI 10.1002/biot.20070004*

[164] Changfu Zhu, Tanja Gerjets, Gerhard Sandmann, ***Nicotiana glauca* engineered for the production of ketocarotenoids in flowers and leaves by expressing the cyanobacterial crtO ketolase gene**, *Transgenic Res (2007) 16:813–821 DOI 10.1007/s11248-007-9151-6*

[165] Tomohisa Hasunuma, Shin-Ichi Miyazawa, Satomi Yoshimura, Yuki Shinzaki, Ken-Ichi Tomizawa, Kazutoshi Shindo, Seon-Kang Choi, Norihiko Misawa, Chikahiro Miyake, **Biosynthesis of astaxanthin in tobacco leaves by transplastomic engineering***, The Plant Journal (2008) 55, 857–868 doi: 10.1111/j.1365-313X.2008.03559.x*

[166] Anja Röding, Lars Dietzel, Hagen Schlicke, Bernhard Grimm, Gerhard Sandmann, Claudia Büchel, **Production of ketocarotenoids in tobacco alters the photosynthetic efficiency by reducing photosystem II supercomplex and LHCII trimer stability***, Photosynth Res (2015) 123:157–165 DOI 10.1007/s11120-014-0055-z*

[167] Kay Grünewald, Christoph Hagen & Wolfram Braune (1997) **Secondary carotenoid accumulation in flagellates of the green alga *Haematococcus lacustris*** *, European Journal of Phycology, 32:4, 387-392, DOI: 10.1080/09670269710001737329*

[168] Kurniasih, S.D., Yamasaki, T., Kong, F. et al., **UV-mediated *Chlamydomonas* mutants with enhanced nuclear transgene expression by disruption of DNA methylation-dependent and independent silencing systems**, *Plant Mol Biol (2016) 92: 629. https://doi.org/10.1007/s11103-016-0529-9*

[169] Tao Zhao, Guanglin Li, Shijun Mi, Shan Li, Gregory J. Hannon, Xiu-Jie Wang, Yijun Qi, **A complex system of small RNAs in the unicellular green alga *Chlamydomonas reinhardtii***, *GENES & DEVELOPMENT 21:1190–1203 2007*

[170] Schroda, M. 2006. **RNA silencing in *Chlamydomonas*: Mechanisms and tools**. *Curr.Genet.49:69–84.*

[171] Kim EJ, Cerutti H., **Targeted gene silencing by RNA interference in *Chlamydomonas***, *Methods Cell Biol. 2009;93:99-110. doi: 10.1016/S0091-679X(08)93005-3.*

[172] Oey M, Ross IL, Stephens E, Steinbeck J, Wolf J, et al. (2013) **RNAi Knock-Down of LHCBM1, 2 and 3 Increases Photosynthetic H2 Production Efficiency of the Green Alga *Chlamydomonas reinhardtii***. *PLOS ONE 8(4): e61375. https://doi.org/10.1371/journal.pone.0061375*

[173] Linden H, **Carotenoid hydroxylase from *Haematococcus pluvialis*: cDNA sequence, regulation and functional complementation**. *Biochim Biophys Acta. 1999 Sep 3;1446(3):203-12.*

[174] Matthias Emanuel Bauch, **Identifizierung und Quantifizierung der Ketocarotinoide in Dauerstadien von Grünalgen und Ketocarotinbiosynthese im Modelorganismus *Chlamydomonas reinhardtii***, *Dissertation zur Erlangung des Grades Doktor der Naturwissenschaften am Fachbereich Biologie der Johannes Gutenberg - Universität Mainz (2011)*

[175] Pröschel M, Detsch R, Boccaccini AR and Sonnewald U (2015) **Engineering of metabolic pathways by artifiial enzyme channels**. *Front. Bioeng. Biotechnol. 3:168. doi: 10.3389/fbioe.2015.00168*

[176] Cordero BF, Couso I, León R, Rodríguez H, Vargas MA. **Enhancement of carotenoids biosynthesis in *Chlamydomonas reinhardtii* by nuclear transformation using a phytoene synthase gene isolated from *Chlorella zofingiensis***. *Appl Microbiol Biotechnol. 2011;91(2):341–351. doi:10.1007/s00253-011-3262-y*

[177] Lu, S., Van Eck, J., Zhou, X., Lopez, A. B., O'Halloran, D. M., Cosman, K. M., Conlin, B. J., Paolillo, D. J., Garvin, D. F., Vrebalov, J., Kochian, L. V., Küpper, H., Earle, E. D., Cao, J., & Li, L. (2006). **The cauliflower or gene encodes a DnaJ cysteine-rich domain-containing protein that mediates high levels of beta-carotene accumulation**. *Plant Cell, 18, 3594–3605.*

[178] Ramos-Martinez EM, Fimognari L, Sakuragi Y, **High-yield secretion of recombinant proteins from the microalga *Chlamydomonas reinhardtii***, *Plant Biotechnol J. 2017 Sep;15(9):1214-1224. doi: 10.1111/pbi.12710. Epub 2017 Apr 11.*

[179] Doshi, R., Nguyen, T., & Chang, G. (2013). **Transporter-mediated biofuel secretion**. *Proceedings of the National Academy of Sciences of the United States of America, 110(19), 7642–7647. doi:10.1073/pnas.1301358110*

[180] Verwaal, R. , Jiang, Y. , Wang, J. , Daran, J. , Sandmann, G. , van den Berg, J. A. and van Ooyen, A. J. (2010), **Heterologous carotenoid production in *Saccharomyces cerevisiae* induces the pleiotropic drug resistance stress response**. *Yeast, 27: 983-998. doi:10.1002/yea.1807*

[181] Kerfeld CA, Melnicki MR, Sutter M, Dominguez-Martin MA, **Structure, function and evolution of the cyanobacterial orange carotenoid protein and its homologs**, *New Phytol. 2017 Aug;215(3):937-951. doi: 10.1111/nph.14670. Epub 2017 Jul 4.*

[182] Michele Cianci, Pierre J. Rizkallah, Andrzej Olczak, James Raftery, Naomi E. Chayen, Peter F. Zagalsky, John R. Helliwell, **The molecular basis of the coloration mechanism in lobster shell: β-Crustacyanin at 3.2-Å resolution**, *Proceedings of the National Academy of Sciences Jul 2002, 99 (15) 9795-9800; DOI: 10.1073/pnas.152088999*

CURRICULUM VITAE

Persönliche Daten:

Name/ Vorname:	Tran, Nam Trung
Geburtsdatum:	10.07.1988
Geburtsort:	Hai Phong, Vietnam
Anschrift:	Stockhornstraße 47, 68169 Mannheim
E-Mail:	*namtrungtran.0788@gmail.com*

Ausbildung

04. 2015 – 2019	Promotion an der TU Darmstadt Fachrichtung: Biologie/ Biotechnologie Thema: Metabolic Engineering von Mikroalgen
10. 2012 – 12. 2014	Masterstudium an der TU Darmstadt Studiengang: Master-Biomolecular Engineering Schwerpunkt: Grüne Biotechnologie
10. 2009 – 09. 2012	Bachelorstudium an der TU Darmstadt Studiengang: Bachelor-Biomolecular Engineering
09.2008 – 07. 2009	Studienkolleg Darmstadt
09.2007 - 04.2008	Deutsch-Sprachkurs an der Hanoi Universität (Vietnam)
07.2006	Oberschulabschluss in Haiphong (Vietnam)

Publikationen

05.2019	*Research Article:* Nam Trung Tran and Ralf Kaldenhoff, **Metabolic Engineering of Ketocarotenoids Biosynthetic Pathway in *Chlamydomonas reinhardtii* strain CC-4102** eingereicht bei Applied Microbiology and Biotechnology
05.2019	*Review:* Nam Trung Tran and Ralf Kaldenhoff, **Achievements and challenges of genetic engineering of the model green alga *Chlamydomonas reinhardtii*** eingereicht bei Algal Research

Ehrenwörtliche Erklärung:

Ich erkläre hiermit ehrenwörtlich, dass ich die vorliegende Arbeit entsprechend den Regeln guter wissenschaftlicher Praxis selbstständig und ohne unzulässige Hilfe Dritter angefertigt habe.

Sämtliche aus fremden Quellen direkt oder indirekt übernommenen Gedanken sowie sämtliche von Anderen direkt oder indirekt übernommenen Daten, Techniken und Materialien sind als solche kenntlich gemacht. Die Arbeit wurde bisher bei keiner anderen Hochschule zu Prüfungszwecken eingereicht.

Darmstadt, den ……

.....